Contents

List of Figures **4**

List of Tables **5**

Symbols and Abbreviations **6**

1 Introduction **8**
1.1 Rationale . . . 8
1.2 The Potato Tuber . . . 10
1.2.1 History and Occurrence . . . 10
1.2.2 Nutritional Value and Importance as a Source of Starch . 10
1.2.3 Potato Plant and Tuber Life Cycle . . . 11
1.2.4 Tuber Carbohydrate Metabolism . . . 13
1.2.5 Post-Harvest Physiology and Cold-Sweetening . . . 15
1.3 Modelling Plant Sink Metabolism . . . 19
1.4 Scope of the Thesis . . . 22

2 Theoretical Background **24**
2.1 Metabolic Modelling . . . 24
2.1.1 Metabolic Models . . . 24
2.1.2 Two Types of Metabolites . . . 25
2.1.3 Reactions and their Formalisation . . . 26
2.1.4 Model Variables . . . 27
2.1.5 Stoichiometry Matrix . . . 28
2.1.6 Steady State . . . 28
2.2 Structural Analysis . . . 29
2.2.1 Structural Model . . . 29
2.2.2 Main Concepts of Structural Analysis . . . 29
2.2.3 Conserved Moieties . . . 30
2.2.4 Enzyme Subsets . . . 32
2.2.5 Elementary Modes . . . 33
2.2.6 Realisation of Structural Analysis . . . 35
2.3 Kinetic Modelling . . . 36
2.3.1 Kinetic Models of Metabolism . . . 36
2.3.2 Numerical Steady State . . . 37
2.3.3 Metabolic Control Analysis . . . 38
2.3.4 Dynamic Simulations . . . 39

2.3.5 Realisation of Structural Analysis 39

3 Principal Metabolites and Reactions 40
3.1 Principal Metabolites 40
3.1.1 Starch 40
3.1.2 Hexose Phosphates 41
3.1.3 Sucrose 42
3.1.4 Reducing Sugars 43
3.1.5 Sugar Nucleotides 44
3.1.6 Nucleotides 44
3.1.7 Triose Phosphates 45
3.1.8 Pyruvate 46
3.1.9 Inorganic Phosphates 46
3.1.10 Other Metabolites 47
3.2 Reactions: Enzymes and Transporters 48
3.2.1 Enzymes Located in the Amyloplast 48
3.2.2 Cytosolic Enzymes - Sucrose Metabolism 54
3.2.3 Cytosolic Enzymes - Glycolytic Pathway 62
3.2.4 Transporters of the Amyloplast Membrane 66
3.2.5 Other Reactions or Pathways 68

4 The Model 70
4.1 Model Design 70
4.1.1 Simplification and Boundary Decisions 70
4.1.2 Compartmentation 72
4.1.3 Assembly 74
4.1.4 Oxidative Phosphorylation 76
4.1.5 Growing Tubers - “Attached” Model 77
4.1.6 Adding Kinetics 78
4.1.7 Compartmental Metabolite Concentrations 83
4.2 Model Interrogation 84

5 Structural Analysis 86
5.1 Building and Analysing the Structural Model 86
5.2 Results of Structural Analysis 87
5.2.1 Connectivity of Metabolites 87
5.2.2 Conservation Relationships 87
5.2.3 Enzyme Subsets 88
5.2.4 Elementary Modes 92
5.2.5 Attached Tuber Model 99
5.3 ‘Scenarios’ 105
5.3.1 Varying oxidative phosphorylation 105
5.3.2 Varying Directionality 105
5.3.3 Adding a cytosolic PPase 106
5.3.4 Adding a hexose isomerase 106
5.4 Conclusions 106

6 Enzyme Activity Measurements **110**
6.1 The Selection . . . 110
6.2 Methods . . . 111
6.2.1 Plant Material . . . 111
6.2.2 Tuber Cultivation / Growth Conditions . . . 111
6.2.3 Harvest and Storage . . . 111
6.2.4 Protein Extraction . . . 112
6.2.5 Enzyme Assays . . . 112
6.3 Results . . . 113
6.4 Conclusions . . . 115

7 Kinetic Modelling **118**
7.1 Initialisation of the Model . . . 118
7.2 Simulation and Steady-State . . . 119
7.2.1 Steady-State Results (Validation) . . . 119
7.2.2 Metabolic Control Analysis (Interrogation) . . . 123
7.3 'Scenarios' . . . 126
7.4 Detached Tuber Model . . . 128
7.4.1 1st Step: Detachment . . . 128
7.4.2 2nd Step: Low Temperature . . . 131
7.4.3 Control Analysis of the Detached Tuber Model . . . 132
7.5 Conclusions . . . 134

8 General Discussion **136**
8.1 Discussion . . . 136
8.2 Future Directions - Outlook . . . 138
8.3 Summary . . . 140

References **141**

A Experimental Data (from Literature) **160**
A.1 Metabolite Data . . . 160
A.2 Flux Data . . . 161

B The Model **162**
B.1 Reactions - Rate Equations . . . 162
B.1.1 Enzymes . . . 162
B.1.2 Transporters (Amyloplast Membrane) . . . 166
B.1.3 Further Reactions or Pathways . . . 167
B.2 Reactions - Parameter Consensus List . . . 168
B.3 Model Script (ScrumPy) . . . 173
B.4 Stoichiometry Matrix N . . . 182

C Published Material **183**

List of Figures

1.1 Potato plant, schematic. 12
1.2 Cross section of mature potato tuber, schematic. 13
1.3 Main metabolic fluxes in potato tuber cells, schematic. 14
1.4 Sugar concentration(s) *vs.* storage time. 15
1.5 Sucrose accumulation, schematic. 17

2.1 Scheme of a linear pathway of three reactions. 24

3.1 The hexose phosphate pool. 42

4.1 Reaction network of the model of carbohydrate metabolism in potato tuber cells. 76
4.2 Comparison of experimental and fitted values of AGPase rate. . . 81

5.1 Elementary mode with the highest ATP yield. 95
5.2 Elementary mode with substantial starch turnover. 96
5.3 Elementary mode with substantial sucrose cycling. 97
5.4 Optimal elementary mode in terms of efficiency of starch deposition. 104

6.1 Total amylolytic activity in three potato varieties after different periods of cold-storage. 114
6.2 Total starch-phosphorylating activity in three potato varieties after different periods of cold-storage. 115
6.3 Hexose-phosphorylating activities in tubers of *S.tuberosum* cv *Desirée* after different periods of cold-storage. 116

7.1 Relative changes in modelled metabolite concentrations for PFK-overexpression and for invertase-overexpression. 126
7.2 Response of the model to detachment. 129
7.3 Response of the model to transfer to low temperatures. 132

B.1 Stoichiometry matrix $\mathbf{N}$. 182
B.2 Vectors $\boldsymbol{S}^T$ and $\boldsymbol{v}$. 182

List of Tables

4.1 Subcellular volumes in growing potato tuber tissue. 73
4.2 List of reactions that are included in the model. 75

5.1 Conserved moieties. 88
5.2 Enzyme subsets. 90
5.3 Elementary modes. 93
5.4 Reactions in sucrose-accumulating and -consuming modes. 99
5.5 Enzyme subsets for attached tuber model. 101
5.6 Elementary flux modes in the attached model. 102
5.7 Stoichiometries of all elementary flux modes that produce starch. 103

6.1 Results of measurements of maximal enzyme catalytic activities in cold-stored potato tubers. 113

7.1 Cytosolic and plastidic metabolite concentrations in developing tubers. 120
7.2 Flux control coefficients. 124
7.3 Comparison of experimentally determined and modelled flux control coefficients. 125
7.4 Response coefficients with regard to sucrose and pyruvate. 125
7.5 Concentration control coefficients. 130
7.6 Response coefficients in cold-stored tuber. 133

A.1 Metabolite concentrations. 160
A.2 Metabolic fluxes. 161

Symbols and Abbreviations

ADP	adenosine diphosphate
ATP	adenosine triphosphate
BSA	bovine serum albumine
CTP	cytidine triphosphate
Da	Dalton
DHAP	dihydroxy acetone phosphate
DTT	dithiothreitol
(dwt)	(dry weight)
EC	Enzyme Commission number
EDTA	ethylene diamine tetraacetic acid
F16BP	fructose 1,6-bisphosphate
F26BP	fructose 2,6-bisphosphate
F6P	fructose 6-phosphate
(fwt)	(fresh weight)
gFW	gram fresh weight
G16BP	glucose 1,6-bisphosphate
G1P	glucose 1-phosphate
G6P	glucose 6-phosphate
GAP	glyceraldehyde 3-phosphate
GTP	guanosine triphosphate
HEPES	N-2-Hydroxyethylpiperazine-N'-2-ethanesulfonic acid
$\mathbf{I}$	unity matrix
$\mathbf{K}$	null space matrix of $\mathbf{N}$
K_i	inhibition constant (concentration of 50% inhibition)
K_m	Michaelis constant or half-saturation concentration
$\mathbf{L}$	link matrix
MCA	Metabolic Control Analysis
MFA	Metabolic Flux Analysis
μM	micromol per litre
$\mathbf{N}$	stoichiometry matrix
NAD^+	oxidised form of nicotinamide adenine dinucleotide

NADH	reduced form of nicotinamide adenine dinucleotide
O.D.	optical density
P_i	orthophosphate
PP_i	pyrophosphate
PEP	phosphoenolpyruvate
1,3-PGA	1,3-diphosphoglycerate
2-PGA	2-phosphoglycerate
3-PGA	3-phosphoglycerate
$S_{0.5}$	substrate concentration corresponding to $V_{max}/2$
S_i	metabolite
$[S]$	concentration of metabolite S
$\boldsymbol{S}$	vector of metabolite concentrations
S.cerevisiae	*Saccharomyces cerevisiae*
S.tuberosum	*Solanum tuberosum*
S6P	sucrose 6-phosphate
UDP	uridine diphosphate
UDPG	uridine diphosphate glucose
UTP	uridine triphosphate
v_i	reaction rate
$\boldsymbol{v}$	vector of reaction rates
V_{max}	limiting rate
$\boldsymbol{\epsilon}$	matrix of ϵ-elasticities

Chapter 1

Introduction

1.1 Rationale

The purpose of this thesis is to describe the construction and interrogation of a metabolic model of the central carbohyrate metabolism in stored potato tubers. The model was built in order to gain understanding of plant sink metabolism in general, and, more specifically, to predict modifications with the potential of decreasing the undesired metabolic process of cold-sweetening in potato tubers, *i.e.* the accumulation of reducing sugars during storage at temperatures below 6°C (Burton 1989).

The potato tuber is the vegetative storage organ of the potato plant *Solanum tuberosum*. It contains approximately 78% water and 22% dry matter. About 82% of the dry matter is carbohydrates that occur mainly as the polysaccharide starch. The importance of starch lies in its nutritional value and in its use as a renewable raw material in a variety of industrial purposes, *e.g.* as thickener, filler, binder or sweetener (Burrell 2003, Jobling 2004).

Conventional breeding as well as transgenic approaches have been used to date to manipulate the carbohydrate metabolism in potato tubers (Dale and Bradshaw 2003) in order to achieve a higher starch content of mature tubers (a higher yield) or to produce 'designer' starches; the former through increasing the ability to metabolise photoassimilates or the ability to synthesise and store starch (quantity), the latter through enhancing starch functionality to suit each type of industry by modification of the physical and chemical properties of the starch (quality).

The physiology of growing potato tubers has been studied, and all enzymes believed to be involved in the conversion of sucrose via hexose phosphates to starch are well characterised (Kruger 1997, Pozueta-Romero et al. 1999), as well as the enzymes of the glycolytic pathway (ap Rees 1985, Plaxton 1996). Progress made in the last decade has led to the cloning of many of the genes encoding for these enzymes, and the generation of a large range of transgenic potato lines (Fernie et al. 2002). In these plant lines the expression levels

of genes are altered, *i.e.* increased or decreased (sense and antisense), either for an individual gene or for a combination of several genes. Investigating the phenotypes of these transgenic potatoes enhances our knowledge of plant physiology but it also raises new questions.

To achieve a certain change in the tuber's physiology by growing transgenic plants is very time-consuming. It requires the transformation (*i.e.* the production of a genetically modified plant) and a growth period of 13-17 weeks. If the metabolic function to be investigated is to find the factors affecting cold-induced sweetening, an extra period of storage after the harvest of the tubers has to be added. At this stage the experiment already lasts several months before the measurements in which one is actually interested can be performed.

Nevertheless, the storage-related problem of low-temperature sweetening (LTS) has been approached by means of transgenesis. Examples are alterations in the expression of ATP-dependent phosphofructokinase (Burrell et al. 1994) and pyrophosphate-dependent phosphofructokinase (Hajirezaei et al. 1994), the two enzymes that catalyse the phosphorylation of fructose 6-phosphate. This reaction marks the entry of hexose phosphates into the glycolytic pathway, and it was believed to exclusively control the glycolytic flux.

When Burrell et al. (1994) overexpressed ATP-dependent phosphofructokinase, the transgenic plants showed less sweetening but the transformation also resulted in an unfavourable lower yield. Hajirezaei et al. (1994) studied plants with up to 90% decreased activities of pyrophosphate-dependent phosphofructokinase (this enzyme is assumed to primarily act in the direction of dephosphorylation of fructose 1,6-bisphosphate), which showed no change in phenotype in terms of sucrose accumulation.

Thus, the two attempts were not successful in terms of reducing cold-induced sugar accumulation, and provided no solution regarding the mechanism causing the imbalance between starch breakdown and glycolysis that results in cold-sweetening. To date, no commercially acceptable cultivar that can be taken out of $\leq 4^{o}$C storage and processed directly has been identified (Dale and Bradshaw 2003).

However, the fact that many of the enzymes converting carbohydrates are well characterised (see above) makes it reasonable to design a mathematical model of this part of metabolism. This model of carbohydrate metabolism can serve as a tool to study this complex system thoroughly *in silico* and to produce new hypotheses of where the control over sucrose accumulation resides. It may help to discover suitable targets for repressing unwanted cold-sweetening.

In the following sections of this chapter some background information on the biological system in question is given, and the modelling approach is introduced and explained.

1.2 The Potato Tuber

1.2.1 History and Occurrence

The solanaceous potato plant, *Solanum tuberosum*, originates from the highlands of South America and was cultivated in the Andes for several millenia before its introduction into Europe in the 16th century. Since then it has spread throughout the whole world and has gained importance. Along with maize, rice and wheat, it is one of the main crops in the world with a production of 321 million tonnes and covering more than 19 million hectares in 2002 (from FAOSTAT database 2004, last accessed September 2004).

S. tuberosum is tetraploid with 48 chromosomes. It belongs to the nightshade family (its members contain the alkaloid solanine) and is divided into two subspecies or groups, namely *Andigena* and *Tuberosum*, with about 3800 cultivars or varieties altogether, a collection of which is established in the International Potato Center in Lima (www.cipotato.org).

1.2.2 Nutritional Value and Importance as a Source of Starch

The potato tuber is the sink organ of the potato plant and its only part utilised by humans. Because of its high content of glycoalkaloids the plant is completely poisonous except for the tubers.

Tubers are enlarged portions of underground stems. More than 80% of their dry matter is carbohydrates which occur mainly as starch. Furthermore, the tubers contain protein (accounting for 11% of its dry weight), trace elements and substantial amounts of vitamins (amongst them at least 12 essential vitamins and minerals, *e.g.* vitamin C and potassium), thiamine, iron, folic acid and some fibre. According to the FAO (Food and Agriculture Organization of The United Nations), a single medium-sized potato contains about half the daily adult requirement of vitamin C. All this points out the high nutritional value of the potato tuber.

In addition, there is a processing or industrial value of the starch that is contained in the tubers. The following are the main commercial uses of potatoes:

1. as a food crop, *i.e.* for human consumption ("foodstuff").
   It can be consumed fresh or processed, *e.g.* as crisps, chips, instant mashed potatoes, novelty snacks, *etc.*;

2. as a feed crop, *i.e.* in the diet of live-stock ("feedstuff");

3. as a source of the renewable raw material starch in:
   - starch pastes and modified starches for various applications, *e.g.* paper adhesives, glues, size (paper surface coating);
   - biodegradable plastic or as 'filler'.

The diversity of the uses of starch in its processed form is increasing continuously, especially with the recent development of the production of customised starches. Now, a raw material that matches the needs of industrial users can be 'designed', *e.g.* by varying the ratio of amylose and amylopectin. In these 'designer starches', the composition or the physico-chemical properties, *e.g.* gelatinisation temperature or pasting behaviour , can be modified to suit a certain purpose (Sivak and Preiss 1998, Jobling 2004).

Because of the importance of the potato tuber as a crop and as a source of the renewable raw material starch, there is extensive scientific interest in tuber development and physiology. Many reviews are published that describe the present knowledge of tuber growth (*e.g.* Cutter 1978 or Burton 1989), or, at a molecular level, the formation and constitution of the reserve polysaccharide starch (*e.g.* Smith 1999, or Kossmann and Lloyd 2000).

1.2.3 Potato Plant and Tuber Life Cycle

Potato plant

The potato plant is a bushy, dark green plant with compound leaves. It has white, pale blue or purple 2.5-cm-wide 5-petaled flowers which, if not sterile, produce small seeds. Potato plants can be cultivated from these 'true seeds' but, more commonly, they are propagated by seed tubers (or pieces of tubers that include at least one bud or 'eye'). These are planted and, under certain temperature and humidity conditions, start to sprout. Growth of roots, growth of the tops, and leaf expansion follows. When leaf growth slows down, the plant begins to flower, and tubers are initialised. Tuber formation is followed by a period of tuber growth accompanied by rapid deposition of starch in the form of semi-crystalline granules that are confined to the plastids. Maturation of the tubers is coupled with senescence of the tops. If not harvested then, after a period of dormancy, the sprouting of the tubers would again start a new potato plant life cycle. For a schematic illustration of all organs of a potato plant, see Figure 1.1.

Productive plants have two or more main stems with 5 to 15 mature tubers found on each plant at harvest. The number of tubers per plant is called a 'tuber set'. Shape, size and weight of mature tubers greatly depends on the variety. For *cv Desirée*, the tubers are oval and the typical weight at harvest is over 60g. The differentiation of tissues in a mature tuber is shown in the illustration of a tuber's cross section in Figure 1.2.

Tuber life cycle

The potato tuber's life cycle is composed of many individual developmental stages including tuber formation, tuber development, dormancy and sprouting (Burton 1989).

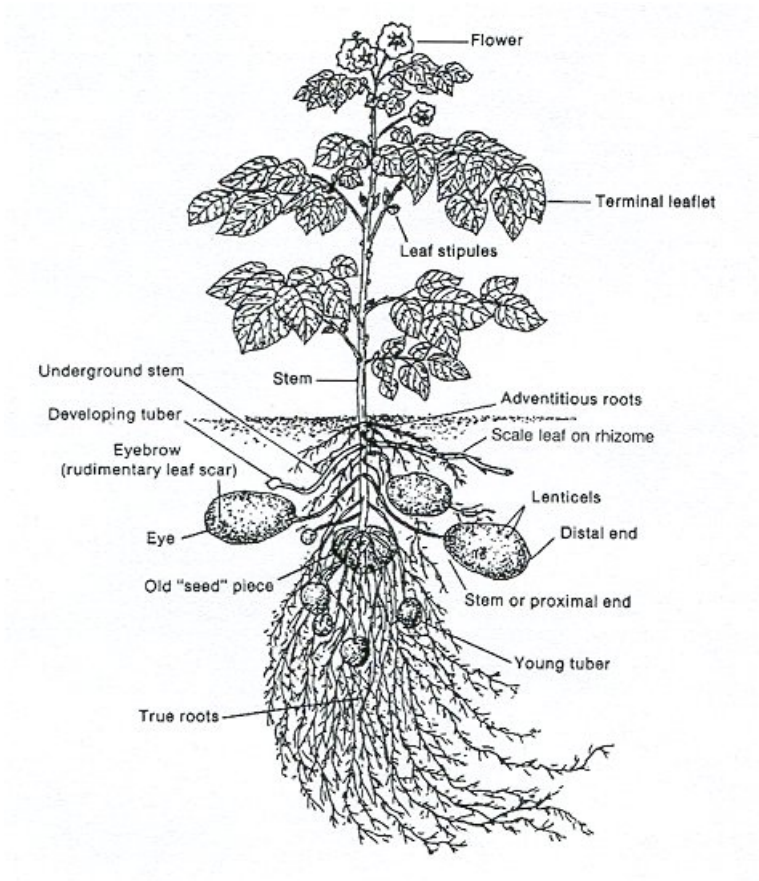

Figure 1.1: Potato plant, schematic.
(from http://www.gov.mb.ca/agriculture/crops/potatoes)

1. **Tuber Formation (Tuberisation)** appears after growth of the tops and leaf expansion. Underground stems (stolons) begin to branch out and swell at their tips. Starch is deposited at the ends of the stolons, enlarging these portions of the underground stems, and thereby forming tubers.

2. **Tuber Development** is characterised by rapid deposition of large quantities of starch in specialised plastids (amyloplasts). When supplied with sucrose, produced in the photosynthetic tissue of mature leaves (source) and transported via the vascular system to the rest of the plant including the stolons (sink), the cells in the internal part of the tuber, the medulla, increase in size and number. Tuber growth lasts for 13 to 17 weeks[1], and, eventually, the starch granules account for the bulk of the dry weight of

[1]Tubers harvested from 10-week-old plants usually are referred to as 'developing' tubers. At this stage, plants are completely green and tubers (20-40 g fresh weight) are still growing. Developing tubers are commonly used for the study of growing tuber metabolism, and comparison of metabolite data between tubers harvested from plants between 8 and 12 weeks old is readily possible (Farré et al. 2001).

the tubers. Figure 1.2 shows a tuber cross section. Mature tubers can survive in the soil for many months, till the next growing season.

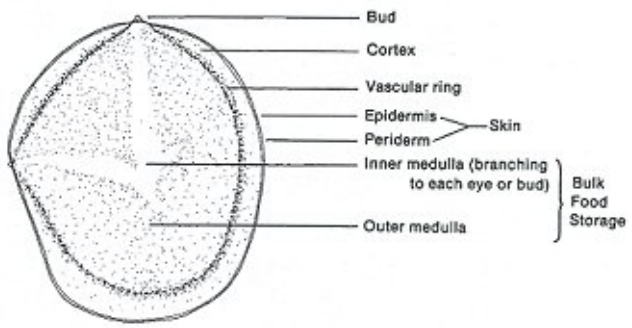

Figure 1.2: Cross section of mature potato tuber, schematic.
(from http://www.gov.mb.ca/agriculture/crops/potatoes)

3. **Dormancy and Sprouting** follow if the tubers are not harvested for consumption or processing. Dormancy is the state of a plant when growth has ceased for the year and other activities in the whole plant have slowed down, usually during winter. Only after this period of dormancy, during which a tuber remains unable to germinate, sprouting appears. Sprouting is characterised by the demobilisation of the starch reserves. Starch forms the source of carbon from which sucrose can be synthesised for export into the growing sprout or shoot. Sprouting completes the potato plant's natural life cycle.

4. **Harvest and Storage** of the tubers are human interventions. Toward the end of their bulking or growth stage, the tubers are dug from the ground and removed from the plant's remains. They are either processed immediately or stored for later use. The storage temperature usually is in the range of 6-12°C for reasons of preservation and to prevent shrinkage, disease loss and sprouting.

From the stages described above, only tuber development (2.) and tuber storage (4.) were investigated in the course of this project. They are discussed in the following.

1.2.4 Tuber Carbohydrate Metabolism

The direction of the main physiological fluxes involving starch changes from synthesis to breakdown, corresponding to the tuber's life stage. In the phase of tuber growth (pre-harvest), the photosynthate sucrose, delivered from the green parts of the plant and imported into the tuber cell, is degraded and, via hexose phosphates, converted to starch, which is partly deposited (see Figure 1.3**A**). In the phase of tuber storage (post-harvest), the deposited starch is partially remobilised for the supply of free energy for the cell (compare Figure 1.3**B**).

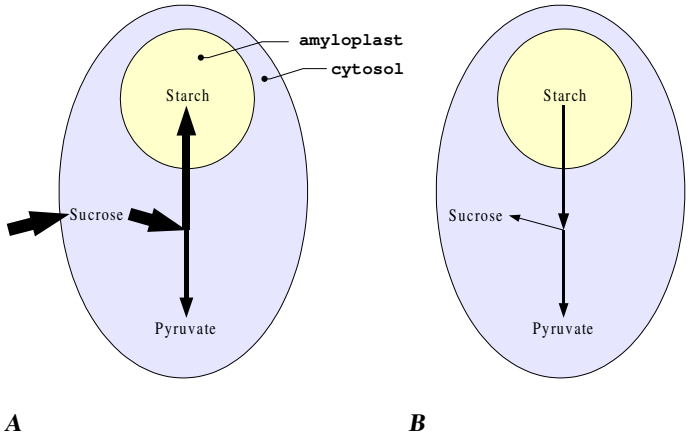

Figure 1.3: Main metabolic fluxes in potato tuber cells, schematic.
A: Sucrose-to-starch conversion in developing tubers;
B: Starch breakdown during storage/dormancy.
The cytosolic fluxes branch at the central hexose phosphate pool.

Sucrose-to-starch conversion defines the tuber's sink strength, whereas net starch breakdown becomes dominant after tuber maturation. In the stored tuber, opposed to during the other life stages, the sole function of carbohydrate metabolism is to provide the cell with vital amounts of precursors for maintenance respiration, which again has to produce enough molecules of ATP and NADH to keep their levels relatively stable (no growth just maintenance).

As mentioned above, the conversion of sucrose to starch is the dominant metabolic flux during tuber development. Sucrose-to-starch conversion has been extensively studied throughout the last century, and there has always been much interest in understanding the regulation of this conversion (Kruger 1997, or reviews by Fernie et al. 2002 or Geigenberger 2003). However, there are still major gaps in the knowledge about the 'reversed' conversion, namely the degradation of starch to hexose phosphates, sucrose or even further to pyruvate. The latter will be addressed herein.

A comprehensive compilation and description of reactions relevant for the model of potato tuber carbohydrate metabolism will be given later in Chapter 3. It also holds more details on starch, sucrose and other sugars that are the cornerstones of carbohydrate metabolism.

Sugars play a manifold role in plants. They function as intermediate metabolites, sink metabolites, or transport metabolites, they regulate the cellular osmotic potential, and they act as signal molecules.

One special aspect of tuber storage and processing quality, namely the phenomenon known as cold-induced sweetening, is discussed in the subsequent section.

1.2.5 Post-Harvest Physiology and Cold-Sweetening

Why cold storage?

Potato plants are best grown in moderate climates where continous production throughout the year is unfeasible. Therefore, long-time storage of harvested tubers is essential. If not immediately processed, sprouting of the potato tubers has to be controlled or prevented. This can be done through treatment with dormancy-prolonging chemicals or through storage at low temperatures and under high humidity conditions (Burton 1989). Further benefits of cold-storage are less shrinkage, less disease loss and decreased sprouting.

What is cold-sweetening?

A storage-related problem is cold-induced sweetening of potato tubers. In tubers stored at low temperatures, namely $\leq 6^{o}$C (Pollock and ap Rees 1975b), starch is degraded, the disaccharide sucrose accumulates, followed by a release of its two components, the reducing hexoses glucose and fructose. The accumulation of all these sugars over the time of storage is called cold-sweetening or LTS (abbreviated for low-temperature sweetening), it is illustrated by Figure 1.4 showing the increasing sugar content in potato tubers.

The phenomenon of low-temperature sweetening was first reported in 1882 (by Müller-Thurgau in Landw.Jahrbuch 11: 751-828), and was a topic of commercial and scientific interest since (*e.g.* Tishel and Mazelis 1966, Pollock and ap Rees 1975a, ap Rees et al. 1988, Hill et al. 1996, Zrenner et al. 1996, Nielsen et al. 1997, Deiting et al. 1998, Krause et al. 1998, Wismer et al. 1998, Blenkinsop et al. 2003, Dale and Bradshaw 2003, Gupta and Sowokinos 2003, Hajirezaei et al. 2003, *etc.*).

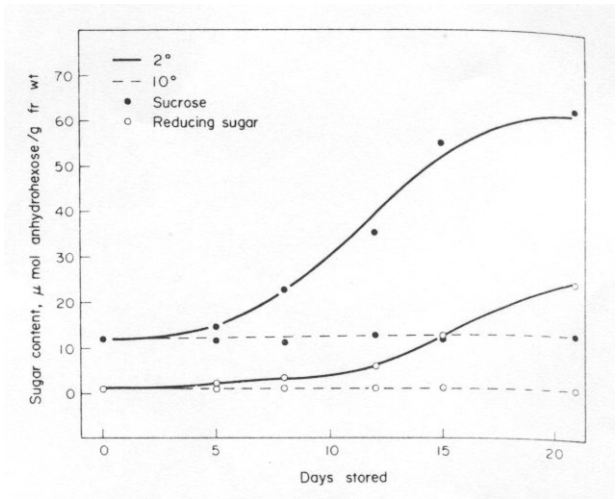

Figure 1.4: Sugar concentration(s) *vs.* storage time.
(from Pollock and ap Rees 1975a)

Cold-sweetening and processing quality

Tubers with higher concentrations of reducing sugars are less suitable for the processing industry. Potatoes with high levels of glucose and fructose make dark chips and fries. As raw potatoes are sliced and processed at high frying temperatures, the reducing sugars react with abundant free amino acids in a non-enzymatic Maillard-type reaction[2]. This leads to disadvantageous or unacceptable discolorations (brown- to black-pigmented) or bitter taste of the products, *e.g.* potato crisps[3]. Processors strive to control crisp colour by the manipulation of oil temperature, slice thickness and length of frying period but the colour of potato crisps is largely determined by the sugar content of the processed potato tubers (Rodriguez-Saona et al. 1997).

Because of this negative effect on the processing qualities of tubers, LTS is recognised as one of the most serious problems of the food-manufacturing industry (Burton 1989). To ensure an acceptable process colour, market quality of process potatoes (to be processed into crisps, chips, and other frozen potato products) includes a low reducing sugar content.

A correlation between the glucose and fructose levels of tubers and the content of acrylamide, a possible carcinogen, of processed product was reported more recently (Chuda et al. 2003, Amrein et al. 2004). This poses a further motive for growing potatoes that show less sweetening because the use of raw products with low sugar content also effectively controls the formation of acrylamide (Chuda et al. 2003).

Besides the storage conditions, the concentrations of chemical constituents, such as reducing sugars, depend also on several other factors (for an overview see Kumar et al. 2004). One of them is tuber maturity, and the state of maturity of a tuber is affected by growth conditions and time of harvest (Richardson et al. 1990, Hertog et al. 1997). Another factor is the potato variety (Sowokinos et al. 1997, Hertog et al. 1997).

Cold-sweetening in different varieties

Comparison studies show that different *S.tuberosum* varieties differ in their response to low-temperature storage (*e.g.* Sowokinos et al. 1997 or Hertog et al. 1997); sugar accumulation is cultivar-dependent. The existence of cultivars in which even cold-sweetening resistance has been observed (*e.g.* *cv Snowden*, reported by Gupta and Sowokinos 2003) gives reason to assume that

[2]The Maillard Reaction or 'non-enzymatic browning' has been known since 1912. It takes place in most foods on heating. It is a complex set of reactions between amines (from proteins) and carbonyl compounds (from the reducing sugars glucose, fructose or maltose). Through it many by-products are formed with an impact on flavour and appearance of cooked or fried food, and it also causes a loss of essential amino acids.

[3]Quality or industry standard potato crisps have a light colour and little vascular discolouration and no bitter or other off-flavours.

it is likewise possible to prevent it in non-resistant but more commercial varieties. Furthermore, simply comparing the metabolism of the resistent cultivars and of cultivars commonly used in agriculture could be a potential route for investigation.

Attempts to reduce or prevent cold-sweetening

Enhancement of the processing quality of potato tubers by reducing sugar accumulation is desirable. To achieve such a reduction, an understanding of the underlying mechanism is necessary. During the second half of the last century a few possible causes for cold-sweetening were proposed.

In the 1970s it was known that some enzymes of central carbon metabolism exhibit cold-lability whereas others do not, *e.g.* cold-lability of the glycolytic enzyme phosphofructokinase (Pollock and ap Rees 1975a) and relative cold-stability of the UDP-glucose and ADP-glucose pyrophosphorylases (Sowokinos 1976). An influence of the latter two, therefore, was doubted, whereas it was hypothesised that cold sensitivity of glycolytic enzymes diverts the products of starch breakdown towards sucrose formation.

This idea was further generalised in the 1980s, when it was proposed by ap Rees et al. (1988) that sucrose accumulates as a consequence of an imbalance between the rate of starch degradation and the rate of glycolysis. This is visualised in Figure 1.5 (or see Figure 1.3**B** again).

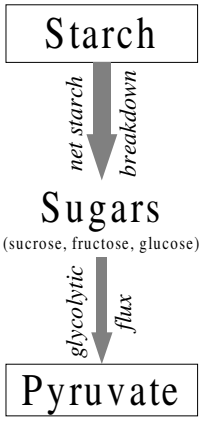

Figure 1.5: Sucrose accumulation caused by an imbalance between the rate of starch degradation and the rate of glycolysis (represented by the width of the arrows).

According to this idea, an increase in the glycolytic flux or a decrease in starch breakdown will presumably offset the claimed imbalance and lead to a lower amount of free sugars in the tubers.

Direct intervention into (or reasoned changes of) metabolism like these became possible only in the 1990s with genetic manipulation techniques. It was attempted to increase the glycolytic flux by transgenic alterations of the expres-

sion of the enzyme phosphofructokinase. Burrell et al. 1994 overexpressed the ATP-dependent enzyme (PFK), and Hajirezaei et al. 1994 experimented with the PP_i-dependent form (PFP). The entry into the glycolytic pathway was then believed to be the 'rate-limiting step' of glycolysis. But manifold change in the expression of the two phosphofructokinases caused no significant change in the glycolytic flux (Burrell et al. 1994, Hajirezaei et al. 1994, see also discussion of the two examples earlier in Paragraph 1.1).

'Trial and error' genetic manipulation of the potato plant to either find the crucial enzyme or to gain a transgenic plant with less cold-sweetening have so far failed to bring the desired result. This is due to the redundancy of plant metabolism, which in a review by Kruger (1997) is explained as follows: "...a decrease in flux through a particular pathway resulting from experimental manipulation is often accompanied by an increase in flux through a complementary series of reactions, thus reducing the metabolic consequences of the original manipulation. Such metabolic flexibility appears to be a central feature of plants, and probably accounts for the absence of major metabolic effects of many transgenic manipulations..."

Two further examples for transgenic manipulations with their consequences diverging from expectations are:
1. Four-fold increase in AGPase activity (Sweetlove et al. 1996a) had no effect on starch accumulation (Sweetlove et al. 1996b). AGPase is directly involved in starch synthesis, forming its precursor ADP-glucose. It is allosterically regulated, and seen as the gateway for carbon entry into transient and storage starch in plants. This led to the assumption that its up-regulation would result in enhanced starch synthesis. It did. But starch was also broken down faster, and, consequently, there was no effect on starch deposition.
2. Enhancement of the capacity to metabolise sucrose by overexpressing cytosolic invertase was assumed to lead to an increased starch accumulation. As might be expected, the sucrose content of potato tubers from transgenic lines with specific expression of a yeast invertase was reduced by 95% (Sonnewald et al. 1997). Unexpectedly, this was accompanied by a reduction of the starch content of up to 15%. The tubers also accumulated large quantities of glucose. Trethewey et al. (1998) introduced a bacterial glucokinase into this invertase-expressing line with the intention of mobilising the excess glucose for starch synthesis but the additional higher glucokinase activity only led to a further dramatic reduction in starch content.

In general, great difficulties are encountered in achieving the desired outcome by genetic manipulation of plant central metabolism (Morandini and Salamini 2003).

The theoretical approach

The exclusively experimental approach of manipulating central carbohydrate metabolism as described above did not bring the desired results, nor did it clarify or reveal the initialising factors for the increase in the tubers' sugar content.

In order to provide more insight into cause and mechanism of sugar accumulation and for a more rational and selective alteration of metabolism, the modern biochemical and genetic tools should be combined with the modern mathematical modelling tools (Burrell 2003).

The theoretical approach, *i.e.* building a mathematical model of the potato tuber carbohydrate metabolism and interrogating it, can further the prospects of enhancing the processing quality of potato tubers. By predicting the effect that alterations in an enzyme activity have on metabolite concentrations, it may help to solve the problem of cold-induced sweetening. Especially metabolic control analysis can serve as a tool for interpretation of experimental failures and as a guide for manipulators (Morandini and Salamini 2003).

Also, the usefulness of modelling for 'metabolic engineering', *i.e.* rationally engineering the plant cell for enhanced production of a secondary metabolite (of the plant itself or from a foreign species), becomes more and more recognised (Morgan and Rhodes 2002).

1.3 Modelling Plant Sink Metabolism

The aim of biological modelling in general is to understand the structure, dynamics, control pattern, and design principles of the biological system under investigation. Metabolic models especially can be adopted to supplement or even to replace *in vivo* or *in vitro* experiments. They can be employed either to generate or to test hypotheses. The constructive interrogation of a metabolic model can serve the purpose of:

- Bioproduction optimisation (*e.g.* maximising the yield of a target product through the improvement of the strain or through the improvement of the growth conditions);
- Drug discovery or target validation, *e.g.* for anti-parasitic or other drugs (by finding/predicting the most effective compounds or by modelling the side effects of drugs);
- Furthering insight into and understanding of biological complexity.

There are two tendencies in metabolic modelling: whole cell models (or models of cell cultures), and very elaborate and detailed models for individual processes and events in organisms that are of general significance or show a very special behaviour. The model described in this thesis is of the latter type, and it is

concerned with the central carbohydrate metabolism in potato tubers and with the process of sugar accumulation.

This model is not the first attempt of modelling plant metabolism. A few models of carbohydrate metabolism in plants already exist (see review by Morgan and Rhodes 2002). Some of them deal with sink metabolism.

Existing models of carbohydrate metabolism in plant sinks

1. A kinetic model of glycolysis in potato tubers has been described by Thomas et al. (1997b). These authors considered a pathway segment beginning with G1P and ending with pyruvate. Using their model and measured amounts of glycolytic metabolites (from Mooney 1994), elasticities were calculated, and subsequently, by means of the matrix method, control coefficients. This led to the prediction that PFK has only little control over glycolysis, which is in agreement with experimental findings (Burrell et al. 1994). Furthermore, it was concluded that the major portion of respiratory control lies outside the glycolytic sequence.

   This model consists of 9 reactions.

2. Sugar cane sucrose metabolism was modelled by Rohwer and Botha (2001). They validated their kinetic model by comparison with independant experimental results, and then used it to assess different enhancement strategies for increasing sucrose accumulation in sugar cane. The activities of the enzymes with the largest control coefficients on futile cycling of sucrose were varied in the model and conversion efficiencies from hexose into sucrose for these enzymes determined.

   There are 11 reactions in this model.

3. Amthor (2003) performed a theoretical analysis of metabolic costs of plant lignin biosynthesis in terms of consumption of sucrose.

   This structural model considers more than 100 reactions.

4. Björn Junker included a kinetic model of sucrose breakdown in his PhD-Thesis regarding potato plants transformed with an inducible invertase (Junker 2004). The model was employed to simulate the quantitative effects of the introduction of a yeast invertase in the cytosol of potato tubers. It did not include starch metabolism, and it did not account for any cellular compartmentation.

   This model consists of 15 reactions.

Two types of models, structural and kinetic, appear in the above list. The first type only considers the structure of a metabolic network (3.), and the second

type also its dynamic behaviour (1., 2. and 4.). Further explanation of this distinction will be given in the subsequent Chapter 2.

The model described and interrogated herein:

The type of a model depends on the particular biological system in question, on the amount of data available, as well as on the purpose that is to be answered.

This model's purpose is to make suggestions of how the demand for a 'cold-processing potato', with improved long-term tuber quality, can be met by genetically manipulating the potato plant.

Several examples of unexpected effects where specific genes were genetically manipulated in potato were mentioned in Paragraph 1.2.5 (PFK, PFP, AGPase, invertase). They illustrate the difficulties that are encountered in achieving a desired outcome, *e.g.* an increase in starch yield or a reduction in cold-sweetening, by genetic manipulation techniques only. By investigating the potato tuber central carbohydrate metabolism in a mathematical model prior to the experiment, it is aimed at avoiding or minimising such disappointments. This approach can offer a more directed improvement strategy than cumbersome gene-by-gene manipulation. The model should guide and rationalise gene manipulations.

The advantages of the theoretical approach in gaining greater understanding have already been discussed (in Section 1.1). They also include, for instance, the possibility of simulating knockouts as opposed to experimentally generating them (Thorneycroft et al. 2001), or the interpretation of experimental failures by pointing out any intrinsic limits to raising starch yield (Morandini and Salamini 2003).

Chapter 4 describes the design of the model to be analysed.

Structural Analysis allows to investigate the structure or topology of the modelled metabolic network (Poolman et al. 2004). Details regarding Structural Analysis will be given in Section 2.2.

Metabolic Control Analysis (MCA) of the model quantifies the effects of a perturbation (*e.g.* altering the rate of one of its reactions) on steady state fluxes through the system or steady state metabolite concentrations (see recent overviews in Kacser et al. 1995, Heinrich and Schuster 1996a, or Fell 1997). Response coefficients, as defined in MCA, describe the response of metabolite concentrations or fluxes to finite changes in enzyme and effector concentrations and can be used to understand the control and regulation of a metabolic system. More details regarding MCA will be given in Section 2.3.

How can MCA be applied to the problem of sugar accumulation? Control analysis of a validated model can be carried out that gives concentration control coefficients of all the reactions in the system toward the concentrations of

the reducing sugars relevant for cold-sweetening. Additionally, simulations are useful, since sugar accumulation is a rather large response to the environmental stress of low temperature and probably brought about by large changes on the molecular level.

1.4 Scope of the Thesis

The overall aim of this work is the prediction, by theoretical means of metabolic modelling, of suitable target enzymes for genetic transformations of *S.tuberosum* with the effect of reducing cold-induced sweetening in stored potato tubers.

All commercial potato cultivars presently used for the production of potato chips and fries accumulate excess free reducing sugars when exposed to cold stress (Sowokinos et al. 1997). The disadvantages of this sugar accumulation were mentioned in the previous Section 1.2.5, and its inhibition or repression is necessary for a better processing quality.

Possible strategies for limiting the accumulation of reducing sugars in stored tubers (by genetically modifying potato plants) are to prevent sucrose accumulation or to prevent the conversion of sucrose to reducing sugars. The prevention of sucrose accumulation can be achieved either by inhibiting sucrose producing reactions or by enhancing sucrose consuming reactions. The prevention of sucrose cleavage into reducing sugars can only take place at the invertase or sucrose synthase step.

Unfortunately, as has been found in many experiments (Morandini and Salamini 2003, see also the four examples given in Paragraph 1.2.5), the effect of changes in the level of a single enzyme in order to reduce sucrose concentration cannot easily be predicted. The system's response to alterations is non-trivial due to the high complexity of plant carbohydrate metabolism.

Understanding of this complexity can be attempted through a theoretical approach, requiring a model of the system, and by using theoretical tools to interrogate this model, such as *e.g.* Structural Analysis or Metabolic Control Analysis. Calculation of the concentration control coefficients on sucrose for all the enzymes in the metabolic network will indicate those reactions that have the greatest influence on sucrose concentration. In order to perform a control analysis, a comprehensive kinetic model of the metabolic network of carbohydrate metabolism in potato tuber is needed.

On the basis of theoretical modelling, the main objective is to identify enzymes with a high degree of control over the concentration of sucrose in tubers. With this information promising targets for genetic manipulation (so called 'candidate genes') can be proposed, or less promising possibilities eliminated.

The objective was achieved by completing the following tasks:

- Construction of a (computer) model of potato tuber carbohydrate metabolism;
- Implementation, validation and refinement of the model;
- Interrogation of the model: structural analysis of the model (*e.g.* detection of elementary modes *etc.*), knock-out analysis, steady state calculation, comparison with experimental data of fluxes and metabolite concentrations, and with 'scenarios' (changed properties of transgenic potato plants), dynamic simulations, control analysis of the kinetic model and calculation of sensitivities of the control coefficients.

Background and details about the theory of metabolic modelling can be found in Chapter 2. The construction of the metabolic model, using the information obtained from a thorough review of the relevant literature (collected in Chapter 3), is described in Chapter 4.

By means of the software *ScrumPy*, a package of *Python*[4] modules for metabolic modelling (M. G.Poolman and D. A.Fell 2002), a structural analysis of the model (*i.e.* detection of conserved moieties, enzyme subsets and elementary flux modes) was carried out. The results of this analysis are documented in Chapter 5. Furthermore, simulations, steady state calculation and control analysis of the model were performed, and Chapter 7 holds a description of this as well as the obtained results.

Chapter 6 describes the methods and results of measurements of maximal catalytic activities of some of the enzymes. The acquired values were incorporated in the model, they serve as kinetic parameters in the kinetic model.

Finally, in Chapter 8, the conclusions from the structural analysis and dynamic simulations are presented and discussed.

[4] *Python* is an interpreted, interactive and object-oriented programming language (visit http://www.python.org).

Chapter 2

Theoretical Background

A motivation for modelling in the biological sciences was given in Section 1.3. In this chapter, the background for modelling is explained: model definition, model design and construction, and methods that have been successfully applied in modelling.

2.1 Metabolic Modelling

2.1.1 Metabolic Models

Models are used to capture and reproduce the essential behaviour of a system or describe its composition of basic units. Metabolic models do so for metabolism.

In metabolism, the basic units are metabolites and reactions. Metabolites are formed, changed or interconverted by biochemical reactions, or they are transported between compartments (imported and exported). The ensemble of reactions and transport processes constitutes the metabolism.

A metabolic model accounts for the interactions of metabolites and enzymes. It is a list of coupled biochemical reactions, representing the network that the reactions form by connecting the metabolites.

In analogy to graph theory, the reactions resemble vertices and the metabolites nodes.

For example, a simple biochemical system of three reactions connecting the reactant X_1 and the product X_2 is depicted in Figure 2.1 schematically.

$$X_1 \longrightarrow S_1 \longleftrightarrow S_2 \longleftrightarrow X_2$$

Figure 2.1: Linear pathway of three reactions converting the reactant X_1 into the product X_2 via the intermediate metabolites S_1 and S_2.

A metabolic model is a list of reactions and information associated to the reactions. For instance, the appendant list of reactions R for the simple network

of Figure 2.1 reads:

$$
\begin{aligned}
R1: &\quad X_1 \longrightarrow S_1 \\
R2: &\quad S_1 \longleftrightarrow S_2 \\
R3: &\quad S_2 \longleftrightarrow X_2
\end{aligned}
$$

For a structural model, a reaction list as shown above is sufficient, whereas for a kinetic model much more information is needed. What additional information is necessary for a kinetic model will be explained shortly (Paragraph 2.1.3), and the potential of a structural model will be discussed in Section 2.2.

In metabolic models there can be any number of reactions describing the interactions between any number of metabolites (though often there are more reactions than metabolites). For instance, the models that were mentioned before in Section 1.3 as examples consisted of between 9 and over 100 reactions: 9, 11 and 15 for the kinetic models, and over 100 for the structural models.

2.1.2 Two Types of Metabolites

Out of all metabolites considered in a metabolic model, some metabolites are designated 'external'. They are often located at the boundaries of a model (*i.e.* defining them), as for instance in Figure 2.1. There are different reasons for defining a metabolite as external. They are *e.g.*:
1. The metabolite is buffered by reactions not considered in the model but regulated by the environment, *e.g.* CO_2, H_2O or extracellular metabolites;
2. The metabolite is buffered by many reactions, *e.g.* currency metabolites such as ATP, ADP, NAD^+, NADH *etc.*, or inorganic compounds such as P_i;
3. The metabolite is present in large excess so that its concentrations at a short time scale is virtually unaffected by the reactions considered in the model;
4. Plant polysaccharides, such as starch, cellulose, *etc.* (or, more generally, any biopolymer, *e.g.* DNA, collagen, glycogen, *etc.*). In these polymeric molecules, the molarity or number of reactive sites or end groups is usually not affected by addition or removal of one monomer, hence, the kinetics of their formation or degradation are not strongly dependent on the degree of polymerisation. But these polymers pose slight problems for the representation of mass-balance when attempting to write down their stoichiometries. Therefore, it is better not to express stoichiometries for biopolymers but to consider them external.

On the other hand, all remaining intermediates are 'internal' metabolites. They are consumed or produced by the reactions in the model, and their concentrations change accordingly.

The concentration of a metabolite S_i often is denoted by brackets, *i.e.* $[S_i]$, but in the following these brackets will be omitted for more clarity. Mentioning of a metabolite S_i also implies its concentration.

2.1.3 Reactions and their Formalisation

The term 'reaction' refers to either a biochemical reaction catalysed by a single enzyme, or to a sequence of several enzyme-catalysed reactions lumped together, or to a transport process. Reactions connect metabolites. They can be described or formalised in the following way (the formalisation of the reaction $R2$ from the example on the previous page is given as an example in parentheses):

0. **Reaction name:** identifier for the reaction ($R2$);
1. **Reactants and products:** variables S_i for all substrates of the reaction (S_1, S_2);
2. **Stoichiometry:** given by the stoichiometric coefficients of the substrates; The stoichiometric coefficients are dimensionless. They describe the proportions of molecularities of all the substrates involved in a reaction. One could identify them with molecules or moles of substance. They are usually integers; if not they should be scaled accordingly. The coefficients of substrates that are used in the reaction are negative, whereas coefficients of substrates that are formed are positive. (-1, 1) (as in: $\mathbf{1}S_1 \leftrightarrow \mathbf{1}S_2$);
3. **Directionality:** states if the reaction is reversible or irreversible[1] (rev./~~irrev.~~);

These items (0.-3.) are compulsory, they are always needed for setting up a metabolic model. Also, they are sufficient for doing a structural analysis. A model that only consists of this information is a structural model.

The following information on a reaction is not needed for structural modelling but it is essential for kinetic modelling.

4. **Rate equation:** a function $v(S_i)$ for the velocity v that specifies $\frac{dS_i}{dt}$, the amount of substrate used or formed in a certain period of time; The equation for v emulates the assumed reaction mechanism or approximates the observed phenomology of the reaction, *e.g.* Michaelis-Menten equation, Reversible Hill equation, *etc.* A compilation of reaction mechanisms, *e.g.* allosteric, ping-pong, sequential, *etc.*, with applicable rate equations can be found in the enzyme kinetics book by Segel (1993). $\left(v_{R2} = V_{max}\frac{\frac{S_1}{K_{mS_1}} - \frac{S_2}{K_{mS_2}}}{1+\frac{S_1}{K_{mS_1}}+\frac{S_2}{K_{mS_2}}}\right)$;

[1] Only if the irreversibility of reactions is considered at all: most biochemists now agree that all reactions in metabolism should be considered potentially reversible (Hofmeyr and Cornish-Bowden 1997, Cornish-Bowden and Cárdenas 2001).

5. **Kinetic parameters:** set of values for the various kinetic parameters V_{max}, K_m, K_i, *etc.* These are phenomenological parameters, as opposed to the elementary rate constants k_+, k_-, *etc.* The substrate specifity of an enzyme is expressed by the K_m, and the catalytic efficiency *in vivo* by V_{max}. The number of kinetic parameters depends on the type of rate equation, *e.g.* three parameters in a reversible uni-uni Michaelis-Menten kinetics where one reactant is converted into one product, and six in a reversible bi-bi Michaelis-Menten kinetics where two reactants are converted into two products. Inhibition or activation by effectors, expressed by K_i and K_a, also increase the number of parameters. (V_{max}, K_{mS_1} and K_{mS_2} for $R2$).

2.1.4 Model Variables

The data in a metabolic model consists of two distinct groups, the entirety of system parameters and the system variables. System parameters are: stoichiometric coefficients (item 2 in the previous paragraph), kinetic parameters (item 5 *ibid.*), the concentrations of external metabolites, and any other entities of the model that are assigned a fixed value. The set of variables, on the other hand, is composed of the set of internal metabolite concentrations and the set of reaction rates.

The rates (velocities) v_i of all reactions Each reaction rate is a function of its kinetic parameters, of the concentrations S_i of its substrates, as well as of the concentrations of its effectors (metabolites that inhibit or activate the reaction). The rates change over time until a steady state is reached. They are calculated according to the rate equations, and are variables of the system.

The concentrations S_i of all internal metabolites As explained above (Paragraph 2.1.2), the concentrations of the external metabolites are fixed, their values kept constant throughout any simulation with the model, which is why they are system parameters.

All remaining intermediates, though, are 'internal' metabolites. They are consumed or produced by the reactions in the model. Their concentrations change over time according to the rates of these reactions until a steady state is reached. At steady state they must fulfil a balance equation implying that production equals consumption (see Paragraph 2.1.6) which is why they are sometimes also called 'balanceable'. The concentrations of internal metabolites are system variables.

Model variables, therefore, are 1. the rates (or velocities) v_i of all reactions and 2. the concentrations S_i of all internal metabolites.

2.1.5 Stoichiometry Matrix

The stoichiometry matrix, a mathematical presentation of the structure of a metabolic model, is derived from the list of reactions, using the information from items 1 and 2 of Paragraph 2.1.3 only.

To illustrate the derivation of the stoichiometry matrix, consider the simple biochemical system of three reactions connecting the reactant X_1 and the product X_2 (shown in Figure 2.1) and the appendant list of reactions R (given in Paragraph 2.1.1).

The internal metabolite S_1 is produced by reaction $R1$ with the rate of v_1, and it is consumed by reaction $R2$ with the rate of v_2. Thus, changes in the concentration of S_1 are a function of all reaction rates v_i, and can be expressed in a differential equation as follows:

$$\frac{dS_1}{dt} = 1 \cdot v_1 - 1 \cdot v_2 + 0 \cdot v_3 \tag{2.1}$$

The same relation can be written out for all of the internal metabolites, and combining all (two) equations gives:

$$\begin{pmatrix} \frac{dS_1}{dt} \\ \frac{dS_2}{dt} \end{pmatrix} = \begin{pmatrix} 1 & -1 & 0 \\ 0 & 1 & -1 \end{pmatrix} \begin{pmatrix} v_1 \\ v_2 \\ v_3 \end{pmatrix} \tag{2.2}$$

or in vector notation:

$$\frac{d\boldsymbol{S}}{dt} = \begin{pmatrix} 1 & -1 & 0 \\ 0 & 1 & -1 \end{pmatrix} \boldsymbol{v} \tag{2.3}$$

where $\boldsymbol{S}$ and $\boldsymbol{v}$ denote the vector of metabolite concentrations and the vector of reaction rates, respectively.

The matrix relating $\boldsymbol{S}$ and $\boldsymbol{v}$ is called the stoichiometry matrix. Its elements are the stoichiometric coefficients of all reactions in the reaction list. It is assigned the symbol $\mathbf{N}$, and Equation 2.3 can be reformulated to:

$$\frac{d\boldsymbol{S}}{dt} = \mathbf{N}\boldsymbol{v} \tag{2.4}$$

Equation 2.4, also called balance equation, holds for any network consisting of the reactions v_i and the internal metabolites S_i (Heinrich and Schuster 1996b). $\mathbf{N}$ links the two variable vectors by relating changes in the metabolite concentrations S_i to the reaction rates v_i. For a metabolic network that contains m internal metabolites and n reactions the stoichiometry matrix $\mathbf{N}$ has the dimension $m \times n$.

2.1.6 Steady State

A biochemical system is described as being in a steady state, if the concentrations of all internal metabolites S_i remain constant, *i.e.* they do not change

over time[2].

$$\frac{d\boldsymbol{S}}{dt} = \mathit{0} \tag{2.5}$$

This *steady state condition* is satisfied (combine Equation 2.4 and Equation 2.5) if the vector $\boldsymbol{v}$ of reaction rates v_{i} fulfils the equation:

$$\mathbf{N}\boldsymbol{v} = \mathit{0} \tag{2.6}$$

Equation 2.6 holds for every steady state of the system (Heinrich and Schuster 1996b). The *steady state condition* also is the key assumption for most theoretical analysis.

The entirety of solutions $\boldsymbol{v}$ of Equation 2.6 is the kernel or null space of the stoichiometry matrix $\mathbf{N}$. The columns of the null space matrix $\mathbf{K}$ span the null space (Reder 1988), or:

$$\mathbf{NK} = \mathbf{0} \tag{2.7}$$

2.2 Structural Analysis

2.2.1 Structural Model

According to the above description in Paragraph 2.1.5, every list of biochemical reactions can be represented by a stoichiometry matrix $\mathbf{N}$. Knowledge about the structure or topology of a metabolic network, reflected by its stoichiometry matrix $\mathbf{N}$ and details of its reactions' reversibility are sufficient to build a structural model.

Analysing the structural model, *i.e.* $\mathbf{N}$, one can determine a variety of model properties that could not be found by any other means.

Another advantage of structural analysis is that for the construction of a structural model no information is needed on concentrations of metabolites or on volumes of compartments, nor any knowledge of kinetic parameters of enzymatic or non-enzymatic reactions.

The steady state condition, as given in Equation 2.6, is the premise for some of the concepts in structural modelling but not for all, *e.g.* the conservation relationships hold true at every point in time.

2.2.2 Main Concepts of Structural Analysis

Once the structural model of a metabolic network has been defined, a structural analysis can be carried out on the stoichiometry matrix $\mathbf{N}$. It may detect one or more of the following:

1. **Conserved Moieties** are sets of internal metabolites with a fixed total concentration (Hofmeyr et al. 1986); metabolites that contribute to such a moiety are not free to take on every concentration but are dependent on the concentrations of the other metabolites contributing.

[2]Constancy of rates follows directly, since they are functions of the S_{i}.

2. **Enzyme Subsets** are defined as groups of enzymes that operate jointly in fixed flux proportions at steady state (Pfeiffer et al. 1999).

3. **Elementary Modes** are defined as minimal sets of reactions that can operate at steady state with all irreversible reactions proceeding in the appropriate direction (Schuster and Hilgetag 1994). The concept of elementary flux modes provides a mathematical tool to define and comprehensively describe all metabolic routes that are stoichiometrically feasible for a certain reaction network. Schuster et al. (2002) give an overview, a calculation algorithm and an example for this concept.

Since the principles 1., 2. and 3. are the subjects of examination later on, more details are given in the following three Sections 2.2.3-2.2.5, including explanations of the algorithms used for their calculation/detection, a brief discussion of each principle's usefulness, and some examples.

But the three concepts introduced above are not the only consequences arising out of the structure of a modelled network. Other contributions of structural analysis have been proposed, *e.g.* connectivity of metabolites (Wagner and Fell 2001), minimal cut sets (Klamt and Gilles 2004), Metabolic Flux Analysis (Avignone-Rossa et al. 2002), *etc.*

2.2.3 Conserved Moieties

The relationships defining conserved sums hold at every point in time (whereas the other two principles mentioned above are valid only for a steady state, when it is assumed that the system in question satisfies Equation 2.6).

Conserved moieties are chemical entities participating in a reaction system without loss of integrity and always remaining in the system (Heinrich and Schuster 1996c). This can be expressed in equations, namely the so called conservation relationships. The metabolites contributing to a conservation relationship are not independent but dependent on each other, in that their total concentration is fixed (Hofmeyr et al. 1986). Conservation relationships take the form:

$$\boldsymbol{g}^{\mathrm{T}} S = ConservedSum = \text{const.} \tag{2.8}$$

where a row vector $\boldsymbol{g}^{\mathrm{T}}$ is multiplied with the vector $\boldsymbol{S}$ of metabolite concentrations. Non-zero elements g_j in $\boldsymbol{g}$ ($g_j \neq 0$) cause the corresponding internal metabolite S_j to enter the conservation relationship.

Equation 2.8 written out gives:

$$\sum_j g_j S_j = \text{const.} \tag{2.9}$$

The concentrations S_j do not change independently but are interrelated such that:

$$\sum_j \frac{dS_j}{dt} = 0 \tag{2.10}$$

There are as many different vectors $\boldsymbol{g}$ as there are linearly independent conserved moieties in a network.

Conserved moieties in the network reveal themselves as linear dependencies in the rows of the stoichiometry matrix (see also example below).

Whenever the network exhibits conserved moieties, there will be dependencies among the rows of $\mathbf{N}$, and the rank of $\mathbf{N}$ is less than m, the number of rows of $\mathbf{N}$ ($rank(\mathbf{N}) < m$). The rows of $\mathbf{N}$ can be rearranged so that the top $rank(\mathbf{N})$ rows are linearly independent. The metabolites which correspond to these rows are the independent species, and the remaining $m - rank(\mathbf{N})$ at the bottom of the rearranged matrix are the dependent species.

Often the Gauss-Jordan method is used to identify linear dependencies in the stoichiometry matrix $\mathbf{N}$ and determine the corresponding conserved moieties, see Hofmeyr (1986) for a worked through example, or Sauro and Ingalls (2004) for a recent review.

An example for conserved moieties is the redox couple NAD^+/NADH. NADH is formed when NAD^+ is consumed and *vice versa*. The row for NADH in $\mathbf{N}$ is dependent on the row for NAD^+, it is exactly its negative.

If the vector of metabolite concentrations $\boldsymbol{S}$ is sorted such that NAD^+ and NADH are positioned at the top, the general representation of conservation relationships (according to Equation 2.8) reads:

$$\begin{pmatrix} 1 & 1 & 0 & \dots \end{pmatrix} \begin{pmatrix} NAD^+ \\ NADH \\ \vdots \end{pmatrix} = SumNADs = \text{const.} \tag{2.11}$$

Or written out as a conserved sum:

$$[NAD^+] + [NADH] = \text{const.} \tag{2.12}$$

Also, observe:

$$\frac{d[NAD^+]}{dt} + \frac{[NADH]}{dt} = 0 \tag{2.13}$$

and

$$\frac{d[NAD^+]}{dt} = -\frac{[NADH]}{dt} \tag{2.14}$$

This last equation again reflects that the row for NADH is exactly the negative of the row for NAD^+ in $\mathbf{N}$.

2.2.4 Enzyme Subsets

The network structure frequently implies that the interplay of enzymes is so tight that several enzymes always operate together, *i.e* there is only one independent flux going through this set. Such sets are called enzyme subsets. The concept was first introduced by Pfeiffer et al. (1999), and these authors defined enzyme subsets as groups of enzymes that operate together in fixed flux proportions in all steady states of a system. This definition has been extended herein to 'groups of reactions' in order to include transport processes.

The reactions found to be in an enzyme subset always occur simultaneously and with an unchanged ratio in every steady state or in every elementary mode. Note that the reactions do not have to be connected. They can occur anywhere in the metabolic network, and can form a non-adjacent set.

Enzyme subsets are herein sorted into the following categories:

i enzyme subset of all 'dead' reactions;
One single enzyme subset is formed by all 'dead' reactions. Because strictly balanced or 'dead' reactions do not carry any flux in the steady state their fixed flux proportion is zero. Thus, they all appear in one subset. Strictly balanced or 'dead' reactions were first reported by Schuster and Schuster (1991).

ii trivial enzyme subsets with exactly one (independent) reaction;
Many 'subsets' consist of exactly one reaction. These reactions are not considered as enzyme subsets hereafter.

iii proper enzyme subsets with $\geq$2 members.

A group of reactions is an enzyme subset if for any two members Ri and Rj of the set the following two conditions are fulfilled: in all flux vectors $\boldsymbol{v}$ satisfying the steady state condition (Equation 2.6) the ratio v_i/v_j has the same value and the orientations of the irreversible reactions involved do not contradict each other (Pfeiffer et al. 1999).

From the properties of the null space of $\mathbf{N}$ (see Paragraph 2.1.6), it follows immediately that this condition can alternatively be written as follows: in all column vectors $\boldsymbol{k}$ of the kernel $\mathbf{K}$ of $\mathbf{N}$, the ratio of the elements k_i/k_j has the same value. This leads to an algorithm for detecting the enzyme subsets that was developed and first implemented by Pfeiffer et al. (1999):
1. Detect all row vectors of $\mathbf{K}$ that are null vectors.
2. Normalise each of the remaining row vectors of $\mathbf{K}$ by dividing by its greatest common divisor.
3. Compare any normalised row vector with any other. If they are the same and there are no contradictions in the directionalities of irreversible reactions,

the corresponding reactions belong to the same subset. The quotient of the normalisation factors gives the flux ratios.

All 'dead' reactions appear to have the same pattern of usage over all elementary modes, their corresponding row vector in the null space matrix **K** of **N** is a null vector. Such a set of 'dead' reactions was first reported by Schuster and Schuster (1991) as a 'strictly detailed balanced subnetwork'.

Suggested roles *in vivo* for enzyme subsets are that they might be functional units in terms of regulation of metabolism, performing coordinated metabolic regulation.

Schuster et al. (2002) found a correlation between relative change in gene expression upon the diauxic shift in yeast and enzyme subsets of yeast central metabolism.

Reed and Palsson (2004) investigated an *E.coli* genome-scale model. They found that sets of reactions that are always used together in optimal solutions (*i.e.* enzyme subsets) showed moderate agreement with the currently known transcriptional regulatory structure in *E.coli* and available expression data.

For bacteria a connection between enzyme subsets and operons has been proposed (work in progress, by Bhushan Bonde).

Furthermore, the detection of enzyme subsets is very useful for model reduction; by lumping all reactions of an enzyme subset into one lumped reaction the stoichiometry matrix **N** can often be condensed considerably. This reduction in complexity may facilitate the structural analysis just by minimising the numerical cost, *i.e.* by shortening the computation time for the decomposition in elementary modes.

Side note: enzyme subsets are related to *monofunctional units* as introduced by Rohwer et al. (1996) (but monofunctional units or 'super-enzymes' have even more restrictions, they are a principle from control analysis and control everything outside in a coherent way), and to *activity sets* (Nuno et al. 1997).

2.2.5 Elementary Modes

Provided that the system in question satisfies the steady state condition, a calculation of elementary modes is possible. The concept of elementary modes arose from the quest for all admissable steady state fluxes (vectors $\boldsymbol{v}$) of a given system (Heinrich and Schuster 1996c).

A *mode* of a system is a relative flux distribution that fulfils the steady state condition for intermediates and the sign restriction for irreversible reactions (first mentioned as *fundamental modes* by Leiser and Blum (1985), and

Fell (1990), and then as *elementary modes* by Schuster and Hilgetag (1994)). In other words, it is a solution $\boldsymbol{v}$ of Equation 2.6 ($\mathbf{N}\boldsymbol{v} = \boldsymbol{0}$) that has valid elements only (*i.e.* no negative fluxes where only positive ones are allowed because of irreversibility).

Modes are called *elementary* if they are nondecomposable (Heinrich and Schuster 1996c), *i.e.* if no reaction can be removed from the mode without violating the steady state condition. No proper subset of the set of reactions of an elementary mode is able to realise a mode.

A calculation procedure for the computation of elementary modes has been given by Schuster et al. (2002). It is an algorithm based on tableaus. It uses linear algebra to find the unique decomposition of the stoichiometry matrix $\mathbf{N}$ into elementary modes. The algorithm was sketched earlier in Schuster and Schuster (1993), Schuster and Hilgetag (1994) and then in Pfeiffer et al. (1999); but Schuster et al. (2002) describe and validate it, by proving that it exclusively generates all the elementary flux modes of an arbitrary network.

Elementary modes are distinct from extreme pathways (defined by Schilling et al. 2000) in that extreme pathways are a subset of elementary modes. For a comparison of these two principles see Klamt and Stelling (2003).

Each elementary mode (sometimes also called 'component pathway' or 'direct reaction route'[3] or even 'extremal current'[4]) has an overall or net reaction with the consumption and production of external metabolites. If no external metabolites are consumed nor produced, then the elementary flux mode is an internal cycle.

Elementary flux modes correspond to different basic functions a biochemical system is able to fulfil, *i.e.* functions that are stoichiometrically possible. The decomposition of a reaction network into elementary flux modes provides a complete list of all these functions, thereby revealing the diversity and functional richness of a network (Heinrich and Schuster 1996c).

But how can this diversity (in form of the list of all elementary modes) be explored?

One way is to investigate the number of modes employing a certain reaction. Relative frequency of a reaction might indicate *e.g.* the importance or even essentiality of an enzymatic reaction, or demonstrate the requirement for a certain transporter in enabling various metabolic pathways. Moreover, the incidence of elementary modes with identical overall net reactions is a measure

[3]But this term is misleading because the route from consumed to produced metabolite does not have to be 'direct' at all; it only must be balanced.

[4]Sometimes a similar concept is found in other fields, *e.g.* in chemistry or engineering.

of redundance in metabolism.

Testing the robustness of a network confronted to gene-knockouts or other gene mutations (by removing of reaction(s) or by introducing new ones) or to environmental changes and stress (by changing the set of external metabolites) is another way.

It is maybe beneficial to note that the elementary flux modes are *potential* metabolic routes. *In vivo*, some modes might not be used at all, others might be dominant in particular tissues and give them their specificity. Or else, there might be a correspondence between elementary modes and different physiological functions of one and the same tissue. (The cellular phenotype is characterised by the set of all molecular fluxes, also called the fluxome.)

All flux distributions of a metabolic network that are possible at steady state are linear combinations (or superpositions) of the fluxes carried by elementary modes. The appropriate assignment of actual flux values to the elementary modes (in order to agree with the observed metabolic fluxes) is an issue that was solved only very recently by Poolman et al. (2004).

Over the last years, elementary mode analysis has been applied successfully, for instance in bioengineering (*e.g.* Schuster et al. 2002, Carlson et al. 2002 and Carlson and Srienc 2004) or in functional genomics (for assigning functions to orphan genes).

Schuster et al. (2002): reported on the use of elementary mode analysis to maximise the synthesis of cyclooctadepsipeptides PF1022 in the fungus *Mycelia sterilia*;

Carlson et al. (2002): used elementary mode analysis to investigate possible effects of biochemical network modifications and altered culturing conditions, in order to optimise poly-beta-hydroxybutyrate (PHB) production in recombinant yeast;

Poolman et al. (2003): investigated and compared dark/light metabolism in a model of Calvin-cycle and oxidative pentose phosphate pathway (OPPP) by means of elementary modes;

Carlson and Srienc (2004): described the prediction of unique pathways in *E.coli* for efficient conversion of glucose and O_2 into new cells and maintenance energy under different growth conditions, plus reported the agreement of predictions with experimental observations and the complete determination of all metabolic fluxes.

2.2.6 Realisation of Structural Analysis

As noted, conserved moieties, enzyme subsets and elementary modes can be calculated from a given stoichiometry matrix **N**. But for metabolic networks with many reactions this matrix is large; the structural analysis becomes exceedingly

extensive and can only be performed using the aid of the computer[5].

In this thesis, the structural analysis was carried out using the software package *ScrumPy* that consists of *Python* modules especially developed for the tasks of metabolic modelling.

The *ScrumPy* method `.ConsMoieties()` uses the Gauss-Jordan algorithm (see Paragraph 2.2.3) for the calculation of conservation relationships; enzyme subset detection (`.EnzSubsets()`) is performed by a shortened version of the algorithm described in Paragraph 2.2.4, in which the normalisation step is skipped; and for the computation of elementary modes, the method `.ConsElModes()` of *ScrumPy* uses the procedure as provided by Schuster et al. (2002).

2.3 Kinetic Modelling

2.3.1 Kinetic Models of Metabolism

Kinetic models are the model type best known to most biochemists. Kinetic modelling deals with the changes in substance concentrations over time as a result of biochemical reactions. The dynamics of a whole network of biochemical reactions is often described mathematically by a system of ordinary differential equations (ODE's).

These differential equations involve reaction rates, linear or non-linear expressions, also called 'rate equations'. The rate equations comprise numerous kinetic parameters, *e.g.* in Michaelis-Menten kinetics these are catalytic activities, Michaelis constants, inhibition constants, *etc.*

Given a complete set of rate equations and kinetic parameters, a full kinetic model of the system can be built. With a full kinetic model time course simulations can be performed, the steady state(s) of the system can be numerically calculated, the impact of pertubations on the steady state(s) be determined, a variety of scenarios can be simulated and, generally, multiple problems be addressed.

The number of parameters, and therewith the dimension of the parameter space of a kinetic model, increases linearly with the number of reactions included. For instance, a metabolic model containing 20 bi-bi-reactions is equipped with over 100 parameters. This is before consideration of any kind of inhibition or any other effectors.

[5]Nevertheless, for larger genome-scale metabolic models (biochemical reaction networks derived from an organism's genome sequence), as already reported for some microorganisms, the computation of elementary modes still meets with the problem of combinatorial explosion. For instance, most recent studies of *E.coli* use stoichiometry matrices containing 537 metabolites and 739 reactions (Almaas et al. 2004). Such systems actually represent an upper limit to what can be solved by conventional algorithms within reasonable time. Fortunately, combinatorial explosion does not manifest a problem for the model of potato tuber carbohydrate metabolism presented here that contains 30 reactions.

In cases where reaction mechanisms are unknown or not all of the kinetic parameters have yet been determined an incomplete kinetic model can be built. There are ways of analysing such incomplete kinetic models.

One possibility is to use the matrix method of Metabolic Control Analysis (applied *e.g.* by Thomas et al. 1997b, see also page 39).

Another application, positioned in the area between structural and kinetic modelling, is Metabolic Flux Analysis (MFA). It can be employed to alleviate the stoichiometric constraints of biosynthesis. An example for a successful application of MFA is the optimisation of production of antibiotics in *Streptomyces lividans* by Avignone-Rossa et al. (2002).

2.3.2 Numerical Steady State

Initialisation

Before any kinetic calculations can be made the variables in the model have to be initialised, or, to be more precise, only the metabolite concentrations.

The initial rates are determined by subsequent evaluation of the rate equations with kinetic parameters and initial metabolite concentrations, according to the rate equations as stated in the model. In other words, the rates are the dependent variables, and can be computed from the independent variables, the metabolite concentrations.

Numerical calculation of steady state

The steady state is defined as a state in which the reaction rates are such that all metabolite concentrations are balanced and do not change in time. Equation 2.6 gives the mathematical representation of this statement.

Unlike an analytical steady state, a numerical steady state cannot be calculated directly.

It is either found by simulation to the steady state, *i.e.* the numerical steady state is approached when the changes in all variables (reaction rates and concentrations of internal metabolites, see Paragraph 2.1.4) become very small, move below a chosen limit/threshold value, or become virtually zero (non-asymptotical steady states cannot be detected).

Or, it is found by iterative methods, such as the Newton's method, in which the set of non-linear equations (obtained by setting the set of ODE's the kinetic model consists of equal to zero) is numerically solved.

The position of the steady state is determined by the network structure, the kinetic type of each involved reaction (exhibiting linear, hyperbolic or sigmoidal kinetics, being reversible or irreversible, *etc.*), and all kinetic parameters.

A metabolic model might have more than one steady state.

2.3.3 Metabolic Control Analysis

In Metabolic Control Analysis (MCA) a number of control coefficients are defined, which quantify the response of metabolic systems to perturbations (Kacser and Burns 1973, Heinrich and Rapoport 1974). More recent overviews were published by Kacser et al. 1995, Heinrich and Schuster 1996a and Fell 1997.

Elasticity Analysis

All parameters of the model can be tested for their immediate influence on the reaction rates. Some parameters have hardly any influence, *i.e.* they can be changed greatly up or down with only minor effect. Other parameters are very important, in that the rate is very sensitive to changes in them.

To test how sensitive the rate equations are locally towards [a] deviations in their kinetic parameters or [b] deviations in the concentrations of their substrates, so called elasticity coefficients have been defined (Kacser and Burns 1973, Heinrich and Rapoport 1974). It is distinguished between π-elasticities and ε-elasticities according to [a] and [b].

The defininition of π-elasticities reads:

$$\pi_j^i = \frac{p_j}{v_i}\frac{\delta v_i}{\delta p_j}$$

where v_i is a flux through one of the reaction and p_j is a parameter of the system. The π-elasticities are the scaled first derivative of an instantaneous reaction rate (or flux) against a kinetic parameter.

The ε-elasticities defined as follows:

$$\varepsilon_j^i = \frac{S_j}{v_i}\frac{\delta v_i}{\delta S_j}$$

where v_i is a flux through one reaction and S_j is a metabolite. The ε-elasticities are the scaled first derivative of an instantaneous reaction rate (or flux) against a metabolite concentration.

The elasticities can be arranged in a matrix, $\boldsymbol{\varepsilon}$ or $\boldsymbol{\pi}$, respectively. The elements of these matrices can be obtained either experimentally or by derivation from known rate equations (Heinrich and Schuster 1996a).

Control Coefficients

The coefficients of Metabolic Control Analysis are defined as the scaled first derivative of some quantity against another. A good overview over the algebraic framework of MCA is given by Heinrich and Schuster (1998) and Hofmeyr (2001).

Flux control coefficients (C_v^J) are the scaled first derivative of a rate v_j (enzyme activity) against the steady state flux J_i.

$$C_{v_j}^{J_i} = \frac{v_j}{J_i}\frac{\delta J_i}{\delta v_j}$$

By calculating all flux control coefficients the reactions of the model can be inspected for their influence on the outcome, the steady state flux.

Concentration control coefficients (C_v^S) are the scaled first derivative of an enzyme activity against a steady-state metabolite concentration.

$$C_{v_j}^{S_i} = \frac{v_j}{S_i}\frac{\delta S_i}{\delta v_j}$$

By calculating all concentration control coefficients the reactions of the model can be examined for their influence on the outcome, the steady state metabolite concentrations. Generally, the C_v^S have much larger ranges of values than the C_v^J (Fell 2004).

It is also possible to evaluate control coefficients from the set of elasticities using the matrix method (Sauro et al. 1987). This has been done with experimental data of metabolite concentrations in potato tuber (Thomas et al. 1997b).

2.3.4 Dynamic Simulations

A modelled system does not have to reach a steady state (*e.g.* oscillations or chaos) or it can do so slowly. Meanwhile, its dynamics can be studied by performing time course simulations. The time-dependent behaviour of the model, *i.e.* changes in metabolite concentrations or changes in metabolic fluxes, can be explored.

The dynamics of a metabolic model, such as the one dealt with herein, are determined by (a) the network structure, (b) the (initial) concentrations of all metabolites (internal and external), (c) the kinetic type of each reaction, and (d) the set of kinetic parameters.

2.3.5 Realisation of Structural Analysis

In *ScrumPy* several methods are provided for kinetic modelling.

Time course simulations can be performed by means of the method `.Simulate()` in which the overall simulation time is settable.

`.FindSS()` uses the Newton's method to attempt a steady state evaluation of the model.

The `.ScaledSensits()` method is very versatile, it can be modified to calculate any of the above described coefficients of Metabolic Control Analysis.

Chapter 3

Metabolites and Reactions of Central Carbohydrate Metabolism

This chapter's focus is on the reactions and intermediate metabolites of central carbohydrate metabolism in cells of the non-photosynthetic storage tissue of potato tubers. The present knowledge, according to published plant science literature and databases (*e.g.* BRENDA database 2004 or MetaCyc database 2004), is reviewed here, in order to provide the necessary information for assembling a metabolic model of this biological system.

Two compartments, cytosol and amyloplast, are considered. The metabolites are dealt with first (Section 3.1), followed by the reactions (Section 3.2) covering enzymatically catalysed reactions as well as transport processes.

3.1 Principal Metabolites

3.1.1 Starch

Starch is an end product of carbon fixation by photosynthesis and a reservoir for metabolic energy. It is found practically in all types of plant tissue as the means of storage for D-glucose. It is synthesised and stored in the plastids. In the chloroplasts of photosynthetic cells starch functions as a temporary store of energy and carbon. The amyloplasts of non-photosynthetic cells are specialised in starch synthesis and long-term storage.

Starch can be broken down rapidly to provide energy (by respiration) and/or building blocks for new growth. It is just one of the storage polysaccharides of plants but its adavantage is that it can be stored in large amounts because of its negligible osmotic pressure (only one single reducing end group in the center or 'hilum'), *e.g.* fructans lower the freezing point of sap and are osmotically active (Sivak and Preiss 1998).

Starch granules consists of two major components, the polymers amylose

and amylopectin (≈ 30% and 70%). Amylose is essentially linear and consists of helices of ≈1500 glucosyl units. Amylopectin is highly branched with 20-25 units average chain length (Sivak and Preiss 1998). The highly ordered and dense packing of glucan chains is organised in a large insoluble (semicrystalline) granule. For reviews of starch structure see *e.g.* Preiss 1982, Martin and Smith 1995 or Kossmann and Lloyd 2000.

The review by Ellis et al. 1998 is concerned with the industrial uses, origins and structure of starch. Two thirds of agriculturally produced starch is utilised as food or feed stuff, one third is employed in a variety of industrial purposes that take advantage of its unique properties (Sivak and Preiss 1998). Other sources of starch besides potato tubers are: fruits or seeds (*e.g.* banana, plantain, rice, wheat, pea, corn) and starchy roots (*e.g.* yam, sweet potato). In storage tubers and roots the percentage of starch can be 65-90% of the dry weight, this being the result of 8-30 weeks of starch deposition (Sivak and Preiss 1998).

Starch granules also contain small amounts of phosphate (Burrell 2003).In potato, phosphorus is esterified to certain glucose residues in amylopectin (G6P-residues). The degree of the phosphorylation of starch in potato tubers has been investigated by Nielsen et al. 1994, who found 0.5% of the glucose residues of starch to be phosphorylated. So, only for about 200 glucosyl units added to the polysaccharide (or removed), one molecule of phosphorus will be removed (or released) from the plastids phosphate pool. Therefore, the phosphorylation of starch itself is negligible in this modelling context.

3.1.2 Hexose Phosphates

The various subparts of carbohydrate metabolism, starch turnover (starch formation and degradation), sucrose metabolism (sucroneogenesis and sucrose breakdown), glycolytic pathway, gluconeogenesis and pentose phosphate pathway are all arranged around the hexose phosphate pool.

Glucose 1-phosphate (G1P), glucose 6-phosphate (G6P) and fructose 6-phosphate (F6P) take a central position in the carbohydrate metabolism of plants.

The various flows into and out of the pool containing these three hexose phosphates are schematically summarised in Figure 3.1.

It is known that both compartments have the enzymic capacity to metabolise hexose phosphates. This rises the question whether there are two independant pools or whether the hexose phosphate concentrations are balanced so that there is just one single pool of hexose phosphates?

For photosynthetic tissue the existence of independent hexose phosphate pools in the plastids and the cytosol has been shown Stitt 1997. Although it remains uncertain for non-photosynthetic tissue, the observed ability of amyloplast membranes to import G6P or G1P (Schott et al. 1995) suggests that

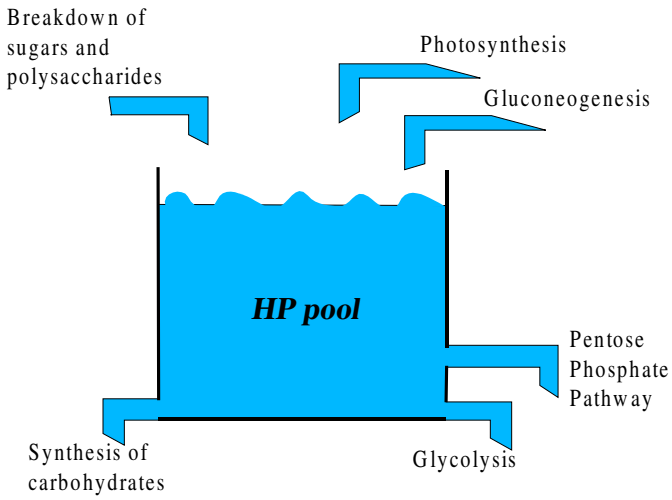

Figure 3.1: The hexose phosphate pool.
Hexose phosphates are **a)** derived from triosephosphates which are formed during photosynthesis and gluconeogenesis or **b)** products of the cleavage of sucrose or of the hydrolysis of starch. The synthesis of these two carbohydrates in contrast constitutes part of the flow out of the hexose phosphate pool. The glycolytic and the pentose phosphate pathway also reduce the amount of hexose phosphates.

there is a direct link between the two pools of intermediates.

Long-time experimental difficulties (Wischmann et al. 1999) have overcome by a new technique that allows the measurement of metabolite concentrations within different compartments (Farré et al. 2001). Farré et al. 2001 circumvent difficulties with purification of amyloplasts by using electron photographs and the principle of Delesse. This will be explained further in Section 4.1.7.

3.1.3 Sucrose

Sucrose, the nonreducing disaccharide of D-glucose and D-fructose, is universal in plants and fulfils many roles: as a transport sugar (A), as a storage reserve (B), as a signal compound (C) and as a compatible solute (D). Consequently, sucrose synthesis is highly regulated (Lunn and MacRae 2003).

A: Sucrose and its derivatives represent the major transport forms of photosynthetically assimilated carbon in plants. Sucrose synthesized in green leaves is exported via the phloem, the long-distance distribution network for assimilates, to supply nonphotosynthetic organs with energy and carbon resources (Oparka 1986). Sucrose not only functions as a transport metabolite but also contributes to the osmotic driving force for phloem translocation (mass flow).

B: Sucrose can function as a storage reserve, *e.g.* in sugarcane. Sucrose accumulation in certain fruits and vegetables is responsible for their sweetening just prior to harvest (ripening). In fact, sucrose content is often one of the major determinants of fruit quality. Interestingly, the sucrose that accumulates in fruit tissues is not simply received from leaves but is actually synthesized within the fruit itself.

C: Sucrose serves as a signal to activate or repress specific genes in a variety of different tissues. As a signal molecule it controls glycolysis and respiration through carbohydrate-modulated gene expression (Koch 1996).

D: Finally, in potato tuber metabolism, sucrose plays the role of a compatible solute.

Sucrose is the major carbohydrate translocated to potato tubers. It is transported from the green photosynthesising parts of the plant to the tuber, constituting its main source of carbon for polysaccharide synthesis and respiration (carbohydrate metabolism). It enters the tuber cells, and is metabolised in the cytosol to hexose phosphates which can be imported into the amyloplast, the site of starch synthesis and accumulation. Sucrose provides the starting point for sucrose-starch-conversion.

Sucrose is found mainly in cytosol and vacuoles, excluded from plastids or mitochondria (Heldt and Sauer 1971)

3.1.4 Reducing Sugars

Sugars play a multifold role in plants. They function as intermediate metabolites, as sink metabolites (*e.g.* fructose in apples and many other fruits), as transport metabolites, they regulate the cellular osmotic potential, and they act as signal molecules. Gene expression is regulated in response to sugar status via sugar-sensing mechanisms (*e.g.* HXK-triggered signals (Koch 1996 and Jang et al. 1997).

Fructose is a product of sucrose degradation, either by invertase or by the reversible reaction of sucrose synthase. Simultaneously, it is a reactant for sucrose biosynthesis, again by sucrose synthase activity. It can also be phosphorylated by fructokinase and by hexokinase.

After 10 days in cold storage at 4°C, fructose levels in tubers start to increase (Hill et al. 1996).

Glucose is the other product of sucrose degradation by invertase. It is also one end product of amylolytic degradation of starch. It can be phosphorylated by hexokinase. After 10 days of tuber storage at 4°C, glucose levels start to increase (Hill et al. 1996).

Maltose Maltose is the third reducing sugar. It is one of the products of starch degradation by α-amylase and β-amylase. Unfortuately, no concentrations were measured or provided by any of the papers consulted. It was not considered in the model.

3.1.5 Sugar Nucleotides

Adenosine diphosphoryl glucose (ADPG) was discovered and investigated by Leloir and collegues in the middle of the last century (Recondo and Leloir 1961). It is formed from G1P in a reaction catalysed by ADP-glucose pyrophosphorylase. The main, if not the sole, function of ADPG in plant cells is as a precursor of the glucosyl residues in starch (Preiss 1973). ADP-glucose was found to be exclusively located in the amyloplast (Farré et al. 2001).

Uridine diphosphate glucose (UDPG) in potato tuber is involved in sucrose metabolism. It is a substrate for the reactions catalysed by UDP-glucose pyrophosphorylase (UGPase) and sucrose synthase (SuSy). Depending on the direction these two proceed in, UDPG is either contributing to sucrose degradation or to sucrose biosynthesis. It is also substrate for sucrose phosphate synthase (SPS) which catalyses the formation of sucrose 6-phosphate (S6P).

F6P + UDP-glucose $\leftrightarrow$ S6P + UDP

Furthermore, UDP-glucose is a precursor for cellulose biosynthesis:

UDP-glucose + (1,4-alpha-D-glucosyl)$_n$ $\leftrightarrow$ UDP + (1,4-alpha-D-glucosyl)$_{n+1}$

catalysed by cellulose synthase, and it is involved in galactose metabolism and trehalose biosynthesis.

It does not play a major role in starch synthesis, as it was shown by Recondo and Leloir (1961) that ADPG was 10-fold more active than UDPG in the transfer of glucose from the sugar nucleotide to the starch granule.

UDPG is usually considered cytosolic only. The high concentrations of UDPG in the amyloplastid fraction (data not shown) measured by Farré et al. (2001), these authors explain by comigration of cell wall fractions with the amyloplastid fraction.

3.1.6 Nucleotides

The "currency metabolites" ATP, ADP, AMP, UTP and UDP are the most ubiquitous intermediates in metabolism, found in every cell. In the section of carbon metabolism investigated here, they are involved in several kinase reactions as well as in the formation of precursors such as ADPG and UDPG.

ATP and UTP or ADP and UDP can be readily interconverted into each other by the equilibrating activity of nucleoside diphosphokinase (NDPK).

Any other contributions to metabolic pathways in potato central carbohydrate metabolism are listed below.

UTP and UDP: Uridine-5'-triphosphate or, shorter, UTP, is involved in the reversible formation of UDPG from G6P by the UDP-glucose pyrophosphorylase reaction (UGPase).

Uridine diphosphate or, shorter, UDP, is involved in the reversible synthesis of sucrose from fructose by sucrose synthase (SuSy) and in the synthesis of sucrose 6-phosphate (S6P) from F6P by sucrose phosphate synthase (SPP). The latter one is considered virtually irreversible because of the channeling of S6P and immediate removal by sucrose phosphate phosphatase (SPP).

UTP and UDP are usually considered cytosolic only. Measured high concentrations of uridine phosphates in the amyloplastid fraction (Farré et al. 2001) were explained by the authors with a comigration of cell wall fractions with the amyloplastid fraction.

ATP and ADP: Adenosine-5'-triphosphate (ATP) and adenosine diphosphate (ADP) occur in both the cytosol and the amyloplast, forming two separate pools each, a cytosolic and a plastidic pool. It is known that translocation between the two pools is mediated by an ATP/ADP-translocator (AATP) Tjaden et al. 1998

AMP: Adenosine monophosphate (AMP) inhibits AGPase allosterically but less effective than orthophosphate (Sowokinos and Preiss 1982).

AMP concentration usually are smaller than ADP concentration (*e.g.* in phloem sap of *R.communis* according to Geigenberger et al. 1993). AMP, ADP, ATP are equlibrated by the swift action of the adenylate kinase (AK) reaction: 2 ADP $\longleftrightarrow$ ATP + AMP

3.1.7 Triose Phosphates

Triose phosphates are the corresponding phosphates to trioses, short chain sugars of the length three.

Dihydroxy-acetone-phosphate (DHAP) and Glyceraldehyde-3-phosphate (GAP) are metabolised in two reactions of glycolysis: cleavage of fructose-1,6-bisphosphate (F16BP) catalysed by aldolase and action of triose phosphate isomerase (TPI).

In order to balance the concentration of DHAP, aldolase and TPI must operate at the same rate.

GAP is also the substrate for the next step in glycolysis, the dehydrogenation of GAP by GAPDH.

Because of the toxicity of the three-carbon sugars glyceraldehyde and dihydroxy acetone, it is probably important that the steady state cellular concentrations of dihydroxyacetone phosphate and 3-phosphoglyceraldehyde be kept low.

1,3-phosphoglycerate (1,3-BPGA) is not considered in the model. It is hidden inside the lumped reaction of GAPDH and PGK. 1,3-BPGA has probably very low concentration, since the concentration of GAP is rather low and K_{eq} of phosphoglycerate kinase (3-PGA/1,3-PGA) has a very high value of 3448.

3-phosphoglycerate (3-PGA) is metabolised by two enzymes of the glycolytic pathway, phosphoglycerate kinase and phosphoglycerate mutase.

3-PGA is an important and potent activator of ADP-glucose pyrophosphorylase (AGPase). It is found in amyloplasts at slightly higher concentration than in cytosol (Farré et al. 2000). It is transported across the amyploplast membrane by a phosphate translocator, either in exchange for P_i or for G6P. But no triose phosphate/phosphate translocator (TPT) was found in the amyloplast membrane (Riesmeier et al. 1993, Fischer et al. 1997). So it was assumed that 3-PGA is translocated by the hexosephosphate/phosphate translocator (GPT), *i.e.* in exchange with G6P (GPT can exchange G6P against orthophosphate or against triose phosphates Flügge et al. 2003).

2-phosphoglycerate (2-PGA) is metabolised in two reactions of the glycolytic sequence: interconversion to 3-PGA by phosphoglycerate mutase (PGlyM), and to phosphoenolpyruvate by enolase.

PGlyM and enolase must operate in a concerted manner in order to balance the concentration of 2-PGA.

Phosphoenolpyruvate (PEP), the product of the enolase reaction, and the reactant for pyruvate kinase, is an important effector of ATP-dependent phosphofructokinase (PFK). This feedback inhibition of glycolytic flux (with PEP, one of its late products regulating the first step) is long known and caused much interest, *e.g.* in the field of control theory (see Thomas et al. 1997aa and Thomas et al. 1997bb).

3.1.8 Pyruvate

Pyruvate is the product of dephosphorylation of phosphoenolpyruvate via pyruvate kinase. Besides taking part in glycolysis, pyruvate is involved in numerous other pathways in the cellular metabolism, such as gluconeogenesis, reductive tricarboxylic acid cycle (TCA), amino acid biosynthesis (*e.g.* lysine, isoleucine, valine *etc.*), amino acid degradation (*e.g.* serine), aerobic respiration, *etc.*

3.1.9 Inorganic Phosphates

Free inorganic phosphates come in two forms, as orthophosphate (P_i) or as pyrophosphate (PP_i).

3.1.9.1 Orthophosphate (P_i)

P_i is formed by hydrolysis of S6P or PP_i. It is utilised by starch degradation via starch phosphorylase, by PP_i-dependent F6P-phosphorylating activity of PFP, and by dehydrogenation of GAP. P_i can be translocated between the two compartments cytosol and lastid via phosphate translocators in exchange with G6P for instance Kammerer et al. 1998.

3.1.9.2 Pyrophosphate (PP_i)

Pyrophosphate is involved in many reactions. Inorganic pyrophosphatase (PPase) removes PP_i by hydrolysis but removal of PP_i can also be achieved by conserving the free energy of the phosphoanhydride bond of PP_i in phosphorylated metabolites. In the cytosol, two soluble enzymes (UGPase and PFP) use PP_i as a substrate in such energy-conserving reactions. These two reactions plus AGPase can also produce PP_i.

There is no PPase in potato tuber cytosol, only in the amyloplast (Sweetlove et al. 1996a, Farré et al. 2001). Plant tissues are remarkably rich in pyrophosphate, which is essentially limited to the cytosolic compartment (*e.g.* Weiner et al. 1987). The values estimated by Farré et al. 2001 and Tiessen et al. 2002 are, for cytosol and amyloplasts, respectively: 23μM/3μM and 12μM/2.4μM (attached tuber) and 7μM/1μM (detached tuber).

The physiological importance of the cytosolic PP_i pool is substantiated by the observation that expression of a soluble inorganic pyrophosphatase of bacterial origin in the cytosol of transgenic tobacco and potato plants leads to significant alterations in metabolism, growth, and development (Jelitto et al. 1992; Sonnewald 1992), whereas overexpression of pyrophosphatase leads to increased sucrose degradation and starch synthesis, increased activities of enzymes for sucrose-starch interconversions, and increased levels of nucleotides in growing tubers (Geigenberger et al. 1998).

3.1.10 Other Metabolites

Sucrose 6-phosphate (S6P) is an intermediate of sucrose metabolism. No concentration for S6P were given in any of the papers and literature consulted. It is most probably channeled from SPS to SPP (Echeverria et al. 1997), and does not seem to be play a major role anywhere else in metabolism (MetaCyc database 2004).

Fructose 2,6-phosphate (F26BP) Although there is evidence that Fru-2,6-P2 is an important factor in the regulation of photosynthetic carbon metabolism in potato leaves, the direct influence of Fru-2,6-P2 on tuber metabolism is limited (Rung et al. 2004).

Redox couple NAD^+/NADH NADH is formed by the GAPDH reaction from NAD^+. GAPDH oxidises NAD^+ to form NADH. Malate dehydrogenase reduces NADH. It works at mole fractions ($NAD^+/(NAD^+ + NADH)) > 0.9$ only (Amthor 2000). A ratio of NAD^+:NADH between 5 and 25 for soybean seeds was mentioned (Quebedeaux 1981), and in other places it is just said to be 'high'.

3.2 Reactions: Enzymes and Transporters

The reactions are sorted after their occurance and action along the pathway of starch degradation and conversion into sugar and subsequently into pyruvate.

3.2.1 Enzymes Located in the Amyloplast

A considerable part of the carbon metabolism of potato tuber cells takes place in specialised organelles, the achlorophyllous amyloplasts. The amyloplast is the site of starch synthesis from glucosyl units, the site of storage of starch granules, and the site of starch degradation. Large quantities of starch can be synthesised and deposited. The enzymatic reactions responsible for these processes are described in this section.

Starch metabolism is characterised by the triangle formed by ADP-glucose pyrophosphorylase (AGPase), starch synthase (StSynth) and starch phosphorylase (StPase), connecting at the edges glucose 1-phosphate (G1P), ADP-glucose (ADPG) and starch (see Preiss 1982). Starch net biosynthesis, as well as starch turnover, are defined by the combination of these three plus amylolytic degradation.

3.2.1.1 Amylolytic degradation of starch - E_1

The glycosidic linkage is one of the most stable bonds found in natural polymers but a class of enzymes, the glycoside hydrolases (E.C. 3.2.1.-), catalyse the hydrolysis of the glycosidic bond (Yip and Withers 2004).

The amylolytic degradation of starch in the potato amyloplast is the result of the activity of several enzymes. In some way involved are: α-amylase and β-amylase (EC 3.2.1.1), alpha-glucosidase (EC 3.2.1.20), debranching enzyme or isoamylase (EC 3.2.1.68), and disproportionating enzyme (EC 2.4.1.25) or D-enzyme. For other plants also involvement of pullulanase (EC 3.2.1.41) has been reported.

α-amylase and β-amylase acting on starch results in maltodextrins and maltose, whereas amylase and disproportioning enzyme results in glucose.

For the model only a summary equation of all these different activities, namely the successive removal of glucose from starch, is considered (see also Maltose on page 44):

$(\text{glucan})_n + H_2O \longrightarrow (\text{glucan})_{n-1} + \text{Glucose}$

A very simple rate equation with just some product inhibition by glucose has been incorporated in the model, see page 162 for the formula.

The cold-induced expression of a new isoform of α-amylase has been described by several groups (Hill et al. 1996, Nielsen et al. 1997 and Deiting et al. 1998). Measurements conducted in the course of this project also showed an increase of total amylolytic activity during the first weeks of storage at 6°C (see Section 6.3 for these values).

3.2.1.2 Starch phosphorylase (EC 2.4.1.1) - E_2

The reversible formation of starch from glucose 1-phosphate catalysed by (starch) phosphorylase

$(\text{glucan})_n + P_i \longleftrightarrow (\text{glucan})_{n-1} + \text{G1P}$

was first reported in 1940 by Hanes 1940. Starch phosphorylase (StPase) is ubiquitous in plants. It catalyses **1.** the synthesis of starch by using G1P as a substrate for elongating the polysaccharide chain of an α-glucan primer (see also other glycosyltransferases in section 3.2.1.5), as well as **2.** its reversed reaction, the phosphorolytical degradation resulting in hexose phosphates.

Two isoforms of α-glucan phosphorylase exist in higher plants, type L and type H, with different affinities for various glucans (hence, l(ow) and h(igh)). In potato tubers the content of type L enzyme exceeds by far the content of type H enzyme (Gerbrandy and Doorgeest 1972). Isoform L has been localised in amyloplasts, and H is located within the cytosol (Brisson et al. 1989). Duwenig et al. (1997) and Duwenig et al. (1997) report that antisense inhibition of cytosolic phosphorylase (type H) in potato plants affects tuber sprouting and flower formation with only little impact on carbohydrate metabolism. Now the L type isozyme is called Pho1 and the H type isozyme Pho2 enzyme.

The isoform that is considered here in connection with plastidic starch metabolism is the L type or Pho2.

StPase is an equilibrium reaction with a K_{eq} of 0.3 for G1P-formation (Kruger 1997). Because starch deficiency was never found to correlate with StPase deficiency, its role *in vivo* is now believed to be the starch degradation rather than starch synthesis (Sivak and Preiss 1998). This is also supported by the ratios of P_i and G1P ($\frac{P_i}{G1P} = 10.8|6.7|3.1$ for pH 5|6|7 respectively, Hanes (1940)). With their excess P_i, although the mass action ratios are not too far removed from the equilibrium (0.09 for pH5, 0.15 for pH6, 0.32 for pH7), they indicate the direction of starch degradation. Additionally, there is the fact that all published K_m(G1P) values are one or two magnitudes higher than measured G1P. K_m(G1P) were found between 1mM and 3mM (Whelan 1955, Mori et al. 1993), and $K_m(P_i)$ usually is about twice this value.

StPase catalyses the reaction $(\text{glucan})_n + \text{P}_\text{i} \leftrightarrow (\text{glucan})_{n-1} + \text{G1P}$ and its equilibrium ratio $\text{G1P}/\text{P}_\text{i}$ is 0.15 (Whelan 1955). According to measurements by Tiessen et al. (2002) the ratios of the concentrations of G1P and P_i in the amyloplast are as follows:

Tuber	G1P	P_i	$\frac{\text{G1P}}{\text{P}_\text{i}}$
attached	17.4μM	870μM	0.02
detached	64μM	500μM	0.128

In both cases the ratio is smaller than 0.15 which means that the dominant catalytic direction is most probably the starch-phosphorylating one. Starch degradation even seems to be much faster if the tuber is still attached to the plant. This implies a huge cycling flux, since in the attached case there is actually net starch production and deposition. Other explanations are that the enzyme is strongly regulated by some other factor(s) resulting in a decisive change in the limiting rate or that the metabolite measurements have to be refined.

Whelan (1955) reports that StPase is quite sensitive to low temperatures. Its activity decreases to 10% after 53 days at 4°C. Contrarily, the measurements performed in the course of this project showed an increase in StPase activity in potato tubers between measurements at 10 days and 80 days of storage at 6°C.

Mori et al. 1993 measured for the L enzyme a ratio $\frac{V_+}{V_-} = 0.42$. This can be used, together with the K_m values, to calculate a K_{eq} according to the Haldane relationship. It gave the value 0.18 which is close to the mass-action ratio at pH6.

For the rate equation and the kinetic parameters used in the model see Appendix B.1 and B.2, respectively.

StPase activity can be measured as orthophosphate-liberation, *i.e.* the amount of P_i released when G1P is added to a primer. Starch itself is phosphorylated to a certain degree, which shifts the thereby obtained result slightly. According to Nielsen et al. (1994), less then 1% of the glucose residues of starch are phosphorylated (see also Paragraph 3.1.1 about starch). Thus, the phosphorylation of starch is neglected, and does not contribute to the phosphate pool in the model.

3.2.1.3 Phosphoglucomutase (EC 5.4.2.2) - E_3

The monomeric enzyme phosphoglucomutase (abbreviated as PGM) catalyses the reversible intermolecular transfer of a phosphate group between the 1- and 6-positions of glucose.

$\text{G1P} \longleftrightarrow \text{G6P}$

Takamiya and Fukui 1978 found that the enzyme appears to have a "ping-pong" mechanism and that it absolutely requires α-D-glucose 1,6-bisphosphate (G16BP) and Mg^{2+}. Maximum activity of this reaction is only obtained in the

presence of a catalytic amount of G16BP. This biphosphate is an intermediate in the reaction, being formed by transfer of a phosphate residue from the enzyme to the substrate, but its dissociation from the enzyme complex is much slower than the overall isomerisation (for more details about the phospho- and dephospho-form of PGM and the reaction mechanism see Ray and Peck 1972a).

E + G1P + G16BP $\longleftrightarrow$ E + G16BP + G6P

With less efficiency, 1,3-PGA can substitute for G16BP and transfer its phosphate to the enzyme, thereby activating it.

E + G1P + 1,3-PGA $\longleftrightarrow$ E + G16BP + 3-PGA

PGM occurs in both the cytosol and the plastids and operates near equilibrium in both (Farré et al. 2001). The equilibrium constant of the phosphate transfer is $K_{eq} \simeq 17$ (NIST database 2004). Farré et al. 2001) measured mass action ratios of 6.8 in cytosol and 12.0 in amyloplast of growing tubers (20-40g fresh weight). This indicates that both isoenzymes operate not far from equilibrium *in vivo*. PGM maximal catalytic activity in potato tuber cells is quite high (published values range from 1457 to 6145 nmol min^{-1} gFW^{-1}, Trethewey et al. 1998, Sweetlove et al. 1999).

Takamiya and Fukui (1978) measured the Michaelis constants K_m for G1P for two isoforms of PGM as 0.06mM and 0.12mM.

Phosphate acts as an inhibitor (Pressey 1967) but at non-physiologically high concentrations only, which is why this is omitted in the rate equation.For PGM a reversible uni-uni Michaelis-Menten kinetics (one substrate consumed, one produced) was assumed, see rate equation in the appendix B.1.

Various papers describe the effects in antisense potato plants: antisense plastidial PGM (Tauberger et al. 2000, Fernie et al. 2001), antisense cytosolic PGM (Fernie et al. 2002), and both (Fernie et al. 2002).

3.2.1.4 ADP-glucose pyrophosphorylase (EC 2.7.7.27) - E_4

ADP-glucose pyrophosphorylase (AGPase) catalyses the reversible conversion of ATP and glucose 1-phosphate to ADP-glucose and pyrophosphate (PP_i).

ATP + G1P $\longleftrightarrow$ ADP-glucose + PP_i

AGPase is highly regulated. It is heterotetrameric (in higher plants it consists of two regulatory large subunits (LS) and two catalytic small subunits (SS) Okita et al. 1990), and it has been suggested that different combinations of large and small subunits in different tissues show differential sensitivity to allosteric regulation (Kruger 1997). Other evidence suggests that the enzyme's activity is regulated by its reductive state (Ballicora et al. 2004). AGPase from potato tuber has an intermolecular disulfide bridge that links the two small subunits by the Cys12 residue. It is activated by reduction of the Cys12 disulfide linkage (Fu et al. 1998) but more information about the biochemistry of the amyloplast is needed to make any conclusions about the role of reductive activation in the regulation of AGPase from potato tuber *in vivo*.

The ADP-glucose (ADPG) produced by AGPase activity is the precursor for starch synthesis in both photosynthetic and non-photosynthetic cells. In 1955 Leloir found evidence for ADPG, and it was concluded that biosynthesis and degradation of starch occur by different pathways.

A close correlation between distribution of AGPase and inorganic pyrophosphatase in cell fractionation studies of developing tubers strongly suggests that the intracellular location of AGPase is the amyloplast Sweetlove et al. 1996a. Kim et al. 1989 also localised it in plastids, and it is even used as plastid marker (*e.g.* by Tiessen et al. 2002). Thus, it is concluded that AGPase is exclusively plastidial.

Stark et al. 1992 found that genetic manipulation of AGPase activity (by expressing a gene that encodes a regulatory variant) in potato tuber led to an increase in starch production, andconcluded that it is the rate-limiting step for starch synthesis. Also, antisense inhibition of AGPase in transgenic potatoes leads to sugar-storing tubers and influences tuber formation and expression of tuber storage protein genes (Müller-Röber et al. 1992). All this evidence shows the importance of AGPase for starch synthesis.

The reaction itself is readily reversible with a $K_{eq} \simeq 1$ but it is believed that inside the amyloplast it is made irreversible by the action of alkaline inorganic pyrophosphatase (extremely high activity in plastids, Weiner et al. 1987) which rapidly hydrolyses the pyrophosphate produced. Also, according to Farré et al. 2001 the molar mass action ratio of AGPase in plastids is 0.002 which is in fact much smaller than its equilibrium constant of 1.1 (NIST database 2004). Therefore, this reaction is essentially irreversible *in vivo*.

3-phosphoglycerate (3-PGA) is a strong activator (Burger et al. 2003) and orthophosphate is an inhibitor inducing sigmoidal kinetics. Thus, AGPAse is regulated by the ratio of 3-PGA and P_i. This represents a regulation by the level of glycolytic intermediates on one side and a regulation by the energy state in the cell on the other side.

The reaction mechanism of AGPase is very complicated, one has to consider two substrates, two products, the activator 3-PGA and the inhibitor P_i. Sowokinos and Preiss 1982 modeled the rate as a Hill equation (with K_m(ATP)=0.19mM and K_m(ADPG)=0.24mM).

In Section B.1 a parameter fit for another rate equation is described.

AGPase activity has a very high value in young tubers and decreases during the bulking stage. Tiessen et al. (2002) report its decrease from over 1200 nmol min^{-1} gFW^{-1} in 6-week-old plants to ∼400 nmol min^{-1} gFW^{-1} in 12-weeks-old plants. The same trend was observed by Sowokinos (1976) who also reported on the enzyme's relative cold-stability.

3.2.1.5 Starch synthase (EC 2.4.1.21) - E_5

The reaction of incorporating into starch a glucosyl unit from the precursor ADP-glucose is performed not by just one single enzyme but by several enzymes. Besides soluble starch synthase (SS) and granule-bound starch synthase (GBSS), the action of at least two more glycosyltransferases (enzymes with EC numbers 2.4.1), namely branching enzyme (SBE - EC 2.4.1.18) and disproportionating enzyme (DPE - EC 2.4.1.25) have been shown.

Branching enzyme (EC 2.4.1.18) is essentially irreversible (Barman 1969). 1,4-alpha-glucan branching enzyme (SBE) (oformerly Q-enzyme) transfers a segment of a 1,4-alpha-D-glucan chain to a primary hydroxyl group in a similar glucan chain, *i.e.* it is necessary for amylopectin synthesis. **Disproportionating enzyme** (EC 2.4.1.25) or D-enzyme was first found in potato tubers (Peat et al. 1953). D-enzyme is most abundant in developing and mature tubers compared to other organs of the potato plant(Takaha et al. 1993). But its direct requirement for starch synthesis is not proven, since Takaha et al. 1998 demonstrated normal starch content and composition in tubers of antisense potato plants lacking D-enzyme.

Starch synthase catalyses α-1,4-linked chain elongation:

$(\text{glucan})_n + \text{ADPG} \longrightarrow (\text{glucan})_{n+1} + \text{ADP}$

There are two forms, a soluble and a granule-bound. The soluble form of the enzyme can be primer-dependent or primer-independent (catalysing a primed or unprimed reaction, respectively).

Starch synthase is essentially irreversible. Values of measured maximal catalytic activities of StSynth are available in the literature. Often it is distinguished between soluble and granule-bound synthase activities. For soluble starch synthase activities of 102 to 143 nmol min^{-1} gFW^{-1} were measured (Sweetlove et al. 1999, Regierer et al. 2002) and for the granule-bound isoform smaller values between 25-31 nmol min^{-1} gFW^{-1}) (*ibid.*). In the model, the sum of soluble and granule-bound synthase activities will be used.

Recondo and Leloir 1961 showed that ADPG was 10-fold more active than UDPG in the transfer of glucose from the sugar nucleotide to the starch granule by StSynth.

3.2.1.6 Inorganic pyrophosphatase (EC 3.6.1.1) - E_6

Inorganic pyrophosphatase (official enzyme name: diphosphate phosphohydrolase) catalyses the cleavage of pyrophosphate into two orthophosphate molecules.

$\text{PP}_\text{i} \longrightarrow 2\ \text{P}_\text{i}$

Hydrolysis of PP_i is highly exergonic with a ΔG of -33.5 kJ mol^{-1} l^{-1} (Patrick du Jardin et al. 1995). This approximates to a K_{eq} of 750000.

For the soluble/alkaline inorganic pyrophosphatase (PPase), activity was

detected exclusively in the plastid (Farré et al. 2001), and it is often used as a plastid marker in assays of other enzymes (Sweetlove et al. 1996a).

As already mentioned in Paragraph 3.2.1.4, PPase renders the formation of ADP-glucose in the amyloplast thermodynamically irreversible. With its extremely high activity in plastids (Weiner et al. 1987) it rapidly hydrolyses the pyrophosphate produced.

According to plastidic metabolite concentrations provided by Tiessen et al. (2002), the mass action ratio of P_i*P_i/PP_i is $(870\mu M)^2/2.36\mu M$= 320720 for attached tubers, and $(500\mu M)^2/0.68\mu M$= 367647 for tubers detached for 1 day. Both are very similar and not far from the estimated equlibrium constant. A near-equlibrium rate equation for PPase can therefore be assumed for incorporation into the model (see Paragraph B.1).

Only two sources with measurements of catalytic activity of potato PPase were found: Geigenberger et al. (1998) measured 478±54 nmol min^{-1} gFW^{-1} in 12-weeks-old plants, and 154±31 nmol min^{-1} gFW^{-1} after 56 days of storage at 4°C; Sweetlove et al. 1999 measured 500±21 nmol min^{-1} gFW^{-1} in 10-weeks old developing tubers.

3.2.2 Cytosolic Enzymes - Hexose Phosphate Pool and Sucrose Cleavage/Resynthesis

Sucrose metabolism includes sucrose synthesis and degradation.

Sucrose synthesis occurs via sucrose synthase (SuSy) acting in the synthetic direction or via sequential action of sucrose 6-phosphate synthase (SPS) and sucrose phosphate phosphatase (SPP). SPP activity is high and very specific, it rapidly removes sucrose 6-phosphate, thereby displacing the equilibrium of the reversible SPS (Winter and Huber 2000).

Sucrose mobilisation can occur via reversible cleavage (as a result from SuSy activity in the non-synthetic direction, conserving the binding energy of the glycosidic bond in UDP-glucose) or from irreversible hydrolysis by invertase. The route of sucrose degradation that involves a UDP-dependent cleavage is unique to plants (Bologa et al. 2003).

Several enzymes catalyse interconversion of the species of the cytosolic hexose phosphate pool (see also Paragraph 3.1.2 on hexose phosphates).

3.2.2.1 Phosphoglucomutase (EC 5.4.2.2) - E_8

PGM has been described in the previous section on page 50. It is also present in the amyloplast, where it catalyses interconversion of G1P and G6P just the same as in the cytosol.

3.2.2.2 UGPase (EC 2.7.7.9) - E_9

ADP-glucose pyrophosphorylase (AGPase) and UDP-glucose pyrophosphorylase (UGPase) were shown to be separate enzymes (Sowokinos 1976). The latter catalyses the reversible conversion of glucose 1-phosphate and UTP to UDP-glucose and pyrophosphate.

UTP + G1P $\longleftrightarrow$ UDP-glucose + PP_i

The ubiquitous enzyme UGPase is cytosolic only, it is often used as a cytosolic marker (Tiessen et al. 2002). It is very specific, the nucleoside phosphates ATP, CTP and GTP, as well as ADPG are no substrates for UGPase (Sowokinos et al. 1993).

UDP-glucose is the precursor (glycosyl donor) for cellulose synthesis. Cellulose, the foundational polymer in cell walls, is a strong, essentially irreversable carbon sink. But tubers do not contain a strong cellulose sink, being mostly composed of parenchyma cells with primary walls.

Depending on the physiological state of the tuber the reaction may be channeled towards the formation of UDPG or towards the synthesis of G1P. The NIST database (2004) and Kruger (1997) provide K_{eq} values of 0.14 - 1.5 and 3.2, respectively. $K_{eq} = 0.6$ was reported by Katsube et al. (1991). Assuming the ratio of forward and backward reaction $\frac{V_+}{V_-}$ as 0.08 (Sowokinos et al. 1993) and calculating K_{eq} according to the Haldane relationship, with all the K_m from the same paper, $K_{eq} = 0.15$ can be obtained.

UGPase has a very high catalytic activity in potato tubers. Values between 8100 and 34707 nmol min^{-1} gFW^{-1} were measured (Sowokinos et al. 1993, Sweetlove et al. 1999, Tauberger et al. 2000, Fernie et al. 2002).

According to Sowokinos (1981), 3-phosphoglycerate has no effect on UGPase (in contrast to AGPase), and UGPase activity follows normal Michaelis-Menten kinetics. Therefore, a simple bi-bi rate equation was assumed. The rate equation used in the model can be seen in the Appendix B.1.1.

Sowokinos (1976) reported that UGPase is relatively cold-stable. Because of this and its very high catalytic activity it was long thought to not have any control over cold sweetening. Recently, Gupta and Sowokinos (2003), and Sowokinos et al. (2004) reported on attempts to relate the properties of certain UGPase isoforms to cold-sweetening resistence.

3.2.2.3 Phosphoglucoisomerase (EC 5.3.1.9) - E_7

Phosphoglucoisomerase (PGI), also called Lohmann's isomerase after its discoverer (Lohmann 1933), is ubiquitously and abundantly present in nature. It catalyses the isotopic equilibration between glucose 6-phosphate (G6P) and fructose 6-phosphate (F6P).

G6P $\longleftrightarrow$ F6P

In peas it possesses a nearly absolute specifity for this metabolite pair, *i.e.* it

neither acts on phosphorylated sugars other than G6P and F6P nor on any free sugars. The activity for the metabolite pair glucose and fructose is only 1/50 in comparison (Takeda et al. 1967).

The reaction has an equilibrium constant of 0.21-0.51 (Barman 1969, Kruger 1997 and NIST database 2004). Some experimentally observed mass action ratios F6P/G1P are: 0.5 in the cytosol and 0.26 in the amyloplast (Farré et al. 2001), and 0.29 in the cytosol (Tiessen et al. 2002). Hence, phosphoglucoisomerase operates very close to equilibrium.

The reaction is inhibited by 6-phosphogluconate, the inhibition constant of which is $K_i = 0.013$mM (Takeda et al. 1967). Further inhibitors are the glycolytic metabolites phosphoenolpyruvate and fructose 1,6-bisphosphate with high inhibition constants of K_i(PEP)=1.1mM and K_i(F16BP)=7.5mM (Noltmann 1972b, rabbit muscle).This K_i for F16BP is 1000× higher than its concentration in tuber cells. This inhibition, therefore, is not considered in the modelling of a rate equation for PGI (see Appendix B.1).

There is data on substrate specifity from PGI of several higher plants but not from potato. For peas, Takeda et al. (1967) measured a Michaelis constant K_m of 0.27mM for G6P. The K_m for F6P is usually one-half to two-thirds of K_m(G6P) according to Noltmann (1972b).
Schnarrenberger and Oeser (1974) found in spinach leaves the K_m for F6P to be 0.3mM for both the chloroplastidic and cytosolic isoenzyme. Also in spinach leaf, Backhausen et al. (1997) measured a similar K_m of 0.58mM for both substrates.

According to Noltmann (1972b), despite its strategic location, PGI is difficult to control because of (a) its K_{eq} being close to unity, (b) its ubiquitous presence in relatively high concentration, and (c) its high catalytic efficiency.

The reaction can be modelled as a reversible uni-uni Michaelis-Menten mechanism with competitive inhibition by PEP. The rate equation is shown in Appendix B.1).

3.2.2.4 Sucrose phosphate synthase (EC 2.4.1.14) - $\mathbf{E}_{10}$

In the reaction catalysed by sucrose phosphate synthase F6P joins UDP-glucose to form sucrose 6-phosphate (S6P).

F6P + UDP-glucose $\longleftrightarrow$ S6P + UDP

Potato tuber SPS has an absolute substrate specifity, UDP-glucose being its only glucosyl donor (Slabnik et al. 1968). SPS activity is strictly compartmented to the cytosol (see review by Winter and Huber 2000).

According to Lunn and ap Rees (1990) the reaction has a reversible equilibrium constant K_{eq} beween 5 and 62. Kruger (1997) reported a K_{eq} of 10.

Reimholz et al. (1994) investigated the allosteric regulation of potato tuber SPS by the metabolites G6P and P_i. G6P activates and P_i inhibits SPS. The two effectors act antagonistically to each other, changing the affinity for its

substrates UDPG and F6P (presence of G6P and absence of P_i lowers the K_m, whereas absence of G6P and presence of P_i increases them. Effector sensibility is altered by reversible protein phosphorylation (see more about this below). Allosteric control of SPS by its activator/inhibitor pair G6P/P_i constitutes a 'fine' regulation.

'Coarse' regulation via covalent modification has been reported for leaf SPS in many plants. Two kinetically distinct forms of the enzyme were detected, a less active phosphorylated and a more active dephosphorylated form, with the SPS phosphorylation status altered by light activation via a protein phosphatase (Huber and Huber 1992). Although, tubers are always in the dark, the tuber protein seems to be similarly regulated, comparing the results from measurements of catalytic activity by means of selective *vs.* non-selective assay. The selective assay contains P_i whereas the non-selective assay does not. Measurements of the SPS activities, V_{sel} and V_{max} (for 'selective' and 'non-selective'), show that catalytic activity depends on the protein phosphorylation status of the protein ($V_{sel} \ll V_{max}$). An 'activation state' V_{sel}/V_{max} of 0.4 - 0.5 was reported by Reimholz et al. (1994), and of <0.1 by Sweetlove et al. (1999) and Fernie et al. (2002). (For the model the data from non-selective assays were chosen, since the tubers are not exposed to light that could change its phosphorylation status.)

Hill et al. (1996) found in *cv Desirée* tubers that V_{sel} raises from about 150 to about 300 with 4 days of storage at 4°C.

Murata (1972a): the enzyme from potato tuber tissue exhibited a hyperbolic substrate saturation curve for UDPG, obeying the ordinary Michaelis-Menten type kinetics. $K_{m\mathrm{UDPG}}$ = 2.0 - 2.5mM. The substrate saturation curve with respect to F6P deviated from the Michaelis-Menten equation, it was sigmoidal in shape. But the data fitted well to a Hill equation with $n = 1.4$ and $S_{0.5\mathrm{F6P}}$ = 0.9mM.

SPS is subject to a complex regulation involving protein phosphorylation at multiple serine residues. Moreover, biochemical evidence suggest that SPS *in vivo* is associated into a multiprotein complex comprising other enzymes of the pathway and regulatory protein components such as protein kinases and 14-3-3 proteins[1]. SPS is possibly associated to SPP, PK_{III} and even UGPase.

Echeverria et al. (1997) showed physical and kinetic evidence for a complex with SPP (in spinach and rice leaves). They propose channeling[2] of S6P through a multienzyme complex of SPS and SPP ('metabolic unit').

No data could be found yet on S6P concentrations.

[1] 14-3-3 proteins are a group of small acidic proteins ubiquitously found in eukaryotes which bind to phosphorylated motives within their diverse target proteins. As a consequence client proteins become altered in their activity, stability or subcellular localisation. 14-3-3 protein again can bind further proteins and so on.

[2] Metabolite channeling: to speed up (see Schuster and Heinrich 1991) or to avoid interaction of the channeled metabolite with rest of metabolism (if its toxic for instance).

Reimholz et al. (1994) give sufficient SPS assay data to be used to model a rate equation but a lumped reaction, combining SPS and SPP in one rate equation, was opted for instead.

3.2.2.5 Sucrose phosphatase (EC 3.1.3.24) - E_{10}

Sucrose 6-phosphate phosphohydrolase, or sucrose phosphatase, catalyses the hydrolysis of sucrose 6-phosphate with release of orthophosphate.

S6P $\longrightarrow$ Sucrose + P_i

A very high change in free energy thermodynamically favours the right side, Sucrose and P_i. The reaction catalysed by sucrose phosphatase (SPP) is essentially irreversible. The high equilibrium constant (777 according to Kruger 1997) pulls the reaction catalysed by SPS (with S6P as its product) into the direction of net sucrose synthesis.

Echeverria and et al. (1995) determined that in storage cells of red beet and turnip hypocotyl as well as in carrot root, SPP is located in the cytoplasm.

SPP was purified from sugarcane and carrot root by Hawker and Hatch (1975). It was found to be activated by Mg^{2+}. It was not inhibited by glucose or fructose but by sucrose (with K_i<5mM for carrot root). This inhibition is partially competitive since a 100% inhibition is never reached (not even in vacuole where Sucrose>600mM). Furthermore, inhibition was observed for unphysiologicallly high concentrations of P_i or PP_i (30mM). The Michaelis constant towards S6P was measured to be 0.15mM (in carrot root).

The proposed channeling of S6P between SPS and SPP (Echeverria et al. 1997) has been explained in the previous paragraph that dealt with SPS. No data is available on S6P concentrations. Together, these facts led to the decision to lump SPS and SPP together in one reaction. In the rate equation for the lumped reaction SPS-SPP, which is given in Appendix B.1, the K_{eq} is the product of the two K_{eq} of SPS and SPP (10·777), and $V_{+/-}$ was set to be 1000 in order to achieve a high equilibrium constant. The mass action ratio is only small, close to unity. Competitive inhibition by sucrose was also considered.

3.2.2.6 Sucrose synthase (EC 2.4.1.13) - E_{13}

Sucrose synthase or, abbreviated, SuSy catalyses the freely reversible reaction:

Fructose + UDP-glucose $\longleftrightarrow$ Sucrose + UDP

ADP-glucose is also quite a good glucosyl donor, reaching about half the V_{max} of the reaction with UDP-glucose (Slabnik et al. 1968) but the enzyme is strictly compartmented to the cytosol (see review by Winter and Huber 2000), where no ADP-glucose is found. Fu and Park (1995) identified two genes in potato: *Sus3* and *Sus4*. The *Sus4* isoform of the enzyme is expressed primarily in the storage and vascular tissue of tubers and appears to facilitate sink function. It

also has sucrose inducebility, *i.e.* it can be induced by high levels of sucrose (Fu et al. 1995).

Specific reduction of the activity of the *Sus4* isoform, through expression of antisense RNA, severely reduces starch content in the tuber (Zrenner et al. 1995).

SuSy is believed to mainly act in the direction of degrading sucrose. The equilibrium constant K_{eq} for sucrose formation is between 1.3 and 6.7 (NIST database 2004). *In vivo* mass action ratios $\frac{\text{Fructose}\cdot\text{UDPG}}{\text{Sucrose}\cdot\text{UDP}}$ were estimated by Geigenberger and Stitt (1993) for developing tubers as 0.42 (no strong compartmentation of the four compounds was assumed, since they were not compartment-specific measurements). This value resembles K_{eq} well (note that the ratio is for the sucrose cleavage direction, whereas the reaction is defined above in the sucrose synthesis direction), therefore, Geigenberger and Stitt (1993) conclude that the reaction catalysed by SuSy is a readily reversible reaction, and SuSy operates relatively near to equilibrium.

From the cytosolic metabolite concentrations given in Tiessen et al. (2002) more mass action ratios can be derived. In attached tubers $\frac{\text{Sucrose}\cdot\text{UDP}}{\text{Fructose}\cdot\text{UDPG}}$ is 5.5, and in detached tubers it is 1.6. Thus, if the *in vivo* K_{eq} is indeed between 1.6 and 5.5, a switch from net synthesis to net degradation of sucrose is possible, *e.g.* sucrose cleavage in growing tubers (phloem unloading), and then sucrose synthesis (cycling) in detached tubers.

SuSy is present at high activities in growing tubers (values between 900 and 1900 nmol min^{-1} gFW^{-1}, measured by different groups: Geigenberger and Stitt 1993, Sweetlove et al. 1999, Tauberger et al. 2000, Geigenberger et al. 2001) but it shows large changes in activity during development and in response to sugar. Tiessen et al. (2002) detected a decrease of SuSy activity from over 1000 nmol min^{-1} gFW^{-1} in 6-week-old plants to ca. 100 nmol min^{-1} gFW^{-1} in 12-weeks-old ones. It also decreases by 87% within 8 days of storage of harvested tubers (Geigenberger and Stitt 1993).

Sucrose synthesis via SuSy is inhibited by ADP and UDP but both have unphysiologically high inhibition constants K_i of 3mM (Slabnik et al. 1968). It is also inhibited by free glucose and fructose. Sebkova et al. (1995) found that SuSy from carrots (*Daucus carota*) is uncompetitively inhibited by glucose (K_i=4.3mM) and non-competitively by fructose (K_i=17.2mM).

Avigad (1982) lists Michaelis constants for UDPG, fructose, UDP and sucrose: 1-2mM, 1-5mM, 0.1-0.7mM and 50-100mM. Geigenberger and Stitt (1993) measured concentrations of 157nmol/gFW, 0.48μmol/gFW, 8.8nmol/gFW and 20.8μmol/gFW. When multiplied by 10 because cytosol represents about 10% of cell volume ($\approx$fresh weight) in developing potato tubers, all reactants occur *in vivo* at concentrations which resemble their K_m.

Rohwer and Botha 2001 modelled the rate of SuSy with a reversible ordered bi-reactant mechanism, UDP-glucose binding first, and UDP dissociating last.

Because SuSy appears to operate near equilibrium (see above) a more simplified rate equation was used for this model. The physiological concentrations of fructose, ADP and UDP are much below the K_i values (see Appendix A.1), therefore, only uncompetitive inhibition by glucose was included. The resulting rate equation can be found in the Appendix B.1.1. Kinetic parameters (K_m's and apparent K_m's) were taken from Slabnik et al. (1968) and Murata (1972b), see Appendix B.2 for a full listing.

3.2.2.7 Invertase (EC 3.2.1.26) - $\mathbf{E}_{11}$

Sucrose can be hydrolyzed in the presence of an enzyme called invertase or sucrase (official name: β-fructofuranosidase). This cleavage of sucrose generates an equimolar mixture of the monosaccharides glucose and fructose (invert sugar).

Sucrose $\longrightarrow$ Fructose + Glucose

Plant invertases are classified according to their solubility and pH optima. There is soluble and insoluble invertase. There is acid(ic) and neutral/alkaline invertase, with pH optima of 5 and 7.5, respectively. Acid invertase is found in vacuoles and associated to cell walls, whereas alkaline invertase is probably restricted to the cytosol.

Only the neutral/alkaline and the acid(ic) isoforms of soluble invertase are of interest here, since they occur in the cytosol and the vacuole, respectively.

The hydrolytic cleavage of sucrose is highly exothermic. It has a very large overall free energy change (26.5 kJ mol^{-1} according to Goldberg et al. (1989), and 29.3 kJ mol^{-1} according to Kruger (1997)), which makes it effectively irreversible ($K_{eq} \approx 136000$ for the second value).

The maximal catalytic activity of acid and alkaline invertases (also called sucrolytic activity) is very low in developing tubers, therefore sucrose synthase must be the dominant route of sucrose breakdown (ap Rees et al. 1988).

Fructose inhibits invertase competitive and glucose inhibits non-competitive (Isla et al. 1991). Glucose is a non-competitive classical inhibitor whose inhibitory action is not suppressed by proteins. Isla et al. 1991 report on acid soluble invertase: K_i(Fructose) = 0.18-0.2mM, K_i(Glucose) = 0.98-1mM. K_i(Glucose) is small compared to concentrations in tuber organelles (from 16 to 32 mM (Farré et al. 2001 and Tiessen et al. 2002)), hence, the reaction must be inhibited very strongly *in vivo*.

The information on invertase inhibition led to the formulation of a rate equation for invertase with irreversible Michaelis-Menten-kinetics for sucrose and competitive/non-competitive inhibition by glucose/fructose. See Appendix B.1 for more details.

The invertase K_m for sucrose is much lower than the sucrose concentration (K_m(Sucrose) = 20-28mM according to Isla et al. 1991). Invertase is irre-

versible, and there is no evidence for strong regulation (Kruger 1997). But regulation is needed because through invertase activity every sucrose molecule is replaced by two osmotically active molecules, which can be removed only by hexokinase or fructokinase.

The invertase rate was modelled as the sum of acid and alkaline invertase. This gives a higher activity but it also incorporates vacuolar sucrose cleavage: asuming that hexoses can easily cross the vacuolar membrane, it is just as if $v_{inv} = V_{inv_{cyt}} + v_{inv_{vac}}$.

3.2.2.8 Hexokinase (EC 2.7.1.1) - $\mathbf{E}_{12}$

Hexokinase exhibits glucose- and fructose-phosphorylating activity.

Hexose + ATP $\longleftrightarrow$ Hexose 6-P + ADP

Three isoforms exist of a hexose-phosphorylating enzyme (HK1, HK2, HK3, see Renz et al. 1993) with high affinity for glucose as well as mannose (Renz and Stitt 1993) but much lower affinity for fructose (hence, they are referred to as hexokinases and not glucokinase). Fructose appears to compete with glucose as a substrate but only for very high concentrations.

Hexokinase is exclusively cytosolic (Winter and Huber 2000).

The ΔG for the reactionwith glucose is -16,7 kJ/mol (Kruger 1997) which makes the product site thermodynamically much more favoured (K_{eq} $\approx$840), and the reaction virtually irreversible.

Renz et al. 1993 and Renz and Stitt 1993 measured the activities of all three isozymes. The activity of HK3 was negligible in comparison (Renz et al. 1993), therefore, the focus is on HK1 and HK2 here. ADP acts as a competitive inhibitor to ATP (K_i=0.04 for HK1 and 0.108mM for HK2). Isoform HK1 additionally showed inhibition by G6P, non-competitively to glucose. The concentrations of the metabolites 3-PGA, PEP, F16BP, P_i, PP_i and F26BP were shown not having an effect on the activity of the hexokinases.

The values of K_m(ATP) were found to be at least tenfold lower than for any other nucleoside triphosphate. The kinetic characteristics described in Renz and Stitt (1993) were used for fitting a rate equation. Assay data was extracted from several figures in this paper. Renz and Stitt (1993) describe that HK activity was inhibited by ADP and G6P The procedure and results of fitting, and the included rate equation are discussed in Paragraph 4.1.6.3.

3.2.2.9 Fructokinase (EC 2.7.1.4) - $\mathbf{E}_{14}$

Unlike hexokinase, fructokinase specifically phosphorylates fructose.

Fructose + ATP $\longleftrightarrow$ F6P + ADP

Renz et al. (1993) found three isoforms, FK1, FK2 and FK3, of fructokinase. They are highly specific for fructose (less than 0.3% activity with glucose).

FK is substrate-inhibited by Fructose (Renz and Stitt 1993). ADP acts as a competitive inhibitor to ATP, and F6P as a non-competitive inhibitor.

FK2 has a very high affinity for fructose, and also a much higher activity than FK1. Therefore, it is the only one of the three isozymes considered herein. The assumed rate equation and some parameters that had to be fitted to achieve a better similarity to the enzyme assay data from Renz and Stitt (1993) are described in Paragraph 4.1.6.3.

3.2.3 Cytosolic Enzymes - Glycolytic Pathway

The glycolytic pathway which converts F6P to pyruvate is well studied in a variety of organisms (Plaxton 1996). Glycolysis is linked to the hexose phosphate pool via the phosphorylation of F6P to F16BP. Two enzymes are responsable for this first step of the reaction chain, PFK and PFP.

In the subsequent steps of glycolysis F16BP is further metabolised to pyruvate with a concomitant production of ATP. The glycolytic pathway produces four molecules of ATP and two molecules of NADH, after prior investment of two molecules of ATP in the "sparking" reactions of glycolysis, hexokinase (or fructokinase) and ATP-dependent phosphofructokinase. (If glycolysis proceeds via PFP instead, one molecule of pyrophhosphate is utilised, which itself has to be formed in an UTP-consuming reaction.)

There are two alternative reactions that can utilize PP_i rather than nucleoside triphosphates (NTPs) as a phosphoryl donor, namely PFP and UGPase. Both reactions are reversible, *i.e.* equally able to produce PP_i.

3.2.3.1 ATP-dependent phosphofructokinase (EC 2.7.1.11) - E_{15}

PFK or ATP-dependent phosphofructokinase has a crucial position in the highly conserved glycolytic pathway, representing the first unique step in it. PFK catalyses the phosphorylation of F6P to F16BP.

F6P + ATP $\longrightarrow$ F16BP + ADP

Because of its position it was long seen as the 'rate-limiting step' of glycolysis. But it was shown later to have little control over respiration and glycolytic pathway (Burrell et al. 1994). This finding was later analysed theoretically for an explanation (Thomas et al. 1997a).

PFK is one of the slowest enzymes in the system under consideration. Maximal catalytic activity has been measured in the range of 31 to 135 nmol min^{-1} gFW^{-1} (Geigenberger et al. 1998, Trethewey et al. 1998).

Phosphofructokinase is tetrameric, and it is allosterically (multifaceted) regulated, with PEP being its most important inhibitor *in vitro*. Substrate and effector kinetics of PFK were modelled by Thomas et al. (1997b). The reaction mechanism chosen was a Monod-Wyman-Changeux mechanism with exclusive binding of PEP to the T state. A parameter fit gave: L=1, n=2, K_m(F6P)=210μM and K_m(PEP)=18μM (Thomas et al. 1997b).

3.2.3.2 PP_i-dependent phosphofructokinase (EC 2.7.1.90) - E_{16}

Instead of ATP, pyrophosphate:fructose 6-phosphate phosphotransferase (PFP) utilises pyrophosphate as the primary phosphoryl donor but shares the ability to catalyse the transfer of phosphate to the 1-position of fructose 6-phosphate with PFK. It catalyses the freely reversible reaction:

$F6P + PP_i \longleftrightarrow F16P + P_i$.

The enzyme is markedly activated by nanomolar levels of fructose 2,6-bisphosphate (F26BP). Mg^{2+} is a requirement. Values for maximal catalytic activity of PFP were reported in the range of 177 to 1266 nmol min^{-1} gFW^{-1} (Mooney 1994, Trethewey et al. 1998).

Although it is an important regulator of glycolysis in animals and fungi, this is not so for plants. Transgenic potato plants with only 2% activity of PFP show no visible phenotype and only minor changes in metabolic fluxes in their tubers (Hajirezaei et al. 1994).

It shows large changes during development, having higher activity in growing tissues (Stitt 1990).

3.2.3.3 Fructose-1,6-bisphosphate aldolase (EC 4.1.2.13) - E_{17}

Fructose-bisphosphate aldolase succeeds PFK and PFP in the glycolytic pathway. It catalyses the cleavage of fructose 1,6-bisphosphate (F16BP) into glyceraldehyde 3-phosphate (GAP) and dihydroxyacetone 3-phosphate (DHAP).

$F16BP \longleftrightarrow GAP + DHAP$

This splitting follows an ordered uni-bi mechanism (Thomas et al. 1997b), in which GAP is released first from the enzyme-substrate-complex.

The reaction is readily reversible, and Barman 1969 gives an equlibrium constant of

$$K_{eq} = \frac{\text{GAP} \cdot \text{DHAP}}{\text{F16BP}} = 81\mu M^{-1}$$

. The concentrations of all its three substrates are of the same magnitude in tuber cells (*e.g.* Mooney 1994) They are low due to the toxicity of dihydroxy acetone and glyceraldehyde.

Aldolase has a high affinity towards its substrate(s). Moorhead and Plaxton 1990 observed Michaelis-Menten kinetics for F16BP cleavage in the cytosol of carrot storage root cells with a K_m(F16BP) of 6μM. Aldolase in *Daucus carota* is inhibited by MgAMP, G1P and phosphoenolpyruvate but only at an I_{50} of over 1mM (*ibid.*).

The enzymes catalytic activity is medium with measured values of 430±25 nmol min^{-1} gFW^{-1} (Trethewey et al. 1998) and 461±63 nmol min^{-1} gFW^{-1} (Tauberger et al. 2000).

For an ordered uni-bi mechanism, GAP released first, a rate equation can be derived. This is shown on Page 165 in the Appendix B.1.1.

3.2.3.4 Triosephosphate isomerase (EC 5.3.1.1) - E_{18}

Glyceraldehyde-3-phosphate aldose-ketose-isomerase or, more conveniently, TPI (short for triosephosphate isomerase)[3] is the next following reaction after aldolase. It catalyses the isomerisation of GAP and DHAP, the two products of F16BP cleavage.

GAP $\longleftrightarrow$ DHAP

Thus, it controls the symmetrical conversion of the two halves of hexose to pyruvate in glycolysis. TPI is easily isolated and the transformation it catalyses has an equilibrium constant K_{eq} between 10 and 24 (NIST database 2004).

TPI has the highest catalytic capacity amongst the glycolytic enzymes (Noltmann 1972c). In the list of enzymes considered in this metabolic model it takes the second place behind UGPase only. Published values of catalytic activity of TPI range from 4438 to 19700 nmol min^{-1} gFW^{-1} (Trethewey et al. 1998, Trethewey et al. 1999).

In some higher plants TPI is inhibited by ATP, F16BP, F6P, G1P and G6P (BRENDA database 2004) but always with relatively high K_i. Therefore, these inhibitions were not considered herein.

The Michaelis constants for both substrates are sub-mM. Tomlinson and Turner (1979) measured K_m(GAP) = 0.44mM and K_m(DHAP) = 0.88mM for garden pea *Pisum sativum*. Thomas et al. (1997b) used K_m(GAP) = 0.33mM and K_m(DHAP) = 0.64mM, averaged from several organsims values, in their model of potato tuber glycolysis. In both cases, the ratio of K_m(DHAP) and K_m(GAP) is 1:2 approximately.

A reversible uni-uni-MMK rate equation was assumed for TPI. The rate equation used in the model is shown in Paragrah B.1.1.

3.2.3.5 GAPDH (EC 1.2.1.12) and phosphoglycerate kinase (EC 2.7.2.3) - E_{19}

GAPDH

GAP dehydrogenase catalyses the following reaction:

GAP + NAD^+ + P_i $\longleftrightarrow$ 1,3-BPGA + NADH

In soybean root, it was found to follow a bi-uni-uni-uni-ping-pong mechanism in which NAD^+ and phosphate interact sequentially with the enzyme, followed in turn by the release of 1,3-BPGA, the addition of GAP, and the release of NADH (Copeland and Zammit 1994).

Maximal catalytic activities were measured by several authors. Values for GAPDH range from 301 to 2100 nmol min^{-1} gFW^{-1} (Trethewey et al. 1998, Geigenberger et al. 2001).

[3] sometimes also abbreviated as TIM, *e.g.* in Stryer 1995

PGK

Phosphoglycerate kinase catalyses:

1,3-BPGA + ADP $\longleftrightarrow$ 3-PGA + ATP

The maximal catalytic activity of PGK is very high, published data ranges from 1379 to 3044 nmol min^{-1} gFW^{-1} (Trethewey et al. 1998, Mooney 1994).

3.2.3.6 Phosphoglycerate mutase (EC 5.4.2.1) - E_{20}

The enzyme phosphoglycerate mutase (abbreviated as PGlyM) catalyses a reversible intramolecular rearrangement. It shifts a phosphoryl group from the 3- to the 2-positions of phosphoglycerate.

3-PGA $\longleftrightarrow$ 2-PGA

The cofactor 2,3-diphosphoglycerate (2,3-DPGA) has an activating effect (Ray and Peck 1972b), possibly similar to the reaction mechanism of PGM described on page 50. Of the two types of PGlyM, cofactor-dependent and cofactor-independent PGlyM, the independant type, where no regulatory mechanisms is known, occurs in plants (Westram et al. 2002).

The standard free energy change for this reaction is 4.2 kJ mol^{-1} which is equivalent to a K_{eq} of 0.18, so the reaction is readily reversible. K_{eq} in the range of 0.08 to 0.2 are listed by NIST database 2004.

PGlyM activity in potato tuber cells is medium fast (published values: 206 nmol min^{-1} gFW^{-1} in Burrell et al. 1994 and 541 nmol min^{-1} gFW^{-1} in Trethewey et al. 1998).

It is inhibited by pyrophosphate but no quantitive details are given (Ray and Peck 1972b).

Thomas et al. 1997b cite a paper by Botha & Dennis from 1986, in which the K_m for 3-PGA and 2-PGA where measured as 330μM and 60μM in *R.communis*.

For want of any more recent or potato-specific data, these values were also employed in this model, as kinetic parameters for a reversible uni-uni Michaelis-Menten equation (see Appendix page 166 for the rate equation and page 171 for the parameters).

3.2.3.7 Enolase (EC 4.2.1.11) - E_{21}

Enolase or phosphopyruvate hydratase catalyses the interconversion of 2-phosphoglycerate and phosphoenolpyruvate.

2-PGA $\longleftrightarrow$ PEP

The K_{eq} of this reaction is 6.3 according to Barman (1969), and between 0.33 and 5.15 according to the NIST database (2004). In any case, it is not far from unity.

Values of maximal catalytic activity were measured by three groups: Mooney (1994) assayed it at 10, 15, 20, 25 and 30°C in mature tubers and found 558, 829, 1120, 1337±98 and 1700 nmol min^{-1} gFW^{-1}. Trethewey et al. (1998)

report 448±27 nmol min^{-1} gFW^{-1}, and Tauberger et al. (2000) 405±34 nmol min^{-1} gFW^{-1}, both in developing tubers.

As for kinetic parameters: Thomas et al. (1997b) in their model of potato tuber glycolysis used substrate specifities of $K_m = 0.15$mM for both 2-PGA and PEP. This was an average of values from different plant species ranging from 0.04mM to 0.83mM, and the same (averaged) values will be used for the model.

There are only two substrates, 2-PGA and PEP, and the rate of enolase was modelled simply by Michaelis-Menten kinetics.

3.2.3.8 Pyruvate kinase (EC 2.7.1.40) - E_{22}

Pyruvate kinase (PK) catalyses the dephosphorylation of PEP:

PEP + ADP $\longrightarrow$ pyruvate + ATP

This reaction is strongly exothermic ($K_{eq} = 6451.6$ according to Barman 1969), and therefore virtually irreversible (Stryer 1995).

It is unlikely to approach equilibrium *in vivo* and, although PK does not appear to be as strongly regulated in plant as it is in mammalian tissues, there is evidence that its kinetics are sensitive to a number of metabolites (Podesta and Plaxton 1991).

Values of maximal catalytic activity were reported between 127±9 nmol min^{-1} gFW^{-1} (Trethewey et al. 1998) and 562±23 nmol min^{-1} gFW^{-1} (**?**).

PK is often considered irreversible.

For an enzyme like pyruvate kinase, with an equilibrium constant of about 10^5, this is very helpful, because in such cases it is unlikely that any reliable kinetic constants for the reverse reaction are available from experimental measurements (Cornish-Bowden and Cárdenas 2001).

The rate equation and kinetic parameters used in the model can be found on pages 166 and 171.

3.2.4 Transporters of the Amyloplast Membrane

Amyloplasts are leucoplasts (colourless plastids). Thus, they are double membrane organelles, *i.e.* surrounded by an envelope composed of inner and outer membrane with an intermembrane space, and all exchange of metabolites or ions must proceed via channels or transporters. A review of all plastidic transport processes was published recently (Weber et al. 2004).

The knowledge of which metabolites are exchanged between cytosol and amyloplast *in vivo* and by which mechanism is a precursory for the definition of a model with two compartments.

3.2.4.1 Hexose transport - T_1

The finding that *A.thaliana* plants lacking the chloroplast envelope hexose transporter accumulate starch indicates that the phosphorolytic pathway of starch breakdown and export cannot replace the amylolytic pathway (Trethewey and ap Rees 1994).

Trethewey et al. (1998) found an unexpected dramatic reduction in starch content after combined overexpression of glucokinase and invertase, and explained it with a diversion of flux into glycolysis at the expense of starch synthesis (change in partitioning) but there is an alternative interpretation of this result. It is that it supports the idea that there is hexose transport out of the amyloplast. If extra GK is introduced to add to hexose-phosphorylating activity, this drains the cytosolic glucose pool first, and then the plastidic one, which in turn reduces the product inhibition of amylolytic degradation, thereby enhancing starch turnover. Thus, the findings presented by Trethewey et al. (1998) strongly suggest the presence of a hexose transporter (HT).

Hexose transport has been shown for the chloroplasts of many plants (Weber et al. 2000.

3.2.4.2 Glucose 6-phosphate translocator (GPT) - T_2 and T_3

The plastidic phosphate translocators, which share inorganic phosphate as a substrate, but exchange this for different specific sugar phosphates, have a central and crucial role in linking plastid and cytosolic carbon metabolism. In recent years, the molecular cloning and functional characterization of these transporters, together with information on their role *in vivo* from mutants and antisense plants with reduced or absent expression, has allowed a comprehensive picture to emerge of this area (Flügge et al. 2003).

There are three classes of phosphate translocators: TPT, PPT and GPT.

TPT is found in potato in chloroplasts only, where it facilitates a strictly concentration-dependant counter-exchange (Riesmeier et al. 1993, Fischer et al. 1997). PPT transports phosphoenolpyruvate (Weber 2004) into the plastid but this is not considered in this model.

GPT

GPT facilitates the counterexchange of hexose phosphate and P_i.

The GPT has been cloned from storage tissues of a number of plant species where it is the main route for the supply of carbon into the plastid for starch biosynthesis (Kammerer et al. 1998). This gene is not normally expressed in photosynthetic tissues. This source of carbon (G6P) would normally be used only in heterotrophic storage tissues.

Substrate specifities of GPT were investigated by Kammerer et al. (1998). These authors suggest that orthophosphate or triose phosphates can be ex-

changed for hexose phosphate.

There are still divergent opinions whether it is G1P (Kosegarten and Mengel 1994) or G6P (Schott et al. 1995, Kammerer et al. 1998, Wischmann et al. 1999) that is transported into tuber amyloplasts.

But Tauberger et al. 2000 seem to offer a solution. Their mutants with more than 50% reduced plastidial PGM activity show a decrese in starch and increase in sucrose and glucose. Both can be explained by PGM being involved in the starch synthetic pathway and G6P being the main carbon entering the amyloplast.

Counterexchange of G6P with either P_i or 3-PGA was included in the model (two separate reactions).

3.2.4.3 ADP/ATP transporter (AATP) - T_4

3.2.4.4 Transport of orthophosphate - T_5

The occurence of P_i-transport in potato amyloplasts membranes has not been proven yet.

3.2.5 Other Reactions or Pathways

3.2.5.1 Nucleoside diphosphate kinase (NDPK) (EC 2.7.4.6) - E_{23}

Nucleoside diphosphate kinase equilibrates the adenylate and uridine pools.

ATP + UDP $\longleftrightarrow$ ADP + UTP

There are three types of NDPK, each located in a different subcellular compartment: type I in the cytosol, type II in the chloroplast stroma, and NDPK III in the mitochondrial inter membrane space Sweetlove et al. 2001.

NDPK is readily reversible with a K_{eq} of 1 (NIST database 2004). No data on substrate specifity or catalytic activity in potato were found. Thus, the simplest assumption was made, and the rate modelled as a reversible mass action kinetic type with $k_+ = k_-$ in order to account for the equilibrium constant being unity.

3.2.5.2 ATP utilisation (E_{24})

ATP utilisation rate was modelled in the style of the equation for ATP utilisation in Bakker et al. (1997). Following this approach, ATP utilisation depends on the ratio of ATP and ADP only (see page 167 for the rate equation).

3.2.5.3 Sucrose import (T_0)

Import of sucrose and other solutes into sink tissue may occur through plasmodesmata or sucrose transporters, *i.e.* symplastical or apoplastical transport (Oparka 1986).

Most plants studied contain multiple sucrose transporters (SUTs), also known as sucrose carriers (SUCs), which likely have different functions in phloem loading and/or unloading or in the import of sucrose into sink tissues.

SUT1/SUC2 expression has been found in sink tissues in roots, pollen, seeds, and elsewhere (Riesmeier et al. 1993). However, the direct mechanism and function of such phloem-associated H^+/sucrose symporters in sink tissues remains unclear.

In the model, therefore, the type of uptake was neglected. A minimalistic rate equation (mass-action-kinetic with K_{eq}=1 and very fast, basically in equilibrium) was assumed for sucrose import into the tuber cell.

3.2.5.4 Adenylate kinase (EC 2.7.4.3)

Adenylate kinase or ATP:AMP phosphotransferase is described as a crucial enzyme maintaining the pool sizes of various adenylates at equilibrium (Noda in Enzymes VIII 1972). It provides unique buffering role against rapid concentration changes of any component of the adenylate pool.

There is an amyloplastidic isoform (*St*pADK, see Regierer et al. 2002) and a cytosolic one (found in rice, Kawai and Uchimiya 1995).

3.2.5.5 Hexose isomerase

There is no enzyme in plants that catalyses the interconversion of reducing sugars: Glucose $\longleftrightarrow$ Fructose

Aldose-ketose isomerases acting on nonphosphorylated sugars have mainly been found to occur in microorganisms (Noltmann 1972a).

Urbanczyk-Wochniak et al. 2003, though, introduced a bacterial xylose isomerase into *S.tuberosum*. This additional xylose isomerase led to minor changes in the levels of tuber glucose and fructose but not in sucrose, and an elevated sucrose (re)synthetic flux (*i.e.* cyclings).

Chapter 4

The Model

In the previous chapter the molecular and biochemical background of plant sink carbohydrate metabolism was reviewed. This summary constitutes the source of information; and in this chapter, the actual reconstruction of the metabolic network is described, resulting in a model of potato tuber central carbohydrate metabolism. Where the model deviates from biological reality, due to necessary simplification and for the sake of modelling, this is indicated and explained.

4.1 Model Design

4.1.1 Simplification and Boundary Decisions

The basic presumption for designing a metabolic model is to consider the biochemical system to be modelled as a relatively closed reaction system except for few substances that are consumed and produced. These substances can cross the boundaries of the system, and inside the 'black box' there is a reasonable number of reactions that carry out conversions which connect them.

In this case here, each cell of a stored potato tuber is considered to be a bounded reaction system with starch as the sole carbon source and the respiration product CO_2 as the carbon sink. (Similarly, before harvest, in the attached model, sucrose is the carbon source, and starch and CO_2 are the carbon sinks.)

There are two levels of simplification for the sake of modelling, firstly, a qualitative one, *i.e.* the metabolism is assumed to be identical in each tuber cell, irrespective of differences in different types of tissues or developmental stage, and secondly, a quantitative one, *i.e.* only a section of the metabolism is considered, a portion of the central carbohydrate metabolism, and all the reactions outside are neglected.

4.1.1.1 Qualitative assumption regarding metabolism

In a potato tuber, there are several different tissues, *e.g.* parenchyma, epidermis, *etc.* (see tuber cross section in Figure 1.2), with differentiated cells. The

diverse features of metabolism in these various cell types is not mirrored in the model but a homogeneous tissue consisting of "general tuber cells", with a generalised metabolism, is assumed. The model represents an average medulla cell, since medulla cells are the most prevalent cells, and they cause the bulking of the tuber by synthesising and storing starch.

Admittedly, this is a simplification but it reflects what was stated by Renz et al. (1993): "A potato tuber is a relatively homogeneous tissue which undergoes a series of marked changes in its carbohydrate metabolism during its life-history. The growing tuber is a 'sink' which imports and degrades sucrose. Later, during storage, starch is partially remobilized and large amounts of sucrose and free hexose are accumulated, especially in the cold..."

Stored tubers are not static entities but inside a constant flow of carbohydrates is released from starch for respiration (Burton 1989). In the stored tuber, the whole metabolism serves maintenance[1] only, whereas in the bulking stage of growing tubers the rapid deposition of starch in the amyloplasts dominates the metabolic fluxes (cell differentiation and cell division is completed at this stage).

4.1.1.2 Quantitative assumption regarding model boundaries

Generally, the network of central carbohydrate metabolism encompasses the following sub-networks:
- starch turnover (starch formation and degradation inside plastids);
- sucrose metabolism (sucrose breakdown and sucroneogenesis in the cytosol);
- glycolytic pathway (in cytosol and plastids);
- gluconeogenesis[2];
- pentose phosphate pathway[2].

They are arranged around a pool of the hexose phosphates glucose 1-phosphate (G1P), glucose 6-phosphate (G6P) and fructose 6-phosphate (F6P). These three hexose phosphates take a central position in the carbohydrate metabolism of plants.

But in this work only a selection of these reactions is considered, including the turnover of the carbohydrates starch and sucrose, and the shunt to glycolysis. The adjacent pathways of pentose phosphate pathway (PPP) (which according to ap Rees and Beevers 1960 utilises 20% of F6P), cell wall synthesis (diverts its precursors from the UDPG pool), respiration (pyruvate to CO_2),

[1]Definition of maintenance by Penning de Vries (1975a): it includes processes that maintain cellular structures and intracellular gradients of ions and metabolites, along with cellular acclimation (phenotypic adjustment) to environmental changes. Dominant maintenance processes are macromolecular turnover (*i.e.* simultaneous breakdown and resynthesis) and active transport that offsets membrane leaks. The 'purpose' is to maintain cellular functionality.

[2]Unclear compartmentation: gluconeogenesis and pentose phopsphate pathway are variously distributed between cytosol and plastids in different tissues, organs and plants (see Emes and Dennis 1997, Debnam and Emes 1999 and Neuhaus and Emes 2000)

etc., are neglected.

Thus, the model refrains from including all parts of the metabolism found in potato tubers but it concentrates on the two compartments cytosol and amyloplast and on the dominating metabolic fluxes therein. The metabolites and reactions chosen for the composition of the model were listed and described in the previous Chapter 3.

The terms 'internal' metabolite and 'external' metabolite for the intermediates of the biochemical reactions in a metabolic model were introduced earlier in Section 2.1.4.

Out of all metabolites in the network, starch and pyruvate were designated as external. This choice is explained as follows:

Starch is defined external because of its abundance.
Defining starch as external circumvents problems with expressing and mass-balancing the stoichiometries for this polysaccharide. It is also appropriate for the kinetics because the molarity or number of reactive sites of the starch polymer is not much affected by addition or removal of glucosyl units (see also Paragraph 3.1.1).

Pyruvate is the product of the irreversible reaction pyruvate kinase and it does not affect any of the other reactions in the model. It also is situated at the end position of the relatively unbranched glycolytic pathway (Paragraph 3.1.8).

The highly abundant starch in the plastid and the cytosolic pyruvate are assigned to be external metabolites, whereas all the remaining 28 metabolites are internal.

Also, but only in the attached model, extracellular sucrose which is supplied by the green parts of the plant is an additional external metabolite.

ADP and ATP are often considered external in other metabolic models. The pools of cytosolic and of plastidic ADP and ATP became internal in this model by adding an irreversible ATP dephosphorylation reaction that substitutes for all reactions or processes in the cell that consume ATP.

4.1.2 Compartmentation

Compartmentalisation of biochemical pathways and processes, characteristic of eukaryotic metabolism, enables cells to **control** and to **optimise** different metabolic functions (in separate spaces).

In plants, metabolism is highly compartmented such that the major transport carbohydrate, sucrose, is found in the cytosol and vacuole, whereas the major storage carbohydrate, starch, is restricted to the plastides (Emes and Dennis 1997, Neuhaus and Emes 2000). For potato tuber cells, this means that there is a spatial separation of sucrose metabolism and starch metabolism, the

former takes place outside the amyloplast, whereas the latter is confined to the amyloplast.

The separation of synthesis of starch and of sucrose into two distinct compartments allows independent regulation of these two important storage and transport metabolites in the cell (Dennis and Greyson 1987). Since it is such a distinct feature of plant sink cells, it was aspired to build the model such that it accounts for this separation.

Amyloplasts take up about 15% of the volume of tuber cells. The cytosol accounts for a volume slightly less than the plastid volume, and the vacuole takes up the biggest part. Table 4.1 shows an overview of the compartmental volumes in tuber cells of 10-weeks-old plants.

Table 4.1: Subcellular volumes in growing potato tuber tissue.
Farré et al. 2001 calculated these relative volumes (percentage of total cell volume) from electron micrographs according to the principle of Delesse (CR Acad.Sci.(Paris), 1847).

Compartment	Relative volume
vacuole	67 %
plastid	14.8 %
cytosol	12 %
cell wall	5 %
mitochondria and nucleus	1.2 %

These individual compartmental volumes of potato tuber cells were determined by Farré et al. 2001, through a method only recently described (*ibid.*). With the knowledge of the relative volumes, these authors then also estimated the subcellular concentrations of several central metabolites (see Table A.1 in the Appendix).

Metabolic models deal with concentrations, which is why volumes have to be considered. But how can the volumes of the cytosol and the amyloplast and the distribution of metabolites between the two fractions be modelled in a simple way?

The solution is **pseudocompartmentation**, an exploitation of the fact that cytosol and amyloplasts have nearly the same volumes, namely 12% and 14.8% of the total volume of the tuber cell (Table 4.1). For the model, it is assumed that the two volumes are identical. Under this condition, metabolite exchange between cytosol and plastids translates exactly to equal but opposite changes in metabolite concentrations in the two compartments. Now separate pools for metabolites that occur in both compartments can be created simply by renaming or labelling metabolite names with the extensions **_cyt** and **_am** (for 'cytosol' and 'amyloplast'). Metabolites that, thus, can be simulated to exist in both compartments are: glucose, G1P, G6P, ADP, ATP, pyrophosphate and orthophosphate.

This approach represents a 'pseudocompartmentation' because, in principle, the model is designed like an uncompartmented model.

4.1.3 Assembly

For writing the *ScrumPy*-script describing the model, the vast quantity of information on the reactions (collected and presented in the previous Chapter 3) was reduced to:
1. Stoichiometries (given by the list of reactions);
2. Rate equations and kinetic parameters.

The distribution of enzymes between the two compartments cytosol and amyloplast was also described in Chapter 3. Some enzymes were found to be present in both compartments. Phosphoglucomutase is one example, and for phosphoglucomutase even the ratio of the catalytic activities between cytosol and amyloplast is known (Fernie et al. 2002). Others were shown to exclusively occur in one of the two compartments only, *e.g.* PP_i-dependent phosphofructokinase and hexokinase in the cytosol (according to Dennis and Greyson 1987, and Kosegarten and Mengel 1994), or pyrophosphatase in the plastids (according to Sweetlove et al. 1996a).

All reactions of sucrose metabolism were included, as well as, two phosphofructokinases (ATP- and PP_i-dependent), the whole glycolytic pathway from aldolase to pyruvate kinase (similar to Thomas et al. 1997b), and reactions of starch synthesis and degradation.

Orthophosphate transport across the plastid membrane (reaction T_4) has been included, although not experimentally confirmed yet; investigating its necessity for metabolism of the tuber is part of this project.

Table 4.2 lists all the reactions that have been included, for each compartment, and in Figure 4.1 a schematic presentation of the network described by this list is shown.

Altogether, the model contains 29 reactions, 24 enzyme-catalysed reactions and five transport steps, which interconvert 28 internal or balanceable metabolites ('balanceable' because their formation and consumption are balanced according to the steady state assumption) and two external metabolites (buffered by connection to reservoirs and considered to be 'source' and 'sink').

Most of the reactions are reversible. Nevertheless, one direction of these reactions has to be assigned the forward direction. In the model definition, by convention, for every reaction this is the direction as shown in Table 4.2.

Eight reactions are considered irreversible because they catalyse hydrolytic reactions or because their equilibrium constant is so high or the ratio of sub-

Table 4.2: List of all 29 reactions that are included in the model.
E - enzymatic reactions; T - transports
$\longrightarrow$ - irreversible reaction; $\longleftrightarrow$ - reversible reaction

No.	Stoichiometry	Reaction or Enzyme
	amyloplast	
E_1	$(\text{glucan})_n \longleftrightarrow (\text{glucan})_{n-1} + \text{Glucose}$	α- and β-amylase, glucosidase and disproportioning enzyme
E_2	$(\text{glucan})_n + P_i \longleftrightarrow (\text{glucan})_{n-1} + \text{G1P}$	starch phosphorylase
E_3	$\text{G6P} \longleftrightarrow \text{G1P}$	phosphoglucomutase
E_4	$\text{G1P} + \text{ATP} \longleftrightarrow \text{ADPG} + \text{PP}$	ADP-glucose pyrophosphorylase
E_5	$(\text{glucan})_n + \text{ADPG} \rightarrow (\text{glucan})_{n+1} + \text{ADP}$	starch synthase
E_6	$PP_i \longrightarrow 2\ P_i$	pyrophosphatase
	transports: amyloplast ‖ cytosol	
T_1	$\text{Glucose}_{am} \longleftrightarrow \text{Glucose}_{cyt}$	hexose transport
T_2	$\text{G6P}_{am} + P_{icyt} \leftrightarrow \text{G6P}_{cyt} + P_{iam}$	G6P/phosphate translocation
T_3	$\text{3-PGA}_{cyt} + \text{G6P}_{am} \leftrightarrow \text{3-PGA}_{am} + \text{G6P}_{cyt}$	triose phosphate/G6P translocation
T_4	$\text{ADP}_{am} + \text{ATP}_{cyt} \longleftrightarrow \text{ADP}_{cyt} + \text{ATP}_{am}$	adenylate translocation
T_5	$P_{iam} \longleftrightarrow P_{icyt}$	phosphate exchange
	cytosol	
E_7	$\text{G6P} \longleftrightarrow \text{G1P}$	phosphoglucomutase
E_8	$\text{G1P} + \text{UTP} \longleftrightarrow \text{UDPG} + PP_i$	UDP-glucose pyrophosphorylase
E_9	$\text{G6P} \longleftrightarrow \text{F6P}$	phosphoglucoisomerase
E_{10}	$\text{F6P} + \text{UDPG} \longrightarrow \text{Sucrose} + \text{UDP} + P_i$	sucrose phosphate synthase and sucrose phosphatase merged
E_{11}	$\text{Fructose} + \text{UDPG} \longleftrightarrow \text{Sucrose} + \text{UDP}$	sucrose synthase
E_{12}	$\text{Sucrose} \longrightarrow \text{Glucose} + \text{Fructose}$	invertase
E_{13}	$\text{Glucose} + \text{ATP} \longrightarrow \text{G6P} + \text{ADP}$	glucokinase
E_{14}	$\text{Fructose} + \text{ATP} \longrightarrow \text{F6P} + \text{ADP}$	fructokinase
E_{15}	$\text{F6P} + \text{ATP} \longrightarrow \text{F16BP} + \text{ADP}$	ATP-dependent phosphofructokinase
E_{16}	$\text{F6P} + PP_i \longleftrightarrow \text{F16BP} + P_i$	PP_i-dependent phosphofructokinase
E_{17}	$\text{F16BP} \longleftrightarrow \text{GAP} + \text{DHAP}$	aldolase
E_{18}	$\text{DHAP} \longleftrightarrow \text{GAP}$	triosephosphate isomerase
E_{19}	$\text{GAP} + \text{ADP} + P_i \longleftrightarrow \text{3-PGA} + \text{ATP}$	GAP dehydrogenase and phosphoglycerate kinase merged
E_{20}	$\text{3-PGA} \longleftrightarrow \text{2-PGA}$	phosphoglycerate mutase
E_{21}	$\text{2-PGA} \longleftrightarrow \text{PEP}$	enolase
E_{22}	$\text{PEP} + \text{ADP} \longrightarrow \text{pyruvate} + \text{ATP}$	pyruvate kinase
E_{23}	$\text{ATP} + \text{UDP} \longleftrightarrow \text{ADP} + \text{UTP}$	nucleoside diphosphokinase
E_{24}	$\text{ATP} \longrightarrow \text{ADP} + P_i$	ATP utilisation
	transport: cell exterior ‖ cytosol	
T_0	$\text{external Sucrose} \longrightarrow \text{Sucrose}$	sucrose supply from phloem

strates is so much removed from it that the reaction was found empirically to be virtually irreversible. They are: amylolytic starch degradation (E_1), starch synthase (E_5), sucrose synthase via S6P (E_{10}), invertase (E_{12}), Hexokinase and Fructokinase (E_{13} and E_{14}), PFK (E_{15}), and finally pyruvate kinase (E_{22}). More details on these irreversible reactions were given in the corresponding paragraphs in Chapter 3.

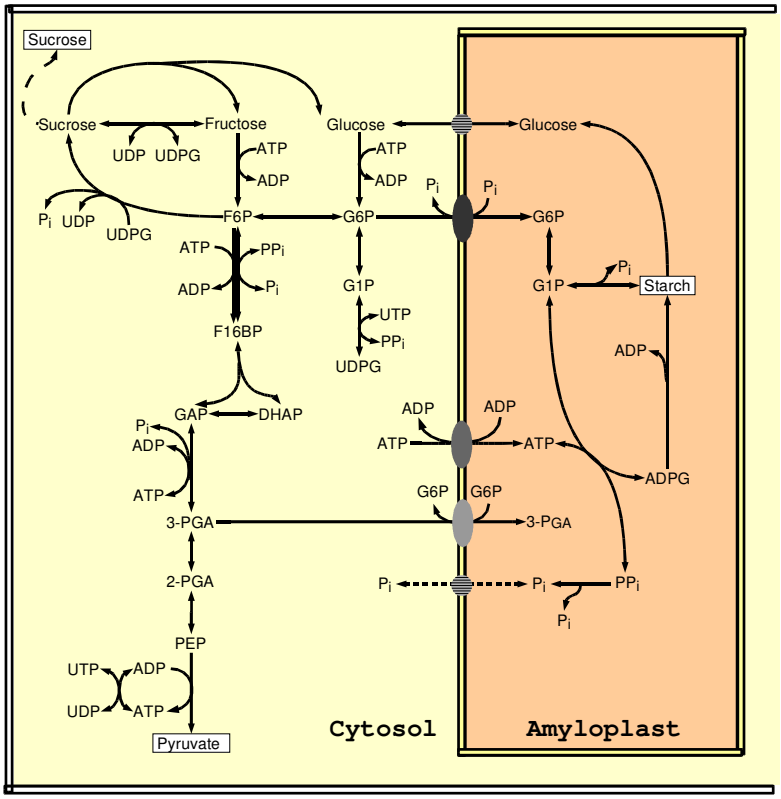

Figure 4.1: Reaction network of carbohydrate metabolism in potato tuber cells. External metabolites are framed. The metabolite tags **_cyt** and **_am** are not shown in order to retain clarity. Unidirectional arrows indicate irreversible reactions (except in transport steps). See Table 4.2 for a complete list of reactions.

While ATP-dependent phosphofructokinase is considered irreversible, PP_i-dependent phosphofructokinase, which occurs only in plants and in bacteria (BRENDA database 2004), is reversible.

Since the reaction of ATP utilisation (E_{24}) was incorporated into the model only to monitor any surplus ATP (but should not introduce any ATP itself), it is set as irreversible too.

4.1.4 Oxidative Phosphorylation

After interrogation of a predecessor model it was decided to include oxidative phosphorylation. The extra ATP yield from this oxidative phosphorylation was incorporated at the lumped GAPDH/PGK step. GAPDH oxidises NAD^+ to form NADH.

For the model it is assumed that the concentrations of NAD^+ and NADH

are balanced, *i.e.* that all NADH formed is reduced producing more ATP. Thereby, the introduction of two more internal metabolites, namely the moiety conserved redox couple NAD^+/NADH, could be avoided. Also, the location of the oxidative phosphorylation is neglected, so that no further compartment (mitochondria) needed to be considered.

The question is the yield of moles ATP per mole NADH. Different ratios for oxidative phosphorylation, namely 3ATP/2NADH, 11ATP/6NADH and 2.5ATP/1NADH, were reported in the literature.

Brand (1994) discusses a yield of 2.5 moles ATP per NADH. For plant photosynthetic tissue (see recent review by Amthor 2000), a ratio of 1.5 ATP per 1 NADH was reported. Whereas, a phenomonological stoichiometry of 1.83 ATP per NADH (equal to 11/6) in potato tubers was found in experiments by Groen et al. (1992).

The investigation and comparison of four possible ratios (0, 1.5, 1.83 and 2) might reveal distinct system behaviour for these different possibilities, and thereby hypotheses for what these ratios imply for the plant's metabolism. Thus, it was attempted to incorporate different yield ratios of oxidative phosphorylation by investigating four different versions of the model (hereafter called: "no-oxphos-model", "1.5-oxphos-model", "1.83-oxphos-model" and "2.0-oxphos-model"). The four lumped reactions GAPDH/PGK in the model script (comments are marked by a hash #) read:

```
GAPDH/PGK: # GAPdehydrogenase/PGK + no oxidative phosphorylation (0)
GAP_cyt + ADP_cyt + P_cyt <> PGA3_cyt + ATP_cyt ~

GAPDH/PGK: # GAPdehydrogenase/PGK + oxidative phosphorylation (1.5)
2 GAP_cyt + 5 ADP_cyt + 5 P_cyt <> 2 PGA3_cyt + 5 ATP_cyt ~

GAPDH/PGK: # GAPdehydrogenase/PGK + oxidative phosphorylation (1.83)
6 GAP_cyt + 17 ADP_cyt + 17 P_cyt <> 6 PGA3_cyt + 17 ATP_cyt ~

GAPDH/PGK: # GAPdehydrogenase/PGK + oxidative phosphorylation (2.0)
GAP_cyt + 3 ADP_cyt + 3 P_cyt <> PGA3_cyt + 3 ATP_cyt ~
```

(Note that the ATP yielded by oxidative phosphorylation is added to the ATP formed by the action of phosphoglycerate kinase.)

4.1.5 Growing Tubers - "Attached" Model

In stored tubers there is no sucrose import (nor any other source of carbon) into the tuber cell from the extracellular environment. Unless sprouting has started, the only loss of carbon from cells is as CO_2.

A further extension of the model allows for investigating the metabolic network before harvest, *i.e.* when the tuber is still attached to the potato plant.

Then the source of carbon is translocated sucrose that enters the tuber cells by apoplastic or symplastic transport. In the cytosol, sucrose is metabolised to hexose phosphates which can be imported into the amyloplast, the site of starch synthesis and accumulation.

Sucrose supply from the green parts of the potato plant is modelled by the addition of one new external metabolite (representing the concentration of sucrose in the phloem sap) and one new reaction that connects this external sucrose with the cytosolic sucrose pool. It was not distinguished between apoplastic and symplastic transport, since the difference between the two is not relevant for modelling the sucrose import.

The attached state of the tuber, thus, is modelled simply by enabling the sucrose uptake reaction T_0 (see Table 4.2). The number of reactions of the model increases by one (`SucSupply`), the number of external metabolites increases by one (`x_Sucrose`), and the number of internal metabolites remains the same.

Additionally, this way of modelling the cellular metabolism of an attached tuber allows for the investigation of the transition from attached to detached tuber in one and the same model, since harvesting (or stopping the supply of sucrose from the green parts of the potato plant to the tuber cells) can be simulated simply by reversing the procedure described before, namely by removing or disconnecting reaction T_0.

Therewith the structural model is completed.
It contains 28 internal metabolites, 2(+1) external metabolites, and 29(+1) reactions.

4.1.6 Adding Kinetics

For a kinetic model each reaction present in the structural model has to be matched with a mathematical expression describing its rate. Also, a full set of parameters has to be provided for every single of the 29 reactions from the assembled list. Thus, the construction of a kinetic model depends on the knowledge of reaction mechanisms (translated into rate equations) and the availability of enzyme or transporter kinetic data (incorporated as the limiting rates V_{max} and as kinetic parameters).

Most of the enzyme maximal catalytic activities that are published to date are measured in developing tubers. There have been much fewer measurements in stored or even cold-stored tubers, and these are, in comparison to developing tubers, of a rather incomplete set of enzymes. It was, therefore, decided to build a kinetic model of an attached tuber first instead of a kinetic model a detached tuber.

The kinetic model represents the central carbohydrate metabolism of a cell of a growing tuber.

The rate equations and kinetic parameters were acquired through reviewing and sorting the relevant literature in plant physiology, plant biochemistry and enzymology, and complemented by measurements of enzyme maximal catalytic activities (further details of the experimental work done to determine kinetic data is given in Chapter 6).

4.1.6.1 Rate equations/functions

Most reactions were modelled as MMK-type reactions with different mechanisms, uni-uni, bi-bi, random or ordered (*i.e.* ping-pong or sequential). There are also a few allosterically regulated enzymes, *e.g.* AGPase, PFK *etc.* Sometimes complicated equations were simplified because the rate equations as they are derived in standard literature (*e.g.* book by Segel 1993) seen in the light of experimentally achieved assays are overspecified (Hofmeyr and Cornish-Bowden 1997, Rohwer and Botha 2001 or Chassagnole et al. 2001).

All transport steps were modelled awith a mass-action-kinetic expression and an equilibrium constant of 1, *i.e.* they are driven only by the concentration gradient between the compartments.

Details of the rate equations used can be found in Appendix B.1.

4.1.6.2 Kinetic parameters

The successful construction of a kinetic model depends on the availability of sufficient accurate and relevant enzyme kinetic data. If kinetic parameters could not be discovered in the literature for the potato plant (let alone for potato tuber), kinetic parameters were chosen from the nearest taxonomical neighbour species possible.

Appendix B.2 provides a consensus list of all kinetic parameters used in the model. Parameter values which have been measured or fitted in the course of this project are included.

4.1.6.3 Fitting of rate equations

For some enzymes, inadequate, incomplete, or no rate equations could be found in the literature (less well characterised enzymatic reactions). Then the published experimental data sets were used to fit a function

$v = v(\text{metabolite concentrations; effector concentrations; } etc.)$

to this data by minimising the deviation of the modelled curve and the assay curves. Considering also regulatory effects, such as inhibitions, activations, *etc.*, rate equations could be derived.

The rate equations and kinetic parameters of ADP-glucose pyrophosphorylase, glucokinase and fructokinase were redefined through the fitting of experimental data from the literature (Sowokinos 1981, and Sowokinos and Preiss 1982 for ADP-glucose pyrophosphorylase, Renz and Stitt 1993 for hexokinase).

AGPase

A least-square fit was used to find a rate equation that fits the AGPase-assay data from Sowokinos (1981) and Sowokinos and Preiss (1982). Experiments which were carried out in the absence of any effector provide data for a fit to a simplified equation for an ordered bi-bi Michaelis-Menten mechanism (see page 563 in Segel 1993).
With K_{eq} set as 1 (it is 1.1 according to NIST database 2004) the equation to fit becomes:

$$v_{AGPase} = V_{app} \frac{(\mathrm{G1P} \cdot \mathrm{ATP} - \mathrm{ADPG} \cdot \mathrm{PP_i})}{(K_{m_{\mathrm{G1P}}}(1 + \frac{\mathrm{PP_i}}{K_{m_{\mathrm{PP_i}}}}) + \mathrm{G1P})(K_{m_{\mathrm{ATP}}}(1 + \frac{\mathrm{ADPG}}{K_{m_{\mathrm{ADPG}}}}) + \mathrm{ATP})}$$

Data from experiments, in which the concentration of G1P or ATP or ADPG, respectively, was varied, allowed a parameter fit for all four Michaelis constants.

Reactants: $K_{m_{\mathrm{G1P}}} = 100\mu\mathrm{M}$ $K_{m_{\mathrm{ATP}}} = 180\mu\mathrm{M}$
Products: $K_{m_{\mathrm{ADPG}}} = 280\mu\mathrm{M}$ $K_{m_{\mathrm{PP_i}}} = 260\mu\mathrm{M}$

The values of the apparent limiting rate V_{app} for the different experiments changed dramatically dependent on the concentrations of activator 3-PGA or inhibitor $\mathrm{P_i}$ in the various assays. V_{app} was assumed to obey the following function:

$$V_{app} = V_{max} \frac{1 + \frac{\mathrm{3PGA}}{K_{a_{\mathrm{3PGA}}}}}{1 + \frac{\mathrm{P_i}}{K_{m_{\mathrm{P_i}}}}}$$

and the parameter fit for this gave:
$K_{i_{\mathrm{P_i}}} = 160\mu\mathrm{M}$
$K_{a_{\mathrm{3PGA}}} = 10\mu\mathrm{M}$
A comparison of some of the experimental results (data from Sowokinos and Preiss 1982 was chosen that is representative of physiological concentrations of 3-PGA and $\mathrm{P_i}$ according to data shown in Table A.1) and the corresponding calculated curves (according to the fitted rate equation above) are shown in Figure 4.2.

GK (HXK)

The enzyme hexokinase is not very specific, in that it also phosphorylates fructose.

But in a metabolic model, obviously, the equation for every reaction is very specific, and it must be distinguished between glucose- and fructose-phosphorylating activity, *e.g.* compare reactions E_{13} and E_{14}.

Renz et al. (1993) found three isoforms of hexosekinases in potato plants but the two isoforms most active in tubers (HK1 and HK2) have the lowest specifity towards fructose compared to glucose (3% and 4% relative activity).

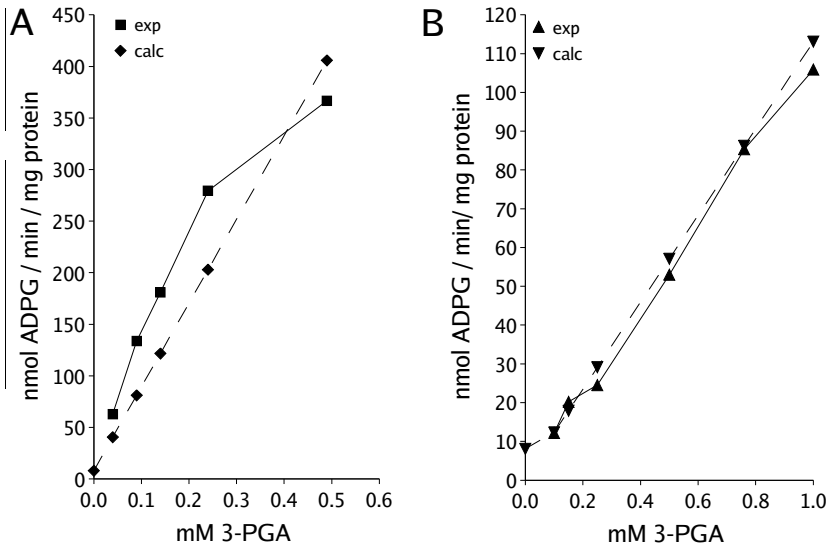

Figure 4.2: Comparison of experimental and fitted values of AGPase activity. Two sets of data are shown, in one set there was no P_i added to the assay (**A**) and in the other one the concentration of P_i was 1.0mM (**B**). The values according to measurements (Figure 4 and Figure 6b in Sowokinos and Preiss 1982) are connected by a continous line, whereas the fitted rate is shown with a dashed line.

This justifies to concentrate only on the glucose-phosphorylating activity of hexokinase. In the following this reaction is referred to as glucokinase (as it is already called in the model), thus, the name 'glucokinase' refers to the actual enzyme hexokinase (HXK) but only its glucose-phosphorylating potential.

In the measurements conducted in this project, it was distinguished between the two activities by adding the appropriate substrate solution to the crude extracts, glucose or fructose, respectively (see Chapter 6).

The experimental results from Renz and Stitt (1993) were used for a fit of the kinetic characteristics of glucokinase (GK). Assay data was extracted from Figures 4A, 4C and 5A in this paper. The authors describe that GK activity was product-inhibited by ADP. Also, the competitive inhibition by fructose (as another substrate for the reaction) was considered, and the following rate equation was formulated:

$$v_{GK} = V_{max} \frac{\frac{\text{Glucose}\cdot\text{ATP}}{K_{m_{\text{Glucose}}} K_{m_{\text{ATP}}}}}{(1 + \frac{\text{Glucose}}{K_{m_{\text{Glucose}}}} + \frac{\text{Fructose}}{K_{m_{\text{Fructose}}}})(1 + \frac{\text{ATP}}{K_{m_{\text{ATP}}}} + \frac{\text{ADP}}{K_{i_{\text{ADP}}}})}$$

Furthermore, one isoform they found (HK1) was inhibited by non-competitively G6P. In the rate equation, this can be achieved by the addition of an inhibition

term to the denominator:

$$v_{GK'} = V_{max} \frac{\frac{\text{Glucose}\cdot\text{ATP}}{K_{m_{\text{Glucose}}} K_{m_{\text{ATP}}}}}{(1 + \frac{\text{Glucose}}{K_{m_{\text{Glucose}}}} + \frac{\text{Fructose}}{K_{m_{\text{Fructose}}}})(1 + \frac{\text{ATP}}{K_{m_{\text{ATP}}}} + \frac{\text{ADP}}{K_{i_{ADP}}})(1 + \frac{\text{G6P}}{K_{m_{\text{G6P}}}})}$$

The slightly changed parameters obtained by a parameter fit of these two equations toward data from experiments in which the concentration of glucose or ATP or ADP had been altered are listed:

which parameter	value fitted for HK1	value fitted for HK2
parameter:	fitted for HK1:	fitted for HK2:
$K_{m_{\text{Glucose}}}$	41μM	130μM
$K_{m_{\text{Fructose}}}$	11.0mM	22mM
$K_{m_{\text{ATP}}}$	80μM	280μM
$K_{i_{\text{ADP}}}$	20μM	100μM
$K_{i_{\text{G6P}}}$	4100μM	-

The activities of HK1 and HK2 were approximately the same according to Renz and Stitt (1993). Also, in calculations with the newly fitted rate equations and over a range of physiological substrate concentrations, the two rates were always very close. One of the isoforms has a very low K_m for fructose but is inhibited by higher concentrations of this sugar. This might be important for the regulation of carbohydrate metabolism. Therefore, it was decided to model the rate of glucokinase as the sum of the above two equations, whereby half the V_{max} was assigned to each of the two partial activities.

FK

Of the three fructokinases reported by Renz et al. (1993) FK2 had the highest activity in tubers.

The kinetic characteristics described in Renz and Stitt (1993) were used for this fit. Assay data was extracted from Figures 1, 2A, 2C, 7A, 8C, 8D in this paper (most relevant because of physiological metabolite concentrations). Renz and Stitt (1993) describe that FK activity was product-inhibited by ADP and F6P. ADP acts as a competitive inhibitor to ATP, and F6P as a non-competitive inhibitor. Furthermore, it is substrate-inhibited by fructose (Renz and Stitt 1993) at high fructose concentrations.

FK2 has a very high affinity for fructose, and also a much higher activity than FK1. Therefore, it is the only one of the 3 enzymes considered in the following. The following rate equation was assumed, and some parameters had to be fitted to achieve a better similarity to the enzyme assay data extracted from Renz and Stitt (1993). The following rate equation was formulated:

$$v_{FK} = \frac{V_{app}(\frac{[Fruc][ATP]}{K_m(Fruc)K_m(ATP)})}{(1 + \frac{\text{Fructose}}{K_{m_{\text{Fructose}}}})(1 + \frac{\text{ATP}}{K_m\text{ATP}} + \frac{\text{ADP}}{K_{i_{\text{ADP}}}} + \frac{\text{Fructose}}{K_{i_{\text{Fructose}}}})(1 + \frac{\text{Fructose}}{K_{i_{\text{Fructose}}}})(1 + \frac{\text{F6P}}{K_{i_{\text{F6P}}}})}$$

and the parameter fit gave:
$K_{m_{\text{Fructose}}} = 90\mu\text{M}$
$K_{i_{\text{Fructose}}} = 5000\mu\text{M}$
$K_{m_{\text{ATP}}} = 35\mu\text{M}$
$K_{m_{\text{ADP}}} = 13\mu\text{M}$
$K_{i_{\text{F6P}}} = 1300\mu\text{M}$
All this was incorporated into the model.

4.1.6.4 Enzyme catalytic activities

A characteristic parameter for each reaction is the limiting rate V_{max}. For the model, it was endeavoured to find measurements of maximal catalytic activities in crude or compartmental extracts of potato tubers for each reaction that is included. Although, much of it is from the same variety, cv *Desirée*, the collected data is very heterogenous, there is considerable inter-tuber and inter-plant variance.

Two strategies can be followed when incorporating the V_{max} into the kinetic model: Either, one decides to collect as many measured values of maximal enzyme catalytic activities as possible, and then uses an average value for the model. Or, one cattempts to use as few different data sources as possible. At least, the sets of measurements taken from one published paper usually come from one extract from one tuber or one tuber set, which is better for compatibility of the values and ensuring coherence of the model (*e.g.* for a set of values for glycolytic enzymes from one paper, the ratios between all of them are more reliable).

The values that were eventually considered in the model are listed in the table in Appendix B.2.

The variation of those maximal catalytic activities collected from biochemistry and plant physiology literature covers three orders of magnitude, *i.e.* it ranges from 10 to 20000 nmol min^{-1} gFW^{-1}. The slowest ones ($\leq$100 nmol min^{-1} gFW^{-1}) are invertase and PFK ; the fastest ones (>1000 nmol min^{-1} gFW^{-1}) are UGPase, TPI, PGM and NDPK; the remainder is medium (between 100 and 1000 nmol min^{-1} gFW^{-1}).

Therewith the kinetic model is completed.
It has 120 parameters altogether (incl. 22 V_{max}).

4.1.7 Compartmental Metabolite Concentrations

Prerequisite and essential information for the construction of a kinetic model of metabolism is the knowledge of cellular and subcellular variation in metabolite

levels, *i.e.* the availability of metabolite concentration data. Since the model considered here is a compartmented one (see Paragraph 4.1.2), *i.e.* it takes into account the spatial separation of sucrose and starch metabolism in plant sink cells, metabolite data from inside the plastids is a necessity. Such data was long lacking (Fehr et al. 2004), mainly due to starch granules destroying the compartments during purifiction. The purification of potato amyloplasts was, until recently, the most difficult step when measuring metabolite concentrations because of disruption of the organelles caused by the large starch grains inside the plastids (Neuhaus et al. 1993).

Four years ago, Farré et al. (2001) described a modified fractionating method, and they provided the first report on metabolite distributions between the vacuolar, cytosolic and plastidial compartments of potato tuber cells. Their technique closes a gap because it overcomes the experimental hardships that hindered earlier attempts of measurements. It allows for differential determination of metabolite concentrations in the compartments of a plant cell, cytosol, plastids, and vacuoles, without prior physical separation or purification of the organelles. The method requires special equipment (*e.g.* a transmission electron microscope), and its duplication was not feasible within the framework of this project.

Table A.1 in the Appendix gives an overview of metabolite concentrations that have been acquired and quantified through this fractionation method since the introduction of the new technique (Farré et al. 2001 and Tiessen et al. 2002). The data collected from these two papers (published by groups at the Max-Planck-Institute of Plant Physiology in Golm, Germany) provides a basis for the initialisation of the metabolite concentrations, as well as a reference state for the steady state, (*i.e.* a 'snapshot' of metabolism that the model should reproduce). For any purpose in the model that required metabolite concentrations (*e.g.* fitting the model or steady state validation), the data produced in Golm was used.

4.2 Model Interrogation

For interrogation of the model the software package *ScrumPy* has been used. *ScrumPy* provides tools for many aspects of modelling, *i.e.* for model definition and for model interrogation. It holds tools for structural modelling and tools for kinetic modelling, such as time course simulations and data analysis. It is written in *Python*, an open source interpreted programming language (see http://www.python.org). *ScrumPy* was developed by Mark Poolman in the Cell Systmes Modelling group at Oxford Brookes University, UK.

Some available functions and methods in *ScrumPy* for the analysis of a structural model and for interrogation of a kinetic model were already mentioned in

Section 2.2.6 and in Section 2.3.5. Since the program is based on *Python*, it allows the user to flexibly define more functions or methods for model interrogation.

ScrumPy scripts are plain ascii files. The model is written down as an input file or 'script' for the program *ScrumPy*. See Appendix B.3 for this script, including all the rate equations and kinetic parameters as well as the initialisation.

The results of the structural analysis and the conclusions drawn are described in Chapter 5, and Chapter 7 shows the outcome of dynamic simulations and control analysis.

(possible) Extensions

The model is somehow complete but it can also be regarded as a core model. It can be refined (by getting more details on existent elements of the model) or extended (by adding more reactions to include further aspects of metabolism) at will anytime.

The model can be made more complicated (or simpler, for that matter!) by:
1. Exploring the limits of depth or accuracy of the model: lumping/de-lumping of reactions, level of simplification in rate equations, specificity/accuracy of parameters, *etc.*;
2. Moving the physical boundaries of the model: decisions of which reactions to include/exclude, choice of external metabolites, *etc.*

Some of these possibilities (vacuole, Maltose, cell wall synthesis, F26BP, *etc.*) will be briefly discussed later in Chapter 8.

Chapter 5

Structural Analysis

In the preceeding chapter a model of the central carbohydrate metabolism in potato tubers was defined. This chapter focuses on the investigation of the structural or topological properties of the metabolic network as defined by the model.

5.1 Building and Analysing the Structural Model

As described earlier, for the structural analysis, only the details on stoichiometry and reversibility (and direction, in the case of irreversible reactions) of all reactions are needed. The stoichiometry matrix **N** is at hand, it can be easily extracted from the list of all reactions in the model (as was described in Paragraph 2.1.5).

Because the model has 28 internal metabolites and 29 reactions, and their number equals the number of rows and columns, respectively, **N** has the dimension 28×29 (for a listing of **N** see the Appendix B.4). If all reactions were considered reversible, the biochemical system (potato tuber carbohydrate metabolism) would be fully described by the stoichiometry matrix **N** only. Since some of the reactions are considered irreversible, the additional information about reversibility is an essential part of the structural model.

The main concepts of structural analysis have already been introduced thoroughly in Section 2.2 before. In the following section, the results of the structural analysis are given. Conservation relationships, enzyme subsets and elementary flux modes are characteristics of the system at steady state.

The structural analysis relies on the steady state assumption (given in Equation 2.6). An important step is the calculation of the null space matrix **K** of the stoichiometry matrix **N**. The analysis (matrix algebra and computation of large tableaus) was performed with the software package *ScrumPy*.

5.2 Results of Structural Analysis

The results of the structural analysis, conserved moieties, enzyme subsets and an overview of all elementary flux modes of this biochemical network, are shown and discussed in the following.

5.2.1 Connectivity of Metabolites

The connectivity of metabolites and the specific distribution of the connectivities in metabolism was discussed by Wagner and Fell (2001), Wuchty and Stadler (2003) and Ma and Zeng (2003). For the model, a simple count was performed of how many reactions each (internal) metabolite partakes in:

8: ATP_cyt, ADP_cyt;

6: P_cyt;

5: G6P_cyt, F6P_cyt;

4: P_am;

3: G6P_am, UDP_cyt, Sucrose_cyt, Fructose_cyt, Glucose_cyt, F16BP_cyt, GAP_cyt, PGA3_cyt, UDPG_cyt, G1P_am;

2: UTP_cyt, Glucose_am, DHAP_cyt, G1P_cyt, PGA2_cyt, PEP_cyt, PP_cyt, PP_am, ATP_am, ADPG_am, ADP_am;

1: PGA3_am.

This itemisation shows that cytosolic ATP and ADP are the most highly connected intermediates in the model. These currency metabolites are followed in the ranking by orthophosphate and the hexose phosphates G6P and F6P.

A metabolite with a connectivity of 1 is a so called 'dead-end' metabolite, as is a metabolite that is connected by irreversible reactions only which are all either producers or consumers of this metabolite.

5.2.2 Conservation Relationships

The structural analysis revealed the four conservation relationships inherent in the network (see detailed explanation in Section 2.2). Almost all of the 28 internal metabolites participate in at least one of these relationships. There are dependencies between the species of the phosphate pool and of the nucleoside pool (*e.g.* ATP, ADP, UTP, UDP, pyrophosphate and orthophosphate).

Metabolite pools that are conserved are 1.) and 2.) the sums of all adenosine phosphates within the two compartments cytosol and amylolast, respectively, 3.) the sum of all uridine phosphates (in cytosol only), and 4.) the sum of all

phosphates and phosphorylated metabolites[1]. They are listed in Table 5.1.

Table 5.1: Conserved moieties.
Metabolites contributing to a conservation relationship are constrained in that their concentrations sum up to a constant value, the conserved sum.

Metabolites in a conservation relationship	Description of conserved sum (metabolite pool)
ATP_cyt, ADP_cyt	cytosolic adenosine phosphates
ATP_am, ADP_am, ADPG_am	plastidic adenosine phosphates
UTP_cyt, UDP_cyt, UDPG_cyt	(cytosolic) uridine phosphates
G1P_cyt, G6P_cyt, F6P_cyt, 2×F16BP_cyt GAP_cyt, DHAP_cyt, 3-PGA_cyt, 2-PGA_cyt, PEP_cyt ATP_cyt, UTP_cyt, P_cyt, 2×PP_cyt G1P_am, G6P_am, 3-PGA_am, ATP_am, P_am, 2×PP_am	phosphorylated metabolites and phosphates

The concentrations of ATP_cyt, ATP_am and UTP_cyt each occur in two conserved sums, and the concentrations of all the other intermediates are contained in one conserved sum.

All metabolites, except the sugars, occur in at least one of the four conservation relationship calculated. The sugars are: amyloplastidic glucose, cytosolic glucose, cytosolic fructose and cytosolic sucrose. These are the only unconstrained metabolites. The concentrations of these sugars are not topologically constrained, and therefore not restricted by an upper limit. Their concentrations can attain arbitrarily high values (always for a particular steady state which depends on the parameter set). This is essential for them being allowed to accumulate. (The hexose molecules for such an accumulation come from the reserve starch.)

It is notable that this is not a feature which was added intentionally but arises solely from the structure of the model.

5.2.3 Enzyme Subsets

There is one 'dead' reaction: the exchange of 3-PGA with P_i across the plastid membrane (PGA3imp). A 'dead' reaction is a reaction that does not carry any flux under the steady state assumption (more explanations were already given in Section 2.2.4). This is most obviously the case where one of the converted or transported metabolites is a 'dead-end' metabolite. A dead-end metabolite

[1]The phosphorylation of starch itself was neglected (according to Nielsen et al. (1994), less then 1% of the glucose residues of starch are phosphorylated, see also Paragraph 3.1.1 about starch). Any phosphate released from mobilised starch does not contribute to the phosphate pool in the model.

can only either be produced or consumed (or transported), there is no reaction to balance its concentration at steady state.

The transport of 3-PGA across the amyloplast membrane (PGA3imp) is a 'dead' reaction because there is no reaction inside the amyloplast that has 3-PGA as a substrate. One can ask why the reaction has been included. Its involvement is legitimate because it transmits information on the status of glycolysis into the plastid, by "sensing" the cytosolic 3-PGA concentration and "signaling" it into the amyloplast, where 3-PGA is a strong activator of AGPase.

All 'dead' reactions of the system form one enzyme subset (compare Section 2.2.4). Furthermore, there are 'trivial' sets with exactly one member, *i.e.* reactions whose activities are not perfectly correlated with any other single reaction in the network.

There are also several 'proper' enzyme subsets in the model, *i.e.* groups of at least two reactions that always operate in a concerted manner. All six of them are listed in Table 5.2.

It was mentioned before (in Section 2.2.4) that it is possible to merge or lump the reactions of an enzyme subset into one integrated reaction without losing any topological information. This new summary reaction then has an overall reaction with 'external' metabolites (external only to this lumped reaction) and metabolites that are hidden inside. The inside metabolites are balanced by the concerted action of the reactions of the subset. Table 5.2 also shows the overall reactions for the six enzyme subsets.

An interesting subset is set 1. It consists of plastidic enzymes only, and inspection shows that the concerted action of the five enzymes causes the addition of one glucosyl unit to the starch pool in time with consuming one ATP molecule from the cytosol (see overall reaction of the subset in Table 5.2), whereas it balances the concentrations of ADP-glucose and of pyrophosphate inside the amyloplast. Its members include the ATP/ADP translocator and the orthophosphate transport across the plastid membrane. Its existence strengthens the notion (Neuhaus and Maass 1996, Fischer and Weber 2002) that ATP transport into the plastid, and hence plastidic ATP-dependent metabolism, cannot be sustained in the absence of a mechanism transporting free phosphate in the opposite direction. A disscussion of this enzyme subset and its implications was published in Poolman et al. (2004) (see reprint in Appendix C on Page 183).

The second subset contains the most reactions, six reactions of the glycolytic pathway, seven reactions altogether (set 2 in Table 5.2). The most remarkable feature of this subset is that it also includes phosphoglucoisomerase (E_9). PGI is not adjacent to the other reactions in this subset (see also Figure 4.1). Its substrates G6P and F6P are neither substrate nor product of any of the other reactions (no overlap). Hence, the enzyme subset is not *connected*. This is

Table 5.2: (Non-trivial) enzyme subsets.
Reactions that belong to the same enzyme subset operate together in fixed flux proportions in all steady states of the system. pf - proportional factor (given only if pf≠1); * - indicates that the reaction is considered irreversible, this causes the whole subset to be irreversible; Note that the metabolites of set 3 and set 4 are all cytosolic.

Set	Reaction No.	Enzyme/Reaction	pf	Irr.
1	E_4	ADP-glucose pyrophosphorylase		
	E_5	starch synthase		*
	E_6	pyrophosphatase		*
	T_4	adenylate translocation		
	T_5	orthophosphate exchange		
	ATP_cyt + G1P_am → starch + ADP_cyt + P_cyt			
2	E_9	phosphoglucoisomerase		
	E_{17}	aldolase		
	E_{18}	triosephosphate isomerase		
	E_{19}	GAPDH/phosphoglycerate kinase	2	
	E_{20}	phosphoglycerate mutase	2	
	E_{21}	enolase	2	
	E_{22}	pyruvate kinase	2	*
	G6P_cyt → F6P_cyt **and** F16BP_cyt + 4 ADP_cyt + 2 P_cyt → 2 pyruvate + 4 ATP_cyt			
3	E_{12}	invertase		*
	E_7	cytosolic PGM	-1	
	E_8	UDP-glucose pyrophosphorylase		
	E_{23}	nucleoside diphosphokinase		
	E_{16}	PP_i-dependent phosphofructokinase		
	Sucrose_cyt → Fructose_cyt + Glucose_cyt **and** F6P + G6P + UDP + ATP → F16BP + UDPG + ADP + P			
4	E_{14}	fructokinase		*
	E_{10}	SPS/SPP		*
	Fructose + ATP + UDPG → Sucrose + ADP + UDP + P			
5	E_3	plastidic PGM		
	T_2	G6P/P translocator		
	G1P_am ↔ G6P_cyt			
6	E_1	amylolytic degradation		*
	T_1	glucose export		
	starch → Glucose_cyt			

an example of non-adjacency in enzyme subsets which was postulated in Paragraph 2.2.4.

The rest of subset 2 comprises all enzymes of glycolysis from aldolase down-

wards. It is a typical example of an enzyme subset. It forms an unbranched pathway, and none of the metabolites along the line is withdrawn at any point. For the system to maintain the steady state, the fluxes through each of the reactions must be fixed in a certain proportion. The aldolase and triosephosphate isomerase reaction carry only half the flux of the rest of the reactions, *i.e.* the flux proportions are 1:1:2:2:2:2 for E_{17}, E_{18}, E_{19}, E_{20}, E_{21} and E_{22}.

Set 3 balances G1P, then UTP and then pyrophosphate in the cytosol. There is no pyrophosphatase in this compartment (very low PPase activity in cytosol according to Geigenberger et al. (1998)), and every molecule of PP_i that is formed must be used in some other reaction. Enzyme subset 3 comprises UDP-glucose pyrophosphorylase and pyrophosphate-dependent phosphofructokinase, the only two enzymes in the network that utilise cytosolic pyrophosphate. Both the reactions they catalyse are reversible but appear in the subset such that the concentration of cytosolic pyrophosphate is kept constant. This set of enzymes, through its concerted action, also keeps the concentrations of G1P and UTP in the cytosol constant.

Sucrose, fructose and glucose, the substrates of invertase, are not involved in the other four reactions. Invertase is disconnected from the rest of the set. This makes enzyme subset 3 another non-adjacent grouping. The membership of invertase in the subset can be explained as follows: the flux through invertase equals the difference between the fluxes through SPS/SPP and SuSy, which means that there is an equally amounting formation of UDP-glucose, which again links invertase to this enzyme subset because UDP-glucose can only be utilised by UDP-glucose pyrophosphorylase.

Another interesting enzyme subset listed in Table 5.2 is set 4. Fructokinase and the enzyme complex of sucrose phosphate synthase and sucrose phosphatase (SPS/SPP) are linked via sucrose and invertase and SuSy. This enzyme subset cannot easily be found by inspection but follows from the combination of reactions in the cytosol. Its biological significance for the moment stays unclear.

Sets 5 and 6 are not particularly interesting, they arise because their reactions form unbranched (but rather short) chains of (two) reactions.

Enzyme subset 5 is the only reversible one.

Only five out of the 29 reactions do not belong to an enzyme subset with at least one other reaction, namely E_2 (StPase), E_{11} (SuSy), E_{13} (GK), E_{15} (PFK) and E_{24} (ATPutil). They form 'trivial' single-reaction subsets.

The high incidence of reactions that belong to 'proper' or non-trivial subsets is due to the fact that the model covers only a rather small section of metabolism. When sucrose uptake from the phloem is considered (see 5.2.5) the number and the size of subsets from Table 5.2 decreases (compare Table 5.5).

5.2.4 Elementary Modes

Elementary modes are minimal sets of reactions (here subsets of the 29 included reactions) that operate at steady state obeying all sign restrictions for one-directional reactions. In Section 2.2.5 an introduction and explanation of elementary modes was given.

There are only two external metabolites, starch and pyruvate. And because pyruvate kinase is irreversible there is only one possible overall reaction in the system, namely the breakdown of starch to pyruvate. Nevertheless, by decomposition, 22 elementary modes were detected. They correspond to 22 different routes of net starch breakdown, and all 22 routes realise the same net reaction:

$$(\text{glucan})_n \longrightarrow (\text{glucan})_{n-1} + 2 \text{ pyruvate}$$

This manifests an amazing variety of different pathways for this one and only possible overall reaction of the network.

Nevertheless, the number is still small enough to allow the modes to be individually examined.

Four different ratios for the yield of ATP per NADH in oxidative phosphorylation were investigated: 0ATP/1NADH; 3ATP/2NADH; 11ATP/6NADH and 2ATP/1NADH. Oxidative phosphorylation was incorporated in one lumped GAPDH-PGK reaction to avoid introduction of NAD^+ and NADH, as was explained in Section 4.1.4.

All networks with oxidative phosphorylation have the same number of elementary modes but these slightly differ in surplus ATP (which is used up by the ATPutil reaction) and cycling. This is shown in Table 5.3.

In the models with oxidative phosphorylation, only 6 out of the 22 pathways produce extra ATP (5 out of 18 for no-oxphos). This was ascertained by checking for use or non-use of the ATP utilisation reaction E_{24}.

The amount of ATP produced by a mode is between 1mole and 7mole, and it strongly depends on the efficiency of oxidative phosphorylation chosen. Higher ratios of ATP/NADH result in modes with more ATP.

This implies not that the remaining 16 modes (13 for no-oxphos) are wasting resources. These still form pyruvate that awaits further utilisation. None of the six(five) ATP-generating modes employs enzyme subset 1, the sequence combining AGPase, StSynth, PPase, AATP and phosphate export, *i.e.* all 9(7) routes that employ AGPase and starch synthase to produce starch use up all the ATP provided by any other process.

The mode producing the most surplus ATP in the 1.5-oxphos-model, namely 3 moles per mole of pyruvate, is shown in Figure 5.1 on page 95. It is a direct route from starch to pyruvate with no cycling, and it uses starch phosphorylase

Table 5.3: Elementary modes; sorted according to ATP production.
The fractional numbers arise only for the 1.83oxphos-model with its rather complicated stoichiometry for the GAPDH/PGK reaction, see page 77.

surplus ATP	Number of modes				
per glucosyl unit from starch	no-oxphos	1.5	1.83	2.0	2.5
0	13	16	16	16	16
1	2	-	-	-	-
2	2	-	-	-	-
3	1	1	-	-	-
$\frac{11}{3}$	-	-	1	-	-
4	-	2	-	1	-
$\frac{14}{3}$	-	-	2	-	-
5	-	2	-	2	1
$\frac{17}{3}$	-	-	2	-	-
6	-	1	-	2	2
$\frac{20}{3}$	-	-	1	-	-
7	-	-	-	1	2
8	-	-	-	-	1
0-7	18	22	22	22	22

for starch breakdown.

Let the *size* of an elementary mode simply be defined as the number of reactions contributing to this mode, then the average size of all elementary modes in this model is 17 for the no-oxphos-model and 18.3 for all oxphos-models. The average size of ATP-producing modes is smaller, only 15.6 for the no-oxphos-model and only 16 for all oxphos-models.

PFP is always going in the phosphorylating direction because invertase, which is considered irreversible, is in enzyme subset 3 together with PFP and three more reactions.

PFP is used in 14 modes (10 in no-oxphos-model), and PFK in only 8 modes. PFK and PFP act as strict alternatives: only one of them occurs in each mode, never both together.

(A futile cycle with F6P phosphorylated by PFK and then dephosphorylated again by PFP is not possible in the model because ADP, ATP, P_i and PP_i are not external, as they often are in other models.)

How carbon from starch breakdown is exported from the amyloplast and imported into the cytosol:
8(6) modes export glucose only, 8 modes export glucose 6-phosphate only, and 6(4) modes export glucose and simultaneously import G6P (resulting in or

equivalent to starch turnover).

Robustness in the network was tested for by successively simulating the knock-out of each reaction. The number of elementary modes remaining after removal of a reaction was for:

```
PGI, ald, TPI, GAPDH_PGK, PGlyM, eno, PK: 0;
GK: 3;
inv, cPGM, UGPase, NDPK, PFP, pPGM, G6Pexp, degr, Gexp, StPase: 8;
FK, SPS_SPP, SuSy: 12;
AGPase, StSynth, PPase, Pexp, ATTP: 13;
PFK: 14;
ATPutil: 16;
PGA3imp: 22.
```

This compilation (note that all enzymes that share an enzyme subset must appear in the same row) shows that seven reactions (namely the glycolytic pathway and PGI) are essential. GK-deficiency leaves only three modes (GK seems quite important), and PFK is the least called upon enzyme. For the no-oxphos-model (data not shown), the results were very similar. Only, subset 1 and 4 were used in fewer modes (i.e. more modes left when knocked out). This is due to a want of ATP because the reactions of subset 1 and 4 are not situated directly along the route of starch degradation and represent cycling if used.

The three elementary modes that do not employ glucokinase (- GK) are also the most "extreme": In the 1.5-oxphos-model one of them produces 6 mole surplus ATP, one cycles through sucrose 6× (through `SPS_SPP - SuSy - FK`), and the last one cycles through starch 6× (through `AGPase - StSynth - StPase`), while only one glucosyl unit from starch is channeled through to glycolysis and converted into pyruvate. (Cycling and surplus ATP in these three "extreme" modes is 3 for the no-oxphos-model, 20/3 for the 1.83-oxphos-model and 7 for the 2.0-oxphos-model.)

The three most "extreme" elementary modes for the 1.5-oxphos-model are shown in Figures 5.1-5.3.

All remaining 19 modes pass through GK, and their cycling and surplus ATP are set somewhere in between the extremes seen in the three GK-free modes. Thus, the glucose-phosphorylating reaction GK has an attenuating effect.

It also implies that, if ATP utilisation or demand does not increase, the cycling shoots up in GK-antisense or GK-knockout potatoes. This hypothesis should be experimentally testable.

Substrate cycling

There is considerable substrate cycling. Most of the 22 elementary modes involve cycling either through starch, or through sucrose, or both even. The largest cycling fluxes (relative to the number of hexose units removed from starch) occur in the GK-free modes.

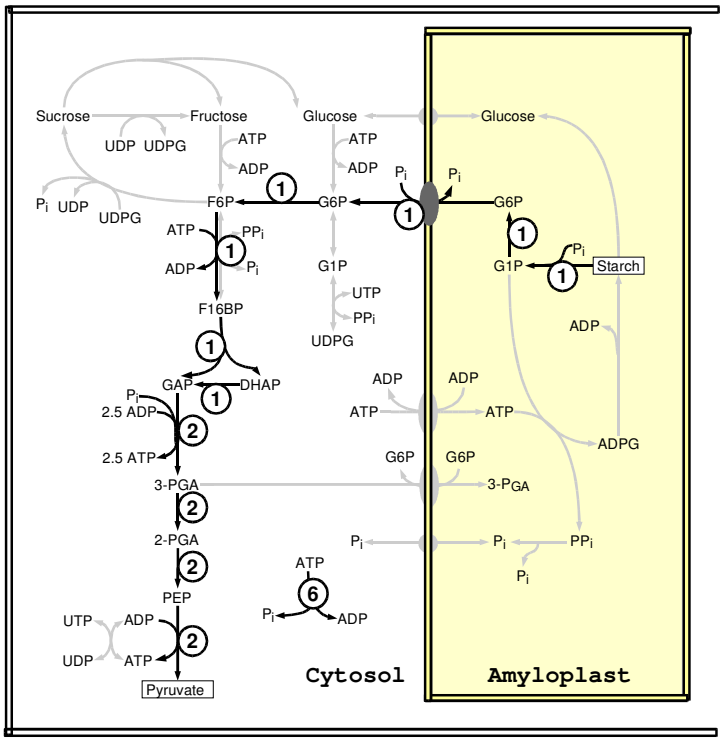

Figure 5.1: Elementary mode with the highest ATP yield.
Only the reactions represented by solid black arrows in the network scheme belong to the mode. The numbers in circles show the proportions between the fluxes going through each of the reactions.

There the ratio of starch turnover and starch degradation can reach 6 (Figure 5.2). But in other modes the ratios 3, 4 and 5 occur. For starch turnover there are two possibilities, elementary modes can follow one of two principal routes. The two groups of modes are: firstly, modes with amylolytic starch breakdown, glucose export and re-uptake as G6P (there are 6 of them, as mentioned above), and secondly, modes that synthesise starch via AGPase and starch synthase, *e.g.* the mode depicted in Figure 5.2.

The ratio of sucrose turnover and starch degradation can be 1, 3, 5 or 6. Figure 5.3 shows a substrate cycle of sucrose synthesis and cleavage that employs sucrose phosphate synthase and phosphorylase for sucrose synthesis and sucrose synthase in the non-synthetic direction. Other options of sucrose cycling involve invertase.

Such sucrose cycling has been found experimentally in developing tubers ((Geigenberger and Stitt 1993)).

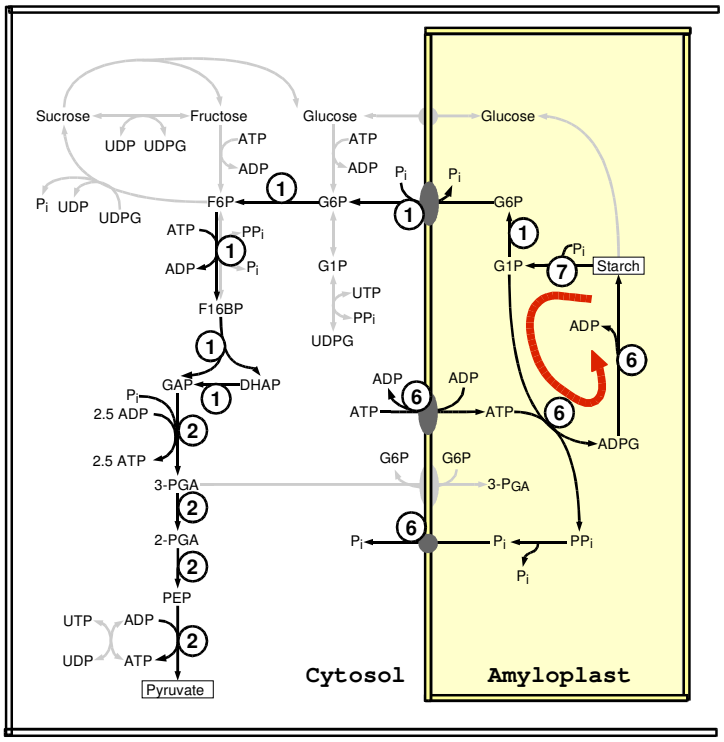

Figure 5.2: Elementary flux mode with substantial starch turnover.
Note that in every node of the network, for example F6P, all the incoming fluxes balance the sum of the outgoing ones.

The detected elementary flux modes represent the achievable cellular functions of the tuber during storage, namely the degradation of starch and, at the same time, generation of free energy (in form of ATP) or reducing potential (in form of NADH), as well as extensive substrate cycling.

Directionality

In principle, there are three possibilities for a reaction: to proceed in the forward direction (positive flux); to proceed in the backward direction (negative flux); or not to proceed at all (no flux). Because of the restrictions imposed through membership in an enzyme subset (if one reaction in there is irreversible, neither of the rest can proceed in both directions at steady state) there are really only four reactions, namely SuSy, StPase, G6Pexp and pPGM, that are reversible (note that PGI is always proceeding in the direction defined as forwards because of its membership in enzyme subset 2, see Table 5.2).

Analysing the model after making all reactions reversible in two steps:

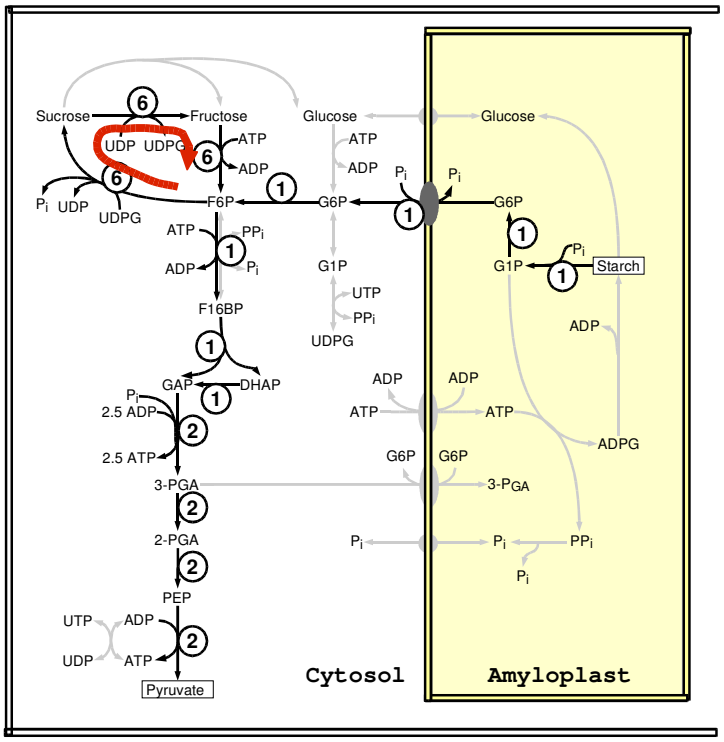

Figure 5.3: Elementary flux mode with substantial sucrose cycling.

1^{st}step Altering the `ATPutil` reaction to reversible results in four new elementary modes. These are internal, *i.e.* have no net reaction, and are driven by ATP provided by the reverted ATP utilisation. They represent cycling of sucrose, or starch (two possibilities), or both starch cycles combined.
sucrose cycling: `-SuSy; -ATPutil; FK; SPS\_SPP`
starch turnover I: `Pexp; StPase; PPase; AGPase; -ATPutil; AATP; StSynth`
starch turnover II: `-G6Pexp; degr; Gexp; HK; -pPGM; -StPase; -ATPutil`
starch turnover I+II:
`-G6Pexp; degr; Pexp; Gexp; HK; -pPGM; PPase; AGPase; -2ATPutil; AT; StSynth`

2^{nd}step Changing all of the reactions to reversible generates 67 modes altogether, 19 of which are internal (11 undriven, 6 driven by ATP, 2 modes even produce ATP by using PFK backwards)
These numbers demonstrate how the decomposition itself as well as the examination of the elementary modes is greatly facilitated by considering some reactions as irreversible.

Sucrose accumulation

The analysis above is based on the steady state assumption that the concentration of all internal metabolites do not change over time. It is known, though, that sucrose accumulates, and fructose and glucose follow with a delay of several days (*e.g.* Hill et al. 1996).

In order to investigate how sucrose can accumulate in the detached tuber, an extra reaction, called `SucAcc`, was added that mimics sucrose accumulation. It creates a shunt/drain out of the pool of internal metabolites. This additional sucrose accumulation reaction reads:

Sucrose_cyt $\longrightarrow$ x_accSucrose

where x_accSucrose denotes the sucrose pool able to accumulate. (It is depicted in the uppermost left corner of the scheme in Figure 4.1 representing the model's reaction network.)

The addition of this sucrose accumulation reaction causes enzyme subset 4 to break apart. Fructokinase and sucrose phosphate synthase are no longer carrying proportional fluxes. FK and SPS_SPP are a subset in the balanced model, in other words, they have to act jointly to keep the sucrose concentration constant, regardless of the action of invertase and sucrose synthase. A change in their ratio upsets the balancing of the sucrose concentration. Now that this co-operation is no longer constraining, the two reactions can carry fluxes that are independent from each other; but will this inevitably result in changes in sucrose?

To answer this question, elementary modes were re-computed too. Their number increased to 75. There were 53 more elementary modes in the system of which 8 are sucrose-accumulating, and 45 are sucrose-consuming. Instead of inspecting all the sucrose-neutral modes as before, the sucrose-producing and sucrose-consuming modes could now be compared.

The 8 new sucrose-producing modes all have the following overall reaction:

3 x_starch $\longrightarrow$ 1 x_accSucrose + 2 x_pyruvate

whereas the sucrose-consuming modes show a variety of net stoichiometries. These will be discussed in the subsequent Section 5.2.5. For now, the interest is solely on the difference between these two sets in the context of usage of reactions. Table 5.4 shows an overview of the dictribution or pattern of usage for all the 67 new modes. The reactions are sorted according to their contribution to sucrose-accumulating modes.

The first observation that can be made is that there seems to be no clear separation of reactions, most of them do contribute both to sucrose-forming and to sucrose-utilising elementary modes.

Interestingly, because unexpected, SuSy is never employed in the sucrose

Table 5.4: Number of elementary modes in which the specified reaction (left column) occurs, and direction of occurence (forward, not at all, or backward).

Direction of reaction used in # of modes	pos/neg	pos/neg
SucAcc	8 / 0	0 / 45
ald, TPI, GAPDH/PGK, PGlyM, eno, PK	8 / 0	45 / 0
-cPGM, UGPase, NDPK, PFP	8 / 0	21 / 12
PGI	8 / 0	11 / 8
SPS_SPP	8 / 0	18 / 0
GK	5 / 0	35 / 0
degr, Gexp	5 / 0	8 / 0
StPase	4 / 1	8 / 15
AGPase, StSynth, PPase, Pexp, AATP	3 / 0	23 / 0
pPGM, G6Pexp	3 / 2	0 / 34
ATPutil	2 / 0	12 / 0
FK	2 / 0	45 / 0
SuSy	0 / 2	9 / 18
inv	0 / 0	33 / 0
PFK	0 / 0	24 / 0

synthesis direction in the sucrose-producing modes (but even in the cleavage direction in two of them; these are the two modes that also employ FK, hence there is sucrose cycling in them).

Looking at the distribution in Table 5.4, four reactions can be distinguished that do never contribute to sucrose-accumulation. They are: invertase and PFK (carrying no flux in all 8 modes), as well as FK and SuSy (which do participate in sucrose cycling in two modes but not directly in sucrose-accumulation). Thus, invertase, PFK, FK and SuSy have no share in sucrose accumulation. But they can still contribute to sucrose-consuming modes.

Fructokinase is the most interesting in this respect. It operates in all 45 sucrose-degrading modes, and is therefore essential for sucrose consumption.

All four are good candidates but because there are still sucrose-degrading modes that do not use invertase or PFK (12 and 21, see Table 5.4 bottom, difference to 45), there is still a possibility that these are the ones predominantly used *in vivo*, and that invertase and PFK are bypassed.

According to this analysis, FK is the best candidate for preventing sucrose accumulation. It does not contribute to it but is essential for its counteracting process, no sucrose-consuming mode can escape its influence.

5.2.5 Attached Tuber Model

The transition of the model of a stored tuber to a developing (still attached to plant) tuber is done just by adding a sucrose uptake reaction (see on the

left in Figure 5.4). This reaction T_0 (SucSupply) is irreversible, it only allows uptake. (The drain of UDPG into cell wall formation and other anabolic pathways again are neglected, since during the bulking stage of tuber growth the sucrose-to-starch-conversion really is the main metabolic function.)

There are several differences to the enzyme subsets found in the detached tuber model (page 90), as shown in Table 5.5. Nevertheless, enzyme subset 1 remains unaffected by detachment. Therefore, the same conclusions as drawn on page 89 regarding the plastid phosphate balance apply. Set 1 is the same in both, and this conclusion holds for developing as well as for harvested tubers but it is even more significant in growing tubers. The meaning of enzyme subset 1 is that, if the model was considered without the phosphate exchange reaction, there would not be any starch synthesis via ADP-glucose phosphorylase and starch synthase.

Starch synthesis might be possible without ATP import into the amyloplast, namely via starch phosphorylase exclusively (an example pathway is depicted in Figure 5.4) but the dominant catalytic direction of this enzyme is most probably the starch phosphorylating one (see also page 49).

Subset 2 and 3 each consist of one member less then in the detached model. Both become fully connected subsets.

For set 3 this also results in becoming reversible, since invertase was the only irreversible reaction before, thereby restricting the direction of the other four. For developing tubers it is very important that there is a reaction which produces pyrophosphate because UDP-glucose, which is formed when sucrose is broken down via sucrose synthase activity, can only enter the hexose phosphate pool through the reaction catalysed by UDP-glucose pyrophosphorylase, the second substrate of which is pyrophosphate. Or in other words: pyrophosphate is required to convert UDP-glucose through to hexose phosphate (Geigenberger et al. 1998).

For the tuber considered to be still attached to the potato plant (positive flux through sucrose uptake reaction T_0), the number of distinctive elementary flux modes derived from the stoichiometry matrix of the network increases to 67. Table 5.6 lists all the net reactions that occur.

There are three possible net reactions: a net breakdown of starch (J1), complete degradation of sucrose into pyruvate (J2), and partial deposition of hexoses from sucrose into starch (J3). An overview of the number of elementary modes each is shown in Table 5.6 in which the modes have been sorted according to the stoichiometries of their net reactions. (Furthermore, a listing for the four different oxphos ratios, 0, 1.5, 1.83 and 2, is provided.)

The expression '1 starch unit' stands for the polysaccharide chain being

Table 5.5: Enzyme subsets for the attached tuber model.
There are several differences to the subsets found in the detached tuber model.
pf - proportional factor (only shown if pf≠1); * - indicates that the reaction is considered irreversible, causing the whole subset to be irreversible.

Set	Reaction No.	Enzyme/Reaction	pf	Irr.
1	E_4	ADP-glucose pyrophosphorylase		
	E_5	starch synthase		*
	E_6	pyrophosphatase		*
	T_4	adenylate translocation		
	T_5	phosphate exchange		
2	~~E_9~~	~~phosphoglucoisomerase~~		
	E_{17}	aldolase		
	E_{18}	triosephosphate isomerase		
	E_{19}	GAPDH/phosphoglycerate kinase	2	
	E_{20}	phosphoglycerate mutase	2	
	E_{21}	enolase	2	
	E_{22}	pyruvate kinase	2	*
3	~~E_{11}~~	~~invertase~~		*
	E_7	cytosolic PGM	-1	
	E_8	UDP-glucose pyrophosphorylase		
	E_{23}	nucleoside diphosphokinase		
	E_{16}	PP_i-dependent phosphofructokinase		
4	~~E_{14}~~	~~fructokinase~~		*
	~~E_{10}~~	~~SPS/SPP~~		*
5	E_3	plastidic PGM		
	T_2	G6P/P translocator		
6	E_1	amylolytic degradation		*
	T_1	glucose export		

extended (or shortened) by 1 glucosyl unit.

Although, there are only the three net reactions (J1-J3), many different stoichiometries for sucrose to starch conversion occur (hence, the summary equation for J3 with variables m and n). These different stoichiometric possibilities are listed separately in Table 5.7).

J1 is the same as it was for the detached model. J2 and J3 utilise the imported extracellular sucrose but only J3 can lead to starch accumulation, which is the major metabolic flux during the bulking stage of growing tubers (Section 1.2.3).

There is not one pathway which converts all of the imported sucrose into starch. This is because the incorporation of glycosyl units into the polysaccha-

Table 5.6: Elementary flux modes in the attached model.
m and n are positive integers.

	Stoichiometry of net reaction	Number of modes			
		no oxphos	1.5	1.83	2.0
J1	1 starch unit → 2 pyruvate	18	22	22	22
J2	1 sucrose → 4 pyruvate	9	11	11	11
J3	$\frac{m}{2} + \frac{n}{4}$ sucrose → m starch units + n pyruvate	17	34	34	34
	all elementary flux modes	44	67	67	67

ride is an ATP-consuming process, and the required ATP must be produced somewhere else within the network.

Since there are only three external metabolites that can act as the start- and endproducts for the net reaction of all modes, the large number of elementary modes impressively illustrates the enormous flexibility and redundancy inherent in plant sink metabolism. The network is constructed in such a way that the same or a similar overall net reaction can be achieved by many different possible reaction routes.

In Table 5.7 all possible stoichiometries of starch deposition via sucrose utilisation are listed. The differing stoichiometries result from different levels of starch turnover (defined as starch degradation occuring during net starch synthesis according to Sweetlove et al. 1996b) and sucrose cycling. Both these processes consume ATP which is formed in the lower part of glycolysis.

The ability of heterotrophic tissue to import and metabolise photoassimilates is called sink strength. In order to quantify the starch deposition or 'yield' that is possible through action of the computed elementary modes, the term *eff* (for efficiency) is introduced. It is defined as the ratio of starch extension and sucrose uptake, *i.e.* the number of glucosyl units added to the ends of polysaccharide chains per imported sucrose molecule.

efficiency of starch deposition Starch deposition is defined as the net increase of starch (difference between synthesis and degradation). An efficiency term *eff* can be derived as follows:

$$eff = \frac{\text{number of glucosyl units added to starch polysaccharide chain}}{\text{number of glucosyl units imported as sucrose}} \quad (5.1)$$

The efficiency *eff* can be calculated for every elementary mode from its net reaction.

Starch deposition efficiency of growing tubers varies from $\frac{1}{3}$ to $\frac{13}{14}$ (calculated from the net stoichiometries shown in Table 5.7). For instance, for the

Table 5.7: Stoichiometries of all elementary flux modes that produce starch (corresponding to J3 in Table 5.6).
Sucrose to starch conversion is achieved by several different stoichiometries. The term *eff* is defined as the ratio of glucosyl units added to starch per monosaccharides coming from sucrose. All values of *eff* greater than 0.5 are in bold.

Net stoichiometry	*eff*	Number of modes			
		no oxphos	ATP/NADH 1.5	1.83	2.0
1 sucrose → 1 starch unit + 2 pyruvate	0.5	13	26	26	26
2 sucrose → 3 starch units + 2 pyruvate	0.75	-	**1**	-	**1**
3 sucrose → 2 starch units + 8 pyruvate	0.33	1	-	-	-
3 sucrose → 4 starch units + 4 pyruvate	0.67	**1**	**1**	-	**1**
3 sucrose → 5 starch units + 2 pyruvate	0.83	**1**	**1**	-	**1**
4 sucrose → 5 starch units + 6 pyruvate	0.625	**1**	-	-	-
5 sucrose → 6 starch units + 8 pyruvate	0.6	-	**1**	-	-
5 sucrose → 7 starch units + 6 pyruvate	0.7	-	-	**1**	-
5 sucrose → 8 starch units + 4 pyruvate	0.8	-	**1**	-	**1**
* 6 sucrose → 11 starch units + 2 pyruvate	0.917	-	**1**	-	-
7 sucrose → 10 starch units + 8 pyruvate	0.714	-	**1**	-	**1**
7 sucrose → 11 starch units + 6 pyruvate	0.786	-	**1**	**1**	-
7 sucrose → 12 starch units + 4 pyruvate	0.857	-	-	-	**1**
7 sucrose → 13 starch units + 2 pyruvate	0.93	-	-	-	**1**
8 sucrose → 13 starch units + 6 pyruvate	0.81	-	-	-	**1**
10 sucrose → 17 starch units + 6 pyruvate	0.85	-	-	**1**	-
17 sucrose → 22 starch units + 24 pyruvate	0.647	-	-	**1**	-
17 sucrose → 28 starch units + 12 pyruvate	0.824	-	-	**1**	-
20 sucrose → 37 starch units + 6 pyruvate	0.925	-	-	**1**	-
23 sucrose → 34 starch units + 24 pyruvate	0.654	-	-	**1**	-
23 sucrose → 37 starch units + 18 pyruvate	0.71	-	-	**1**	-
$\frac{m}{2} + \frac{n}{4}$ sucrose → m starch units + n pyruvate	0.33–0.93	17	34	34	34

1.5-oxphos-model the most optimal mode has a 92% yield. It is depicted in Figure 5.4 and in Table5.7 it is marked with a * star.

One can see from Table 5.7 that the higher the ratio of ATP won by oxidative phosphorylation, the more choice is there for modes with higher starch yield. In fact, for the model without oxphos, there are only three modes with *eff*>0.5, whereas the models that consider some degree of oxidative phosphorylation have 8 such modes, and these mostly have higher *eff*-values as well.

This leads to the formulation of the hypothesis that **starch synthesis at such high rates as observed in potato tubers (0.5-0.7) depends on non-cytosolic sources of free energy.**

Direction of PGI

All modes with *eff* higher than 0.5 do proceed via PGI in the backwards direction (F6P→G6P). If PGI is not used at all, *eff* equals 0.5, the yield of

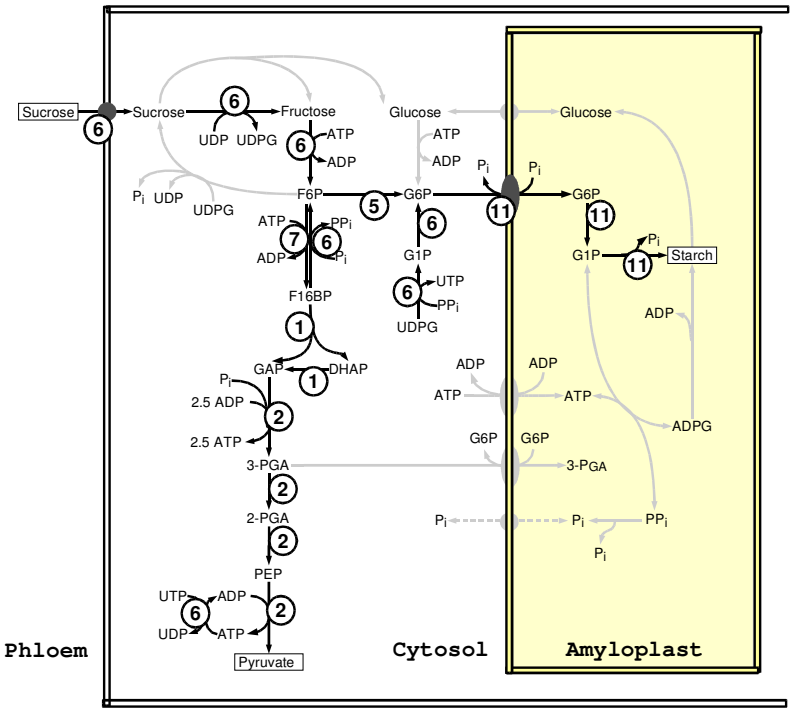

Figure 5.4: Elementary mode with optimal starch yield.

starch is exactly half of the sucrose taken up. If it proceeds in forward direction (G6P→F6P) only complete degradation of starch or sucrose is possible (J1 and J2).

Whereas in the detached model PGI was in an enzyme subset together with all reactions from lower glycolysis, and its direction was therefore fixed (only forward), in the attached model it does not belong to this enzyme subset nor any other subset. It is free to carry flux both ways or none (before it was essential, and now it is not).

Since it is known that more than 50% of the imported sucrose is deposited as starch *in vivo*, the direction for PGI is already preassigned.

Fructokinase

Another observation is that fructokinase is employed in every of the 45 sucrose-consuming modes, no matter if they ultimately deposit starch or convert all of the sucrose taken up into pyruvate, *i.e.* a FK-knock-out model cannot proceed with the conversion of sucrose into starch.

The following listing shows how many starch-producing modes remain when the reaction (on the right) is deleted from the model ("knock-out"):

```
0 :  ['G6Pexp', 'SucSupply', 'ald', 'TPI', 'eno', 'GAPDH_PGK', 'pPGM',
```

```
      'FK', 'PGlyM', 'PK']
7 :  ['GK']
9 :  ['NDPK', 'inv', 'cPGM', 'UGPase', 'PFP']
14 :  ['SuSy']
15 :  ['StPase', 'Pexp', 'AATP', 'AGPase', 'PPase', 'StSynth']
16 :  ['PFK']
21 :  ['SPS_SPP']
26 :  ['degr', 'Gexp', 'ATPutil', 'PGI']
34 :  ['PGA3imp']
```

FK and G6Pexp are the only essential reactions apart from the glycolytic pathway.

5.3 'Scenarios'

This following interrogation convincingly shows the usefulness of the whole structural approach because changes in the model can be made with little effort, and then the model can immediately be analysed all over again.

5.3.1 Varying oxidative phosphorylation

The results for a model in which no oxidative phosphorylation was considered or for models with oxidative phosphorylation but at different degrees of ATP/NADH ratio were partly shown already. The analysis was done in parallel. No-oxphos results were shown along with the results of oxphos-models.

The conserved sums and enzyme subsets were the same. There were many differences in the elementary modes decomposition.

5.3.2 Varying Directionality

These are no biological meaningful scenarios (*e.g.* glycolysis backwards *etc.*). They are merely mentioned because the numbers (numbers of modes for examination, number of seconds elapsed for calculation) excellently demonstrate the enormous impact the directionality has, how the decomposition itself as well as the examination of the elementary modes is greatly facilitated by considering some reactions as irreversible.

1. ATPutil reversible ⇒ 8 new modes arise. Four of them are internal cycles with no net reaction at all but driven by ATP (futile cycling of sucrose, or starch, or both starch cycles, or combined cycling through starch and sucrose). Four modes use sucrose taken up to produce starch without glycolysis.

2. All reactions reversible ⇒ The system consists of a total of 261 elementary modes (219 in no-oxphos-model). 19 modes are internal: 2 driven by ATP, 11 undriven, 6 even produce ATP via reversed PFK (numbers are 3, 11, 5 in the no-oxphos-model).

5.3.3 Adding a cytosolic PPase

The addition of a pyrophosphatase to the cytosol gives rise to 28 new elementary modes. These new modes have as net reaction J1, J2 or J3 with maximal *eff*=0.5 which means that PPase added to the cytosol cannot contribute to increased starch synthesis (as reported by Jelitto et al. 1992 and Geigenberger et al. 1998 after addition of *E.coli* PPase to the cytosol especially). Rather, the observed changes in carbon partitioning in these transgenic plants must be a secondary effect, resulting from concomitantly increased activities of enzymes for sucrose-starch interconversions.

5.3.4 Adding a hexose isomerase

Addition of a reaction that interconverts hexoses gives rise to 86 new modes, it more than doubles the number of stoichiometrically balanced pathways in the network. 37 of the new modes use hexose isomerase in fructose-to-glucose direction, and 49 use it in the opposite direction. This abundance of pathways has not been examined yet but it is expected that a closer inspection might yield interesting insights, especially in the context of comparing with and explaining of observations with transgenic tubers (Urbanczyk-Wochniak et al. 2003).

5.4 Conclusions

Qualitative analysis such as the structural analysis described above is seen to be a tool for inspecting and/or verifying larger networks for consistency and biological meaningfulness. The basic functions and behaviour of the system can be checked prior to exhaustive dynamic simulation studies. If the model does not behave as observed, or not in a biologically meaningful way; then the model should be amended first before carrying on, thus saving resources.

The model built herein reproduces the main features of sugar metabolism in tubers, namely ATP production through maintenance glycolysis and substantial cycling both through starch (starch turnover) and through sucrose (cleavage and resynthesis). This claim is supported by the elementary mode analysis which shows that the achievable cellular functions during tuber storage, according to this model, include the deposition of starch, cycling of sucrose and starch, as well as generation of free energy (ATP) or reducing power (NADH). This is consistent with what is documented on potato tuber metabolism.

Further findings for the model of a detached tuber are:

1. **Conserved sums:** The fact that only sucrose, fructose and glucose are not constrained by conservation relationships, and are, therefore, not limited by a conserved sum (see page 87).

2. **Phosphate across amyloplast membrane (export):** The detection of enzyme subset 1 (see discussion on page 89) strengthens the notion that ATP transport into the plastid, and hence plastidic ATP-dependent metabolism, cannot be sustained in the absence of a mechanism transporting free phosphate in the opposite direction (Neuhaus and Maass 1996 and Fischer and Weber 2002). Phosphate is imported into the amyoloplast in the form of ATP, and used inside for ADP-glucose formation, but there must also be some mechanism for the phosphate to leave the amyloplast again.

3. **Non-adjacent enzyme subsets:** The reactions of two enzyme subsets (sets 2 and 3 in Table 5.2 on page 88) are not all adjacent. This is more a theoretical issue but interesting, nevertheless. Intuitively, reactions that form unbranched sub-pathways are enzyme subsets, and these would be not difficult to detect, but only with the help of the algebraic method for calculation of enzyme subsets (as described in Section 2.2.4), these non-adjacent sets can be detected.

4. **Diverse routes of starch breakdown:** Although there is only one overall or net reaction (starch → pyruvate) there are 22 unique ways of achieving it. The metabolic function of degradation of starch to supply free energy and pyruvate can be realised by many routes that show different degrees of cycling and ATP production. Substrate cycling of sucrose (*i.e.* sucrose cleavage and formation) and (macromolecular) turnover of starch (*i.e.* simultaneous breakdown and resynthesis of starch) are substantial.

5. **GK-deficiency:** Investigation of the elementary modes that proceed without usage of the glucokinase reaction revealed an interesting attenuating effect of GK (see explanations on page 94).

6. **Possible role of FK for sucrose accumulation:** As was discussed in Section 5.2.4 on page 97, fructokinase is the only reaction that contributes to all modes involved in sucrose degradation, whereas it does not contribute to any mode that leads to sucrose accumulation. It is therefore reasonable to assume that overexpression of fructokinase could be beneficial in preventing accumulation of sucrose in stored tubers.

Further conclusions could be drawn from the structural analysis of the model of an attached tuber:

7. **Diverse routes for sucrose-to-starch conversion:** 67 unique modes with different levels of efficiency (starch per sucrose) and different degrees of substrate cycling and ATP production (see Table 5.6 and Table 5.7) were detected. The elementary modes obtained show that the achievable cellular functions during tuber development include the deposition of starch, cycling of sucrose and starch, as well as generation of free energy (ATP)

or reducing power (NADH). This is consistent with knowledge of potato tuber metabolism, and it substantiates the validity of the model, in terms of its structure.

8. **Redundancy and robustness:** Redundancy is expressed by the numbers of modes. The number and diversity of elementary modes in this model substantiate the notion that plants have evolved unique cellular and biochemical strategies to cope with their sessile lifestyle, *i.e.* extensive biosynthetic capabilities and metabolic redundancy. Robustness of the system is more concerned with the question of ability to maintain function (in the attached tuber: starch formation plus energy/pyruvate supply; in the detached detached: just energy/pyruvate supply) when subjected to environmental perturbations. Knock-out versions of the model were checked for this ability (see page 94 and page 104).
   Generally, in plants, as it was found here, there is a tendency to employ more than one "road" to get somewhere, *e.g.*: invertase (hydrolysis) and sucrose synthase for sucrose degradation; amylolysis and phosphorylation (StPase) for starch degradation; similarly two possibilities for synthesis of the two; and two enzymes for phosphorylation of F6P; *etc.*

9. **PGI directions** The direction of phosphoglucoisomerase action is very important. Without PGI, the partitioning of carbon is 1:1 exactly in growing tubers, so PGI is needed for any diversion from that ratio, whereas in harvested tubers it is used in forward direction in each of the elementary modes for starch breakdown.

10. **The 'free-energy hypothesis':** The amount of surplus ATP produced by the elementary modes of the versions of the model with no oxidative phosphorylation with those of the models with different stoichiometry of oxidative phosphorylation was compared. This led to the formulation of the hypothesis that the high efficiency of starch synthesis found in growing potato tubers is not possible with cytosolic ATP-production only but non-cytosolic sources of free energy are needed.

11. **Role of FK for sucrose-to-starch conversion:** Fructokinase is employed in each of the 45 sucrose-consuming modes, regardless of whether they ultimately deposit starch or convert all of the sucrose taken up into pyruvate. Fructokinase is concluded to be essential for utilising imported sucrose within the tuber cell.

This indicates FK as a promising candidate, not only for preventing or reducing sucrose accumulation, considering item 6 above, but also for enhancing sink strength, considering item 11.

Overall, structural analysis serves in revealing structural features of the given metabolic network but to what extent or in what proportion to each other the elementary modes are realised in the tuber cells cannot be answered. Further investigations, performed with the kinetic model of carbohydrate metabolism that was built, are shown in Chapter 7 which deals with kinetic modelling and analysis.

Items 5, 6 and 11 from above (glucokinase with its attenuating effect, fructokinase with its effect on sucrose accumulation) also motivated measurements of sugar-phosphorylating activities. The enzyme activity measurements conducted are documented in the following chapter.

Chapter 6

Enzyme Activity Measurements

To supplement the data of enzyme catalytic activities (see Section 3.2.1 - 3.2.3) additional measurements were conducted in crude extracts from the tissue of cold-stored potato tubers. The choice of enzymes, the methods of measurement and the results of the measurements conducted are described in this chapter.

6.1 The Selection

The (maximal) catalytic activities of enzymes are important parameters of the kinetic model, in which they are represented by the limiting rates V_{max} (see Section 2.3). It is known that they do change during storage at low temperatures (Pollock and ap Rees 1975a). This led to the decision to generate more data for certain enzymes. Four catalytic activities in the tubers of wild-type potato plants were determinated, after a short and a long period of storage. They were: total amylolytic activity, starch-phosphorylating activity, and the glucose- and fructose-phosphorylating activities.

It is known that the amylolytic activity changes dramatically during the first two weeks of cold storage (Hill et al. 1996, Nielsen et al. 1997 and Deiting et al. 1998). This is due to the marked increase of one specific form of amylase in potato tubers. More data is available from developing tubers of cv *Desirée* (Sweetlove et al. 1999, Fernie et al. 2002) but prolonged storage was not investigated. Therefore, measurements of total amylolytic activity (combined α- and β- amylase and debranching enzyme) in stored tubers were conducted.

Only little data is available for the limiting rate of starch phosphorylase, which is why starch-phosphorylating activity was also included in the list of measurements. A single value was published recently from cv *Desirée* (486±8 nmol min^{-1} gFW^{-1}, Fernie et al. 2002), and it can be compared with values

obtained in cv *Prairie* (200-260 nmol min^{-1} gFW^{-1}, Dr. Steve Coates, personal communication) and with the results presented here.

Hexokinase data is available of tubers (cv *Desirée*) that were stored for 5 months at 4°C (Renz et al. 1993), and a ratio of 0.67 for fructose- to glucose-phosphorylating activity is reported. One more value for glucokinase activity, again in developing tubers of cv *Desirée*, could be found in Trethewey et al. (1998) (160 nmol min^{-1} gFW^{-1}). Results from the structural analysis of the model showed a crucial role of glucokinase and fructokinase. Thus, hexose-phosphorylating activity was included into the measurements.

Three varieties of *S.tuberosum* which show differing levels of cold-sweetening were chosen: *Hermes* (a low sweetener), *Prairie* (a moderate sweetener) and *Desirée* (a high sweetener). *Desirée* is also the variety used for the majority of measurements and experiments reported in the literature. Activities that were collected from published data mostly came from tubers of *Desirée* plants. Since varieties differ in catalytic activities, it was thought appropriate to include cv *Desirée* in the measurements (to both ensure comparability of the data and compatibility with the model).

Growth conditions for the potato plants, protein extraction procedures and enzyme assay methods are described in the following section.

6.2 Methods

6.2.1 Plant Material

The original stock plants for *Solanum tuberosum* L. cv *Prairie*, cv *Hermes* and cv *Desirée*, propagated at ATC, came from the Scottish Crop Research Institute (SCRI) in Dundee.

6.2.2 Tuber Cultivation / Growth Conditions

Wild-type potato plants of the three varieties *Prairie*, *Hermes* and *Desirée* were grown from seed tubers. They were raised on soil in a greenhouse with automatic watering and 70% relative humidity. One plant each was cultivated in a 7-inch-pot under a 16-h-light regime at 16-22°C. Three plants of cv *Prairie* and five plants of cv *Hermes* were grown from November 2002 to March 2003. Five plants of cv *Desirée* were grown from February 2003 to May 2003.

6.2.3 Harvest and Storage

The tubers were harvested (tubers with a diameter of less than 1cm were discarded) and transferred to cold storage at 6°C. After different storing periods,

10 days and 80 days for cv *Prairie* and cv *Hermes*, 34 and 111 days for cv *Desirée*, tubers were removed from cold storage and used for measurements.

6.2.4 Protein Extraction

An extraction procedure was used that is optimised for potato tubers and established in the ATC laboratories.

Tissue samples with a weight of approximately 1g were taken from the centres of the tubers with a cork borer (diameter 7mm) and homogenised in extraction buffer containing 100mM HEPES (pH 7.0), 5mM EDTA, 5mM DTT 0.5% (w/w) BSA and polyvinylpyrrolidone. The samples were ground with a pestle and mortar and the homogenate was centrifuged at 14000rpm ($\sim$ 21910 g). The supernatant was desalted by passage through a PD-10 Sephadex column (G-25 Medium, Amersham Pharmacia Biotech). The collected elute was assayed for total amylolytic activity and starch phosphorylating activity.

The procedure for hexokinase extraction was as described above but with a different composition of extraction buffer: 50mM HEPES (pH 7.5), 1mM EDTA, 1mM KCl, 1mM $MgCl_2$, 5mM DTT and 0.2% (w/w) BSA. The elute from this extraction was assayed for hexose-phosphorylating activity, *i.e.* glucose-phosphorylating and fructose-phosphorylating activity, respectively.

All chemicals were obtained from Sigma (Poole, UK).

6.2.5 Enzyme Assays

Amylolytic activity:

The total amylolytic activity in thus obtained crude extracts was measured as the degradation of an amylopectin solution in a stopped assay. The degradation products were determined colorimetrically according to the method described by Bernfeld (1955).

Protein extract and buffer were mixed first, and then the reaction was started by adding an amylopectin solution. It was stopped at different time intervals with a di-nitro-salicylic acid solution. After the samples were centrifuged for 5 min at 13000 rpm ($\sim$ 18890 g), the absorbance was read at 510 nm in a spectrophotometer (UVICON 932; Kontron Instruments, Neufahrn, Germany). The total maltose content of the reaction mixtures was estimated by comparison of the absorbance with a maltose calibration series prepared immediately before. The changing maltose concentrations, as a function of time, give the catalytic activity.

Starch- and hexose-phosphorylating activities:

The remaining activities were measured with continuous spectrophotometric assays, according to the method of Turner et al. (1977) for hexokinase, and according to the method of Michal (1984) (by formation of G1P) for starch phosphorylase.

In each case, the reactions were started by adding appropriate substrate solutions.

All assay cocktails contained the enzyme glucose 6-phosphate dehydrogenase (G6PDH), and when G6P was formed via phosphorylation of glucose this led to the reduction of $NADP^+$ to NADPH. The production of NADPH in the assay mixture was estimated spectrophotometrically with an Uvicon 932 spectrophotometer by monitoring the increase in absorbance at 340nm. The change in optical density or absorbance (Δ A) is related to the concentration of NADPH as follows:

$$\frac{\Delta \mathrm{A}}{\mathrm{min}} = \frac{6.22 \frac{\mu \mathrm{mol}}{\mathrm{ml}}}{\mathrm{min}} \tag{6.1}$$

The formation of F6P in the fructose-phosphorylating reaction was coupled to G6PDH via phosphoglucoisomerase.

G1P production in the starch-phosphorylating reaction was coupled to G6PDH by adding phosphoglucomutase.

All chemicals were obtained from Sigma (Poole, UK), and the auxilliary enzymes were obtained from Boehringer Mannheim (now: Roche Diagnostics, Lewes, UK).

6.3 Results

An overview of the results of all measurements that were carried out is given in Table 6.1. The measured activities are not compartment-specific, since the crude extracts were produced from homogenised tissue samples.

Table 6.1: Maximal enzyme catalytic activities measured in crude extracts from potato tubers stored at 6°C.
In parentheses the sweetener type of the variety is shown. Results given are mean values ± SD (n=3-5). The number of tubers measured was 3 to 5.
[a] only 2 tubers measured; [b] measurement after storage for 112 days.

Variety	Max. activity	Activity in nmol min^{-1} gFW^{-1} after storage for			
		10 days	34 days	80 days	111 days
Hermes (low)	total amylolytic	238±91		651±77	
	starch-phosphorylating	192±124		657±156	
Prairie (moderate)	total amylolytic[a]	525±58		900±14	
	starch-phosphorylating[a]	141±37		511±34	
Desirée (high)	total amylolytic		825±134		820±200
	starch-phosphorylating		430±128		577±70
	glucose-phosphorylating		36±9		95±19[b]
	fructose-phosphorylating		271±25		172±21[b]

Amylolytic activity: Figure 6.1 shows the results for total amylolytic activity. There clearly is an increase during cold storage. Using a Student's t-test, this increase has a significance level of more than 99% for cv *Hermes* (P<0.001) and of more than 95% for cv *Prairie* (P=0.024). The onset of this increase can not be determined precisely because of the sparseness of the data (only two data points for every variety) but it can be assumed that it takes place before 30 days of storage, since it then seems to reach a plateau (see the data for cv *Desirée* with no significant change between the two periods).

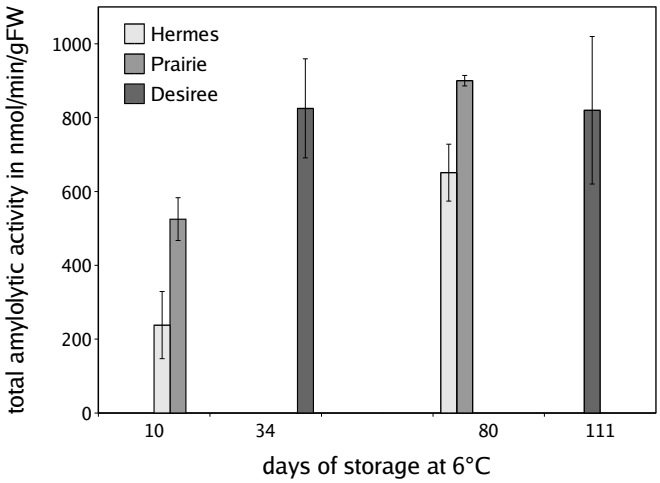

Figure 6.1: Total amylolytic activity in tubers of three potato varieties after different periods of cold-storage.
Results represent means ± SD (n=2-5) and are given in nmol min^{-1} gFW^{-1}. There is a significant increase between the earlier and the later measurement for cv *Hermes* and cv *Prairie* (P<0.001 and P=0.024 in Student's t-test) but no significant change for cv *Desirée*.

Furthermore, it can be noticed that the *Prairie* values are higher than the *Hermes* values, suggesting a correlation to their classification as 'moderate' and 'low' sweeteners, respectively. This trend, however, is not adopted by the values for *Desirée*, which are between the values of *Prairie* and *Hermes*. Therefore, it is not possible to conclude a relationship between amylolytic activities and the level of sweetening occuring in the three varieties.

Starch-phosphorylating activity: Starch-phosphorylating activity (see Figure 6.2) appears to increase continously during cold storage. The statistical test shows that the increase of activity from 10 days to 80 days is significant, whereas no conclusions can be drawn for the further prolonged storage up to 111 days.

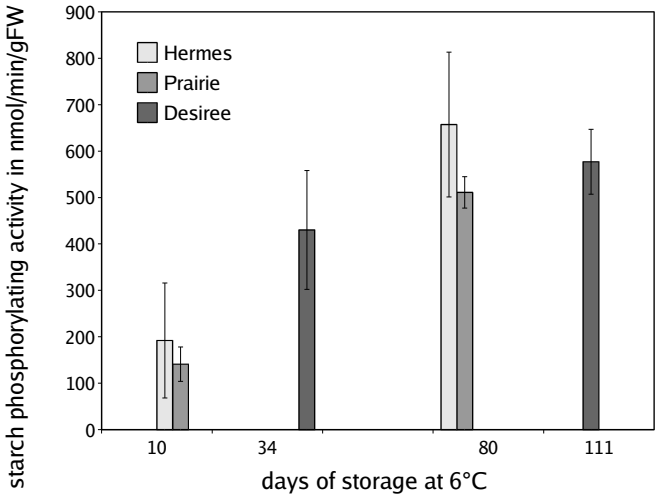

Figure 6.2: Total starch-phosphorylating activity in tubers of three potato varieties after different periods of cold-storage.
Results represent means ± SD (n=2-4) and are given in nmol min^{-1} gFW^{-1}. There is a significant increase between the earlier and the later measurement for cv *Hermes* and cv *Prairie* (P=0.03 and P=0.018 in Student's t-test) but no significant change for cv *Desirée*.

Hexose-phosphorylating activities: The results for hexose-phosphorylating activity in tubers of the variety *Desirée* are shown in Figure 6.3. The observations document a considerable increase in glucose-phosphorylating activity and a considerable decrease in fructose-phosphorylating activity (for statistical test results see Figure 6.3). Furthermore, the ratio of glucose- and fructose-phosphorylating activities can be calculated from the absolute values in Table 6.1. It increases from 0.13 (after 34 days) to 0.55 (after 112 days).

Additional measurements indicated that hexose-phosphorylating activity in the extracts was very temperature-sensitive and decayed quickly (data not shown). Thus, the measured glucose- and fructose-phosphorylation rates (Table 6.1 and Figure 6.3) most probably present an underestimation of the rates of phosphorylation occuring *in vivo*. A more reliable value is the ratio of the two, since the same extract was used for both assays and both measurements were carried out simultaneously.

6.4 Conclusions

From the results (Table 6.1), it was concluded that the total amylolytic activity and the starch-phosphorylating activity rise in stored potato tubers between 10 and 80 days of storage at 6°C. Also, glucose-phosphorylating activity increases between 34 and 112 days of cold-storage, whereas fructose-phosphorylating ac-

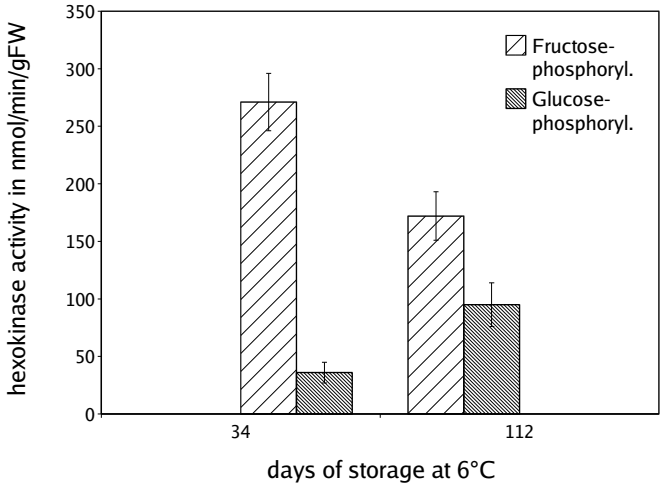

Figure 6.3: Glucose- and fructose-phosphorylating activities in tuber tissue of *S.tuberosum cv Desirée* after different periods of cold-storage.
Results represent means ± SD (n=3-4) and are given in nmol min^{-1} gFW^{-1}. There are significant changes between the earlier and the later measurement for both activities (P-values<0.01 in the Student's t-test).

tivity increases in the same period of time (in the same tubers).

In retrospect, for more precise and quantitative data, activities should ideally have been measured at several time points, *e.g.* after 0, 2, 5, 10, 20 and 80 days of storage. However, the changes seen were significant, and the long cycle time for an experiment from planting to completion of enzyme measurements did not allow further studies to be conducted.

As explained before, the measurements described in this chapter were performed in order to complement the data collected from the literature.

The maximal catalytic activities were incorporated in the kinetic model of the detached tuber. They enter the model as the system parameters V_{max} (limiting rates) for the corresponding reactions.

For total amylolytic activity, the values ascertained here have been included in the model, although the measurements described above were for starch-to-maltose breakdown only. The assumption was made that this rate can serve as an estimate for the rate of starch-to-glucose breakdown.

Plastidic starch-phosphorylating activity in potatoes was found to be induced by sucrose abundance (St-Pierre and Brisson 1995). Since this is a follow-on process, caused by sucrose accumulation, it was decided to incor-

porate only the lower of the measured values, 200±100 nmol min^{-1} gFW^{-1} (after 10 days of storage, see Table 6.1), into the model.

For hexose-phosphorylating activity not only the absolute values are of interest but also the ratio of glucose- and fructose-phosphorylating activities. It can be calculated from the absolute values shown in Table 6.1. It increases from 0.13 (after 34 days) to 0.55 (after 112 days). The two activities appear to change inversely proportional. This observation fits well into the pattern reported by Renz and Stitt (1993) who measured a ratio GK over FK of 0.67 in tubers stored for 5 months (≈150d). If it is assumed that the data is comparable, this suggests a continuous increase of the GK/FK ratio throughout storage. This assumption is also supported by the fact that the ratio of GK and FK was much smaller in growing tubers and increasing above unity in sprouting tubers, as also reported by Renz and Stitt (1993).

Chapter 7

Kinetic Modelling

The findings of the structural analysis discussed in Chapter 5 confirmed that the model reproduces many of the empirically observed features of both potato tuber carbohydrate metabolism in growing and in stored tubers ('attached' and 'detached' model).

Based on the structural model, a kinetic model was built by adding kinetics to the list of reactions. This procedure was described before in Section 4.1.6, where it had also been noted that rather than attempting to build a kinetic model of a stored tuber (detached), because of lack of data, it was decided to focus on a model of a developing or growing tuber (attached).

All rate equations and kinetic parameters incorporated are listed in Appendices B.1 and B.2. External metabolites are system parameters and have to be set in advance. Starch occurs in none of the rate equation, an arbitrary value for glucose equivalents of 1000mM was chosen (emphasising the abundance). Pyruvate appears in the rate equation for pyruvate kinase only. Measurements by Mooney (1994) showed that its concentration is close to the concentration of GAP and PEP, therefore, it was set to be 10μM. Extracellular sucrose was set to 90mM. The version of the model with an ATP-yield of 1.83 from oxidative phosphorylation was chosen (according to Groen et al. 1992, see Section 4.1.4).

7.1 Initialisation of the Model

The complete *ScrumPy* - readable script that represents the model, as used for all the analysis in Chapter 5 and in this chapter, is shown in Appendix B.3. It consists of three parts, firstly, the list of reactions, including reaction names, stoichiometries and rate equations, secondly, a list of all kinetic parameters, and thirdly, the initialisation of metabolite concentrations. (Only metabolite concentrations have to be initialised. Reaction rates are then fully determined through the rate equations.)

When deciding on the values for the third part of the script, the initial metabolite concentrations, the conservation relationships as determined by struc-

tural analysis (see Section 5.2.2) have to be observed. The initial values for metabolites contributing to one or more conserved sums must be chosen carefully, since, once initialised, the total of these metabolite concentrations remains unchanged at each point of time.

There are four conservation relationships in the model, and they are listed in Table 5.1 on page 88. According to these conservation relationships, conserved sums were derived from experimental data, *i.e.* measured concentrations of those metabolites contributing to a relationship were summed up. The data from Tiessen et al. (2002) was used for this calculation (attached tubers, Table A.1 or Table 7.1). The values that were eventually considered are (the sum derived from the experimental data is given in brackets):

1. sum of all cytosolic adenosine phosphates: 380μM [379.3]
2. sum of all plastidic adenosine phosphates: 350μM [349.5]
3. sum of all cytosolic uridine phosphates: 900μM [861.4]
4. sum of all phosphorylated metabolites and free phosphate: 6000μM [>5597.8[1]]

These fixed sums were set in the kinetic model by entering the initial metabolite concentrations accordingly. For example, for cytosolic adenosine phosphates ATP=200μM and ADP=180μM were chosen.

Nucleotide pool sizes are significant, as it was shown that the overall levels of adenine and uridine nucleotides are 2-3 fold higher in PPase-transformants than in wild-type tubers (Geigenberger et al. 1998). One path of investigation not followed on for now is to initiate with different conserved sums and observe any occuring differences in the behaviour of the model.

7.2 Simulation and Steady-State

7.2.1 Steady-State Results (Validation)

The system, as modelled, reaches a (numerical) steady state. In the following, the two sets of variables, internal metabolite concentrations and reaction rates, that the system adopts at this steady state, are presented.

7.2.1.1 Metabolite Concentrations

The model was tested for reproducing the metabolite data as measured in Golm (Farré et al. 2001, Tiessen et al. 2002).

Table 7.1 shows all 28 internal metabolite concentrations at steady state of the kinetic model. For comparison, they are listed together with the published

[1]Because not all of the concentrations required for calculating this conserved sum were measured by Tiessen et al. (2002) this sum had to be approximated.

experimental data from Farré et al. (2001) and from Tiessen et al. (2002). Both sets of measurements are listed in order to illustrate the variance even between two measurements of different plants in different years but by the same lab.

Table 7.1: Metabolite concentrations in the cells of developing tubers.
*measured by Farré et al. 2001; **measured by Tiessen et al. 2002.

Metabolite		Concentration in μM		
in cytosol	in amyloplast	exp.data*	exp.data**	model data
Sucrose		41000	82400	87648
Fructose		<100	1370	13
Glucose		31000	-	38
	Glucose	16000	-	3346
UDP-glucose		830	571	729
UTP		400	238	155
UDP		58	52	16
G1P		51	43	69
	G1P	80	17	28
G6P		340	510	1173
	G6P	970	379	485
F6P		170	147	295
F16BP		-	-	0.5
DHAP		-	-	19
GAP		-	-	0.7
3-PGA		300	296	209
	3-PGA	460	198	86
2-PGA		-	-	25
PEP		57	-	38
	ADP-glucose	-	22	61
ATP		210	292	346
	ATP	495	179	198
ADP		18	87	34
	ADP	240	149	91
pyrophosphate		23	12	2.2
	PP_i	3	2.4	1.0
orthophosphate		-	2400	2025
	P_i	-	870	839

Overall, the agreement is satisfactory. Plastidic and cytosolic pools of metabolites agree closely in absolute values as well as with the gradients between the two compartments (where applicable). The model provides theoretical values for all metabolites incorporated but, as can be seen in Table 7.1, not all of them have actually been determined *in vivo*. For those no comparison is possible.

GAP and DHAP values are very small. Because of the toxicity of the short chain sugars glyceraldehyde and dihydroxyacetone, it is probably important that the steady state concentrations of dihydroxyacetone phosphate and 3-phosphoglyceraldehyde be kept low. Also, the very low concentrations of F16BP, GAP and DHAP might be the reason for them being omitted in measurements.

The modelled ratios of ATP and ADP in the cytosol, ATP and ADP in the amyloplast and of UTP and UDP in the cytosol, are compared with the experimental data from Farré et al. (2001)* and Tiessen et al. (2002)** observed empirically:

ratio	compartment	exp.data*	exp.data**	model
UTP/UDP	cytosol	6.90	4.54	9.78
ATP/ADP	cytosol	11.67	3.34	10.07
ATP/ADP	amyloplast	2.06	1.20	2.18

Generally, the values for the nucleoside triphosphates are higher than has been observed *in vivo*, at the expense of the nucleoside diphosphates which are lower than observed *in vivo*, but ATP/ADP ratios are difficult to measure, since only a slight degree of hydrolysis of ATP during the preparation of the samples will affect the result. NMR measurements *in vivo* generally give higher ratios than biochemical analysis of extracts.

The two cytosolic ratios NTP/NDP are very close because of the swift action of NDPK which is very efficient in the model. It might not be very important to get these ratios right because it is really hard to measure *in vivo* NTP/NDP ratios, as can be seen already from ratios given by the two papers which are quite different.

The most obvious discrepancy of model data compared to experimental data is that fructose and glucose concentrations are much smaller than experimentally verified. This can be related to the low K_m of both glucokinase and fructokinase for their substrates (see parameter consensus list in Appendix B.2). This immediately raises the question: how can these two reducing sugars possibly accumulate in stored tubers? It suggests that GK and FK must be regulated more efficiently *in vivo* than is now considered in the model, maybe by an yet unknown mechanism.

Fructokinase is substrate-inhibited by fructose, so, once fructose levels get over a certain threshold value, FK inhibition by its own reactant will decrease its activity and allow fructose to accumulate (potential for a bistable system, with a high concentration and a low concentration steady state). But it is not apparent how fructose can reach the threshold value (>5mM) needed for the switch to the higher value.

7.2.1.2 Steady State Fluxes

Not all fluxes, or rates of individual reactions, need to be inspected but rather only a selection that characterise the metabolic and biological function of the system at this steady state. Interesting fluxes in this respect are: sucrose uptake (`SucSupply`), net starch formation (starch deposition as it is called herein since page 102), and glycolytic flux (represented by any of the reactions downstream of aldolase). Starch formation or deposition is a composite flux, it can only be expressed as the sum of several individual rates (Equation 7.1) or, with one variable fewer, as a function of sucrose uptake and glycolytic flux (Equation 7.2):

$$J_{StarchDeposit} = v_{StSynth} - v_{StPase} - v_{degr} \tag{7.1}$$

$$J_{StarchDeposit} = 2 \cdot J_{SucroseUptake} - J_{Glycolysis} \tag{7.2}$$

where

$$J_{SucroseUptake} = v_{SucroseSupply}$$

and

$$J_{Glycolysis} = v_{ald} = v_{TPI} = \frac{v_{GAPDH_PGK}}{2} = \frac{v_{PGlyM}}{2} = \frac{v_{eno}}{2} = \frac{v_{PK}}{2}$$

.

Net fluxes in the model at steady state are:

Sucrose uptake	23.5 nmol sucrose min^{-1} gFW^{-1}
Sucrose cycling	21.7% of the sucrose uptake flux
Starch deposition	26.8 hexose nmol min^{-1} gFW^{-1}
Starch cycling	45.7% of starch synthesis, relative to starch synthase reaction

These flux values are comparable with observed values, a collection of which is listed in Table A.2 on page 161 in the Appendix. Turnover of sucrose seems to be a widespread phenomenon in plants, and it has been found experimentally in developing tubers (Geigenberger and Stitt 1993).

The efficiency of starch deposition was defined earlier for the structural model (net stoichiometries only, see Equation 5.1 in Section 5.2.5). Now it can be expressed for the metabolic fluxes in the kinetic model:

$$eff = \frac{J_{StarchDeposit}}{2 \cdot J_{SucroseUptake}} = \frac{v_{StSynth} - v_{StPase} - v_{degr}}{2 \cdot v_{SucroseSupply}} \tag{7.3}$$

Substitution of the numerator, using equation 7.2 decreases the number of variables from four to two. Witness:

$$eff = 1 - \frac{J_{Glycolysis}}{2 \cdot J_{SucroseUptake}} = 1 - \frac{v_{ald}}{2 \cdot v_{SucroseSupply}} \tag{7.4}$$

Insertion of the above values into this equation gives an efficiency of *eff*=0.57.

Overall the steady state results agree well with the experimental data. Extracellular sucrose is taken up by the cell, and its cleavage products contribute to the accumulation of starch or are further metabolised to pyruvate. The fluxes are in the right order of magnitude, even the distribution between glycolysis and starch synthesis (with ≥50% being diverted into starch) closely reproduces the one *in vivo*.

Thus validated, a control analysis was performed on the model.

7.2.2 Metabolic Control Analysis (Interrogation)

For the steady state obtained, flux control coefficients could be calculated. In Table 7.2 the calculated flux control coefficients C_v^J toward sucrose uptake, toward starch deposition, and toward glycolysis are listed. These three fluxes are most representative, they span the metabolic field of functions of the system under investigation. They are also related to each other by Equation 7.2.

All coefficients are rather small, apart from invertase. Invertase has the highest control over starch deposition (*i.e.* much of the control operating at the first step) but the table also shows that this is mainly achieved by controlling sucrose uptake. Invertase also has the highest control coefficient with regard to glycolytic flux, only followed by PK with a value half as high as invertase's.

An interesting point is that both PFK and PK have negative control over starch deposition and positive control over sucrose uptake. They are only two enzyme with this pattern, all other reactions show the same direction of control towards these two metabolic fluxes. Whereas for the control between starch deposition and glycolysis most of the reactions (if they do actually have a value significantly different from zero) do show the opposite sign with regard to the two, *i.e.* if negative for glycolysis then positive for starch deposition, and the other way around.

The control of 3-PGA translocation is zero. This enzyme does not carry a flux at steady state.

Comparison of modelled C_v^J with experimentally determined C_v^J

A few control coefficients were reported in the literature. They can be compared with the values calculated from the model.

1. Trethewey et al. (1999) have shown that sucrose hydrolysis exerts control over glycolysis and respiration in potato tubers. The control coefficient of invertase over glycolytic flux in the model $C_{v_{inv}}^{J_{Glycolysis}}$ is 0.41, and it is also the highest one with regard to glycolysis.

Table 7.2: The three flux control coefficients C_v^J, for sucrose uptake, for starch deposition and glycolysis. Reactions that have a rate equation describing an irreversible mechanism are marked with a star *

Rate	irrev.	Control coefficients		
v_i	*	$C_{v_i}^{J_{SucroseUptake}}$	$C_{v_i}^{J_{StarchDeposit}}$	$C_{v_i}^{J_{Glycolysis}}$
degr	*	- 0.0043	- 0.0182	+ 0.0141
StPase		- 0.0089	- 0.0865	+ 0.0936
pPGM		+ 0.0003	+ 0.0010	- 0.0006
AGPase		+ 0.0160	+ 0.0354	- 0.0097
StSynth	*	+ 0.0062	+ 0.0159	- 0.0065
PPase		+ 0.000024	+ 0.000048	- 0.000007
Gexp		- 0.0041	- 0.0174	+ 0.0135
G6P/P		+ 0.0001	+ 0.0003	- 0.0002
PGA3/P		+ 0.0	+ 0.0	+ 0.0
AATP		+ 0.0032	+ 0.0089	- 0.0042
Pexp		- 0.0030	- 0.0025	- 0.0035
cPGM		- 0.000001	- 0.000001	- 0.000000
UGPase		- 0.000003	- 0.000005	- 0.000000
PGI		+ 0.0000	+ 0.0005	- 0.0005
SPS_SPP		- 0.0151	- 0.0328	+ 0.0084
SuSy		+ 0.0114	+ 0.0108	+ 0.0120
inv	*	+ 0.9129	+ 1.2934	+ 0.4106
GK	*	+ 0.0554	+ 0.0783	+ 0.0253
FK	*	+ 0.0186	+ 0.0263	+ 0.0085
PFK	*	+ 0.0175	- 0.0380	+ 0.0908
PFP		- 0.0057	- 0.0094	- 0.0008
ald		- 0.0042	- 0.0069	- 0.0006
TPI		- 0.0006	- 0.0011	+ 0.0001
GAPDH_PGK		- 0.0006	- 0.0011	+ 0.0000
PGlyM		- 0.0053	- 0.0134	+ 0.0053
eno		- 0.0150	- 0.0382	+ 0.0156
PK	*	+ 0.0185	- 0.1144	+ 0.1939
NDPK		- 0.0003	- 0.0003	- 0.0003
ATPutil		- 0.0001	- 0.1005	+ 0.1323

2. Figure 1 in Sweetlove et al. (2001) suggests that the control of PFK over starch synthesis and respiration is very small. The $C_{v_{PFK}}^J$ calculated for the model are: $C_{v_{PFK}}^{J_{StarchDepos}}$ = -0.038 and $C_{v_{PFK}}^{J_{Glycolysis}}$ = 0.091. These values are not large but they do actually present the 7th and 5th highest absolute values in the list for the corresponding process.

3. A small collection of experimentally determined control coefficients in growing potato tubers was published recently (Geigenberger et al. 2004). Comparison of those coefficients that were calculated for the model with those that are

also in that collection shows quite good agreement for some (SuSy, UGPase, SPS) but not for all (see Table 7.3). Generally, the coefficients are much smaller when calculated from the model but there is agreement in most of them in their signs (+/-).

Table 7.3: Comparison of the flux control coefficients C_v^J collected from various separate experiments by Geigenberger et al. (2004) and those calculated for the model. ?? - marks values that could not be found by Geigenberger et al. (2004).

Enzyme	Control coefficients C_v^J	
	according to	according to model
v_i	Geigenberger et al. (2004)	$C_{v_i}^{J_{StarchDeposit}}$
SuSy	+0.10	+0.0108
UGPase	approximately 0.0	-0.000
GK	approximately 0.0	+0.0783
FK	??	+0.0263
cPGM	+0.15	-0.000001
GPT	??	+0.0003
AATP	+0.98	+0.0089
pPGM	+0.23	+0.0010
AGPase	+0.35	+0.0354
StSynth	+0.12	+0.0159
PPase	??	+0.00005
SPS	-0.15	-0.0328
PFP	+0.25	-0.0094

Response coefficients C_X^J of sucrose uptake, starch deposition and glycolysis were calculated with regard to the two external metabolites sucrose and pyruvate instead of to a reaction. (Starch was omitted because it does not appear in any rate, and all three values are equal to zero.) These coefficients are shown in Table 7.4. Not unexpectedly, the sucrose presented to the cell has a major influence on all metabolic fluxes.

Table 7.4: Response coefficients C_X^J of sucrose uptake, starch deposition and glycolysis with regard to the two external metabolites sucrose and pyruvate.

External metabolite	Control coefficients		
X_i	$C_{X_i}^{J_{SucroseUptake}}$	$C_{X_i}^{J_{StarchDeposit}}$	$C_{X_i}^{J_{Glycolysis}}$
x_Sucrose	0.2640	0.3805	0.1103
x_Pyruvate	-0.0001	0.0004	-0.0008

7.3 'Scenarios'

The comparison of model steady state values with experimental data of metabolite concentrations and metabolic fluxes shows acceptable agreement. The next step for validation of the model is to test if it can reproduce (at least in qualitative terms) so called 'scenarios'. These are observations or experiments that were made by several groups. The experiments were set up in the model, simulated and compared.

1. **PFK-overexpression:** The overexpression in potatoes of bacterial PFK (up to 30×) had no effect on the metabolic fluxes but an increase in the concentrations of metabolites downstream of F6P was observed in aged discs of tubers (Burrell et al. 1994). For growing tubers there is less data. Sweetlove et al. (2001) report that PFK×2.1 and PFK×2.5 developing tubers have 3× higher 3-PGA content and G6P is lowered to 80%.
   This behaviour is matched well by the model: PFK×2.5 and PFK×25 cause little change in sucrose uptake (23.5, 23.8, 24.8 nmol min^{-1} gFW^{-1} of sucrose from outside the cell), sucrose cycling goes down (21.7%, 17.4%, 9.3%), starch cycling (45.7%, 48.8%, 51.8%) and *eff* (0.570, 0.545, 0.515) change only little. For changes in metabolites see Figure 7.1 (note the marked increase in glycolytic metabolites downstream of F6P).

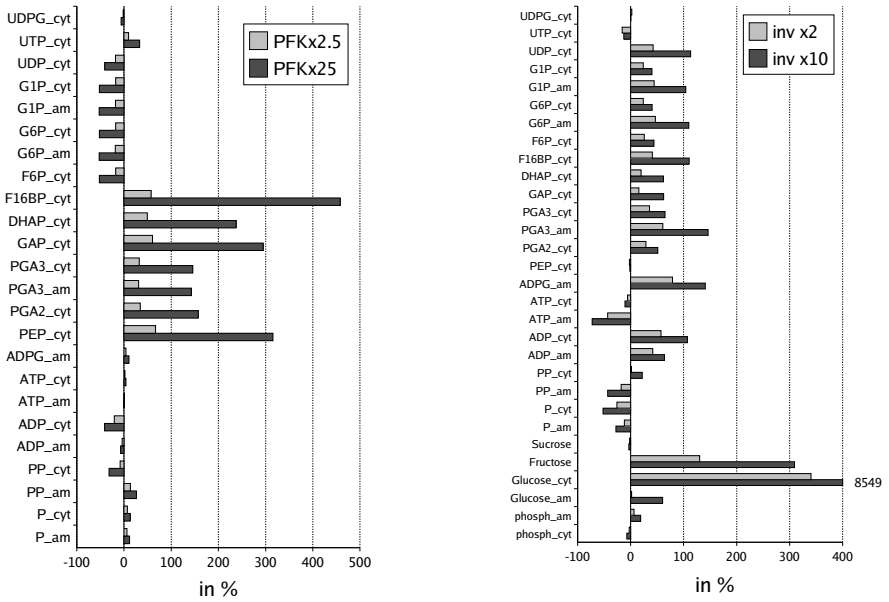

Figure 7.1: Relative changes in metabolites when PFK (left panel) or invertase (right panel) are overexpressed in the model.

2. **PFP-antisense-inhibition:** Hajirezaei et al. (1994) found that antisense transformation of potato, resulting in decreased expression of PFP (by 70-

90% in growing tubers and by 88-99% in stored tubers), did not change cold-induced sugar accumulation but the tubers contained 20-40% less starch. Also, in growing tubers, 3-PGA and PEP went down to 40%, the rest (UDPG, G6P, ATP, ADP, PP_i) was unchanged. And in mature tubers G6P was higher (50%) and 3-PGA was lower. They also did 30d storage at 4°C and UDPG, G6P and F6P went up in those, whereas 3-PGA and PEP went down. Hajirezaei et al. (1994) concluded that PFP does not contribute to the control of glycolytic flux.
The model shows no significant change at all, either in metabolite concentrations or in metabolic fluxes. This probably due to the very small flux PFP carries in the modelled steady state (≈1% of glycolytic flux only).

3. **AGPase-manipulation:** A 4-5-fold increase in activity of the enzyme, achieved by transformation with an *E.coli* AGPase gene (Sweetlove et al. 1996a), had no detectable effect on the starch content of developing or mature tubers (Sweetlove et al. (1996b)). Pulse-chase experiments with labelled sucrose showed that the flux from labelled sucrose into starch increased in the transformed tubers (roughly in proportion to the increase in AGPase activity, C_{AGPase}^{AGPase}=1) but also that it was accompanied by an increased rate of starch turnover. (Note that this implies $C_{AGPase}^{StarchDeposit}$=0 in disagreement with Geigenberger et al. (2004) and in Table 7.3.) Increasing V_{max} of AGPase in the model results in the following changes in metabolic fluxes (original values in brackets):

Sucrose uptake	23.6 nmol sucrose min^{-1} gFW^{-1} [23.5]
Sucrose cycling	13.7% of the sucrose uptake flux [21.7%]
Starch deposition	27.7 hexose nmol min^{-1} gFW^{-1} [26.8]
Starch cycling	54.2% of starch synthesis, rel. to StSynth reaction [45.7%]

4. **Overexpression of invertase:** Sonnewald et al. (1997) reported that specific expression of a yeast invertase in cytosol of tubers led to 95% reduction in sucrose content, but that this was accompanied by a larger accumulation of glucose and a reduction in starch.

   Hajirezaei et al. (2000) report for tubers with elevated cytosolic invertase activity that their hexose phosphate levels and 3-PGA are increased, as well as glucose levels, whereas sucrose levels are decreased.

   These findings can be matched qualitatively by the model. Two-fold and ten-fold overexpression of invertase reduces sucrose, and increases glucose in the cytosol (see Table 7.1, note that relative changes are shown, and sucrose has a rather high steady state concentration in comparison to glucose). But the total amounts are nowhere near the experimental reported results. This, again, can be explained by the action of glucokinase, which

by its activity and very high substrate specifity (low K_m) does not allow for a considerable glucose accumulation.

The metabolic fluxes at the steady states for two- and ten-fold overexpressed invertase change dramatically. Sucrose uptake fastens and the efficiency of starch deposition increases from 0.57 in the original model to 0.66 and even 0.70 in the manipulated model. This is also a reflection of the flux control coefficients that were discussed in the previous section.

Test for FK Of the candidates that were distinguished before (in the strcutural analysis, see page 99) for reducing cold-sweetening, two were discussed so far, PFK and invertase.

For fructokinase no such experiments have been published, and the model was used to simulate the manipulation of the fructose-phosphorylating step:

- 10-fold overexpression of FK results in a minimal change in metabolic fluxes with a minimal decrease in *eff*.
- Downregulation of FK results in fructose levels increasing (but not dramatically). Effects on both sucrose uptake and efficiency of starch deposition start at about -80% only.

7.4 Detached Tuber Model

The model for a cold-stored was obtained in two steps. The first step is the detachment, and then, the second step is the incorporation of changes in tuber physiology caused by storage at low temperature (*i.e.* changes in catalytic activity of some enzymes or changes in their regulation).

7.4.1 1st Step: Detachment

Detachment is modelled as the reverse of what was explained in Section 4.1.5, simply by disconnecting reaction T_0 - `SucSupply`. As initial metabolite concentrations, the metabolite concentrations from the steady state of the attached model are used.

The dynamic response of the system is that immediately after detachment the intracellular sucrose level starts to decrease. Within one day[2] it drops from over 80mM to 56mM, and then further over three more days to to 5mM. Also, in Tiessen et al. (2002) this trend was observed after 1d and 3d of detachment (see Table A.1). Sucrose levels as well as net starch synthesis decrease by ca. 30% after 1 day, and by further 30% after 3 days. This is matched very well by the model. Hexose phosphate levels, though, do not match. In the model they decrease, whereas in the tubers measured by Tiessen et al. (2002) they increase. An overview of changes the model variables undergo is shown in Figure 7.2.

[2]All activities are in nmol min^{-1} gFW^{-1}, hence, 1440 simulation steps represent 1 day.

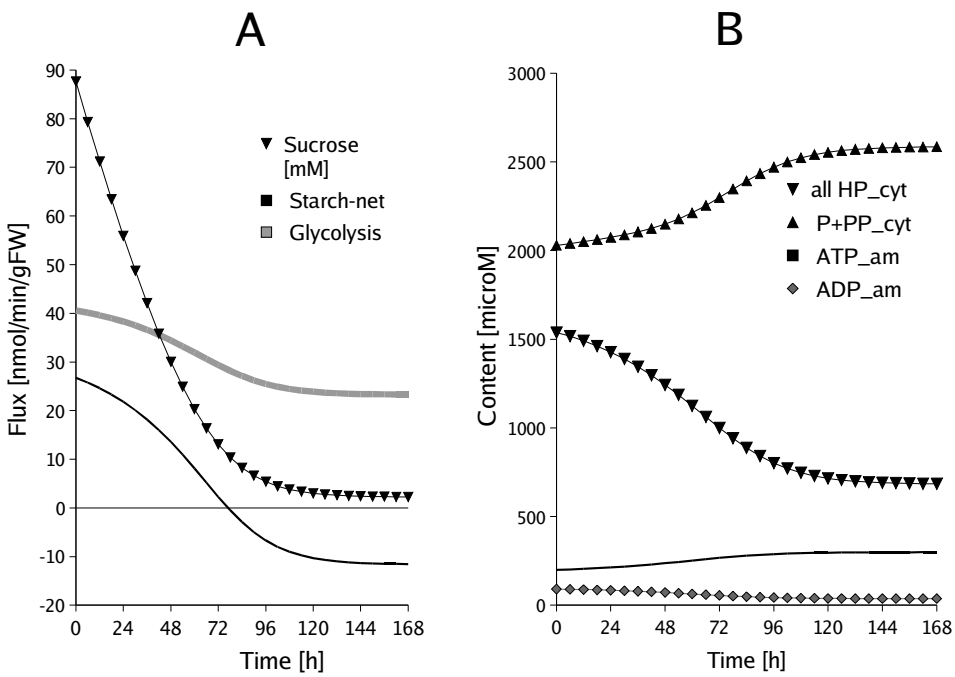

Figure 7.2: Response of the model to detachment.
A Sucrose depletion within 3-4 days. After 3 days starch net synthesis becomes starch net degradation. Glycolytic flux decreases.
B Concentration of free phosphate increases, at the expense of the phosphorylation status of hexoses (HP). The ATP to ADP ratio rises in the amyloplast.

In principal, in this manner, a new steady state is approached, with starch degradation as the only metabolic flux, and channeling of all products into glycolysis. Net starch degradation (or glycolysis) settles at 11.6 nmol min^{-1} gFW^{-1} (in hexose units), and there is 55.9% starch turnover (now: relative to StPase+degr). Sucrose cycling is 2.9 nmol min^{-1} gFW^{-1} that is 25% relative to total starch degradation (or glycolysis).

Since the model settled in a steady state, it is possible to calculate concentration control coefficients according to the definitions in Metabolic Control Analysis (see Section 2.3.3). This was done for the four sugars considered in the model, sucrose, fructose, plastidic and cytosolic glucose. The control coefficients are listed in Table 7.5.

Inspection of Table 7.5 reveals that the concentration of plastidic glucose is completely controlled by its formation via starch degradation and its export into the cytosol. The control by these two reactions is also notable in cytosolic

Table 7.5: Concentration control coefficients C_v^S calculated for the model just after detachment.

Enzyme	Control coefficients C_v^S toward			
	Sucrose	Fructose	Glucose_cyt	Glucose_am
degr	+ 0.0617	+ 0.0653	+ 0.3510	+ 0.5073
StPase	+ 0.8937	+ 0.8901	+ 0.4218	+ 0.0003
pPGM	+ 0.0032	+ 0.0030	+ 0.0014	+ 0.0000
AGPase	- 0.5741	- 0.5286	- 0.2436	- 0.0002
StSynth	- 0.0297	- 0.0276	- 0.0128	- 0.0000
pPPase	- 0.0001	- 0.0001	- 0.0001	- 0.0000
Gexp	+ 0.0599	+ 0.0633	+ 0.3404	- 0.5069
G6P/P	+ 0.0020	+ 0.0019	+ 0.0009	+ 0.0000
AATP	- 0.0200	- 0.0187	- 0.0087	- 0.0000
Pexp	+ 0.0009	- 0.0015	- 0.0009	- 0.0000
cPGM	+ 0.0005	+ 0.0005	+ 0.0002	+ 0.0000
UGPase	+ 0.0007	+ 0.0006	+ 0.0003	+ 0.0000
PGI	+ 0.0085	+ 0.0080	+ 0.0019	+ 0.0000
SPS_SPP	+ 0.4105	+ 0.3970	+ 0.1682	+ 0.0001
SuSy	- 0.0674	+ 0.0991	- 0.0272	- 0.0000
inv	- 0.8722	+ 0.0249	+ 0.0842	+ 0.0001
GK	- 0.0038	+ 0.0002	- 1.0832	- 0.0007
FK	- 0.0044	- 1.0105	+ 0.0003	+ 0.0000
PFK	- 0.3498	- 0.4118	- 0.2049	- 0.0001
PFP	+ 0.4139	+ 0.3892	+ 0.1722	+ 0.0001
ald	+ 0.0105	+ 0.0099	+ 0.0044	+ 0.0000
TPI	+ 0.0017	+ 0.0016	+ 0.0007	+ 0.0000
GAPDH_PGK	+ 0.0011	+ 0.0011	+ 0.0005	+ 0.0000
PGlyM	+ 0.1060	+ 0.0982	+ 0.0454	+ 0.0000
eno	+ 0.3267	+ 0.3028	+ 0.1400	+ 0.0001
PK	- 0.2001	- 0.3199	- 0.1701	- 0.0001
NDPK	+ 0.0104	- 0.0107	+ 0.0041	+ 0.0000
ATPcons	- 0.1904	- 0.0274	+ 0.0134	+ 0.0000

glucose but there it is alleviated, and cytosolic glucose is equally or even stronger controlled by other steps in the network.

Fructose and glucose in the cytosol have a very similar pattern for the whole range of reactions, the most striking difference being the distinction between glucokinase and fructokinase, with a $C_{Hexokinase}^{Hexose}$ of -1 for their respective substrates.

It is questionable, though, if this version of the model, with its very low sugar concentrations, especially of sucrose, reflects the marked changes in cold-stored compared to just stored tubers. Further changes were applied.

7.4.2 2nd Step: Low Temperature

Changes in gene expression can occur within days, and either this or another mechanism, maybe involving the redox status or pH, do lead to changes in some of the enzymes, once the potato tubers have been transferred to (exposed to) low temperatures for storage. The following changes were applied in order to model the transfer of tubers to the cold:

1. A new isoform of amylase appears within several days at 4°C (Hill et al. 1996, Nielsen et al. 1997 and Deiting et al. 1998). This also corresponds with the measurement of rising total amylolytic activity during storage at 6°C reported in Section 6.3. For the modification of the model the activity value of 825 nmol min^{-1} gFW^{-1} measured in cv *Desirée* was used.

2. After 8 days of storage SPS activity is twice as high as before (Geigenberger and Stitt 1993). After only 2 to 4 days in cold-storage SPS activity rises 3-5 fold (Hill et al. 1996 and Deiting et al. 1998). This was rise in SPS activity was modelled by setting V_{max} of this reaction to 4000 nmol min^{-1} gFW^{-1} (was 797 before).

3. Geigenberger and Stitt (1993) reported a decrease in invertase activity in cold-stored tubers. The model value was changed from 33 to 15 nmol min^{-1} gFW^{-1}.

4. Tiessen et al. 2002 studied the enzyme kinetics of AGPase of extracts from 1-day-detached tubers, and they found: when growing potato-tubers are detached from their mother plant there is a rapid inhibition of starch synthesis, involving inhibition of ADP-glucose pyrophosphorylase. This was due to an increased activation constant K_a(3-PGA) of AGPase in response to detachment. In the model the K_a(3-PGA) of 10μM was set to a higher value of 500μM.

5. PFK is long known to be cold-labile (Pollock and ap Rees 1975a). The value from Mooney 1994 (27 nmol min^{-1} gFW^{-1}) was used. This represents a decrease by 80%.

6. Fructokinase activity decreases (see measurements in Chapter 6). V_{max} of FK was adjusted from 376 to 271 nmol min^{-1} gFW^{-1}.

7. In view of the appearance of a new isoform of amylase (see item 1), with presumably unique enzyme kinetics, the K_i(Glucose) of the reaction of amylolytic degradation was set to a higher value of 2500μM.

When these changes were applied to the model in this second step (detachment and now transfer to low temperatures), sucrose accumulates as is shown in Figure 7.3 and glycolytic flux increase from 11.6 nmol min^{-1} gFW^{-1} to 18.4 nmol min^{-1} gFW^{-1} (in hexose unit).

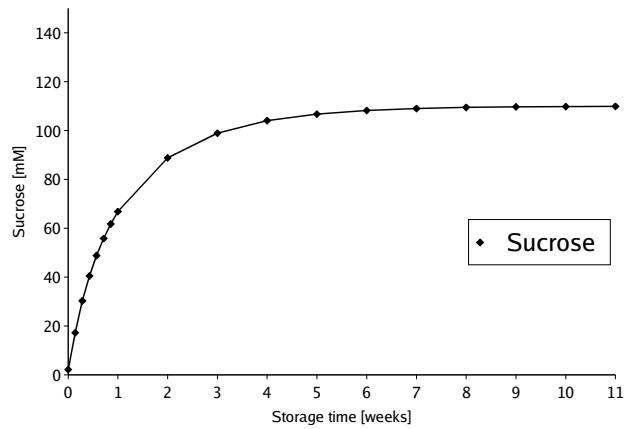

Figure 7.3: Sucrose accumulation after modelling the transfer to low temperatures.

This modified model can now be used to simulate the response to alterations in enzyme catalytic activities.

For example, probing the model with the two ratios of GK/FK from Chapter 6 (decreasing GK/FK ratio from 34 days to 112 days) did show that these ratios brought about an even faster sucrose accumulation with a higher final concentration but this is due to the comparable low GK activity introduced (much higher in the model before). This was also reflected in a very high response coefficient $R_{GK}^{Sucrose}$, see the following section.

7.4.3 Control Analysis of the Detached Tuber Model

Response coefficients were calculated by successively altering the limiting rate of each of the included reactions by 1%, monitoring the asymptotically approached sucrose concentration, and comparing it to the sucrose concentration in the unaltered model (see Figure 7.3). The response of the glycolytic flux was treated similarly, and the two response coefficients obtained, $R_v^{Sucrose}$ and $R_v^{Glycolysis}$, are listed in Table 7.6 below.

The reactions in Table 7.6 are sorted according to the value of their response coefficient. Reactions with a negative coefficient have a sucrose-limiting effect if overexpressed, and reactions with a positive response have a sucrose-limiting effect if their expression is suppressed.

GK, invertase, AGPase, PFK and SuSy are on top of the table, and amylolytic degradation, hexose transport, SPS/SPP, PFP and enolase are at the bottom, suggesting that they are candidates for manipulations. For the reactions in between the coefficient, and therewith the expected effect, becomes too small.

Table 7.6: Response of (final) sucrose concentration and of glycolytic flux. The limiting rates were being varied by 1%. The response coefficient (RC) is 1 if the change in sucrose concentration is also 1%.

	Response coefficients	
Reaction	$R_v^{Sucrose}$	$R_v^{Glycolysis}$
GK	-1.0014	+ 0.1861
inv	- 0.7931	+ 0.1460
AGPase	- 0.4628	- 0.02348
PFK	- 0.434523160528	+ 0.2355
SuSy	- 0.37993256794	+ 0.0190
PK	- 0.194687333624	+ 0.1650
StSynth	- 0.0472120067007	- 0.0033
AATP	- 0.0335919600915	- 0.0029
FK	- 0.0240256659497	+ 0.00418
pPGM	- 0.00790299478137	- 0.0008
G6P/P	- 0.00311187114463	- 0.0004
StPase	- 0.00271989051041	- 0.0005
pPPase	- 0.0000104824867564	- 0.00000005
cPGM	+ 0.00174230747997	+ 0.00009
UGPase	+ 0.0019594772072	+ 0.0001
TPI	+ 0.0020	+ 0.0003
GAPDH_PGK	+ 0.0033	+ 0.000355822588995
ald	+ 0.0058	+ 0.000391314614222
PGI	+ 0.01824	+ 0.00576399127024
PGlyM	+ 0.0381	+ 0.0046
ATPcons	+ 0.0462488978317	+ 0.0738
NDPK	+ 0.0878523798859	- 0.0027
Pexp	+ 0.103908924411	+ 0.0188
eno	+ 0.110317213864	+ 0.01370
PFP	+ 0.388992822052	+ 0.0245
SPS_SPP	+ 0.664614014069	+ 0.0441
Gexp	+ 0.872556558152	+ 0.0701
degr	+ 1.15863890155	+ 0.0927

Reactions that cause a significant reduction in sucrose accumulation in stored tubers but no negative change in starch production of growing tubers are the desired candidates for manipulation.

Therefore, ideal candidates for reducing cold-sweetening should have a large $R_v^{SucroseAcc.}$ in stored tubers but no large negative $C_v^{StarchDepos.}$ when altered. Alternatively, they should have a large negative $R_v^{SucroseAcc.}$ in stored tubers but no large positive $C_v^{StarchDepos.}$ when altered.

Apart from PFK (with a small negative $C_{PFK}^{StarchDepos.}$) all of the candidate

reactions named above confirm to this restriction.

Fructokinase has, despite the predictions made in Chapter 5, a rather small but at least negative response coefficient. The problem is that, especially for glucokinase and fructokinase, the kinetic model is not very accurate. This was noted earlier (see page 7.2.1.1) and it will be discussed in the conclusions below.

There are no inadvisable targets for genetic manipulation really, only, the direction of the manipulation, given by the sign of the control coefficients should be observed in order to avoid unwanted effects.

A very interesting finding, visible in the right column of Table 7.6, is that all reactions have a positive response coefficient for glycolytic flux, except seven of the nine reactions located in the plastid. This is a very distinct separation, which was not detected before in any of the control coefficients looked at before (Table 7.2 or Table 2.3.3).

7.5 Conclusions

Promising target enzymes for genetic manipulation for achieving processing quality improvement are: GK, invertase, AGPase, PFK and SuSy for over-expression, and SPS, PFP and enolase for suppression. Furthermore, hexose transport but the enzyme catalysing it is not known yet, and amylolytic degradation but this is catalysed by a conglomerate of many enzymes, and therefore an unsuitable target.

Because most of the kinetic parameters in the kinetic model are from developing tubers an attached tuber model was built first, and also interrogated first. It was established that the model shows acceptable agreement with experimental metabolite and flux data (see Sections 7.2.1.1 and 7.2.1.2). The model is also able to reproduce some of the behaviour observed in potato tubers subjected to genetic manipulation (compare Section 7.3).

One problem encountered was that the concentrations of glucose and fructose never reached levels as reported from measurements. Reasons for this can be: (a) the sub-mM K_m for glucose and fructose for both GK and FK which makes accumulation impossible; (b) the catalytic activities for these two enzymes are estimated too high and do not reflect *in vivo* values; (c) some other, yet undiscovered regulatory mechanism that does not allow for high activity or rather for high substrate specifity of the hexose-phosphorylating reactions; or (d) the hexoses are separated from the site of activity of GK and FK, the cytosol, but are located and thereby separated from them in the vacuole (in

this case, the hexoses are not actually "seen" by the enzymes because they are in a different compartment). This last option conflicts, though, with the measurements published by Farré et al. (2001). On the other hand, these were the early days of the new method of measuring compartment-specific metabolite concentrations. It would be interesting to find out if more measurements do confirm the high glucose concentrations in the cytosol. Options (a) to (c), though, as listed above, do call for more investigations into the enzyme kinetics of the two hexose phosphorylating enzymes found in potato tubers.

Another problem encountered is the time frame of dynamic changes *in vivo*. Carbohydrate status is a regulatory signal to which a number of plant genes have been shown to respond at the transcriptional level to both sugar accumulation and depletion (reviews Koch 1996; Smeekens, 2000; Rolland et al., 2002).

This implies firstly, that the changes in V_{max} that were applied to the model in order to simulate cold-storage are far too simplistic, and cannot represent the dynamic changes *in vivo* very well (either these changes are not exactly known or not so much is published yet, it is probably a task or application for the upcoming field of systems biology), and secondly, that the sugar accumulation might not only be a consequence of, but also itself a cause for, further changes in metabolism, *e.g.* sprouting *etc.* This complicates the matter further. Or, more to the point, in the model, for example, the initial depletion of sucrose after detachment, occuring over 3-4 days, is such a signal. It might cause effects in the enzymes involved in carbohydrate metabolism which are not entirely known yet, let alone could be incorporated in this model.

For the moment, the model discussed herein is the best one available. Nevertheless, the model can undergo upgrading, by being updated on the basis of ongoing research in the field of plant metabolism.

Chapter 8

General Discussion

8.1 Discussion

A mathematical model of central carbohydrate metabolism in potato tuber cells was built. The reaction network was reconstructed according to agreed knowledge of metabolic pathways in plants. It was complemented with rate equations, using information and kinetic data collected by reviewing the literature, and by measuring enzyme activities in crude extracts of potato tubers.

The distinctive beneficial feature of this model, which sets it apart from existing models of plant sink metabolism, is the introduction of compartments, allowing for separate, compartment-specific metabolite pools. Furthermore, ATP and ADP were considered internal; this was made possible by including a generic ATP-consuming reaction. PFP (plant pyrophosphate-dependent phosphofructokinase) was included. This is the biggest kinetic model of its kind ever attempted in terms of this part of plant metabolism.

Structural analysis of the model as well as kinetic modelling (*i.e.* steady state calculation, control analysis, simulations) were carried out using *ScrumPy*. The model shows satisfactory behaviour, and it is sufficiently realistic.

The motivation for building the model was to create a means of guidance for engineering metabolism, with its predictions giving reasoned directions for the manipulation of the potato for better processing quality. Sugar accumulation in potato tubers stored at low temperatures, *i.e.* cold-sweetening, is a commercial problem because it significantly lowers the processing quality of the tubers (Burton 1989). Glucose and fructose are also the critical factors for acrylamide formation; their reduction represents the most feasible way of reducing acrylamide in potato products (Chuda et al. 2003, Amrein et al. 2004).

The subject of this project was to design a model of carbohydrate metabolism in potato tuber cells with the primary aim of addressing the question: where does the control over sucrose concentration reside? The model described herein is appropriate for this purpose. After contemplating the results of the structural

analysis presented in this thesis (see Section 5.4), and also taking into consideration the results of the control analysis of the kinetic model (Section 7.5), several enzymes can be proposed as promising targets for genetic manipulation.

The 'candidate genes' for reducing sucrose accumulation in cold-stored tubers are, firstly, via overexpression: FK, GK, invertase, AGPase and PFK; and in the second case, via inhibition/downregulation: SPS, PFP and enolase.

Invertase is the obvious choice from the sucrose point of view. It has already been the target in studies with transgenic plants, and its overexpression was shown to result in an accumulation of reducing sugars (Richardson et al. 1990, Sonnewald et al. 1997). Also, PFK and AGPase, which were thought to be the rate-limiting steps for glycolysis or for starch synthesis respectively, were subjected to molecular manipulation techniques (*e.g.* Burrell et al. 1994, and Mooney 1994 for PFK; *e.g.* Stark et al. 1992 and Müller-Röber et al. 1992 for AGPase). GK has been targeted together with invertase, their combined overexpression resulting in an unexpected decrease in starch content (Trethewey et al. 1998).

PFP was subjected to strongly decreased expression but tubers showed no visible phenotype (Hajirezaei et al. 1994). An activation of SPS is known to correlate with the onset of sucrose accumulation (Hill et al. 1996) and a decreased expression resulted in a reproducible but non-proportional decrease of soluble sugars in cold-stored tubers (Krause et al. 1998).

Thus, out of the list of most likely candidates, some have been getting significant attention already. Their potential as targets for crop improvement has been explored experimentally, whereas fructokinase has not yet been a major target for manipulations to meet the aim of better processing quality. Potato fructokinase has, so far, been neglected or escaped attention, for elusive reasons. One single publication (Viola 1996) suggests that FK *in vivo* might represent a limiting factor in sucrose metabolism. As for enolase, no studies concerning its impact on cold-sweetening are known.

As an exhaustive analysis shows (see Chapter 5), the structural approach enables the determination of a variety of model properties that could not be found by any other means. Structural modelling can generate information that is complementary to, rather than a subset of, that obtainable via kinetic modelling (Poolman et al. 2004). Besides the outcome mentioned above concerning the cold-sweetening problem, there are more outcomes of this project that should be mentioned.

Firstly, the number and diversity of elementary modes found by decomposition relates to the extensive biosynthetic capabilities and metabolic redundancy in plants (their way of coping with their sessile lifestyle).

Secondly, not only did the structural analysis support and substantiate the notion of a need for phosphate to vacate the amyloplast, after it has entered

it in the form of ATP (see pages 89 and 100 for the discussion of enzyme subsets), but also for the kinetic model it was only possible to be fitted to the experimental data with a K_{eq}(P_i export) that implies a transport against a concentration gradient (see parameters in Appendix B.2). Both the P_i and the PP_i values are higher in the cytosol than in the amyloplast. This gradient makes a transport of PP_i just as unlikely as the one of P_i, plus there is PPase activity in the amyloplast compartment but not in the cytosol. But how is the balance of plastidial phosphates kept *in vivo*? This really is a question that calls for further investigation.

Furthermore, an increase in the ratio of glucokinase and fructokinase activity during prolonged storage was experimentally confirmed. FK was found to decrease during cold-storage, whereas GK rises. In detached tubers, GK was hypothesised to have an attenuating effect on carbohydrate metabolism (page 94), implying that, if ATP utilisation or demand does not increase, the cycling shoots up in GK-antisense or GK-knockout potatoes (see Section 5.2.4). This hypothesis should be experimentally testable.

Finally, according to the structural analysis, FK was found to be essential for sucrose-consumption. It is employed by each and every elementary mode that leads to sucrose accumulation. It is reasonable to assume that its overexpression affects total sucrose concentration.

When attempting to build a model such as this, one has to accept certain limitations. Some difficult choices have to be made regarding the physical boundaries of the model (decisions of which reactions to include/exclude and the choice of external metabolites); and regarding the depth/accuracy of the model (level of simplification in rate equations, specificity of parameters, *etc.*).

All in all, there is the question of when and where to stop refining and expanding the model in order to start the analytic interrogation. Often, it is not the availability of tools (*i.e.* in this case computing power) but the time of the modeller that forms the limiting factor.

8.2 Future Directions - Outlook

The most immediate step to be undertaken within the scope of this project will be the publication of the model and submission to the JWS[1] database (Olivier and Snoep 2004). Publication of the model in this public database will invite criticism and further the model's improvement with feedback from

[1]JWS Online is an online repository of published cellular systems models ($\approx$ 20 at the moment). JWS takes models described in submitted manuscripts, checks and codes them, then makes them available for reviewers to use in their evaluation of the paper. If the model is sound and the paper is accepted, the model is then moved to the public database. Anyone visiting the site can then use the model to run in simulations of their own, safe in the knowledge that the model has been rigorously validated. The JWS has also been used all over the world for teaching.

other researchers, either plant biochemists or physiologists, or members of the modelling community.

Possible extensions or continuations of this project might include:

- Experiments for testing the claims made in Section 5.4 could be devised and performed.

- Alternatives routes for P_i to cross the amyloplast membrane could be investigated by implementing different options in the model, and then reanalysing it. Such options include, for example:
  1. **additional** pyrophosphate exchange across plastid membrane;
  2. PP_i **instead** of P_i across the plastid membrane;
  3. exchange of P_i or PP_i with some other metabolite.

- The diurnal switch could be simulated by setting different values for external sucrose. Sucrose export from leaves is high during the day and lower at night (see Geigenberger and Stitt 2000).

- The model could be extended in many ways. Some ideas include:
  a) Maltose could be added, as another metabolite, as well as maltose-related reactions. The possibility of maltose production was mentioned in Nielsen et al. (1997) and Chia et al. (2004). Also, a maltose transporter was identified recently in *A.thaliana* (Niittylä et al. 2004);
  b) Vacuolar metabolism (sucrose loading of the tonoplast, sucrose mobilisation via acid invertase and export of reducing sugars) could be modelled. This involves the non-trivial addition of a whole new compartment (within the frame of the existing model a higher V_{max} was used to emulate the vacuolar hydrolytic potential);
  c) A shunt from UDP-glucose into cell wall synthesis or from F6P into the pentose phosphate pathway could be considered. Such diversions of metabolites can be modelled with the addition of one more external metabolite (similar to what was done with '`SucroseAcc`' in Section 5.2.4).

- A reduction of the model complexity could be attempted, by lumping according to timescale, or by mathematical methods (*e.g.* invariant manifolds, see Roussel and Fraser 2001).

- Another project could be to combine the presented model of carbohydrate metabolism with complementary models of other parts of metabolism (existent or future ones), *e.g.* nitrate metabolism, in order to get a fuller and more realistic insight into plant metabolism.

8.3 Summary

The experimental manipulation of plant metabolism, *e.g.* via the generation of transgenic plant lines, is often very expensive and time-consuming, and transgenic plants frequently fall short of the expectations: many of the original manipulations do not show major metabolic effects (Kruger 1997). Many attempts to engineer central metabolism have proven unsuccessful to date and suggest that a greater understanding of the regulatory circuits and networks controlling metabolism is required before engineering can become routine. Therefore, a more theoretical approach, *i.e.* modelling, was applied, which can provide a framework for the planning and execution of experiments.

A problem of great economic interest is the search for transgenic lines of potato (*Solanum tuberosum*) with reduced or suppressed cold-sweetening (the accumulation of sucrose in the tubers during their storage at low temperatures). There are more than 30 enzymes that are immediately involved in potato tuber carbohydrate metabolism, making them all potential targets for genetic modification. How is a sensible choice to be made? To assist the search, promising target enzymes for genetic manipulation were identified by analysing a model of potato tuber carbohydrate metabolism. The metabolic model itself and its analysis were presented herein.

It was shown that the combination of quantitative experimentation with theoretical analysis and numerical simulation on the computer helps to develop strategies for rationally manipulating a system to one's own advantage. Simulations with validated computer models can provide new insights into mechanisms of metabolic control during cold-storage which would be time-consuming and costly to derive from experimentation solely.

This metabolic model can help not only to determine the causes of cold-sweetening and possible targets for its reduction; it will also enhance our general understanding of plant carbohydrate metabolism. The analysis presented herein has only just scratched the surface of what is possible with such a model. The potential of it still awaits exploration.

Now that the model has been constructed and validated, it can be used as a basis for further investigations.

Bibliography

Almaas, E., B. Kovacs, T. Vicsek, Z. Oltvai, and A.-L. Barabási (2004). Global organization of metabolic fluxes in the bacterium Escherichia. Nature 427(6977), 839–843.

Amrein, T., B. Schonbachler, F. Rohner, H. Lukac, Schneider. H., Keiser. A., F. Escher, and R. Amado (2004). Potential for acrylamide formation in potatoes: data from the 2003 harvest. Eur.Food Res.Technol. 219(6), 572–578.

Amthor, J. S. (2000). The McCree-de Wit-Penning de Vries-Thornley Respiration Paradigms: 30 Years Later. Annals of Botany 86, 1–20.

Amthor, J. S. (2003). Efficiency of lignin biosynthesis: a quantitative analysis. Annals of Botany 91, 673–695.

ap Rees, T. (1985). The Organisation of Glycolysis and the Oxidative Pentose Phosphate Pathway in Plants. In R. Douce and D. A. Day (Eds.), Encyclopaedia of Plant Physiology, Volume 18, Chapter 13, pp. 391–417. Berlin: Springer-Verlag.

ap Rees, T. and H. Beevers (1960). Pentose phosphate pathway as a major component of induced respiration of carrot and potato slices. Plant Physiol. 35, 830–838.

ap Rees, T., M. Burrell, T. Entwistle, J. Hammond, D. Kirk, and N. Kruger (1988). Plants and Temperature, Volume 32, Chapter Effects of low temperature on the respiratory metabolism of carbohydrates by plants., pp. 377–393. Society for Experimental Biology, Cambridge.

Avigad, G. (1982). Encyclopedia of Plant Physiology, Volume 13A, Chapter Sucrose and other disaccharides. Springer-Verlag.

Avignone-Rossa, A., J. White, A. Kuiper, P. Postma, M. Bibb, and M. Teixeira de Mattos (2002). Carbon flux distribution in antibiotic-producing chemostat cultures of *Streptomyces lividans*. Metab.Eng. 4(2), 138–150.

Backhausen, J., P. Jöstingmeyer, and R. Scheibe (1997). Competitive inhibition of spinach leaf phosphoglucose isomerase isoenzymes by erythrose-4-phosphate. Plant Sci. 130, 121–131.

Bakker, B. M., P. Michels, F. Opperdoes, and H. V. Westerhoff (1997). Glycolysis in bloodstream form Trypanosoma brucei can be understood in terms of the kinetics of the glycolytic enzymes. J.Biol.Chem. 272(6), 3207–3215.

Ballicora, M., A. Iglesias, and J. Preiss (2004). ADP-glucose pyrophosphorylase: a regulatory enzyme for plant starch synthesis. Photosynthesis Research 79, 1–24.

Barman, T. E. (1969). Enzyme Handbook. Berlin, Heidelberg & New York: Springer Verlag.

Bernfeld, P. (1955). Methods in Enzymology, Volume 1, Chapter 17, pp. 149f. Academic Press.

Blenkinsop, R., L. Copp, R. Yada, and A. Marangoni (2003). A proposed role for the anaerobic pathway during low-temperature sweetening in tubers of Solanum tuberosum. Physiologia Plantarum 118(2), 206–212.

Bologa, K., A. Fernie, A. Leisse, M. Loureiro, and P. Geigenberger (2003). A bypass of sucrose synthase leads to low internal oxygen and impaired metabolic performance in growing potato tubers. Plant Physiol. 132(4), 2058–2072.

Brand, M. D. (1994). The stoichiometry of proton pumping and ATP synthesis in mitochondria. The Biochemist Aug-Sept, 20–24.

BRENDA database (2004). BRENDA: Enzyme DB. online database url: http://brenda.bc.uni-koeln.de. BRENDA team: Prof. Dr. Dietmar Schomburg et al.

Brisson, N., H. Giroux, M. Zollinger, A. Camirand, and C. Simard (1989). Maturation and subcellular compartmentation of potato starch phosphorylase. Plant Cell 1(5), 559–566.

Burger, B., J. Cross, J. Shaw, J. Caren, T. Greene, T. Okita, and L. Hannah (2003). Relative turnover numbers of maize endosperm and potato tuber ADP-glucose pyrophosphorylases in the absence and presence of 3-phosphoglyceric acid. Planta 217(3), 449–456.

Burrell, M. (2003). Starch: the need for improved quality or quantity an overview. J.Exp.Biology 54(382), 451–456.

Burrell, M., P. Mooney, M. Blundy, D. Carter, F. Wilson, J. Green, K. Blundy, and T. ap Rees (1994). Genetic manipulation of 6–phosphofructokinase in potato tubers. Planta 194, 95–101. PFK was overexpressed ¡= 30 fold, respiration measured under high and low respiration rates, no significant difference in flux, some rearrangement of sugar phosphates.

Burton, W. (1989). The Potato. (Third ed.). Harlow: Longman Scientific & Technical.

Carlson, R., D. Fell, and F. Srienc (2002). Metabolic pathway analysis of a recombinant yeast for rational strain development. Biotechnol. Bioeng. 79(2), 121–134.

Carlson, R. and F. Srienc (2004). Fundamental E.coli biochemical pathways for biomass and energy production: Creation of overall flux states. Biotechnol. Bioeng. 86(2), 149–162.

Chassagnole, C., D. Fell, B. Rais, B. Kudla, and J. Mazat (2001). Control of the threonine-synthesis pathway in Escherichia coli: a theoretical and experimental approach. Biochem.J. 356, 433–444.

Chia, T., D. Thorneycroft, A. Chapple, G. Messerli, J. Chen, S. Zeeman, S. Smith, and A. Smith (2004). A cytosolic glucosyltransferase is required for conversion of starch to sucrose in Arabidopsis leaves at night. Plant J. 37(6), 853–863.

Chuda, Y., H. Ono, H. Yada, A. Ohara-Takada, C. Matsuura-Endo, and M. Mori (2003). Effects of physiological changes in potato tubers (Solanum tuberosum L.) after low temperature storage on the level of acrylamide formed in potato chips. Bioscience, Biotechnology, and Biochemistry 67(5), 1188–1190.

Copeland, L. and A. Zammit (1994). Kinetic properties of NAD-dependent glyceraldehyde-3-phosphate dehydrogenase from the host fraction of soybean root nodules. Arch. Biochem. Biophys. 312, 107–113.

Cornish-Bowden, A. and M. Cárdenas (2001). Information transfer in metabolic pathways. Effects of irreversible steps in computer models. Eur.J.Biochem. 268(24), 6616–6624.

Cutter, E. (1978). Structure and development of the potato plant. In P. Harris (Ed.), The Potato Crop., pp. 70–152. London: Chapman & Hall.

Dale, M. and J. Bradshaw (2003). Progress in improving processing attributes in potato. TiPS 8(7), 310–312.

Debnam, P. M. and M. J. Emes (1999). Subcellular distribution of enzymes of the oxidative pentose phosphate pathway in root and leaf tissues. J.Exp.Bot. 50(340), 1653 – 1661.

Deiting, U., R. Zrenner, and M. Stitt (1998). Similar temperature requirement for sugar accumulation and for the induction of new forms of sucrose phosphate synthase and amylase in cold-stored potato tubers. Plant Cell Env. 21(2), 127–138.

Dennis, D. and M. Greyson (1987). Fructose 6-phosphate metabolism in plants. Physiol.Plantarum 69, 395–404.

Duwenig, E., M. Steup, and J. Kossmann (1997). Induction of genes encoding plastidic phosphorylase from spinach (Spinacia oleracea L) and potato (Solanum tuberosum L) by exogenously supplied carbohydrates in excised leaf discs. Planta 203(1), 111–120.

Duwenig, E., M. Steup, L. Willmitzer, and J. Kossmann (1997). Antisense inhibition of cytosolic phosphorylase in potato plants (Solanum tuberosum L.) affects tuber sprouting and flower formation with only little impact on carbohydrate metabolism. Plant J. 12(2), 323–333.

Echeverria, E. and et al. (1995). Intracellular localization of sucrose phosphatase in storage cells. Physiologia Plantarum 95(4), 559–562.

Echeverria, E., M. Salvucci, P. Gonzalez, G. Paris, and G. Salerno (1997). Physical and kinetic evidence for an association between sucrose-phosphate synthase and sucrose-phosphate phosphatase. Plant Physiol. 115, 223–227.

Ellis, R., M. Cochrane, M. Dale, C. Duffus, A. Lynn, I. Morrison, R. Prentice, J. Swanston, and S. Tiller (1998). Starch production and industrial use. J.Sci.Food Agric. 77(3), 289–311.

Emes, M. and D. Dennis (1997). Plant Metabolism (2nd ed.)., Chapter 6. Regulation by compartmentation, pp. 69–80. Harlow: Addison Wesley Longman.

FAOSTAT database (2004). FAOSTAT: Statistical Database of FAO. url: http://faostat.fao.org. FAO (Food and Agriculture Organization of The United Nations).

Farré, E., P. Geigenberger, L. Willmitzer, and R. Trethewey (2000). A possible role for pyrophosphate in the coordination of cytosolic and plastidic carbon metabolism within the potato tuber. Plant Physiol. 123(2), 681–688.

Farré, E., A. Tiessen, U. Roessner, P. Geigenberger, R. Trethewey, and L. Willmitzer (2001). Analysis of the compartmentation of glycolytic intermediates, nucleotides, sugars, organic acids, amino acids, and sugar alcohols in potato tubers using a nonaqueous fractionation method. Plant Physiol. 127, 685–700.

Fehr, M., D. Ehrhardt, S. Lalonde, and W. Frommer (2004). Minimally invasive dynamic imaging of ions and metabolites in living cells. Curr.Opin.Plant Biol. 7(3), 345–351.

Fell, D. (1997). Understanding the Control of Metabolism. London: Portland Press.

Fell, D. (2004). Enzymes, metabolites and fluxes. J.Exp.Bot. 56(410), 267–272.

Fell, D. A. (1990). Substrate cycles: Theoretical aspects of their role in metabolism. Comments Theor. Biol. 1, 341–357.

Fernie, A., U. Roessner, R. Trethewey, and L. Willmitzer (2001). The contribution of plastidial phosphoglucomutase to the control of starch synthesis within the potato tuber. Planta 213, 418–426.

Fernie, A., A. Swiedrych, E. Tauberger, A. Lytovchenko, R. Trethewey, and L. Willmitzer (2002). Potato plants exhibiting combined antisense repression of cytosolic and plastidial isoforms of phosphoglucomutase surprisingly approximate wild type with respect to the rate of starch synthesis. Plant Physiol. Biochem. 40(11), 921–927.

Fernie, A., E. Tauberger, A. Lytovchenko, U. Roessner, L. Willmitzer, and R. Trethewey (2002). Antisense repression of cytosolic phosphoglucomutase in potato (it Solanum tuberosum) results in severe growth retardation, reduction in tuber number and altered carbon metabolism. Planta 214(4), 510–520.

Fernie, A., A. Tiessen, M. Stitt, L. Willmitzer, and P. Geigenberger (2002). Altered metabolic fluxes result from shifts in metabolite levels in sucrose phosphorylase expressing potato tubers. Plant Cell Env. 25, 1219–1232.

Fernie, A., L. Willmitzer, and R. Trethewey (2002). Sucrose to starch: a transition in molecular plant physiology. Trends Plant Sci. 7(1), 35–41.

Fischer, K., B. Kammerer, and M. Gutensohn (1997). A new Class of Plastidic Phosphate Translocators: A Putative Link between Primary and Secondary Metabolism by the Phosphoenolpyruvate/Phosphate Antiporter. The Plant Cell 9, 453–462.

Fischer, K. and A. Weber (2002). Transport of carbon in non-green plastids. Trends Plant Sci. 7(8), 345–351.

Flügge, U.-I., R. E. Haeusler, F. Ludewig, and K. Fischer (2003). Functional genomics of phosphate antiport systems of plastids. Physiologia Plantarum 118, 475–482.

Frydman, R. and C. Cardini (1966). Studies on the biosynthesis of starch. I. Isolation and properties of the soluble adenosine diphosphate glucose: starch glucosyltransferase of *Solanum tuberosum*. Arch. Biochem. Biophys. 116(1), 9–18.

Fu, H., S. Kim, and W. Park (1995). High-level tuber expression and sucrose inducibility of a potato Sus4 sucrose synthase gene require 5'-flanking and 3'- flanking sequences and the leader intron. Plant Cell 7(9), 1387–94.

Fu, H. and W. Park (1995). Sink-associated and vascular-associated sucrose synthase functions are encoded by different gene classes in potato. Plant Cell 7(9), 1369–85.

Fu, Y., M. Ballicora, and J. Preiss (1998). Mutagenesis of the glucose-1-phosphate-binding site of potato tuber ADP-glucose pyrophosphorylase. Plant Physiol. 117(3), 989–996.

Geigenberger, P. (2003). Regulation of sucrose to starch conversion in growing potato tubers. J.Exp.Bot. 54(382), 457–465.

Geigenberger, P., M. Hajirezaei, M. Geiger, U. Deiting, U. Sonnewald, and M. Stitt (1998). Overexpression of pyrophosphatase leads to increased sucrose degradation and starch synthesis, increased activities of enzymes for sucrose-starch interconversions, and increased levels of nucleotides in growing tubers. Planta 205, 428–437.

Geigenberger, P., S. Langenberger, I. Wilke, D. Heineke, H. Heldt, and M. Stitt (1993). Sucrose is metabolized by sucrose synthase and glycolysis within the phloem complex of ricinus-communis l seedlings. Planta 190(4), 446–453.

Geigenberger, P., C. Stamme, J. Tjaden, A. Schulz, P. Quick, T. Betsche, H. Kersting, and H. Neuhaus (2001). Tuber physiology and properties of starch from tubers of transgenic potato plants with altered plastidic adenylate transporter activity. Plant Physiol. 125, 1667–1678.

Geigenberger, P. and M. Stitt (1993). Sucrose synthase catalyzes a readily reversible-reaction in vivo in developing potato-tubers and other plant-tissues. Planta 189(3), 329–339.

Geigenberger, P. and M. Stitt (2000). Diurnal changes in sucrose, nucleotides, starch synthesis and AGPS transcript in growing potato tubers that are suppressed by decreased expression of sucrose phosphate synthase. Plant J. 23(6), 795–806.

Geigenberger, P., M. Stitt, and A. Fernie (2004). Metabolic control analysis and regulation of the conversion of sucrose to starch in growing potato tubers. Plant Cell Env. 27(6), 655–673.

Gerbrandy, S. and A. Doorgeest (1972). Potato phosphorylase isoenzymes. Phytochemistry 11, 403–407.

Goldberg, R. N., Y. B. Tewari, and J. C. Ahluwalia (1989). Thermodynamics of the Hydrolysis of Sucrose. J.Biol.Chem. 264(17), 9901–9904.

Groen, B., H. van Mil, J. Berden, and K. van Dam (1992). The efficiency of oxidative phosphorylation in potato tuber mitochondria is different for succinate and external NADH. Biochimica et Biophysica Acta (BBA) - Bioenergetics 1140(1), 37–44.

Gupta, S. and J. Sowokinos (2003). Physicochemical and kinetic properties of unique isozymes of UDP-Glc pyrophosphorylase that are associated with resistance to sweetening in a cold-stored potato tubers. J. Plant Physiol. 160(6), 589–600.

Hajirezaei, M., U. Sonnewald, R. Viola, S. Carlisle, D. Dennis, and M. Stitt (1994). Transgenic potato plants with strongly decreased expression of pyrophosphate-fructose-6-phosphate phosphotransferase show no visible phenotype and only minor changes in metabolic fluxes in their tubers. Planta 192(1), 16–30.

Hajirezaei, M., Y. Takahata, R. Trethewey, L. Willmitzer, and U. Sonnewald (2000). Impact of elevated cytosolic and apoplastic invertase activity on carbon metabolism during potato tuber development. J.Exp.Bot. 51(Special No.), 439–445.

Hajirezaei, M.-R., F. Bornke, M. Peisker, Y. Takahata, J. Lerchl, A. Kirakosyan, and U. Sonnewald (2003). Decreased sucrose content triggers starch breakdown and respiration in stored potato tubers (Solanum tuberosum). J.Exp.Bot. 54(382), 477–488.

Hanes, C. (1940). The reversible formation of starch from glucose-1-phosphate catalyzed by potato phosphorylase. Proc.R.Soc. London B 129, 174–208.

Hawker, J. and M. Hatch (1975). Methods in Enzymology, Volume 42C, Chapter 55, pp. 341–347. Academic Press.

Heinrich, R. and T. A. Rapoport (1974). A linear steady–state treatment of enzymatic chains; general properties, control and effector strength. Eur. J. Biochem. 42, 89–95.

Heinrich, R. and S. Schuster (1996a). The Regulation of Cellular Systems, Chapter 5, pp. 138–291. Chapman and Hall.

Heinrich, R. and S. Schuster (1996b). The Regulation of Cellular Systems, Chapter 2, pp. 9–74. Chapman and Hall.

Heinrich, R. and S. Schuster (1996c). The Regulation of Cellular Systems, Chapter 3, pp. 75–111. Chapman and Hall.

Heinrich, R. and S. Schuster (1998). The modelling of metabolic systems. Structure, control and optimality. BioSystems 47, 61–77.

Heldt, H. and F. Sauer (1971). The inner membrane of the chloroplast envelope as the site of specific metabolite transport. Biochim.Biophys.Acta 234(1), 83–91.

Hertog, M., L. Tijskens, and P. Hak (1997). The effects of temperature and senescence on the accumulation of reducing sugars during storage of potato (Solanum tuberosum L) tubers: A mathematical model. Postharvest Biol. and Technol. 10(1), 67–79.

Hill, L., R. Reimholz, R. Schröder, T. Nielsen, and M. Stitt (1996). The onset of sucrose accumulation in cold-stored potato tubers is caused by an increased rate of sucrose synthesis and coincides with low levels of

hexose-phosphates, an activation of sucrose phosphate synthase and the appearance of a new form of amylase. Plant Cell Env. 19(11), 1223–1237.

Hofmeyr, J.-H. and A. Cornish-Bowden (1997). The reversible Hill equation: how to incorporate cooperative enzymes into metabolic models. Bioinformatics 13, 377–385.

Hofmeyr, J.-H. S. (1986). Steady state modelling of metabolic pathways: a guide to the prespective simulator. Comp. Appl. Biosci. 2, 5–11.

Hofmeyr, J.-H. S. (2001). Metabolic control analysis in a nutshell. In T.-M. Yi, M. Hucka, M. Morohashi, and H. Kitano (Eds.), Proceedings of the 2nd International Conference on Systems Biology, pp. 291–300.

Hofmeyr, J.-H. S., H. Kacser, and K. J. van der Merwe (1986). Metabolic control of moiety-conserved cycles. Eur.J.Biochem. 155, 631–641.

Huber, S. and J. Huber (1992). Role of sucrose-phosphate synthase in sucrose metabolism in leaves. Plant Physiol. 99, 1275–1278.

Isla, M., M. Vattuone, R. Ordonez, and A. Sampietro (1999). Invertase activity associated with the walls of it Solanum tuberosum tubers. Phytochemistry 50(4), 525–534.

Isla, M., M. Vattuone, and A. Sampietro (1991). Modulation of potato invertase activity by fructose. Phytochemistry 30(2), 423–426.

Jang, J.-C., P. Leon, L. Zhou, and J. Sheen (1997). Hexokinase as a sugar sensor in higher plants. The Plant Cell 9, 5–19.

Jelitto, T., U. Sonnewald, L. Willmitzer, M. Hajirezaei, and M. Stitt (1992). Inorganic pyrophosphate content and metabolites in potato and tobacco plants expressing E.coli pyrophosphatase in their cytosol. Planta 188, 238–244.

Jobling, S. (2004). Improving starch for food and industrial applications. Curr.Opin.Plant Biology 7, 210–218.

Junker, B. H. (2004). Invertase in potato. Ph. D. thesis, Potsdam University.

Kacser, H. and J. Burns (1973). The control of flux. Symp. Soc. Exp. Biol. 27, 65–104.

Kacser, H., J. A. Burns, and D. A. Fell (1995). The control of flux. Biochem. Soc. Trans. 23, 341–366.

Kammerer, B., K. Fischer, B. Hilpert, S. Schubert, M. Gutensohn, A. Weber, and U.-I. Flügge (1998). Molecular Charaecterization of a Carbon Transporter in Plastids from Heterotrophic Tissues: The Glucose 6-Phosphate/Phosphate Antiporter. The Plant Cell 10, 105–117.

Katsube, T., Y. Kazuta, K. Tanizawa, and T. Fukui (1991). Expression in Escherichia coli of UDP-Glucose Pyrophosphorylase cDNA from Potato

Tuber and Functional Assessment of the Five Lysyl Residues Located at the Substrate-Binding Site. Biochemistry 30, 8546–8551.

Kawai, M. and H. Uchimiya (1995). Biochemical properties of rice adenylate kinase and subcellular location in plant cells. Plant Mol. Biol. 27, 943–951.

Kim, W., V. Francheschi, T. Okita, N. Robinson, M. Morell, and J. Preiss (1989). Immunocytochemical localization of ADPglucose pyrophosphorylase in developing potato tuber cells. Plant Physiol. 91, 217–220.

Klamt, S. and E. Gilles (2004). Minimal cut sets in biochemical reaction networks. Bioinformatics 20(2), 226–234.

Klamt, S. and J. Stelling (2003). Two approaches for metabolic pathway analysis? TIBS 21(2), 64–69.

Koch, K. (1996). Carbohydrate-modulated gene expression in plants. Annu.Rev.Plant Physiol.Plant Mol.Biol. 47, 509–540.

Kosegarten, H. and K. Mengel (1994). Evidence for a Glucose 1-Phosphate Translocator in Storage Tissue Amyloplasts of Potato (em Solanum tuberosum) Suspension-Cultured Cells. Physiologia Plantarum 91(1), 111–120.

Kossmann, J. and J. Lloyd (2000). Understanding and influencing starch biochemistry. Crit.Rev.Biochem.Mol.Biol. 35(3), 141–196.

Krause, K., L. Hill, R. Reimholz, T. Nielsen, U. Sonnewald, and M. Stitt (1998). Sucrose metabolism in cold-stored potato tubers with decreased expression of sucrose phosphate synthase. Plant Cell Env. 21(3), 285–299.

Kruger, N. (1997). Plant Metabolism (2nd ed.)., Chapter 7. Carbohydrate synthesis and degradation, pp. 83–104. Harlow: Addison Wesley Longman.

Kumar, D., B. Singh, and P. Kumar (2004). An overview of the factors affecting sugar content of potatoes. Ann.Appl.Biol. 145(3), 247–256.

Leiser, J. and J. J. Blum (1985). On the analysis of substrate cycles in large metabolic systems. Cell Biophysics 11, 123–138.

Lohmann, K. (1933). Biochem.Z. 262, 137.

Lunn, J. and T. ap Rees (1990). Apparent equilibrium-constant and mass-action ratio for sucrose-phosphate synthase in seeds of *pisum sativum*. Biochem.J. 267, 739–743.

Lunn, J. and E. MacRae (2003). New complexities in the synthesis of sucrose. Curr.Opin.Plant Biol. 6, 208–214.

M. G.Poolman and D. A.Fell (2002). ScrumPy software and manual. Available from http://mudshark.brookes.ac.uk/ScrumPy/ScrumPy.html.

Ma, H.-W. and A.-P. Zeng (2003). The connectivity structure, giant strong component and centrality of metabolic networks. Bioinformatics 19(11), 1423 1430.

Martin, C. and A. Smith (1995). Starch biosynthesis. The Plant Cell 7, 971–985.

MetaCyc database (2004). MetaCyc. online database url: http://metacyc.org.

Michal, G. (1984). Methods of Enzymatic Analysis (3rd ed.), Volume VI, pp. 185ff. VCH Verlagsgesellschaft mbH, Weinheim, Germany.

Montavan, P. and N. J. Kruger (1992). Substrate specifity of prophosphate:fructose 6-phosphate 1-phosphotransferase from potato tuber. Plant Physiol. 99, 1487–1492.

Mooney, P. (1994). The fate of photosynthate in a non-photosynthetic cell. Ph. D. thesis, University of London.

Moorhead, G. and W. Plaxton (1990). Purification and characterisation of cytosolic aldolase from carrot storage root. Biochem.J. 269(1), 133–139.

Morandini, P. and F. Salamini (2003). Plant biotechnology and breeding: allied for years to come. Trends Plant Sci. 8(2), 70–75.

Morgan, J. A. and D. Rhodes (2002). Mathematical modelling of plant metabolic pathways. Metabolic Engineering 4, 80–89.

Mori, H., K. Tanizawa, and T. Fukui (1993). A chimeric alpha-glucan phosphorylase of plant type L and H isozymes. Functional role of 78-residue insertion in type L isozyme. J.Biol.Chem. 268(8), 5574–5581.

Müller-Röber, B., U. Sonnewald, and L. Willmitzer (1992). Inhibition of the ADP-glucose pyrophosphorylase in transgenic potatoes leads to sugar-storing tubers and influences tuber formation and expression of tuber storage protein genes. EMBO J. 11(4), 1229–1238.

Murata, T. (1972a). Sucrose phosphate synthetase from various plant origins. Agr.Biol.Chem. 36(11), 1877–1884.

Murata, T. (1972b). Sucrose Synthetase of Rice Grains and Potato Tubers. Agr.Biol.Chem. 36(10), 1815–1818.

Neuhaus, H., O. Batz, E. Thom, and R. Scheibe (1993). Purification of highly intact plastids from various heterotrophic plant tissues: analysis of enzymic equipment and precursor dependency for starch biosynthesis. Biochem.J. 296(2), 395–401.

Neuhaus, H. and U. Maass (1996). Unidirectional transport of orthophosphate across the envelope of isolated cauliflower-bud amyloplasts. Planta 198, 542–548.

Neuhaus, H. E. and M. J. Emes (2000). Nonphotosynthetic metabolism in plastids. Ann.Rev.Plant Physiol.Plant Mol.Biol. 51, 111–140.

Nielsen, T., U. Deiting, and M. Stitt (1997). A beta-amylase in potato tubers is induced by storage at low temperature. Plant Physiol. 113, 503–510.

Nielsen, T., B. Wischmann, T. Enevoldsen, and B. Moller (1994). Starch phosphorylation in potato tubers proceeds concurrently with de novo biosynthesis of starch. Plant Physiol. 105(1), 111–117.

Niittylä, T., G. Messerli, M. Trevisan, J. Chen, A. Smith, and S. Zeeman (2004). A previously unknown maltose transporter essential for starch degradation in leaves. Science 303(5654), 87–89.

NIST database (2004). NIST Standard Reference Database 74. online database url: http://xpdb.nist.gov/enzyme_thermodynamics.

Noltmann, E. (1972a). Aldose-Ketose Isomerases. In P. D. Boyer (Ed.), The Enzymes (3rd ed.), Volume 6, pp. 271–354. Academic Press.

Noltmann, E. (1972b). Glucose 6-phosphate Isomerase. In P. D. Boyer (Ed.), The Enzymes (3rd ed.), Volume 6, pp. 272–301. Academic Press.

Noltmann, E. (1972c). Triosephosphate Isomerase. In P. D. Boyer (Ed.), The Enzymes (3rd ed.), Volume 6, pp. 326–340. Academic Press.

Nuno, J., I. Sanchez-Valdenebro, C. Perez-Iratxeta, E. Meléndez-Hevia, and F. Montero (1997). Network organisation of cell metabolism: monosaccharide interconversion. Biochem.J. 324, 103–111.

Okita, T., P. Nakata, J. Anderson, J. Sowokinos, M. Morell, and J. Preiss (1990). The subunit structure of potato tuber ADPglucose pyrophosphorylase. Plant Physiol. 93, 785–90.

Olivier, B. and J. Snoep (2004). Web-based kinetic modelling using JWS Online. Bioinformatics 20, 2143–2144.

Oparka, K. (1986). Phloem-unloading in the potato tuber. Pathways and sites of ATPase. Protoplasma 131, 201–210.

Patrick du Jardin, Jorge Rojas-Beltran, Christiane Cebhardt, and Robert Brasseur (1995). Molecular Cloning and Characterization of a Soluble lnorganic Pyrophosphatase in Potato. Plant Physiol. 109, 853–860.

Peat, S., W. Whelan, and W. Rees (1953). D-enzyme: a disproportionating enzyme in potato juice. Nature 172(4369), 158.

Pfeiffer, T., I. Sanchez-Valdenebro, J. Nuno, F. Montero, and S. Schuster (1999). Metatool: for studying metabolic networks. Bioinformatics 15(3), 251–257.

Plaxton, W. (1996). The organization and regulation of plant glycolysis. Ann.Rev.Plant Physiol.Plant Mol.Biol. 47, 185–214.

Podesta, F. and W. Plaxton (1991). Kinetic and regulatory properties of cytosolic pyruvate kinase from germinating castor oil seeds. Biochem.J. 279, 495–501.

Pollock, C. and T. ap Rees (1975a). Activities of enzymes of sugar metabolism in cold-stored tubers of *Solanum tuberosum*. Phytochemistry 14, 613–617.

Pollock, C. and T. ap Rees (1975b). Effect of cold on glucose metabolism by callus and tubers of Solanum tuberosum. Phytochemistry 14, 1903–1906.

Poolman, M., H. Assmus, and D. Fell (2004). Applications of metabolic modelling to plant metabolism. J.Exp.Bot. 55(400), 1177–1186.

Poolman, M., K. Venkatesh, M. Pidcock, and D. Fell (2004). A Method for the Determination of Flux in Elementary Modes, and its Application to Lactobacillus rhamnosus. Biotechnol. Bioeng. 88(5), 601–612.

Poolman, M. G., D. A. Fell, and C. A. Raines (2003). Elementary modes analysis of photosynthate metabolism in the chloroplast stroma. Eur. J. Biochem 270, 430–439.

Pozueta-Romero, J., P. Perata, and T. Akazawa (1999). Sucrose-starch conversion in heterotrophic tissues of plants. Crit.Rev.Plant Sci. 18(4), 489–525.

Preiss, J. (1973). Adenosine diphosphoryl glucoe pyrophosphorylase. In P. D. Boyer (Ed.), The Enzymes (3rd ed.), Volume VIII. London: Academic Press.

Preiss, J. (1982). Regulation of the biosynthesis and degradtion of starch in higher plants. Ann.Rev.Plant Physiol. 33.

Pressey, R. (1967). Purification and properties of phosphoglucomutase from potato tubers. Journal of Food Science 32, 381–385.

Quebedeaux, B. (1981). Adenylate and nicotinamide nucleosides in developing soybean-seeds during seed-fill. Plant Physiol. 68, 23–27.

Ray, W. and E. Peck (1972a). Phosphoglucomutase. In P. D. Boyer (Ed.), The Enzymes (3rd ed.), Volume 6, pp. 408–458. Academic Press.

Ray, W. and E. Peck (1972b). Phosphoglycerate mutase. In P. D. Boyer (Ed.), The Enzymes (3rd ed.), Volume 6, pp. 459–475. Academic Press.

Recondo, E. and L. Leloir (1961). Adenosine diphosphate glucose and starch synthesis. Biochem.Biophys.Res.Commun. 6, 85–88.

Reder, C. (1988). Metabolic control theory: a structural approach. J. Theor. Biol. 135, 175–201.

Reed, J. L. and B. O. Palsson (2004). Genome-scale in silico models of E.coli have multiple equivalent phenotypic states: assessment of correlated reaction subsets that comprise network states. Genome Research 14, 1797–1805.

Regierer, B., A. Fernie, F. Springer, A. Perez-Melis, A. Leisse, K. Koehl, L. Willmitzer, P. Geigenberger, and J. Kossmann (2002). Starch content and yield increase as a result of altering adenylate pools in transgenic plants. Nature Biotech. 20, 1256–1260.

Reimholz, R., P. Geigenberger, and M. Stitt (1994). Sucrose-phosphate synthase is regulated via metabolites and protein phosphorylation in potato tubers, in a manner analogous to the enzyme in leaves. Planta 192, 480–488.

Renz, A., L. Merlo, and M. Stitt (1993). Partial-purification from potato-tubers of 3 fructokinases and 3 hexokinases which show differing organ and developmental specificity. Planta 190(2), 156–165.

Renz, A. and M. Stitt (1993). Substrate-specificity and product inhibition of different forms of fructokinases and hexokinases in developing potato-tubers. Planta 190(2), 166–175.

Richardson, D., H. Davies, and H. Ross (1990). An investigation into the factors influencing sugar levels in uk grown potatoes (cv Record). Potato Research 33(2), 235–239.

Richardson, D., H. Davies, H. Ross, and J. . . .-. Mackay, G.R. (1990) (1990). Invertase activity and its relation to hexose accumulation in potato-tubers. J.Exp.Bot. 41(222), 95–99.

Riesmeier, J. W., U.-I. Flügge, B. Schulz, D. Heineke, H.-W. Heldt, L. Willmitzer, and W. B. Frommer (1993). Antisense repression of the chloroplast triose phosphate translocator affects carbon partitioning in transgenic potato plants. PNAS 90, 6160–6164.

Rodriguez-Saona, L., R. Wrolstad, and C. Pereira (1997). Modeling the contribution of sugars, ascorbic acid, chlorogenic acid and amino acids to non-enzymatic browning of potato chips. J.Food Sci. 62(5), 1001–1005.

Rohwer, J., S. Schuster, and H. Westerhoff (1996). How to recognize monofunctional units in a metabolic system. J.Theor.Biol. 179(3), 213–28.

Rohwer, J. M. and F. C. Botha (2001). Analysis of sucrose accumulation in the sugar cane culm on the basis of in vitro kinetic data. Biochem.J. 358, 437–445.

Roussel, M. and S. Fraser (2001). Invariant manifold methods for metabolic model reduction. Chaos 11, 196–206.

Rung, J., H. Draborg, K. Jørgensen, and T. Nielsen (2004). Carbon partitioning in leaves and tubers of transgenic potato plants with reduced activity of fructose-6-phosphate,2-kinase/fructose-2,6-bisphosphatase. Physiologia Plantarum 121(2), 204–214.

Sauro, H. M. and B. P. Ingalls (2004). Computational Analysis in Biochemical Networks: Computational Issues for Software Writers. Biophysical Chemistry 109, 1–15.

Sauro, H. M., J. R. Small, and D. A. Fell (1987). Metabolic control and its analysis: Extensions to the theory and matrix method. Eur. J. Biochem. 165, 215–221.

Schilling, C., D. Letscher, and B. Palsson (2000). Theory for the systemic definition of metabolic pathways and their use in interpreting metabolic function from a pathway oriented perspective. J.Theor.Biol. 203, 229–248.

Schnarrenberger, C. and A. Oeser (1974). Two isoenzymes of glucosephosphate isomerase from spinach leaves and their intracellular compartmentation. Eur.J.Biochem. 45, 77–82.

Schott, K., S. Borchert, B. Müller-Röber, and H. Heldt (1995). Transport of inorganic phosphate and C3- and C6-sugar phosphates across the envelope membranes of potato tuber amyloplasts. Planta 196, 647–652.

Schuster, S. and R. Heinrich (1991). Is metabolite channelling the complicated solution to the easy problem of reducing transient times ? J.Theor.Biol. 152, 57–61.

Schuster, S. and C. Hilgetag (1994). On Elementary Flux Modes in Biochemical Systems at Steady State. J.Biol.Syst. 2, 165–182.

Schuster, S., C. Hilgetag, J. Woods, and D. Fell (2002). Reaction routes in biochemical reaction systems: algebraic properties, validated calculation procedure and example from nucelotide metabolism. J.Math.Biol. 45, 153–181.

Schuster, S., S. Klamt, W. Weckwerth, M. Moldenhauer, and T. Pfeiffer (2002). Use of network analysis of metabolic systems in bioengineering. Bioprocess Biosys. Eng. 24, 363–373.

Schuster, S. and R. Schuster (1991). Detecting strictly detailed balanced subnetworks in open chemical-reaction networks. J.Math.Chem. 6(1), 17–40.

Schuster, S. and R. Schuster (1993). Refined algorithm and computer program for calculating all non-negative fluxes admissible in steady states of biochemical reaction systems with or without some flux rates fixed. Comp. Appl. Biosci. 9(1), 79–85.

Sebkova, V., C. Unger, M. Hardegger, and A. Sturm (1995). Biochemical, physiological, and molecular characterization of sucrose synthase from Daucus carota. Plant Physiol. 108(1), 75–83.

Segel, I. H. (1993). Enzyme Kinetics. Wiley Classics Library.

Sivak, M. N. and J. Preiss (1998). Starch: Basic Science to Biotechnology, Volume 41 of Advances in Food and Nutrition Research. Academic Press.

Slabnik, E., R. Frydman, and C. Cardini (1968). Some Properties of Potato Tuber UDPG:fructose-2-glucosyltransferase (E.C. 2.4.1.14) and UDPG:fructose-6-phosphate-2-glucosyltransferase (E.C. 2.4.1.13). Plant Physiol. 43, 1063–1068.

Smith, A. (1999). Making starch. Curr.Opin.Plant Biol. 2, 223–229.

Sonnewald, U. (1992). Expression of E. coli inorganic pyrophosphatase in transgenic plants alters photoassimilate partitioning. The Plant J. 2(4), 571–581.

Sonnewald, U., M. Hajirezaei, J. Kossmann, A. Heyer, R. Trethewey, and L. Willmitzer (1997). Increased potato tuber size resulting from apoplastic expression of a yeast invertase. Nature Biotech. 15, 794–797.

Sowokinos, J. (1976). Pyrophosphorylases in it Solanum tuberosum 1. Changes in ADP-glucose and UDP-glucose pyrophosphorylase activities associated with starch biosynthesis during tuberization, maturation, and storage of potatoes. Plant Physiol. 57, 63–68.

Sowokinos, J. (1981). Pyrophosphorylases in *Solanum tuberosum* 2. Catalytic properties and regulation of ADP-glucose and UDP-glucose pyrophosphorylase activities in potatoes. Plant Physiol. 68(4), 924–929.

Sowokinos, J. and J. Preiss (1982). Pyrophosphorylases in it Solanum tuberosum 3. Purification, physical, and catalytic properties of ADP-glucose pyrophosphorylase in potatoes. Plant Physiol. 69(6), 1459–1466.

Sowokinos, J., J. Spychalla, and S. Desborough (1993). Pyrophosphorylases in it Solanum tuberosum 4. Purification, tissue localization, and physicochemical properties of UDP-glucose pyrophosphorylase. Plant Physiol. 101(3), 1073–1080.

Sowokinos, J., C. Thomas, and M. Burrell (1997). Pyrophosphorylases in potato 5. Allelic polymorphism of UDP-glucose pyrophosphorylase in potato cultivars and its association with tuber resistance to sweetening in the cold. Plant Physiol. 113, 511–517.

Sowokinos, J., V. Vigdorovich, and M. Abrahamsen (2004). Molecular cloning and sequence variation of UDP-glucose pyrophosphorylase cDNAs from potatoes sensitive and resistant to cold sweetening. J. Plant Physiol. 161(8), 947–955.

St-Pierre, B. and N. Brisson (1995). Induction of the plastidic starch-phosphorylase gene in potato storage sink tissue. Planta 195, 339–344.

Stark, D., K. Timmerman, G. Barry, J. Preiss, and G. Kishore (1992). Regulation of the amount of starch in plant-tissues by ADP-glucose pyrophos-

phorylase. Science 258(5080), 287–292.

Stitt, M. (1990). Fructose-2,6-bisphosphate as a regulatory molecule in plants. Annu.Rev.Plant Physiol.Plant Mol.Biol. 41, 153–185.

Stitt, M. (1997). Plant metabolism (2nd ed.)., Chapter 25. The flux of carbon between the chloroplast and cytoplasm, pp. 382–400. Harlow: Addison Wesley Longman.

Stryer, L. (1995). Biochemistry (4th ed.). New York, U.S.A.: W. H. Freeman.

Sweetlove, L., M. Burrell, and T. ap Rees (1996a). Characterization of transgenic potato (it Solanum tuberosum) tubers with increased ADPglucose pyrophosphorylase. Biochem.J. 320, 487–492.

Sweetlove, L., M. Burrell, and T. ap Rees (1996b). Starch metabolism in tubers of transgenic potato (it Solanum tuberosum) with increased ADPglucose pyrophosphorylase. Biochem.J. 320, 493–498.

Sweetlove, L., N. Kruger, and S. Hill (2001). Starch synthesis in transgenic potato tubers with increased 3-phosphoglyceric acid as a consequence of increased 6-phosphofructokinase activity. Planta 213, 478–482.

Sweetlove, L., B. Mowday, H. Hebestreit, C. Leaver, and A. Millar (2001). Nucleoside diphosphate kinase III is localized to the inter-membrane space in plant mitochondria. FEBS letters 508, 272–276.

Sweetlove, L., B. Müller-Röber, L. Willmitzer, and S. Hill (1999). The contribution of adenosine 5'-diphosphoglucose pyrophosphorylase to the control of starch synthesis in potato tubers. Planta 209, 330 – 337.

Takaha, T., J. Critchley, S. Okada, and S. Smith (1998). Normal starch content and composition in tubers of antisense potato plants lacking D-enzyme (4-alpha-glucanotransferase). Planta.

Takaha, T., M. Yanase, S. Okada, and S. Smith (1993). Disproportionating enzyme (4-alpha-glucanotransferase; EC 2.4.1.25) of potato. Purification, molecular cloning, and potential role in starch metabolism. J.Biol.Chem. 268(2), 1391–6.

Takamiya, S. and T. Fukui (1978). Phosphoglucomutase from potato tubers. Chemical and catalytic properties. J.Biochem. 84(3), 569–574.

Takeda, Y., S. Hizukuri, and Z. Nikuni (1967). Crystallization and properties of pea glucosephosphate isomerase. Biochim.Biophys.Acta 146(2), 568–575.

Tauberger, E., A. Fernie, M. Emmermann, A. Renz, J. Kossmann, L. Willmitzer, and A. Trethewey (2000). Antisense inhibition of plastidial phosphoglucomutase provides compelling evidence that potato tuber amyloplasts import carbon from the cytosol in the form of glucose-6-phosphate. Plant J. 23(1), 43–53.

Thomas, S., P. Mooney, M. Burrell, and D. Fell (1997a). Finite change analysis of glycolytic intermediates in tuber tissue of lines of transgenic potato (it Solanum tuberosum) overexpressing phosphofructokinase. Biochem.J. 322, 111–117.

Thomas, S., P. Mooney, M. Burrell, and D. Fell (1997b). Metabolic control analysis of glycolysis in tuber tissue of potato (it Solanum tuberosum): explanation for the low control coefficient of phosphofructokinase over respiratory flux. Biochem.J. 322, 119–127.

Thorneycroft, D., S. Sherson, and S. Smith (2001). Using gene knockouts to investigate plant metabolism. JXB 52(361), 1593–1601.

Tiessen, A., J. Hendriks, M. Stitt, A. Branscheid, Y. Gibon, E. Farré, and P. Geigenberger (2002). Starch synthesis in potato tubers is regulated by post-translational redox modification of ADP-glucose-pyrophosphorylase: a novel regulatory mechanism linking starch synthesis to the sucrose supply. The Plant Cell 14, 2191–2213.

Tishel, M. and M. Mazelis (1966). The accumulation of sugars in potato tubers at low temperature and some associated enzymatic activities. Phytochemistry 5, 895–902.

Tjaden, J., T. Mohlmann, K. Kampfenkel, G. Henrichs, and H. Neuhaus (1998). Altered plastidic ATP/ADP-transporter activity influences potato tuber (Solanum tuberosum) morphology, yield and composition of tuber starch. Plant J. 16(5), 531–540.

Tomlinson, J. and J. Turner (1979). Pea seed triose phosphate isomerase. Phytochemistry 18(12), 1959–1962.

Trethewey, R. and T. ap Rees (1994). A mutant of arabidopsis thaliana lacking the ability to transport glucose across the chloroplast envelope. Biochem. J. 301, 449–454.

Trethewey, R., P. Geigenberger, A. Hennig, H. Fleischer-Notter, B. Müller-Röber, and L. Willmitzer (1999). Induction of the activity of glycolytic enzymes correlates with enhanced hydrolysis of sucrose in the cytosol of transgenic potato tubers. Plant Cell Env. 22(1), 71–79.

Trethewey, R., P. Geigenberger, K. Riedel, M. Hajirezaei, U. Sonnewald, M. Stitt, J. Riesmeier, and L. Willmitzer (1998). Combined expression of glucokinase and invertase in potato tubers leads to a dramatic reduction in starch accumulation and a stimulation of glycolysis. Plant J. 15(1), 109–118.

Turner, J., D. Harrison, and L. Copeland (1977). Fructokinase of pea seeds. Plant Physiol. 60, 666–669.

Urbanczyk-Wochniak, E., A. Leisse, U. Roessner-Tunali, A. Lytovchenko,

J. Reismeier, L. Willmitzer, and A. Fernie (2003). Expression of a bacterial xylose isomerase in potato tubers results in an altered hexose composition and a consequent induction of metabolism. Plant Cell Env. 44(12), 1359–1367.

van Schaftingen, E., B. Lederer, R. Bartrons, and H.-G. Hers (1982). A kinetic study of pyrophosphate: fructose 6-phosphate phosphotransferase from potato tubers. Eur.J.Biochem. 129, 191–195.

Viola, R. (1996). Hexose metabolism in discs excised from developing potato (Solanum tuberosum L) tubers .2. Estimations of fluxes in vivo and evidence that fructokinase catalyses a near rate-limiting reaction. Planta 198(2), 186–196.

Wagner, A. and D. Fell (2001). The small world inside large metabolic networks. Proc. Roy. Soc. London B 268, 1803–1810.

Weber, A. (2004). Solute transporters as connecting elements between cytosol and plastid stroma. Curr.Opin.Plant Biol. 7, 247–253.

Weber, A., J. Schneidereit, and L. Voll (2004). Using mutants to probe the in vivo function of plastid envelope membrane metabolite transporters. J.Exp Bot. 55(400), 1231–1244.

Weber, A., J. C. Servaites, D. R. Geiger, H. Kofler, D. Hille, F. Gröner, U. Hebbeker, and U.-I. Flügge (2000). Identification, purification, and molecular cloning of a putative plastidic glucose translocator. The Plant Cell 12, 787–801.

Weiner, H., M. Stitt, and H. Heldt (1987). Subcellular compartmentation of pyrophosphate and pyrophosphatase in leave. Biochim.Biophys.Acta 893, 13–21.

Westram, A., J. R. Lloyd, U. Roessner, J. W. Riesmeier, and J. Kossmann (2002). Increases of 3-phosphoglyceric acid in potato plants through antisense reduction of cytoplasmic phosphoglycerate mutase impairs photosynthesis and growth, but does not increase starch contents. Plant Cell Env. 25(9), 1133–1143.

Whelan, W. (1955). Methods in Enzymology, Volume 1, Chapter 22, pp. 192ff. Academic Press.

Winter, H. and S. Huber (2000). Regulation of sucrose metabolism in higher plants: Localization and regulation of activity of key enzymes. Crit.Rev.Plant Sci. 19(1), 31–67.

Wischmann, B., T. Nielsen, and B. Moller (1999). In vitro biosynthesis of phosphorylated starch in intact potato amyloplasts. Plant Physiol. 119, 455–462.

Wismer, W., W. Worthing, R. Yada, and A. Marangoni (1998). Membrane lipid dynamics and lipid peroxidation in the early stages of low-temperature sweetening in tubers of Solanum tuberosum. Physiologia Plantarum 102, 396–410.

Wuchty, S. and P. Stadler (2003). Centers of complex networks. J.Theor.Biol. 223, 45–53.

Yip, V. and S. Withers (2004). Nature's many mechanisms for the degradation of oligosaccharides. Org. Biomol. Chem. 2(19), 2707–2713.

Zrenner, R., M. Salanoubat, L. Willmitzer, and U. Sonnewald (1995). Evidence of the crucial role of sucrose synthase for sink strength using transgenic potato plants. Plant J. 7(1), 97–107.

Zrenner, R., K. Schuler, and U. Sonnewald (1996). Soluble acid invertase determines the hexose-to-sucrose ratio in cold-stored potato tubers. Planta 198(2), 246–252.

Appendix A

Experimental Data (from Literature)

A.1 Metabolite Data

Table A.1: Cytosolic and plastidic metabolite concentrations.
A comprehensive collection of experimentally measured potato tuber metabolite concentrations is shown.
Farré et al. 2001 measured developing tubers from 10-week-old plants.
Tiessen et al. 2002 measured developing tubers from 8 to 9-week-old plants; attached: analysed directly after harvest; detached: tubers analysed 1d after harvest.
- metabolite not measured.

Metabolite	Concentration in μM					
	Farré et al. 2001		Tiessen et al. 2002			
			attached		detached	
	cytosol	amyloplast	cytosol	amyloplast	cytosol	amyloplast
Sucrose	41000	10000	82400	-	47900	-
Fructose	not detected	1110	1370	-	1790	-
Glucose	31000	16000	-	-	-	-
UDPG	830	901	571	-	627	-
UTP	400	84	238	-	121	-
UDP	58	31	52.4	-	37.1	-
G1P	51	80	42.7	17.4	115	64
G6P	340-370	970	510	379	1212	822
F6P	140-170	190-260	147	-	299	-
ADPG	-	-	-	21.5	-	11.2
ATP	210	495	292	179	151	279
ADP	18	240	87.3	149	77	148
PP_i	23	3	12	2.36	6.9	0.68
P_i	-	-	2400	870	2200	500
3-PGA	300	460	296	198	324	244
PEP	57	122	-	-	-	-
Pyruvate	4	38	-	-	-	-

A.2 Flux Data

Flux	Value	Method of determination	Reference
hexose uptake respiration glycolytic flux	44nmol hexose min^{-1} gFW^{-1} 1.1nmol pyruvate min^{-1} gFW^{-1} 17-34nmol hexose min^{-1} gFW^{-1}	incubated tuber discs	Geigenberger and Stitt (1993)
net rate of starch synthesis sucrose uptake	33 nmol min^{-1} gFW^{-1} 24nmol hexose min^{-1} gFW^{-1}	incubated tuber discs tuber discs from growing tubers incubated with 100mM [14C]Sucrose	Viola (1996) Geigenberger et al. (1998)
sucrose uptake sucrose uptake	41.8nmol hexose min^{-1} gFW^{-1} 58.8nmol hexose min^{-1} gFW^{-1}	25 min incubation with 25mM Sucrose 25 min incubation with 100mM Sucrose	Fernie et al. (2002) Fernie et al. (2002)
sucrose accumulation	2.5μmolday^{-1} gFW^{-1} = 1.6nmol min^{-1} gFW^{-1}	(initial rate, slows down after some days)	Hill et al. (1996)
respiration of whole tubers at 4°C	2-3 μmolCO2 day^{-1} gFW^{-1} $\simeq$ 0.46-0.7nmol pyruvate min^{-1} gFW^{-1}		Blenkinsop et al. (2003)

Table A.2: A collection of measured metabolic fluxes.

Appendix B

The Model

B.1 Reactions - Rate Equations

This section holds all rate equations as employed in the model. The kinetic parameters (V_max, K_m, K_i, *etc.*) are provided separately. Appendix B.2 holds a full listing of parameters used.

In order to preserve some clarity (and because of too few space), the suffices _am and _cyt indicating the metabolite's compartmental location are omitted in the below equations. The context of the reactions should provide it. Only, for the transport steps they are given.

B.1.1 Enzymes

E_1: amylolytic degradation of starch

Degradation of starch via amylase is complex, it results from the interplay of several enzymes (see Paragraph 6.1). Therefore no detailed rate equation can be formulated. Nevertheless, a product inhibition by glucose was built in:

$$v_{degr} = V_{max} \frac{1}{1 + \frac{\text{Glucose}}{K_{i_{\text{Glucose}}}}}$$

E_2: starch phosphorylase (EC 2.4.1.1)

Starch is considered as abundant, therefore the rate is modelled as being only dependent on the concentrations of glucose 1-phosphate and orthophosphate:

$$v_{StPase} = \frac{V_+ \cdot \frac{\text{P}_\text{i}}{K_{m_{\text{P}_\text{i}}}} + V_- \cdot \frac{\text{G1P}}{K_{m_{\text{G1P}}}}}{1 + \frac{\text{P}_\text{i}}{K_{m_{\text{P}_\text{i}}}} + \frac{\text{G1P}}{K_{m_{\text{G1P}}}}} = V_{max} \frac{\text{P}_\text{i} - \frac{\text{G1P}}{K_{eq}}}{K_{m_{\text{P}_\text{i}}} + \text{P}_\text{i} + \text{G1P} \frac{K_{m_{\text{P}_\text{i}}}}{K_{m_{\text{G1P}}}}}$$

E_3 + E_7: phosphoglucomutase (EC 5.4.2.2)

The equation for PGM, a reversible uni-uni Michaelis-Menten kinetics, reads:

$$v_{PGM} = V_{max} \frac{\text{G1P} - \frac{\text{G6P}}{K_{eq}}}{K_{m_{\text{G1P}}} + \text{G1P} + \text{G6P} \frac{K_{m_{\text{G1P}}}}{K_{m_{\text{G6P}}}}}$$

For a near-equilibrium assumption, dispensing with the K_m, the rate equals:

$$v_{PGM} = V_{max} \cdot \left(1 - \frac{\frac{\mathrm{G6P}}{\mathrm{G1P}}}{K_{eq}}\right)$$

$\mathbf{E_4}$: ADP-glucose pyrophosphorylase (EC 2.7.7.27)

K_{eq} was set to 1, and the simplified ordered bi-bi Michaelis-Menten equation from Segel 1993 becomes:

$$v_{AGPase} = V_{app} \frac{(\mathrm{G1P} \cdot \mathrm{ATP} - \mathrm{ADPG} \cdot \mathrm{PP_i})}{(K_{m_{\mathrm{G1P}}}(1 + \frac{\mathrm{PP_i}}{K_{m_{\mathrm{PP_i}}}}) + \mathrm{G1P})(K_{m_{\mathrm{ATP}}}(1 + \frac{\mathrm{ADPG}}{K_{m_{\mathrm{ADPG}}}}) + \mathrm{ATP})}$$

The dependencies on the concentrations of activator 3-PGA and inhibitor $\mathrm{PP_i}$ were fitted (see Paragraph 4.1.6.3 at page 80), and the modelled V_{app} obeys:

$$V_{app} = f\,(\mathrm{3PGA}, \mathrm{PP_i}) = V_{max} \frac{1 + \frac{\mathrm{3PGA}}{K_{a_{\mathrm{3PGA}}}}}{1 + \frac{\mathrm{P_i}}{K_{m_{\mathrm{P_i}}}}}$$

$\mathbf{E_5}$: Starch synthase (EC 2.4.1.21)

Starch synthesis was modelled as an irreversible uni-uni Michaelis-Menten kinetics:

$$v_{StSynth} = V_{max} \frac{\mathrm{ADPG}}{\mathrm{ADPG} + K_{m_{\mathrm{ADPG}}}}$$

$\mathbf{E_6}$: Inorganic pyrophosphatase (EC 3.6.1.1)

This plastidic enzyme was modelled by a near-equlibrium equation:

$$v_{PPase} = V_{max} \left(1 - \frac{\frac{\mathrm{P_i}}{\mathrm{PP_i}}}{K_{eq_{\mathrm{PPase}}}}\right)$$

$\mathbf{E_8}$: UGPase (EC 2.7.7.9)

A simple bi-bi rate equation was assumed for the rate of UGPase. No effectors were considered, see also page 55.

$$v_{UGPase} = V_{app} \frac{\mathrm{G1P} \cdot \mathrm{UTP} - \frac{\mathrm{UDPG} \cdot \mathrm{PP_i}}{K_{eq}}}{(K_{m_{\mathrm{G1P}}}(1 + \frac{\mathrm{PP_i}}{K_{m_{\mathrm{PP_i}}}}) + \mathrm{G1P})(K_{m_{\mathrm{UTP}}}(1 + \frac{\mathrm{UDP}}{K_{m_{\mathrm{UDPG}}}}) + \mathrm{UTP})}$$

$\mathbf{E_9}$: Phosphoglucoisomerase (EC 5.3.1.9)

This isomerisation can be modelled as a reversible uni-uni Michaelis-Menten mechanism with competitive inhibition by phosphoenolpyruvate as follows:

$$v_{PGI} = V_{max} \frac{\mathrm{G6P} - \frac{\mathrm{F6P}}{K_{eq}}}{K_{m_{\mathrm{G6P}}} + \mathrm{G6P} + \mathrm{F6P}\frac{K_{m_{\mathrm{G6P}}}}{K_{m_{\mathrm{F6P}}}} + \mathrm{PEP}\frac{K_{m_{\mathrm{G6P}}}}{K_{i_{\mathrm{PEP}}}}}$$

E_{10}: SPS (EC 2.4.1.14) and SPP (EC 3.1.3.24)

The proposed channeling of S6P between SPS and SPP (Echeverria et al. 1997) has been explained in the Paragraphs 3.2.2.4 and 3.2.2.5 on pages 56f. The lumped reaction SPS-SPP was modelled by the following rate equation:

$$v_{SPS-SPP} = V_{max} \frac{\mathrm{F6P} \cdot \mathrm{UDPG} - \frac{\mathrm{UDP \cdot P_i}}{K_{eq}}}{K_{m_{\mathrm{F6P}}} K_{m_{\mathrm{UDPG}}} + \mathrm{F6P} \cdot \mathrm{UDPG} + \frac{V_+}{V_-} \frac{\mathrm{UDP \cdot P_i}}{K_{eq}} + \mathrm{Sucrose} \frac{K_{m_{\mathrm{F6P}}} K_{m_{\mathrm{UDPG}}}}{K_{i_{\mathrm{Sucrose}}}}}$$

where K_{eq} is the product of the two K_{eq} of SPS and SPP, and $\frac{V_+}{V_-}$ is set according to the Haldane equation (from the mass action ratio $\frac{\mathrm{Sucrose \cdot UDP \cdot P_i}}{\mathrm{F6PUDPG}}$ and the K_m)). There is competitive inhibition by sucrose.

E_{11}: Sucrose synthase (EC 2.4.1.13)

Rohwer and Botha 2001 modelled the rate of SuSy with a reversible ordered bi-reactant mechanism, UDP-glucose binding first, and UDP dissociating last. Because SuSy appears to operate near equilibrium (see Paragraph 3.2.2.6) a more simplified rate equation was used for this model. The physiological concentrations of fructose, ADP and UDP are much below the K_i values (see Appendix A.1), therefore, only uncompetitive inhibition by glucose was included. This results in the rate equation:

$$v_{SuSy} = V_{max} \frac{\frac{\mathrm{UDPG \cdot Fructose}}{K_{m_{\mathrm{UDPG}}} K_{m_{\mathrm{Fructose}}}} (1 - \frac{\frac{\mathrm{UDP \cdot Sucrose}}{\mathrm{UDPG \cdot Fructose}}}{K_{eq}})}{(1 + \frac{\mathrm{UDPG \cdot Fructose}}{K_{m_{\mathrm{UDPG}}} K_{m_{\mathrm{Fructose}}}} + \frac{\mathrm{UDP \cdot Sucrose}}{K_{m_{\mathrm{UDP}}} K_{m_{\mathrm{Sucrose}}}})(1 + \frac{\mathrm{Glucose}}{K_{i_{\mathrm{Glucose}}}})}$$

E_{12}: Invertase (EC 3.2.1.26)

For the irreversible rate of invertase, product inhibition by fructose (competitive) and glucose (non-competitive) was considered:

$$v_{inv} = V_{max} \frac{\frac{\mathrm{Sucrose}}{K_{m_{\mathrm{Sucrose}}}}}{(1 + \frac{\mathrm{Sucrose}}{K_{m_{\mathrm{Sucrose}}}} + \frac{\mathrm{Fructose}}{K_{i\mathrm{Fructose}}})(1 + \frac{\mathrm{Glucose}}{K_{i_{\mathrm{Glucose}}}})}$$

E_{13}: Glucokinase (EC 2.7.1.1)

The glucose-phosphorylating step was modelled as irreversible. Fructose competes as a substrate, and there is product inhibition by ADP (competitive) and G6P (uncompetitive):

$$v_{GK} = V_{app} \frac{\frac{\mathrm{Glucose \cdot ATP}}{K_{m_{\mathrm{Glucose}}} K_{m_{\mathrm{ATP}}}}}{(1 + \frac{\mathrm{Glucose}}{K_{m_{\mathrm{Glucose}}}} + \frac{\mathrm{Fructose}}{K_{i_{\mathrm{Fructose}}}})(1 + \frac{\mathrm{ATP}}{K_{m_{\mathrm{ATP}}}} + \frac{\mathrm{ADP}}{K_{i_{\mathrm{ADP}}}})(1 + \frac{\mathrm{G6P}}{K_{m_{\mathrm{G6P}}}})}$$

The rate equation for GK was incorporated as the sum of the rates for two isoforms. They both are expressed at similar levels Renz et al. 1993, and they were assigned half of the limiting rate each. Inhibition by G6P was only found for one of the two isoforms considered (rate as above). For the G6P-insensitive the G6P-term in the denominator is omitted, otherwise the same rate equation applies, only with different kinetic parameters. See page 94 for further details.

E_{14}: Fructokinase (EC 2.7.1.4)

The fructose-phosphorylating step was modelled as irreversible. Product inhibition by ADP (competitive) and F6P (uncompetitive) was considered. Additionaly, fructose has an inhibiting effect at higher concentrations (substrate inhibition):

$$v_{FK} = V_{max} \frac{\frac{\text{Fructose}\cdot\text{ATP}}{K_{m_{\text{Fructose}}} K_{m_{\text{ATP}}}}}{(1 + \frac{\text{Fructose}}{\text{Km}_{\text{Fructose}}})(1 + \frac{\text{ATP}}{K_{m_{\text{ATP}}}} + \frac{\text{Fructose}}{K_{i_{\text{Fructose}}}} + \frac{\text{ADP}}{K_{m_{\text{ADP}}}})(1 + \frac{\text{Fructose}}{K_{i_{\text{Fructose}}}})(1 + \frac{\text{F6P}}{K_{m_{\text{F6P}}}})}$$

See page 104 for further details.

E_{15}: ATP-dependent phosphofructokinase (EC 2.7.1.11)

The reaction mechanism for PFK was modelled as a Monod-Wyman-Changeux mechanism with exclusive binding of PEP to the T state by Thomas et al. 1997b. The rate equation and fitted parameters were taken as given by these authors:

$$v_{PFK} = V_{app} \frac{\frac{\text{F6P}}{K_{m_{\text{F6P}}}} \left(1 + \frac{\text{F6P}}{K_{m_{\text{F6P}}}}\right)}{\left(1 + \frac{rmF6P}{K_{m_{\text{F6P}}}}\right)^n + L \left(1 + \frac{\text{PEP}}{K_{i_{\text{PEP}}}}\right)^n}$$

E_{16}: PP_i-dependent phosphofructokinase (EC 2.7.1.90)

PFP is a readily reversible reaction.

$$V_{max} \frac{\frac{1}{K_{m_{\text{F6P}}} K_{m_{\text{PPi}}}} \left(\text{F6P} \cdot \text{PP} - \frac{\text{F16BP}\cdot\text{P}_\text{i}}{\text{K}_\text{eq}}\right)}{1 + \frac{\text{F6P}}{\text{K}_{\text{m}_{\text{F6P}}}} + \frac{\text{PP}_\text{i}}{K_{m_{\text{PPi}}}} + \frac{\text{F16BP}}{K_{m_{\text{F16BP}}}} + \frac{\text{P}_\text{i}}{K_{m_{\text{Pi}}}}}$$

E_{17}: Fructose 1,6-bisphosphate aldolase (EC 4.1.2.13)

For an ordered uni-bi mechanism, GAP released first, a rate equation can be derived according to the King-Altmann method (see my Diploma Thesis). The method is explained in Segel 1993. The rate equation reads:

$$v_{ald} = V_{max} \frac{\frac{\text{F16BP}}{K_{m_{\text{F16BP}}}} \left(1 - \frac{\frac{\text{GAP}\cdot\text{DHAP}}{\text{F16BP}}}{K_{eq}}\right)}{1 + \frac{\text{F16BP}}{K_{m_{\text{F16BP}}}} + \frac{\text{GAP}}{K_{m_{\text{GAP}}}} + \frac{\text{DHAP}}{K_{m_{\text{DHAP}}}} + \frac{\text{F16BP}\cdot\text{GAP}}{K_{m_{\text{F16BP}}}\cdot K_{i_{\text{GAP}}}} + \frac{\text{GAP}\cdot\text{DHAP}}{K_{m_{\text{GAP}}} K_{m_{\text{DHAP}}}}}$$

E_{18}: Triosephosphate isomerase (EC 5.3.1.1)

Uni-uni Michaelis-Menten kinetics was used for TPI:

$$v_{TPI} = V_{max} \frac{\text{GAP} - \frac{\text{DHAP}}{K_{eq}}}{K_{m_{\text{GAP}}} + \text{GAP} + \text{DHAP} \frac{K_{m_{\text{GAP}}}}{K_{m_{\text{DHAP}}}}}$$

E_{19}: GAPDH/PGK

Again, a near-equilibrium assumption:

$$v_{GAPDH-PGK} = V_{max} \left(1 - \frac{\frac{\text{3PGA}\cdot\text{ATP}}{\text{GAP}\cdot\text{P}_\text{i}\cdot\text{ADP}}}{K_{eq}}\right)$$

E_{20}: PGlyM (EC 5.4.2.1)

The reversible uni-uni Michaelis-Menten kinetics for the rate of PGlyM is:

$$v_{PGlyM} = V_{max} \frac{3\text{PGA} - \frac{2\text{PGA}}{K_{eq}}}{K_{m_{3\text{PGA}}} + 3\text{PGA} + 2\text{PGA}\frac{K_{m_{3\text{PGA}}}}{K_{m_{2\text{PGA}}}}}$$

E_{21}: Enolase (EC 4.2.1.11)

Enolase only has two substrates, and its rate was modelled simply with Michaelis-Menten kinetics as follows:

$$v_{eno} = V_{max} \frac{2\text{PGA} - \frac{\text{PEP}}{K_{eq}}}{K_{m_{2\text{PGA}}} + 2\text{PGA} + \text{PEP}\frac{K_{m_{2\text{PGA}}}}{K_{m_{\text{PEP}}}}}$$

E_{22}: Pyruvate kinase (EC 2.7.1.40)

Pyruvate kinase is considered irreversible. The rate is of a partial rapid equilibrium mechanism (see Segel 1993:

$$v_{PK} = V_{max} \frac{\frac{\text{PEP}\cdot\text{ADP}}{K_{m_{\text{PEP}}} K_{m_{\text{ADP}}}}}{1 + \frac{\text{PEP}}{K_{m_{\text{PEP}}}} + \frac{\text{PEP}\cdot\text{ADP}}{K_{m_{\text{PEP}}} K_{m_{\text{ADP}}}} + \frac{\text{ATP}}{K_{m_{\text{ATP}}}} + \frac{\text{Pyruvate}\cdot\text{ATP}}{K_{m_{\text{Pyruvate}}} K_{m_{\text{ATP}}}}}$$

E_{23}: Nucleoside diphosphate kinase (NDPK) (EC 2.7.4.6)

This very fast reaction was modelled by a mass action rate equation:

$$v_{NDPK} = V_{max} \left(k_+ \cdot \text{ATP} \cdot \text{UDP} - k_- \cdot \text{ADP} \cdot \text{UTP}\right)$$

B.1.2 Transporters (Amyloplast Membrane)

Transport steps got mass-action rate equations with K_{eq}=1.
Here the location of the transported metabolites is important, and therefore the suffices _am and _cyt are shown.

T_1: Hexose transport

$$v_{Gexp} = V_{max} \left(k_+ \cdot \text{Glucose_am} - k_- \cdot \text{Glucose_cyt}\right)$$

T_2: GPT - G6P/P_i translocation

$$v_{G6Pexp} = V_{max} \left(k_+ \cdot \text{G6P_am} \cdot \text{P_cyt} - k_- \cdot \text{G6P_cyt} \cdot \text{P_am}\right)$$

T_3: GPT - 3-PGA/P_i translocation

$$v_{PGA3imp} = V_{max} \left(k_+ \cdot \text{3PGA_cyt} \cdot \text{P_am} - k_- \cdot \text{3PGA_am} \cdot \text{P_cyt}\right)$$

T_4: ADP/ATP transporter (AATP)

$$v_{AATP} = V_{max}\left(k_+ \cdot \text{ATP_cyt} \cdot \text{ADP_am} - k_- \cdot \text{ATP_am} \cdot \text{ADP_cyt}\right)$$

T_5: P_i-transport

$$v_{Pexp} = V_{max}\left(k_+ \cdot \text{P_am} - k_- \cdot \text{P_cyt}\right)$$

B.1.3 Further Reactions or Pathways

E_{24}: ATP utilisation

$$v_{ATPutil} = k_{ATPutil} \cdot \frac{\text{ATP}}{\text{ADP}}$$

T_0: Sucrose import

$$v_{SucSupply} = V_{max}\left(k_+ \cdot \text{phloemSucrose} - k_- \cdot \text{Sucrose}\right)$$

B.2 Reactions - Parameter Consensus List

This is the complete list of kinetic parameters as used in the model.
All V_{max} are given in nmol min^{-1} gFW^{-1}.

E_1: amylolytic starch breakdown (page 48)

$K_{i_{\text{Glucose}}}$	100μM		estimate
V_{max}	478	potato tuber	Fernie et al. (2002)

E_2: starch phosphorylase (page 49)

K_{eq}	0.18		calculated after Haldane
$K_{m_{\text{P}}}$	6.2mM	potato tuber	Whelan (1955)
$K_{m_{\text{G1P}}}$	2.6mM	potato tuber	Whelan (1955)
V_{max}	200	potato tuber	Steve Coates, personal communication

E_3 + E_7: phosphoglucomutase (page 50 and page 54)

K_{eq}	$\simeq$ 17		NIST database (2004)
$V_{max_{\text{plastidic}}}$	1542	potato tuber	Fernie et al. (2002)
$V_{max_{\text{cytosolic}}}$	1842	potato tuber	Fernie et al. (2002)

E_4: adenosine 5'-diphosphate glucose pyrophosphorylase (page 51)

$K_{m_{\text{G1P}}}$	100μM		parameter fit
$K_{m_{\text{ATP}}}$	180μM		parameter fit
$K_{m_{\text{ADPglucose}}}$	280μM		parameter fit
$K_{m_{\text{PPi}}}$	260μM		parameter fit
$K_{a_{\text{3PGA}}}$	10μM		parameter fit
$K_{i_{\text{Pi}}}$	160μM		parameter fit
V_{max}	312	potato tuber	Sweetlove et al. (1999)

E_5: starch synthase (page 53)

$K_{m_{\text{ADPG}}}$	150μM	potato	Frydman and Cardini (1966)
V_{max}	171	potato tuber	Fernie et al. (2002)

E_6: pyrophosphatase (page 53)

K_{eq}	750000		estimated according to ΔG
V_{max}	500	potato tuber	Sweetlove et al. (1999)

E_8: UDP-glucose pyrophosphorylase (page 55)

K_{eq}	0.15		calculated after Haldane with $\frac{V_+}{V_-}$=0.08
$K_{m_{\text{G1P}}}$	80μM	potato tuber	Sowokinos et al. (1993)
$K_{m_{\text{UTP}}}$	120μM	potato tuber	Sowokinos et al. (1993)
$K_{m_{\text{UDPG}}}$	140μM	potato tuber	Sowokinos et al. (1993)

$K_{m_{\mathrm{PP}}}$	130μM	potato tuber	Sowokinos et al. (1993)
V_{max}	8100	potato tuber	Fernie et al. (2002)

$\mathbf{E}_9$: phosphoglucoisomerase (page 55)

K_{eq}	$\simeq 0.25$		NIST database (2004)
$K_{m_{\mathrm{G6P}}}$	270μM	pea seeds	Takeda et al. (1967)
$K_{m_{\mathrm{F6P}}}$	150μM		approximated by comparison of magnitudes of $K_{m\mathrm{G6P}}$ and $K_{m\mathrm{F6P}}$ in Noltmann (1972b)
$K_{i_{\mathrm{PEP}}}$	1100μM	rabbit muscle	Noltmann (1972b)
$K_{i\mathrm{F16BP}}$	7500μM	rabbit muscle	Noltmann (1972b)
V_{max}	1086	potato tuber	Trethewey et al. (1998)

$\mathbf{E}_{10}$: sucrose phosphate synthase and sucrose phosphate phosphatase (page 56f.)

K_{eq}(SPS)	10	potato tuber	Kruger (1997)
$K_{m_{\mathrm{UDPG}}}$(SPS)	2000μM	potato tuber	Murata (1972a)
$K_{m_{\mathrm{F6P}}}$(SPS)	900μM	potato tuber	Murata (1972a)
V_{max}(SPS)	797	potato tuber	Fernie et al. (2002)
K_{eq}(SPP)	777		Kruger (1997)
$K_{i_{\mathrm{Sucrose}}}$(SPP)	<5000	carrot root	Hawker and Hatch (1975)
V_{max}(SPP)	850	carrot root	Hawker and Hatch (1975)
K_{eq}	7770		K_{eq}(SPS)$\times K_{eq}$(SPP)
V_{app}	797	potato tuber	the smaller V_{max}
$\frac{V_+}{V_-}$	1000		estimate

$\mathbf{E}_{11}$: sucrose synthase (page 58)

Γ (K_{eq})	2.4	potato tuber	Geigenberger and Stitt (1993)
$K_{m_{\mathrm{UDPG}}}$	1650μM	potato tuber	Slabnik et al. (1968)
$K_{m_{\mathrm{Fructose}}}$	5900μM	potato tuber	Slabnik et al. (1968)
$K_{m_{\mathrm{UDP}}}$	140μM	potato tuber	Murata (1972b)
$K_{m_{\mathrm{Sucrose}}}$	55mM	potato tuber	Murata (1972b)
$K_{i_{\mathrm{Glucose}}}$	12mM	potato tuber	Murata (1972b)
V_{max}	100	potato tuber	Tiessen et al. (2002)

$\mathbf{E}_{12}$: invertase (page 60)

$K_{m_{\mathrm{Sucrose}}}$	28000μM	potato tuber	Isla et al. (1999)
$K_{i_{\mathrm{Fructose}}}$	180μM	potato tuber	Isla et al. (1999)
$K_{i_{\mathrm{Glucose}}}$	1000μM	potato tuber	Isla et al. (1999)
V_{max}	33	potato tuber	Trethewey et al. (1999)

E_{13}: glucokinase (page 61)

$K_{m_{\text{Glucose}}}$(HK1)	41μM		parameter fit
$K_{i_{\text{Fructose}}}$(HK1)	11000μM		parameter fit
$K_{m_{\text{ATP}}}$(HK1)	80μM		parameter fit
$K_{i_{\text{ADP}}}$(HK1)	20μM		parameter fit
$K_{i_{\text{G6P}}}$(HK1)	4100μM		parameter fit
$K_{m_{\text{Glucose}}}$(HK2)	130μM		parameter fit
$K_{i_{\text{Fructose}}}$(HK2)	22000μM		parameter fit
$K_{m_{\text{ATP}}}$(HK2)	280μM		parameter fit
$K_{i_{\text{ADP}}}$(HK2)	100μM		parameter fit
V_{max}	160		Trethewey et al. (1998)

E_{14}: fructokinase (page 61)

$K_{m_{\text{Fructose}}}$	90μM		parameter fit
$K_{m_{\text{ATP}}}$	35μM		parameter fit
$K_{i_{\text{Fructose}}}$	5000μM		parameter fit
$K_{i_{\text{ADP}}}$	13μM		parameter fit
$K_{i_{\text{F6P}}}$	1300μM		parameter fit
V_{max}	376		Sweetlove et al. (1999)

E_{15}: ATP-dependent phosphofructokinase (page 62)

$K_{m_{\text{F6P}}}$	290μM		Thomas et al. (1997b)
$K_{i_{\text{PEP}}}$	18μM		Thomas et al. (1997b)
n_{PFK}	2		Thomas et al. (1997b)
L_{PFK}	1		Thomas et al. (1997b)
V_{max}	135		Trethewey et al. (1998)

E_{16}: PP_i-dependent phosphofructokinase (page 63)

K_{eq}	3.3		Kruger (1997)
$K_{m_{\text{F6P}}}$	500μM		estimate
$K_{m_{\text{PP}}}$	25μM	potato tuber	Montavan and Kruger (1992)
$K_{m_{\text{F16BP}}}$	10μM	potato tuber	van Schaftingen et al. (1982)
$K_{m_{\text{P}}}$	10μM	potato tuber	van Schaftingen et al. (1982)
V_{max}	1266	potato tuber	Trethewey et al. (1998)

E_{17}: fructose 1,6-bisphosphate aldolase (page 63)

K_{eq}	81μM		Barman (1969)
$K_{m_{\text{F16BP}}}$	6μM	carrot root	Moorhead and Plaxton (1990)
$K_{m_{\text{GAP}}}$			estimate
$K_{m_{\text{DHAP}}}$			estimate
$K_{i_{\text{GAP}}}$			estimate
V_{max}	430	potato tuber	Trethewey et al. (1998)

E_{18}: triosephosphate isomerase (page 64)

K_{eq}	$\simeq 19$		NIST database (2004)
$K_{m_{\mathrm{GAP}}}$	440μM	garden pea	Tomlinson and Turner (1979)
$K_{m_{\mathrm{DHAP}}}$	880μM	garden pea	Tomlinson and Turner (1979)
V_{max}	4438	potato tuber	Trethewey et al. (1998)

E_{19}: phosphoglycerate kinase (page 64)

K_{eq}(GAPDH)	$0.5\mathrm{mM}^{-1}$		Barman (1969)
V_{max}(GAPDH)	301	potato tuber	Trethewey et al. (1998)
K_{eq}(PGK)	3448		Barman (1969)
V_{max}(PGK)	1379	potato tuber	Trethewey et al. (1998)
K_{eq}	$1.724\mu\mathrm{M}^{-1}$		
V_{max}	301	potato tuber	smaller one

E_{20}: phosphoglycerate mutase (page 65)

K_{eq}	$\simeq 0.16$		Ray and Peck (1972b) and NIST database (2004)
$K_{m_{3-\mathrm{PGA}}}$	330μM	castor plant	Thomas et al. (1997b)
$K_{m_{2-\mathrm{PGA}}}$	60μM	castor plant	Thomas et al. (1997b)
V_{max}	541	potato tuber	Trethewey et al. (1998)

E_{21}: enolase (page 65)

K_{eq}	6.3		Barman (1969)
$K_{m_{2-\mathrm{PGA}}}$	150μM	average of -	Thomas et al. (1997b)
$K_{m_{\mathrm{PEP}}}$	150μM	- several plants	Thomas et al. (1997b)
V_{max}	448	potato tuber	Trethewey et al. (1998)

E_{22}: pyruvate kinase (page 66)

K_{eq}	6451.6		Barman (1969)
$K_{m_{\mathrm{PEP}}}$	20μM	derived	Thomas et al. (1997b)
$K_{m_{\mathrm{ADP}}}$	86μM	rabbit muscle	Barman (1969)
$K_{m_{\mathrm{pyruvate}}}$	1000μM	rabbit muscle	Barman (1969)
$K_{m_{\mathrm{ATP}}}$	20μM	derived	Thomas et al. (1997b)
V_{max}	127	potato tuber	Trethewey et al. (1998)

E_{23}: nucleoside diphosphokinase (page 68)

K_{eq}	1.0	NIST database (2004)
k_+	0.001	estimate
k_-	0.001	estimate

E_{24}: ATP utilisation (page 68)

k	3	estimate

T_1: hexose transport (page 67)

k_+	0.001	estimate
k_-	0.001	estimate

T_2 + T_3: phosphate translocator (page 67)

k_+	0.01	estimate
k_-	0.01	estimate

T_4: ATP/ADP translocator (page 68)

k_+	0.002	estimate
k_-	0.002	estimate

T_5: phosphate transport (page 68)

k_+	0.3	estimate
k_-	0.1	estimate

T_0: sucrose supply (page 68)

k_+	0.01	estimate
k_-	0.01	estimate

B.3 Model Script (ScrumPy)

```
##########################################
# 26/02/05                               #
# model, copy of Thesis.spy              #
##########################################

#Structural() #if this option is not commented out
              #ScrumPy will ignore the kinetics and only read the reaction list
              #and the model becomes a structural model.

###########
#reactions#
###########

AGPase:
##### ADP glucose pyrophosphorylase
G1P_am + ATP_am <> ADPG_am + PP_am
Vmax_AGPase*(G1P_am*ATP_am-ADPG_am*PP_am)*(1+PGA3_am/Ka_PGA3_AGPase)/
((Km_G1P_AGPase*(1+PP_am/Km_PP_AGPase)+G1P_am)
*(Km_ATP_AGPase*(1+ADPG_am/Km_ADPG_AGPase)+ATP_am))
/(1+P_am/Ki_P_AGPase)

StSynth:
##### starch synthase
ADPG_am + x_starch -> ADP_am + x_starch
Vmax_StSynth*ADPG_am/(Km_ADPG_StSynth+ADPG_am)

pPPase:
##### plastidic inorganic pyrophosphatase
PP_am <> 2 P_am
Vmax_pPPase*(1 - (P_am*P_am/PP_am)/Keq_pPPase)

StPase:
##### starch phosphorylase
x_starch + P_am <> G1P_am
Vforward_StPase*(P_am - G1P_am/Keq_StPase)/
(Km_P_StPase + P_am + G1P_am*Km_P_StPase/Km_G1P_StPase)

degr:
##### amylolytic starch breakdown
x_starch -> Glucose_am
Vmax_degr/(1+Glucose_am/Ki_Glucose_degr)

Gexp:
##### hexose translocator
Glucose_am <> Glucose_cyt
V_Gexp*(k_forward_Gexp*Glucose_am - k_backward_Gexp*Glucose_cyt)

G6Pexp:
##### G6P/P counterexchange
G6P_am + P_cyt <> G6P_cyt + P_am
V_G6Pexp*(k_forward_G6Pexp*G6P_am*P_cyt - k_backward_G6Pexp*G6P_cyt*P_am)
```

```
pPGM:
##### plastidic phosphoglucomutase
G1P_am <> G6P_am
Vmax_pPGM * (1 - G6P_am/G1P_am/Keq_pPGM)

cPGM:
##### cytoplasmic phosphoglucomutase
G1P_cyt <> G6P_cyt
Vmax_cPGM * (1 - G6P_cyt/G1P_cyt/Keq_cPGM)

PGI:
##### phosphoglucoisomerase
G6P_cyt <> F6P_cyt
Vmax_PGI*(G6P_cyt-F6P_cyt/Keq_PGI)/
(Km_G6P_PGI + G6P_cyt + F6P_cyt*Km_G6P_PGI/Km_F6P_PGI
+ F16BP_cyt*Km_G6P_PGI/Ki_F16BP_PGI + PEP_cyt*Km_G6P_PGI/Ki_PEP_PGI)

PFK:
##### PFK
F6P_cyt + ATP_cyt -> F16BP_cyt + ADP_cyt
Vmax_PFK*(F6P_cyt/Km_F6P_PFK)*((1+F6P_cyt/Km_F6P_PFK)**(n_PFK-1))/
((1+F6P_cyt/Km_F6P_PFK)**n_PFK + L_PFK*((1+PEP_cyt/Ki_PEP_PFK)**n_PFK))

PFP:
##### PFP
F6P_cyt + PP_cyt <> F16BP_cyt + P_cyt
Vmax_PFP*(1/Km_F6P_PFP/Km_PP_PFP)*(F6P_cyt*PP_cyt-F16BP_cyt*P_cyt/Keq_PFP)/
(1+F6P_cyt/Km_F6P_PFP+PP_cyt/Km_PP_PFP+F16BP_cyt/Km_F16BP_PFP+P_cyt/Km_P_PFP)

ald:
##### aldolase
F16BP_cyt <> GAP_cyt + DHAP_cyt
Vmax_ald*(F16BP_cyt/Km_F16BP_ald)*(1 - (GAP_cyt*DHAP_cyt/F16BP_cyt)/Keq_ald)/
(1 + F16BP_cyt/Km_F16BP_ald + GAP_cyt/Km_GAP_ald + DHAP_cyt/Km_DHAP_ald
 + (F16BP_cyt*GAP_cyt)/(Km_F16BP_ald*Ki_GAP_ald)
 + (GAP_cyt*DHAP_cyt)/(Km_GAP_ald*Km_DHAP_ald))

TPI:
##### TPI
DHAP_cyt <> GAP_cyt
Vmax_TPI*(DHAP_cyt - GAP_cyt/Keq_TPI)/
(Km_DHAP_TPI + DHAP_cyt + GAP_cyt*Km_GAP_TPI/Km_GAP_TPI)

GAPDH_PGK:
##### GAPdehydrogenase/PGK + oxidative phosphorylation (1.83)
6 GAP_cyt + 17 ADP_cyt + 17 P_cyt <> 6 PGA3_cyt + 17 ATP_cyt
Vmax_GAPDH/6 * (1 - (PGA3_cyt*ATP_cyt)/(GAP_cyt*P_cyt*ADP_cyt)/Keq_GAPDH)

PGA3imp:
##### G6P/3-PGA counterexchange
PGA3_cyt + G6P_am <> PGA3_am + G6P_cyt
V_PGA3imp * (k_forward_PGA3imp*PGA3_cyt*G6P_am - k_backward_PGA3imp*PGA3_am*G6P_cyt)
```

```
PGlyM:
##### phosphoglycerate mutase
PGA3_cyt <> PGA2_cyt
Vmax_PGlyM*(PGA3_cyt - PGA2_cyt/Keq_PGlyM)/
(Km_PGA3_PGlyM + PGA3_cyt + PGA2_cyt*Km_PGA3_PGlyM/Km_PGA2_PGlyM)

eno:
##### enolase
PGA2_cyt <> PEP_cyt
Vmax_eno*(PGA2_cyt - PEP_cyt/Keq_eno)/
(Km_PGA2_eno + PGA2_cyt + PEP_cyt*Km_PGA2_eno/Km_PEP_eno)

PK:
##### pyruvate kinase
PEP_cyt + ADP_cyt -> x_pyruvate + ATP_cyt
Vmax_PK*PEP_cyt*ADP_cyt/(Km_PEP_PK*Km_ADP_PK)/
(1 + PEP_cyt/Km_PEP_PK + PEP_cyt*ADP_cyt/(Km_PEP_PK*Km_ADP_PK)
+ ATP_cyt/Km_ATP_PK + x_pyruvate*ATP_cyt/(Km_pyruvate_PK*Km_ATP_PK))
#partial rapid equilibrium (see Segel p.592) but irreversible!

UGPase:
##### UDP glucose pyrophosphorylase
G1P_cyt + UTP_cyt <> UDPG_cyt + PP_cyt
Vforward_UGPase*(G1P_cyt*UTP_cyt-UDPG_cyt*PP_cyt/Keq_UGPase)/
((Km_G1P_UGPase*(1+PP_cyt/Km_PP_UGPase)+G1P_cyt)
*(Km_UTP_UGPase*(1+UDPG_cyt/Km_UDPG_UGPase)+UTP_cyt))

SPS_SPP:
##### SPS/SPP
F6P_cyt + UDPG_cyt -> Sucrose_cyt + P_cyt + UDP_cyt
Vapp_SPS_SPP*(F6P_cyt*UDPG_cyt - UDP_cyt*P_cyt/Keq_SPS_SPP)/
(Km_F6P_SPS_SPP*Km_UDPG_SPS_SPP + F6P_cyt*UDPG_cyt
+ UDP_cyt*P_cyt*Vratio_SPS_SPP/Keq_SPS_SPP
+ Sucrose_cyt*Km_F6P_SPS_SPP*Km_UDPG_SPS_SPP/Ki_Sucrose_SPS_SPP)

SuSy:
##### sucrose synthase
Fructose_cyt + UDPG_cyt <> Sucrose_cyt + UDP_cyt
Vmax_SuSy*(Fructose_cyt*UDPG_cyt/(Km_SuSy_Fructose*Km_SuSy_UDPG))
*(1 - Sucrose_cyt*UDP_cyt/Fructose_cyt/UDPG_cyt/Keq_SuSy)/
(1 + Fructose_cyt*UDPG_cyt/(Km_SuSy_Fructose*Km_SuSy_UDPG)
+ Sucrose_cyt*UDP_cyt/(Km_SuSy_Sucrose*Km_SuSy_UDP))/
(1 + Glucose_cyt/Ki_SuSy_Glucose)

SucSupply:
### sucrose uptake
x_sucrose <> Sucrose_cyt
V_SucSupply*(k_forward_SucSupply*x_sucrose - k_backward_SucUptSupply*Sucrose_cyt)
```

```
inv:
##### invertase
Sucrose_cyt -> Fructose_cyt + Glucose_cyt
Vmax_inv*(Sucrose_cyt/Km_Sucrose_inv)/
((1 + Sucrose_cyt/Km_Sucrose_inv + Fructose_cyt/Ki_Fructose_inv)
*(1 + Glucose_cyt/Ki_Glucose_inv))

FK:
##### fructokinase
Fructose_cyt + ATP_cyt -> F6P_cyt + ADP_cyt
Vmax_FK*(Fructose*ATP_cyt/(Km_Fructose_FK*Km_ATP_FK))/
((1+Fructose/Km_Fructose_FK)*(1+Fructose/Ki_Fructose_FK)*(1+F6P_cyt/Km_F6P_FK)
*(1+ATP_cyt/Km_ATP_FK+Fructose/Ki_Fructose_FK+ADP_cyt/Km_ADP_FK))

GK:
##### glucokinase
Glucose_cyt + ATP_cyt -> G6P_cyt + ADP_cyt
(Vmax_GK/2)*(Glucose_cyt*ATP_cyt/(Km_Glucose_HK1*Km_ATP_HK1))/
((1+Glucose_cyt/Km_Glucose_HK1+Fructose/Km_Fructose_HK1)
*(1+ATP_cyt/Km_ATP_HK1+ADP_cyt/Ki_ADP_HK1)*(1+G6P_cyt/Ki_G6P_HK1))
+(Vmax_GK/2)*(Glucose_cyt*ATP_cyt/(Km_Glucose_HK2*Km_ATP_HK2))/
((1+Glucose_cyt/Km_Glucose_HK2+Fructose/Km_Fructose_HK2)
*(1+ATP_cyt/Km_ATP_HK2+ADP_cyt/Ki_ADP_HK2))

NDPK:
##### nucleoside diphosphate kinase
ATP_cyt + UDP_cyt <> ADP_cyt + UTP_cyt
V_NDPK*(k_forward_NDPK*ATP_cyt*UDP_cyt - k_backward_NDPK*ADP_cyt*UTP_cyt)

AATP:
##### adenylate translocator
ADP_am + ATP_cyt <> ATP_am + ADP_cyt
V_AATP*(k_forward_AATP*ATP_cyt*ADP_am - k_backward_AATP*ATP_am*ADP_cyt)

Pexp:
##### orthophosphate export
P_am <> P_cyt
V_Pexp*(k_forward_Pexp*P_am - k_backward_Pexp*P_cyt)

ATPutil:
##### ATP utilisation
ATP_cyt -> ADP_cyt + P_cyt
V_ATPutil*k_ATPutil*(ATP_cyt/ADP_cyt)


############
#parameters#
############

#all Vmax in nmol/min/gFW, all Km in microM

#AGPase
Vmax_AGPase = 312
```

```
Km_G1P_AGPase = 100
Km_ATP_AGPase = 180
Km_ADPG_AGPase = 280
Km_PP_AGPase = 260
Ki_P_AGPase = 160
Ka_PGA3_AGPase = 10

#StSynth
Vmax_StSynth = 171         ### soluble + granule-bound
Km_ADPG_StSynth = 150

#(plastidial) inorganic pyrophosphatase
Vmax_pPPase = 500
Keq_pPPase = 750000

#StPase
Vforward_StPase = 200
Km_P_StPase = 6200
Km_G1P_StPase = 2600
Keq_StPase = 0.18

#amylolytic degradation of starch
Vmax_degr = 114
Ki_Glucose_degr = 100

#Gexp
V_Gexp = 1
k_forward_Gexp = 0.001
k_backward_Gexp = 0.001

#G6Pexport
V_G6Pexp = 1
k_forward_G6Pexp = 0.01
k_backward_G6Pexp = 0.01

#plastidic phosphoglucomutase
Vmax_pPGM = 1542
Keq_pPGM = 17

#cytosolic PGM
Vmax_cPGM = 1842
Keq_cPGM = 17

#phosphoglucoisomerase
Vmax_PGI = 1086
Km_G6P_PGI = 270
Km_F6P_PGI  = 150
Keq_PGI = 0.25
Ki_PEP_PGI = 1100
Ki_F16BP_PGI = 7500

#PFK
Vmax_PFK = 135
```

```
Km_F6P_PFK = 290
Ki_PEP_PFK = 18
n_PFK = 2
L_PFK = 1

#PFP
Vmax_PFP = 1266
Km_F6P_PFP = 500
Km_PP_PFP = 25
Km_F16BP_PFP = 10
Km_P_PFP = 10
Keq_PFP = 3.3

#aldolase
Vmax_ald = 430
Keq_ald = 81
Km_F16BP_ald = 6
Km_GAP_ald = 100
Km_DHAP_ald = 100
Ki_GAP_ald = 1000

#triosephosphateisomerase
Vmax_TPI = 4438
Keq_TPI = 0.0455
Km_GAP_TPI = 440
Km_DHAP_TPI = 880

#GAPdehydrogenase/PGK
Vmax_GAPDH = 301
Keq_GAPDH = 1.724  #1724/mM!

#PGA3imp
V_PGA3imp = 1
k_forward_PGA3imp = 0.01
k_backward_PGA3imp = 0.01

#PGlyM
Vmax_PGlyM = 541
Keq_PGlyM = 0.16
Km_PGA3_PGlyM = 330
Km_PGA2_PGlyM = 60

#enolase
Vmax_eno = 448
Keq_eno= 6.3
Km_PGA2_eno = 150
Km_PEP_eno = 150

#pyruvate kinase
Vmax_PK = 127
#Keq_PK = 6451.6
Km_PEP_PK = 20
Km_ADP_PK = 20
```

```
Km_pyruvate_PK = 1000
Km_ATP_PK = 86

#UGPase
Vforward_UGPase = 8100
Km_G1P_UGPase = 80
Km_UTP_UGPase = 120
Km_UDPG_UGPase = 140
Km_PP_UGPase = 130
Keq_UGPase = 0.15

#SPS/SPP
Vapp_SPS_SPP = 797
Km_F6P_SPS_SPP = 900
Km_UDPG_SPS_SPP = 2000
Ki_Sucrose_SPS_SPP = 5000
Keq_SPS_SPP = 7770
Vratio_SPS_SPP = 1000

#SuSy
Vmax_SuSy = 100
Keq_SuSy = 2.4
Km_SuSy_Fructose = 5900
Km_SuSy_UDPG = 1650
Km_SuSy_Sucrose = 55000
Km_SuSy_UDP = 140
Ki_SuSy_Glucose = 12000

#SucSupply
V_SucSupply = 1
k_forward_SucSupply = 0.01
k_backward_SucSupply = 0.01

#invertase (alkaline invertase)
Vmax_inv = 33
Km_Sucrose_inv = 28000
Ki_Fructose_inv = 180
Ki_Glucose_inv = 1000

#fructokinase
Vmax_FK = 376
Km_Fructose_FK = 90
Km_ATP_FK = 35
Ki_Fructose_FK = 5000
Km_ADP_FK = 13
Km_F6P_FK = 1300

#cytosolic hexokinase
Vmax_GK = 160
Km_Glucose_HK1 = 41
Km_Fructose_HK1 = 11000
Km_ATP_HK1 = 80
Ki_ADP_HK1 = 20
```

```
Ki_G6P_HK1 = 4100
Km_Glucose_HK2 = 130
Km_Fructose_HK2 = 22000
Km_ATP_HK2 = 280
Ki_ADP_HK2 = 100

#nucleoside diphosphate kinase
V_NDPK = 1
k_forward_NDPK = 0.001
k_backward_NDPK = 0.001

#AATP
V_AATP = 1
k_forward_AT = 0.002
k_backward_AT = 0.002

#Pexp
V_Pexp = 1
k_forward_Pexp = 0.3
k_backward_Pexp = 0.1

#ATPtil
V_ATPutil = 1
k_ATPutil = 3


################
#initialization#
################

#all in microM

ADPG_am = 100
UDPG_cyt = 870
UTP_cyt = 20
UDP_cyt = 10
G1P_am = 30
G1P_cyt = 30
G6P_am = 550
G6P_cyt = 500
F6P_cyt = 160
Glucose_cyt = 150
Glucose_am = 3000
Sucrose_cyt = 88000
Fructose_cyt = 20
F16BP_cyt = 1
DHAP_cyt = 5
GAP_cyt = 1
PGA3_cyt = 150
PGA3_am = 160
PGA2_cyt = 20
PEP_cyt = 10
PP_am = 5
```

```
P_am = 2000
PP_cyt = 1
P_cyt = 2000
ATP_am = 150
ADP_am = 100
ATP_cyt = 200
ADP_cyt = 180

x_sucrose = 90000
x_starch = 1000000
x_pyruvate = 10
```

B.4 Stoichiometry Matrix N

$$
\begin{pmatrix}
-1 & 0 & 0 & 0 & 0 & 0 & 0 & 0 & 0 & 0 & 0 & 0 & 0 & 1 & 0 & 0 & 0 & 0 & -1 & 0 & 0 & 0 & 0 & 0 & 0 & 0 & 0 & 0 & 0 & 0 \\
-1 & 0 & 0 & 0 & 1 & 0 & 0 & 0 & 0 & -3 & 0 & 0 & 0 & 0 & 0 & 0 & 0 & 0 & 0 & 0 & 1 & 0 & 0 & 0 & 1 & 0 & 0 & 0 & 0 & 1 \\
1 & 0 & 0 & 0 & 0 & 0 & 0 & 1 & 0 & 0 & 1 & 0 & 0 & 0 & 0 & 0 & 0 & 0 & 1 & 0 & 0 & 0 & 0 & -1 & 0 & 0 & 0 & 0 & 0 & 0 \\
1 & 0 & 0 & 0 & -1 & 0 & 0 & 0 & 0 & 0 & 0 & 0 & 0 & 0 & -1 & 0 & 0 & 2 & 0 & 0 & 0 & 0 & 0 & 0 & 0 & 0 & 0 & 0 & 0 & 0 \\
0 & -1 & 0 & 0 & 0 & 0 & 0 & 0 & 0 & 3 & -1 & 0 & 0 & 0 & 0 & 0 & 0 & 0 & 0 & 0 & -1 & -1 & 0 & 0 & 0 & -1 & 1 & -1 & 0 & 0 \\
0 & -1 & 0 & 0 & 0 & 0 & 0 & 0 & 0 & 0 & 0 & 0 & 0 & 0 & 0 & 1 & 0 & 0 & 0 & 0 & 0 & 0 & 0 & 0 & 0 & 0 & 0 & 0 & 0 & 1 \\
0 & 1 & 0 & 0 & 0 & 0 & 0 & 0 & 0 & -3 & 1 & 0 & 0 & 0 & 0 & 0 & 0 & 0 & 0 & 0 & 1 & 1 & 0 & 0 & 0 & 1 & -1 & 1 & 0 & 0 \\
0 & 1 & 0 & 0 & 0 & 0 & 0 & 0 & 0 & 0 & 0 & 0 & -1 & 0 & 0 & 0 & 0 & 0 & 0 & 0 & 0 & 0 & 0 & 0 & 0 & 0 & 0 & 0 & 0 & 0 \\
0 & 0 & 1 & 0 & 0 & 0 & -1 & 0 & 0 & 0 & 0 & 0 & 0 & 0 & 0 & 0 & 0 & 0 & 0 & 0 & 0 & 0 & 0 & 0 & 0 & 0 & 0 & 0 & 0 & 0 \\
0 & 0 & 0 & -1 & 0 & 0 & 0 & 0 & 0 & 0 & 0 & 0 & 0 & 0 & 0 & 1 & 1 & 0 & 0 & 0 & 0 & 0 & 0 & 0 & 0 & 0 & 0 & 0 & 0 & 1 \\
0 & 0 & 0 & 1 & 0 & 0 & 0 & 0 & 0 & 0 & 0 & 0 & 0 & 0 & 0 & -1 & 0 & 0 & 0 & 0 & 0 & 0 & 0 & 0 & 0 & -1 & 0 & 0 & 0 & 0 \\
0 & 0 & 0 & 1 & 0 & 0 & 1 & 0 & 0 & 0 & -1 & 0 & 0 & 0 & 0 & 0 & 0 & 0 & 0 & 0 & 0 & 0 & 0 & 0 & 0 & 0 & 0 & 0 & 0 & 0 \\
0 & 0 & 0 & 0 & 0 & -1 & 0 & 0 & 0 & 0 & 0 & 0 & 0 & 0 & 0 & 0 & 0 & 0 & 0 & 0 & 0 & 1 & 0 & 0 & 1 & 0 & 0 & 0 & 0 & 0 \\
0 & 0 & 0 & 0 & 0 & 1 & 0 & 0 & 1 & -1 & 0 & 0 & 0 & 0 & 0 & 0 & 0 & 0 & 0 & 0 & 0 & 0 & 0 & 0 & 0 & 0 & 0 & 0 & 0 & 0 \\
0 & 0 & 0 & 0 & 0 & 1 & 0 & 0 & -1 & 0 & 0 & 0 & 0 & 0 & 0 & 0 & 0 & 0 & 0 & 0 & 0 & 0 & 0 & 0 & 0 & 0 & 0 & 0 & 0 & 0 \\
0 & 0 & 0 & 0 & 0 & 0 & 0 & -1 & 0 & 0 & 0 & 0 & -1 & 0 & 0 & 0 & 0 & 0 & 0 & 0 & 0 & 0 & 0 & 0 & 0 & 0 & 0 & 0 & 0 & 0 \\
0 & 0 & 0 & 0 & 0 & 0 & 0 & 0 & 0 & 1 & 0 & 0 & 0 & 0 & 0 & 0 & 0 & 0 & -1 & 0 & 0 & 0 & -1 & 0 & 0 & 0 & 0 & 0 & 0 & 0 \\
0 & 0 & 0 & 0 & 0 & 0 & 0 & 0 & 0 & 0 & 0 & -1 & 0 & 0 & 0 & 0 & 0 & 0 & 0 & 0 & 0 & 0 & 1 & 0 & 0 & 0 & 0 & 0 & 0 & 0 \\
0 & 0 & 0 & 0 & 0 & 0 & 0 & 0 & 0 & 0 & 0 & 1 & 0 & 0 & 0 & 0 & 0 & 0 & 0 & 0 & 0 & 0 & 0 & 0 & 0 & 0 & -1 & 0 & 0 & 0 \\
0 & 0 & 0 & 0 & 0 & 0 & 0 & 0 & 0 & 0 & 0 & 0 & 1 & 0 & 0 & -1 & 0 & 0 & 0 & 0 & 0 & 0 & 0 & 0 & 0 & 0 & 0 & 0 & 0 & -1 \\
0 & 0 & 0 & 0 & 0 & 0 & 0 & 0 & 0 & 0 & 0 & 0 & 1 & 0 & 0 & 0 & 0 & 0 & 0 & 0 & 0 & 0 & 0 & 0 & -1 & 0 & 0 & 0 & 0 & 0 \\
0 & 0 & 0 & 0 & 0 & 0 & 0 & 0 & 0 & 0 & 0 & 0 & 0 & -1 & 1 & 0 & 0 & 0 & 0 & -1 & 0 & 0 & 0 & 0 & 0 & 0 & 0 & 0 & 0 & 0 \\
0 & 0 & 0 & 0 & 0 & 0 & 0 & 0 & 0 & 0 & 0 & 0 & 0 & 0 & 0 & 0 & -1 & 0 & 0 & 0 & 0 & 0 & 0 & 0 & 0 & 0 & 0 & 0 & 0 & 0 \\
0 & 0 & 0 & 0 & 0 & 0 & 0 & 0 & 0 & 0 & 0 & 0 & 0 & 0 & 0 & 0 & 0 & -1 & 0 & 1 & 0 & 0 & 0 & 0 & 0 & 0 & 0 & 0 & 0 & 0 \\
0 & 0 & 0 & 0 & 0 & 0 & 0 & 0 & 0 & 0 & 0 & 0 & 0 & 0 & 0 & 0 & 0 & 0 & 1 & 0 & 0 & 0 & 0 & 0 & 0 & 0 & 0 & 0 & 0 & 0 \\
0 & 0 & 0 & 0 & 0 & 0 & 0 & 0 & 0 & 0 & 0 & 0 & 0 & 0 & 0 & 0 & 0 & 0 & 0 & -1 & 0 & 0 & 0 & 0 & 0 & 0 & 0 & 1 & 0 & 0 \\
0 & 0 & 0 & 0 & 0 & 0 & 0 & 0 & 0 & 0 & 0 & 0 & 0 & 0 & 0 & 0 & 0 & 0 & 0 & 1 & 0 & 0 & 0 & 0 & 0 & 0 & 0 & 0 & -1 & 0 \\
0 & 0 & 0 & 0 & 0 & 0 & 0 & 0 & 0 & 0 & 0 & 0 & 0 & 0 & 0 & 0 & 0 & 0 & 0 & 0 & 0 & -1 & 0 & 1 & -1 & 1 & 0 & 0 & 0 & -1 \\
0 & 0 & 0 & 0 & 0 & 0 & 0 & 0 & 0 & 0 & 0 & 0 & 0 & 0 & 0 & 0 & 0 & 0 & 0 & 0 & 0 & 0 & 0 & 0 & 0 & 0 & 0 & -1 & 1 & 0
\end{pmatrix}
$$

Figure B.1: Stoichiometry matrix **N** of the model.

$$
\boldsymbol{S}^T = \begin{pmatrix}
G6P_am \\ P_cyt \\ G6P_cyt \\ P_am \\ ATP_cyt \\ UDP_cyt \\ ADP_cyt \\ UTP_cyt \\ Glucose_am \\ Sucrose_cyt \\ Fructose_cyt \\ Glucose_cyt \\ F16BP_cyt \\ GAP_cyt \\ DHAP_cyt \\ G1P_cyt \\ PGA3_cyt \\ PGA2_cyt \\ PEP_cyt \\ UDPG_cyt \\ PP_cyt \\ G1P_am \\ PP_am \\ PGA3_am \\ ATP_am \\ ADPG_am \\ F6P_cyt \\ ADP_am
\end{pmatrix}
\qquad
\boldsymbol{v} = \begin{pmatrix}
G6Pexp \\ NDPK \\ degr \\ inv \\ SucSupply^* \\ Pexp \\ ald \\ Gexp \\ cPGM \\ TPI \\ GAPDH \\ HXK \\ eno \\ UGPase \\ pPGM \\ StPase \\ SuSy \\ pPPase \\ PGA3imp \\ AGPase \\ ATPcons \\ PFK \\ PGlyM \\ PGI \\ PFP \\ FK \\ PK \\ AT \\ StSynth \\ SPS_SPP
\end{pmatrix}
$$

Figure B.2: Metabolite concentration vector $\boldsymbol{S}^T$ and reaction rate vector $\boldsymbol{v}$.
* additional, in attached model only.

Appendix C

Published Material

Poolman, Mark G., Assmus, Heike E. and Fell, David A.
Applications of metabolic modelling to plant metabolism.
J.Exp.Bot. 55: 1177-1186.
JXB Advance Access published on June 1, 2004, DOI 10.1093/jxb/erh090.